2009-05-05

# Functional Analysis of Yeast Pheromone Receptors in ER Exit, Ligand-Induced Endocytosis and Oligomerization: A Dissertation

Chien-I Chang
*University of Massachusetts Medical School*

# FUNCTIONAL ANALYSIS OF YEAST PHEROMONE RECEPTORS IN ER EXIT, LIGAND-INDUCED ENDOCYTOSIS AND OLIGOMERIZATION

A Dissertation Presented

By

CHIEN-I CHANG

Submitted to the Faculty of the
University of Massachusetts Graduate School of Biomedical Sciences, Worcester
in partial fulfillment of the requirements for the degrees of

DORTOR OF PHILOSOPHY

MAY 5, 2009

BIOMEDICAL SCIENCES

FUNCTIONAL ANALYSIS OF YEAST PHEROMONE RECEPTORS IN ER EXIT, LIGAND-INDUCED ENDOCYTOSIS AND OLIGOMERIZATION

A Dissertation Presented
By

CHIEN-I CHANG

The signatures of the Dissertation Defense Committee Signifies completion and approval as to style and content of the Dissertation

_____
Duane D. Jenness, Ph.D., Thesis Advisor

_____
Richard E. Baker, Ph.D., Member of Committee

_____
Reid Gilmore, Ph.D., Member of Committee

_____
Trudy G. Morrison, Ph.D., Member of Committee

_____
James B. Konopka, Ph.D., Member of Committee

The signature of the Chair of the Committee signifies that the written dissertation meets the requirements of the Dissertation Committee

_____
Peter M. Pryciak, Ph.D., Chair of Committee

The signature of the Dean of the Graduate School of Biomedical Sciences signifies that the student has met all graduation requirements of the school

_____
Anthony Carruthers, Ph.D.,
Dean of the Graduate School of Biomedical Sciences

Department of Molecular Genetics and Microbiology
May 5, 2009

## Acknowledgements

First I would like to thank my mentor Dr. Duane Jenness for his guidance and patience. He gave me the freedom to do whatever I want in the experiment without interfering too much. I would like to think him for the excellent training I received during these years. This thesis cannot be done without him.

My sincere thanks for my past and current committee members Dr. Peter Pryciak, Dr. Reid Gilmore, Dr. Trudy Morrison, Dr. Richard Baker, Dr. James Konopka and Dr. Donald Tipper for the insight and advice on my academic advancement.

I also want to thank my parents for their unconditional support throughout my graduate years and my life. Last but not least I want to thank my wife Hua-Jung for being there for me.

## Abstract

This study investigates endocytosis and ER export signals of the yeast α-factor receptor and the role that receptor oligomerization plays in these processes. The α-factor receptor contains signal sequences in the cytoplasmic C-terminal domain that are essential for ligand-mediated endocytosis. In an endocytosis complementation assay, I found that oligomeric complexes of the receptor undergo ligand-mediated endocytosis when the α-factor binding site and the endocytosis signal sequences are located in different receptors. Both in vitro and in vivo assays strongly suggested that ligand-induced conformational changes in one Ste2 subunit do not affect neighboring subunits. Therefore, the recognition of endocytosis signal sequence and the recognition of the ligand-induced conformational change are likely to be two independent events, where the signal sequence plays only a passive role in the ligand-induced endocytosis. Four amino acid substitutions (C59R, H94P, S141P and S145P) in TM domains I, II and III were identified that resulted in the accumulation of truncated receptors in the ER but did not block ER export of full-length receptors. The two DXE motifs in the C-terminal tail were required for export of the mutant receptors from the ER; however DXE was not essential for proper cell surface expression of wild-type receptors apparently because the receptors contain redundant ER export signals. An assay for oligomerization of receptors in the ER was developed based on the ability of truncated mutant receptors to exit the ER. The four substitutions (C59R, H94P, S141P and S145P) that caused DXE-dependent ER export failed to form homo-oligomers, suggesting that the DXE motifs and receptor

oligomerization serve as independent ER export signals. Consistent with this view, two of the substitutions (S141P and S145P), when coexpressed, with wild-type receptors, formed hetero-oligomers that exited the ER. Finally, the full-length oligomer-defective mutant Ste2-S141P was sensitive to α-factor, suggesting that receptor monomers that reach the cell surface are able to activate the heterotrimeric G protein. The potential roles that TM1, 2 and 3 play in receptor oligomerization are discussed.

TABLE OF CONTENTS

# LIST OF TABLES AND FIGURES

# CHAPTER I

# INTRODUCTION

In this introduction, I discuss general features among G-protein coupled receptors (GPCRs) that pertain to my thesis research. Most if not all of the GPCRs can form dimer or higher-order oligomeric complexes. The different structural regions of GPCRs such as the N-terminal domain, carboxy terminal domain and transmembrane domains have been implicated in regulating oligomerization of GPCRs. In addition, post-translational modifications including glycosylation, phosphorylation, ubquitination and palmitoylation also affect GPCRs in a variety of ways such as cell surface expression, endocytosis, signal activation and oligomerization. Functional implications of GPCR oligomerization are proposed relating to cell-surface targeting, signal transduction and G-protein coupling. The functional roles of the motif sequences implicated in ER retention, ER export trafficking, and internalization in GPCRs are highlighted. Chaperone proteins are revealed to be important for proper ER export, signal transduction and plasma membrane targeting of GPCR. Finally, I discuss the current understanding of $\alpha$-factor pheromone receptors in yeast and the implications of the oligomeric $\alpha$-factor pheromone receptors in relation to cell surface expression, signal transduction and biogenesis.

The unicellular budding yeast *Saccharomyces cerevisiae* has been used as a model organism to study signaling pathways and other aspects of cellular function.

*S. cerevisiae* grows either as haploid or diploid cells. Haploid cells of two mating types, **a** and α cells, fuse to form diploid cells. Haploid **a** cells respond to the α-factor pheromone that is secreted by α cells. The binding of α-factor pheromone to its receptor (the product of *STE2* gene) initiates a signal transduction pathway that is mediated by the action of a heterotrimeric G protein and a MAP protein kinase cascade. When α-factor mating pheromone binds to its receptor on the surface of **a** cells, the receptors undergo conformation changes that activate the G-protein and ultimately cause the cell to arrest in the $G_1$ phase of the cell division cycle. In this chapter, the basic properties of the mating pheromone receptors of *S. cerevisiae* as well as the G-protein coupled receptor (GPCR) family members are examined.

**G-protein-coupled receptors (GPCRs)**

All G protein-coupled receptors (GPCRs) share a common topological structure that consists of an N-terminal extracellular segment, seven transmembrane (TM) domains and a cytosolic C-terminal segment. The TM domains are connected alternately by intracellular and extracellular loops (David *et al.*, 1997; Hebert and Bouvier, 1998; Bockaert and Pin, 1999). However, the sizes of the N-terminal, extracellular domains and the C-terminal tail vary among GPCRs. Sequence analysis reveals no significant homology between GPCRs. GPCRs serve as a bridge connecting information from the extracellular space to the inside of the cells where cellular responses takes place. They also share a common mechanism to activate trimeric G-proteins. Upon ligand binding, activated GPCRs catalyze the exchange of GTP for GDP resulting in dissociation of

α-GTP and the βγ dimer. The process in turn activates the downstream targets including enzymes and ion channels (Hamm, 1998). GPCRs respond to a variety of extracellular stimuli including light, odorants, hormones, calcium and neurotransmitters. The extracellular and transmembrane regions of the receptors are involved in ligand binding, whereas the intracellular surface is important for G protein activation and function. For example, the third intracellular loop of the α-factor receptor functions in G-protein coupling (Bourne, 1997). The cytoplasmic C-terminal domain of both mammalian and yeast receptors plays a role in ligand-induced endocytosis and desensitization (Rohrer *et al.*, 1993; Schandel and Jenness, 1994). In addition, the cytoplasmic C-terminal domain of *S. cerevisiae* α-factor receptor contributes to the formation of preactivation complexes with its cognate G protein (Dosil *et al.*, 2000).

## Oligomerization of GPCRs

### Evidence for GPCR oligomerization

Examples of GPCRs that form oligomers include β2-adrenergic receptor (Hebert *et al.*, 1996), dopamine receptor (Ng *et al.*, 1996; George *et al.*, 2000), opioid receptor (Cvejic and Devi, 1997; Jordan and Devi, 1999), $Ca2^{+}$-sensing receptor (Bai *et al.*, 1998), GABA receptor (Jones *et al.*, 1998; White *et al.*, 1998), M3 muscarinic receptor (Zeng and Wess, 1999), vasopressin receptors (Zhu and Wess, 1998; Terrillon *et al.*, 2004), α-factor receptor (Overton and Blumer, 2000; Yesilaltay and Jenness, 2000), somatotatin receptor (Rocheville *et al.*, 2000), leukotriene B4 receptor BLT1 (Baneres

and Parello, 2003), alpha2c-adrenergic receptor (Prinster *et al.*, 2006) and neurotensin receptor (White *et al.*, 2007). Evidence for dimerization of GPCRs is based on the results of co-immunoprecipitation analysis, western blot analysis and the bioluminescence resonance energy transfer (BRET) and fluorescence resonance energy transfer (FRET) techniques. The BRET and FRET have been employed to identify interactions between GPCR subunits in *vivo*, early examples include β2-adrenergic receptors (Angers *et al.*, 2000) and α-factor receptors (Overton and Blumer, 2000).

It has become a common theme that GPCRs can form dimers or higher oligomer complexes. However, the effect of ligands on GPCR dimerization varies among the GPCRs. In some cases, GPCR oligomers detected under basal conditions are unchanged in amount after ligand treatment, suggesting that GPCRs exist as stable preformed complexes. For example, muscarinic M3 showed no effect on oligomerization upon agonist treatment (Shea and Linderman, 1997; Zeng and Wess, 1999). The α-factor treatment has no obvious effect on Ste2 oligomerization (Yesilaltay and Jenness, 2000). For other GPCRs, oligomers can be detected under basal conditions, but ligand treatment modulates the extent of oligomerization. For example, GPCR oligomers such as δ-opioid receptor that can be detected by using western blots and co-immunoprecipitation have been shown to undergo agonist-dependent decreases in the amount of higher molecular-weight species (Cvejic and Devi, 1997). In contrast, the β2-adrenergic receptor is also detected under basal condition but agonist increases the amount of the higher-molecular-weight species (Hebert *et al.*, 1996). In addition, the lutropin receptor has been reported to undergo increasing aggregation in response to its agonist (Tao *et al.*,

2004). However, at least some of the diversity among GPCRs reflects the difficulties associated with the various techniques used, although the diversity may reflect the differences among these receptors.

**Structural features of GPCR oligomers**

Current studies reveal that increasing numbers of GPCRs form dimers or oligomeric complexes. Due to the diversity of GPCRs it is not surprising that different interfaces among GPCRs are found to be involved in forming oligomeric complexes. Currently, there is no common set of mechanisms that explain all of the quaternary structures in GPCRs. Below, the different structural domains of GPCRs including the cytoplasmic domain, transmembrane domain (heptahelical domain) and N-terminal domain are discussed in relation to their involvement in oligomerization. The best example for GPCRs forming functional dimers/oligomers comes from rhodopsin with the suggestive evidence coming from atomic force microscopy (Liang *et al.*, 2003) and the possible interfaces for forming dimers or oligomers are discussed below. However, whether GPCR dimers or higher-order oligomers represent different functional states remains elusive. It should also be mentioned that terms dimerization and oligomerization are both used to indicate that GPCRs can form quarternary structures beyond the monomer and the dimerization term is used for the convenience of functional demonstrations in the homooligomeric and heterooligomeric complexes, although, in at least some cases GPCRs, can form higher oligomeric complexes as well. Structural

domains implicated to be involved in GPCR dimerization/oligomerization are shown on Table 1-1.

**Role of C-terminal domain in GPCR Oligomerization**

Previous studies indicated that interaction between the C-terminal tails of GABAb R1 (GB1) and GABAb R2 (GB2) were essential for proper ER export (Margeta-Mitrovic *et al.*, 2000). Therefore, it was assumed that the C-terminus provided an essential dimerization interface. However, subsequent experiments showed that the C-terminal interaction between the two subtypes was only crucial for cell-surface targeting, but was not required for heterodimerization (Pagano *et al.*, 2001). Whether the C-terminal portion of some GPCRs is crucial for dimerization remains unclear. Some truncated GPCRs can still form dimers. For example, a C-terminally truncated Ca-sensing receptor can form a dimer with full-length receptor (Bai *et al.*, 1998). Dimerization of H2 histamine receptor does not require its C-terminal tail (Fukushima *et al.*, 1995).

However, sequences in the C-terminal domain of GPCRs may play a role in regulating oligomerization of GPCRs. Metabotropic glutamate receptor 1b (mGluR1b) containing an RRKK motif near the C-terminus leads to ER retention, and a mutation that converts this RRKK sequence to AAAA results in cell surface expression, suggesting an important role of the RRKK motif in mGluR trafficking (Chan *et al.*, 2001). Interestingly, although mGluR1a also contains the RRKK motif, it can be expressed normally on the cell surface. The function of the ER retention signal in mGluR1a is

TABLE 1-1. Domains of GPCRs implicated in Oligomerization

| Receptor | Involved domains | References |
|---|---|---|
| β-adrenergic receptor | TM VI | (Hebert *et al.*, 1996; Salahpour *et al.*, 2004) |
| Complement C5a receptor | TM (I/II), TMIV | (Klco *et al.*, 2003; Hernanz-Falcon *et al.*, 2004) |
| Rhodopsin | TM IV/V | (Fotiadis *et al.*, 2003; Liang *et al.*, 2003; Fotiadis *et al.*, 2004; Fotiadis *et al.*, 2006) |
| Dopamine D2 receptor | TM IV | (Guo *et al.*, 2003; Guo *et al.*, 2008) |
| α1b-adrenoceptor | TMI, IV (TMII, V, VI) | (Carrillo *et al.*, 2004) |
| Adenosine A2A receptor | TM V | (Thevenin *et al.*, 2005a; Thevenin *et al.*, 2005b) |
| GABA receptor | N-terminal domain | (Rondard *et al.*, 2008) |
| Ca-sensing receptor | N-terminal domain | (Zhang *et al.*, 2001) |
| α-factor receptor | TM I, II, III | (Overton and Blumer, 2002; Overton *et al.*, 2003) This study |
| Metabotropic glutamate receptor 1b (mGluR1b) | C-terminal domain | (Remelli *et al.*, 2008) |

TM= transmembrane domain.

overridden by the activities of other domains in the C-terminus of the mGluR1a (Chan *et al.*, 2001). It has been shown that mGluR1b forms stable homodimers but does not form heterodimers with mGluR1a efficiently, based on co-immunoprecipitation experiments (Remelli *et al.*, 2008). The motif (RRKK) in the C-terminus of the mGluR1b is involved in regulating the receptor dimerization with the other mGluR1 isoforms. Defects in the RRKK motif near the C-terminus of mGluR1b result in heterodimerization of mGluR1a and mGluR1b. The result suggests that the RRKK motif in mGluR1b prevents mGluR1b from dimerizing with other forms of mGluR1 (Remelli *et al.*, 2008). In yeast cells, the C-terminal domain of Ste2 is dispensable for dimerization (Overton and Blumer, 2000; Yesilaltay and Jenness, 2000).

**Role of transmembrane domains in GPCR olimerization**

Increasing evidence indicates that transmembrane domains (TM) of GPCRs play a key role in the dimerization interface for both homodimers and heterodimers. An early study of β2 adrenergic receptor has shown that a peptide derived from transmembrane domain VI inhibits receptor dimerization (Hebert *et al.*, 1996). Studies of the dopamine D2 receptor using cysteine-scanning mutagenesis and chemical crosslinking indicated that transmembrane IV mediated dimerization of the receptors (Lee *et al.*, 2000; Guo *et al.*, 2003). The cysteine cross-linking approach was also used to study the quaternary structure of the complement C5a receptor. The disulfide trapping strategy is used to explore the oligomerization of C5a receptors. The rates of cross-linking between cysteines placed in different positions of the C5a receptors identified the potential

interfaces for C5a oligomers. These cross-linking results compared with the helical orientation and packing of rhodopsins allowed Klco et al (2003) to propose two putative symmetric dimer interfaces in TM4 as well as TM1/TM2. Later, two key residues, Ile52 (TM1) and Val150 (TM4), in the chemokine receptor CCR5 were determined to be crucial for the interaction surface between CCR5 receptors, and mutations affecting these residues resulted in non-functional receptors, defective in dimer formation or signaling (Hernanz-Falcon *et al.*, 2004).

The evidence which shows rhodopsin can form two-dimensional arrays of dimers is supported by the atomic force microscopy analysis (Fotiadis *et al.*, 2003; Liang *et al.*, 2003). In the current model, the transmembrane domains IV and V of rhodopsin are involved in the interaction contact between monomers of a dimer and transmembrane I is involved in the interaction between rows of dimers (Fotiadis *et al.*, 2004; Fotiadis *et al.*, 2006). Another independent approach on opsin was reported. Kota et al (2006) expressed opsin in COS1 cells and used fluorescence resonance energy transfer (FRET) experiments to confirm interactions between opsin dimers. The dimer formation of opsins was assessed by the rate of disulphide bond formation in the presence of cupric orthophenanthroline by using opsin mutants in which specific amino acids were substituted to cysteine. The results are consistent with roles for transmembrane domain IV and V in the dimer interface of opsin.

In the $\alpha$1b-adrenoceptor, multiple interactions between transmembrane helices have been implicated in oligomeric receptor complexes (Carrillo *et al.*, 2004). Based on the co-immunoprecipitation assays of $\alpha$1b-adrenoceptor fragments, a model similar to the

"row" of rhodopsin arrays observed by (Liang *et al.*, 2003) has been proposed, and it indicated that the transmembrane domain I and IV were involved in symmetric interaction between receptor fragments containing these sequences (Carrillo *et al.*, 2004). Transmembrane domains II, V and VI were possibly involved in the non-symmetetrc interactions (Carrillo *et al.*, 2004). For other receptors such as the adenosine A2A receptor, the fifth transmembrane domain is apparently involved in receptor oligomerization (Thevenin *et al.*, 2005a; Thevenin *et al.*, 2005b).

**Role of N-terminal domain in GPCR dimerization**

Limited evidence indicates that the N-terminal extracellular segment of GPCRs plays a role in oligomerization. However, the extracellular domains known as the Venus flytrap domain (VFT) on both GB1 and GB2 interact with each other, and VFT of GB2 controls agonist affinity in GB1 (Liu *et al.*, 2004). The direct interactions between these two subtypes were confirmed by using recombinant soluble extracellular regions in the heterodimeric metabotropic gamma-aminobutyric receptors (Nomura *et al.*, 2008). Rondard et al (2008) have identified a dimerization interface within the VFT dimer of GABA receptors by using a glycan wedge scanning approach. They also show that disruption of this dimer interface affects allosteric interaction between the subunits and the proper trafficking and assembly of the GB1 and GB2 heterodimer on plasma membrane (Rondard *et al.*, 2008).

Disulfide bonds between N-terminal cysteine residues also appear to play a role on some GPCRs. For example, a disulfide bond between Cys129 and Cys131 in

Ca-sensing receptor has been demonstrated in different studies (Ray *et al.*, 1999; Zhang *et al.*, 2001). However, it is implied that non-covalent hydrophobic interactions between Ca-sensing receptors also contribute to dimerization (Zhang *et al.*, 2001).

**Structural regions involved in Ste2 dimerization**

The α-factor receptor (Ste2) has been shown to form homo-oligomeric complexes that are the functional units of endocytosis (Overton and Blumer, 2000; Yesilaltay and Jenness, 2000). Previous data from our lab (Yesilaltay and Jenness, 2000) and from others (Overton and Blumer, 2000) indicate that homo-oligomeric complexes of Ste2p are subject to ligand-induced endocytosis since a receptor that lacks an α-factor binding site or lacks an endocytosis signal sequence can undergo ligand-induced endocytosis when wild-type receptors are also present in the cell. Interactions between α-factor receptors were evaluated by using FRET and co-immunoprecipitation experiments (Overton and Blumer, 2000; Yesilaltay and Jenness, 2000). Evidence indicates that the α-factor receptors form oligomeric complexes in the plasma membrane. When different tagged receptors are expressed in the same cell, both tagged receptors are precipitated with antibodies specific for either of the two tags. The experiments also indicate both C-terminal cytoplasmic domain and intermolecular disulfide bonds are not required for oligomeric formation (Yesilaltay and Jenness, 2000). The oligomeric complexes of Ste2p formed in the plasma membrane have also been identified by coexpressing receptors tagged with different fluorescent proteins and demonstrating fluorescence resonance energy transfer (FRET) (Overton and Blumer, 2000).

Protein-protein interactions between α-factor receptors directed at identifying the subunit interface(s) have been investigated by combining mutagenesis with FRET analysis (Sommers and Dumont, 1997; Overton and Blumer, 2002; Gehret *et al.*, 2006). FRET has also been detected in certain Ste2 mutants with complementary deletion segments (Overton and Blumer, 2002). In FRET experiments, Ste2 segments including the N-terminal extracellular domain and TM1 and TM2 can self-associate efficiently. In addition, TM1 of Ste2 has also been shown to self-associate although with reduced efficiency. The results suggest that TM1 plays an important role in the interface between α-factor receptors and that the N-terminal domain and TM2 facilitate protein-protein interaction (Overton and Blumer, 2002). Later, the Glycophorin A-like motif, $^{56}$GxxxG$^{60}$ in transmembrane domain I was proposed to provide the dimerization contact (Overton *et al.*, 2003). Mutations affecting the $^{56}$GxxxG$^{60}$ motif result in disruption of the oligomerization of Ste2. However, potential roles for structural domains other than TM1in oligomerization have not been investigated. In addition it remains unclear whether Ste2 only forms dimers or whether it can form high-order structures as well.

Although the reduced FRET for the Ste2 mutants affecting the $^{56}$GxxxG$^{60}$ suggest that these mutant receptors are defective for dimerization (Overton *et al.*, 2003), some caution should be exercised in this interpretation. Based on the subcellular location, it is apparent that the dimer-defective mutants are largely retained in the ER. It is possible that ER retained mutant receptors are subject to ER associated degradation, causing CFP and YFP to be clipped off of the Ste2-CFP and Ste2-YFP fusion proteins. The consequence would lead to misinterpretation of the reduced FRET signal. This issue is

addressed in my thesis. In addition, efficient FRET depends on proper orientation between energy donors and acceptors. Therefore reduced FRET may reflect misfolding of the $^{56}$GxxxG$^{60}$ mutants, and the distorted structure of Ste2 subunits may interfere with energy transfer between the Ste2-CFP and Ste2-YFP.

**Functional roles of GPCR dimerization/oligomerization**

It is well known that oligomerization is required for ER exit of some multi spnning membrane proteins and the examples include immune receptors (Reddy and Corley, 1998), glutamate NMDA receptors (Perez-Otano *et al.*, 2001) and GPCRs (Angers *et al.*, 2001; Milligan *et al.*, 2007). Oligomerization of viral glycoprotein subunits has also been shown to be important for ER exit. The vesicular stomatitis virus glycoprotein (VSVG) forms noncovalently linked trimers in the ER before they are delivered to the cell surface (Zagouras *et al.*, 1991). However, coexpression of wild-type VSVG with a mutant subunit containing a C-terminal ER retention signals leads to VSVG heterotrimers that form at a rate similar to wild-type VSVG homotrimers but are retained in the ER (Zagouras *et al.*, 1991). Other examples include the Emp46-Emp47 and Erv41-Erv46 complexes where protein oligomerization has been shown to be important for ER export (Watanabe and Riezman, 2004). Emp47 is required for the transport of the integral membrane protein Emp46 (Sato and Nakano, 2004). For the Erv41-Erv46 complex, multiple export signals are found to be required *in trans* for COPII dependent transport from the ER (Otte and Barlowe, 2002). In this thesis, the

roles that GPCR oligomerization plays in cell-surface delivery and signal transduction are investigated.

**Cell–surface targeting of GPCRs**

The dimerization phenomenon may be a general feature for GPCR. Several lines of evidence indicate that GPCRs form dimers prior to reaching the cell surface. Therefore, dimerization of GPCRs may play a positive role in quality control checkpoints as GPCRs progress through the biosynthetic processes, ensuring that incompletely or improperly folded proteins are retained and targeted for degradation.

The hypothesis that oligomerization of GPCRs is involved in correct trafficking was clearly demonstrated by the extensive studies of the metabotropic GABAb receptors. It is necessary to express two distinct receptor subtypes, GABAb R1 and GABAb R2, in order to obtain receptor function (Jones *et al.*, 1998; White *et al.*, 1998). When expressed alone, the GABAb R1 is retained in the ER as an immature protein. An ER retention signal RXR is present in the C-terminal domain of the GABAb R1 receptor, preventing it from reaching the cell surface. Deletion of ER retention signal in the C-terminal domain of the GABAb R1 receptor leads to plasma membrane targeting (Margeta-Mitrovic *et al.*, 2000). It was reported that GABAb R2 masks the ER retention signal of GABAb R1 through a C-terminal coiled-coil domain, thereby allowing membrane expression of GABAb R1. Calver et al (2001) demonstrated that the C-terminal regions of GABA b receptors mediate receptor trafficking but are not required for proper signaling in receptors.

Several lines of evidence indicate certain mutant GPCRs have dominant negative effects on wild-type receptors that prevent or limit their cell surface delivery when they form a heterodimeric complexes. In D2 dopamine receptors, cell surface expression of wild-type receptors is prevented by coexpressing mutant truncated receptors (Lee *et al.*, 2000).

For a co-receptor of human immunodefiency virus HIV-1, CCR5, it has been shown that a truncated form of CCR5 (CCR5delta32) forms heterodimers with wild-type CCR5 that result in ER retention (Benkirane *et al.*, 1997). The inhibition of wild-type CCR5 by the mutant delays the onset of AIDS by 2-4 years. In the frizzled (Fz) family of Wnt receptors, mutant Frizzled 4 (linked to familial exudative vitreoretinopathy, FEVR) causes wild-type Fz4 to be retained in the ER, thereby blocking its signaling (Kaykas *et al.*, 2004). The cell-surface targeting of $\alpha$2-adrenergic receptors is blocked due to heterodimerization with a transport deficient mutant (Zhou *et al.*, 2006). The dominant-negative effect of mutant melanocortin 1receptor on the wild-type receptor (MC1R), a key regulator of differentiation and proliferation of epidermal melanocytes, is also thought to be the result of heterodimerization (Sanchez-Laorden *et al.*, 2006).

Vasopressin receptors can form dimers in the ER. It has been shown that most common mutant forms of the V2 vasopressin receptor have a dominant negative effect on the wild-type receptor. The mutant protein is thought to dimerize with wild-type receptor, therefore retaining it in the ER and preventing the wild-type receptor from reaching the cell surface (Zhu and Wess, 1998; Morello *et al.*, 2001). However, most of these mutant receptors have been demonstrated to be functional once they reach the cell

surface (Morello *et al.*, 2001). The ER retention of vasopressin receptor mutant is thought to be due to the RXR retention motif in the i3 loop of the receptor (Hermosilla and Schulein, 2001; Hermosilla *et al.*, 2004). Under normal conditions, the cell-surface expression of wild-type V2 vasopressin receptor suggests that the ER retention motif in the i3 loop is masked.

Dimerization of adrenergic receptors plays a role in cell-surface targeting. The proper cell surface targeting of $\alpha_{1D}$-adrenergic receptors is controlled by heterodimerization with $\alpha_{1B}$-adrenergic receptors (Hague *et al.*, 2004b). Distantly related receptors such as β2-adrenergic receptor and olfactory receptors can form heterodimers, and the heterodimerization promotes plasma membrane targeting (Hague *et al.*, 2004a). Homodimerization of the β2-adrenergic receptor is a prerequisite for cell surface targeting (Salahpour *et al.*, 2004). Homodimerization of β2-adrenergic receptors occurs in the ER, and β2-adrenergic receptors lacking the ER-export motif sequence dimerize with wild-type receptors but prevent the trafficking of the complexes to the plasma membrane. The glycophorin-like dimerization motif GxxxGxxxL in the sixth transmembrane region of β2-adrenoceptor suggested a role in proper trafficking to the plasma membrane (Salahpour *et al.*, 2004). Disruption of this motif prevents dimerization and cell surface targeting. Interestingly, this GxxxG-like motif is also present in other receptors such as metabotropic receptors, secretin-like receptors and cannabinoid receptors indicating that this motif may play a common role in receptor oligomerization, even though the motif is located in different transmembrane segments in the different receptors (Overton *et al.*, 2003).

The Ca-sensing receptor (CASR) forms dimers constitutively in the ER, and the Ca-sensing receptor mutants that have different amino acid substitution at residue 583 fail to dimerize is retained in the endoplasmic reticulum (Pidasheva *et al.*, 2006). However, confocal immuno-fluorescence microscopy and perinuclear staining methods have revealed that the wild-type Ca-sensing receptor and the two mutant receptors, R66H and R66C, form dimers in ER. Taken together, the results indicate that CASR dimerization may be required for ER exit; however, dimerization may not be sufficient for trafficking to the cell surface (Pidasheva *et al.*, 2006).

Dimerization is important for cell surface targeting of α-factor receptors. The glycophorin-like motif in transmembrane domain I of the α-factor receptor is important for its dimerization and cell-surface targeting on the truncated receptors. Based on the FRET assay, disruption of the putative dimer interface in the mutant receptor results in ER accumulation of mutant receptors (Overton and Blumer, 2002; Overton *et al.*, 2003). In this thesis, structures involved in Ste2 oligomerization have been investigated.

**Functional roles of GPCR dimerization in signal transduction**

Receptor heterodimers sometimes exhibit unique functional properties. Early observations found that two fully functional opioid receptors, δ and κ, display different binding and functional properties when they are expressed together and when they are expressed alone (Jordan and Devi, 1999). For the chemokine receptor, CCR2b, the loss of function mutant, CCR2b (Y139F), blocks signaling through the wild-type CCR2b by forming dominant-negative hetero-dimers (Rodriguez-Frade *et al.*, 1999). A peptide

derived from the transmembrane domain VI of β2 adrenergic receptors inhibits dimerization as well as adenyl cyclase activation (Hebert *et al.*, 1996). Heterodimerization between some sensory receptors such as T1R2 and T1R3 or T1R1 and T1R3 also indicated that heterodimerization is required to generate functional taste receptors in order to recognize sweet-taste molecules (Nelson *et al.*, 2001; Nelson *et al.*, 2002).

Heterodimerization for some GPCRs modulates receptor function. The GABAb receptors provide an excellent example that the dimeric structure is required for its functional activities. The cell surface targeting in the heterodimers is described in the preceding section. Other roles such as binding activity and receptor-G protein coupling have also been investigated extensively. Neither GABAb R1 or GABAb R2 can activate GIRK-type potassium channels when expressed alone, but in combination both receptors result in activation (Jones *et al.*, 1998). The N-terminal segment of GABAb R1 is responsible for the ligand (GABA) binding, and GABAb R2 itself is critical for G-protein coupling (Galvez *et al.*, 2001). Therefore, GABAb heterodimers exhibit trans-activation where GABAb R1 binds the ligand and GABAb R2 couples to the G-protein.

Other examples of GPCR interactions in heterodimers have also been reported. Heterodimers between angiotensin AT1 and bradykinin receptors show enhanced G-protein activation (AbdAlla *et al.*, 2000). Similar results have been reported for the heterodimers containing the D2 dopamine and SST-5 somatostatin receptors (Rocheville *et al.*, 2000) as well as heterodimers containing the μ and δ opioid receptors (Gomes *et al.*, 2004). Co-expression of μ and δ opioid receptors alternates the G protein selectivity

compared to expression of either receptor alone. In contrast to the individually expressed μ and δ opioid receptors, co-expression of both receptors showed insensitivity to pertussis toxin and continued signal transduction, likely due to interaction with a different subtype of G protein (George *et al.*, 2000). High-affinity agonist binding and G protein coupling of the melatonin receptor 1 (MT1) are inhibited by the orphan receptor GPR50 through heterodimerization (Levoye *et al.*, 2006). Mas-related receptor E (MrgE) has been shown to alter the signaling and internalization activities of MrgD when HEK293 cells coexpress MrgD and MrgE (Milasta *et al.*, 2006).

**Interaction between G-proteins and GPCRs**

GPCR oligomers apparently represent the basic functional unit for GPCRs although recently it has been shown that at least in some monomeric GPCRs can efficiently activate G proteins (Ernst *et al.*, 2007; White *et al.*, 2007; Whorton *et al.*, 2007; Whorton *et al.*, 2008). It should also be mentioned that most functional assays are performed with transfected cell lines. Therefore, the exact cellular processes associated with GPCR dimerization and how they become activated in an organism requires further investigation.

The stoichiometry of the signaling complexes that contain GPCRs and heterotrimeric G proteins remains largely unknown. In principle, both subunits of the GPCR homodimer should be able to interact with the G-protein. Whether GPCR dimers signal through two heterotrimeric G-proteins or interact with only one G-protein is unclear. In the leukotriene B4 receptor (BLT1 receptor) only one G-protein appears to

bind to the receptor dimer in the solution-phase neutron-scattering experiments, (Baneres *et al.*, 2003; Baneres and Parello, 2003). In contrast, the monomeric form of the purified BLT1 receptor can activate a G-protein (Baneres and Parello, 2003). A model has been proposed that subunits of Ste2 contact different regions of G-protein heterotrimer (Chinault *et al.*, 2004). Intracellular loop 1 (ic1), ic3, the C-terminal tail and the intracellular ends of TM2 and TM3 of Ste2 have been implicated in coupling to the G-protein (Dosil *et al.*, 2000; Chinault *et al.*, 2004). Chinault et al (2004) performed complementation experiments combining different mutations of Ste2 and only coexpression of both the ic1 and ic3 mutant receptors *in trans* resulted in increased signaling activity.

Recent results have shown an asymmetric structure of GPCR dimers. Only one glutamate receptor in the receptor dimer appears to be turned on (Goudet *et al.*, 2005; Hlavackova *et al.*, 2005). A similar result has also been reported for the leukotriene $B_4$ receptor dimer, and Damian et al (2006) have shown an asymmetric conformational change in a GPCR dimer that is controlled by G-proteins. The asymmetrically active conformation of BLT1 dimer can be uncoupled from the G-protein by adding GTPγS, and uncoupling of G-protein leads to a symmetric receptor dimer with two activated protomers (Damian *et al.*, 2006). Since such asymmetric conformational changes are not observed in the absence of the G-protein, it is clear that specific contracts between the BLT1 dimer and the G-protein occur. Interestingly, a recent study has shown no trans-activation of the G-protein in a BLT1 heterodimer (Damian *et al.*, 2008). Transactivation in Ste2 heterodimers apparently does not occur since no signaling

activity increase has been detected in yeast cells that coexpress a G-protein coupling defective Ste2 and a ligand-binding defective Ste2 (Chinault *et al.*, 2004).

**Regulation of GPCR Trafficking**

Endocytic and exocytic transport of GPCRs are regulated and affected by several structural features of the receptor including post-translational modification, retention signal motifs, export signal motifs, chaperone or GPCR-interacting proteins and proper GPCR folding. GPCRs can undergo a variety of post-translational modifications such as N-linked glycosylation, palmitoylation, phosphorylation and ubiquitylation. How these factors regulate the GPCR cell-surface targeting, signaling, ER export and protein quality control are discussed below.

**Glycosylation of GPCRs**

The N-linked Glycosylation at the consensus sequence NXS/T is a common post-translational modification on GPCRs. A requirement for glycosylation for GPCRs to target the cell surface expression differs among GPCRs. For example, a mutation affecting the glycosylation sites in AT1R and follicle-stimulating hormone receptor (FSHR) abolished its plasma membrane targeting and caused receptors to accumulate in the peri-nuclear region (Davis *et al.*, 1995; Deslauriers *et al.*, 1999; Jayadev *et al.*, 1999). In β-adrenergic receptors, glycosylation facilitates receptor transport to the plasma membrane (Rands *et al.*, 1990). In contrast, glycosylation of the histamine H2 receptor, m2 muscarinic acetylcholine receptor and $\alpha_1$-adrenergic receptor does not play a

significant role in cell surface expression (Sawutz *et al.*, 1987; van Koppen and Nathanson, 1990; Fukushima *et al.*, 1995). Glyscoylation is dispensible on Ste2 (Mentesana et al., 2001).

**Functional roles of palmitoylation in GPCRs**

Palmitoylation is a reversible process involving attachment of the16-carbon saturated fatty acid, palmitic acid, via a thiolester linkage to cysteine residues in the cytoplasmic C-terminal domain of certain GPCRs (Marchese *et al.*, 2008; Chini and Parenti, 2009). Several properties of GPCR are affected by the absence of palmitoylation including receptor maturation, trafficking, signaling and internalization (Marchese *et al.*, 2008; Chini and Parenti, 2009). Several GPCRs such as dopamine D1 receptor (Ng *et al.*, 1994), Vasopressin V2 receptor (Sadeghi *et al.*, 1997), TSH receptor (Tanaka *et al.*, 1998) and CCR5 (Percherancier *et al.*, 2001; Petaja-Repo *et al.*, 2006) exhibit reduced cell surface expression when they are not palmitoylated. Palmitoylation also regulates signaling and internalization of CCR5 (Kraft *et al.*, 2001) and controls the human A1 adenosine receptor (Gao *et al.*, 1999). However, current data indicates that not all of GPCRs undergo palmitoylation. Receptors such as the gonadotropin releasing hormone (GnRH) receptor (Navratil *et al.*, 2006) and $\alpha$-isoform of the thrombroxane A2 receptor (Reid and Kinsella, 2007) do not undergo palmitoylation. Ste2 lacking the cysteine residues in the C-terminus is not palmitoylated.

**Phosphorylation and ubiquitination in GPCR trafficking**

Phosphorylation is a posttranslational modification that regulates many proteins including GPCRs, and it is well known that phosphorylation of GPCRs modulates GPCR signaling activity at the cell surface and promotes receptor endocytosis (Hanyaloglu and von Zastrow, 2008). Ubiquitination has been shown to play a role in directing GPCR endocytosis and trafficking to the lysosome.

In the presence of agonist, many GPCRs are rapidly phosphorylated by the G protein-coupled receptor kinases (GRKs) predominantly on serine and threonine residues in the C-terminal domain and the third intracellular loop. The activated GPCRs then bind arrestins and undergo internalization. In the $\beta_2$-adrenergic receptor ($B_2AR$), agonist binding induces phosphorylation and ubiquitination of the receptor. Arrestin is also ubiquitinated and recruited to the receptor during internalization. The internalized $\beta_2$ARs are dephosphorylated and recycled back to the cell surface in a pathway mediated by EBP50/ NHERF, NSF and HRS (Shenoy *et al.*, 2001; Marchese *et al.*, 2008). Unlike $\beta_2$AR which forms transient complexes with arrestin, other GPCRs such as angiotensin II type 1A receptor ($AT_{1A}R$) form stable complexes with arrestin (Shenoy and Lefkowitz, 2003a, b).

Ubiquitination is a posttranslational modification of cellular proteins. Ubiquitin is a 76 amino acid polypeptide. The C-terminus of ubiquitin is linked to the target proteins by forming an isopeptide bond to the ε-amino group of a lysine residue on the substrate proteins. It is known that ubiquitination of proteins has functional significance in multiple pathways including proteasomal degradation, signal transduction, transcriptional

regulation and protein trafficking in endocytic and biosynthetic pathways (Marchese *et al.*, 2008). An increasing amount of evidence has shown that ubiquitin serves as an internalization signal for GPCRs that is different from the role of ubiquitin in the proteasome degradation pathway. In yeast GPCRs such as Ste2 and Ste3 receptors, internalization is mediated by ubiquitination (Hicke and Riezman, 1996; Roth and Davis, 1996). In mammalian cell GPCRs such as $\beta_2$AR (Shenoy *et al.*, 2001), CXCR4 (Marchese *et al.*, 2003), $V_2$R (Martin *et al.*, 2003), PAR2 M (Jacob *et al.*, 2005) and sst3 somatostatin receptor (Tulipano *et al.*, 2004), the receptors show an agonist-dependent ubiquitin modification suggestting that ubiquitination plays a role GPCR transport. Interestingly, mutant protease-activated receptor 1 (PAR1) receptors that are defective in ubiquitination lead to increased constitutive internalization suggesting that ubiquitination serves as a negative regulator for PAR1 (Wolfe *et al.*, 2007). In yeast, monoubiquitination functions as an endocytic signal (Terrell *et al.*, 1998).

Ubiquitination of GPCRs has been demonstrated to be important in the biosynthesis and endoplasmic reticulum (ER)-associated protein degradation (ERAD) pathways. For GPCRs such as the opioid receptor (Petaja-Repo *et al.*, 2001), rhodopsin (Illing *et al.*, 2002; Saliba *et al.*, 2002) and thyrotropin-releasing hormone receptor (TRHR) (Cook *et al.*, 2003), polyubiquitination has been demonstrated to play a role in proteasome-medicated degradation.

**Motifs involved in protein export from the ER**

Protein transport from the ER occurs in COPII-coated vesicles. Therefore cargo proteins may need to bind to specific components of COPII coated vesicles for efficient export. However, the sorting signals that are involved in directing proteins into COPII vesicles are not well defined. Protein can exit if they contain an ER exit motif or if they bind to another protein that can exit the ER. Yeast Erv29p is a membrane protein with four transmembrane domains with both termini are exposed to the cytosol. Erv29p cycles between the ER and the Golgi apparatus (Foley *et al.*, 2007). Erv29p acts as a receptor, loading proteins such as the glycosylated α-factor pheromone precursor and carboxypeptidase Y into COPII vesicles (Belden and Barlowe, 2001; Foley *et al.*, 2007).

Two classes of ER export signals in non-GPCR membrane proteins have been characterized. One class consists of a C-terminal domain with a dihydrophobic motif (such as phenylalanine—FF) that provides efficient ER transport in the p24 family of protein (Nakamura *et al.*, 1998) and in ERGIC53 (Kappeler *et al.*, 1997). Mutations affecing the FF motif on these proteins result in ER retention. For the Erv41p-Erv46p complex, multiple export signals have been identified and function *in trans* for COPII-dependent transport from the ER (Otte and Barlowe, 2002). Mutations affecting the C-terminal tail of Erv41 and Erv46 lead to ER accumulation and these C-terminal tail mutants are not packaged into COPII vesicles (Otte and Barlowe, 2002). The IL motif on the C-terminal tail of Erv41p is a COPII-binding motif, and it may be sufficient for the binding of the GTPase Sar1 but is not sufficient for packaging into vesicles (Otte and Barlowe, 2002). In addition, the FY sequence in the C-terminal tail of Erv46p is required

for formation of theSec23/Sec24p pre-budding complex and for packaging of Erv46p into COPII vesicles (Otte and Barlowe, 2002). It has been suggested that signals in both the Erv41p and Erv46p tail sequences are required for specific orientation during the formation of the Erv41p-Erv46p complex since the Erv41p-Erv46p tail-swap chimeras are not exported from the ER (Otte and Barlowe, 2002).

The other class of ER export signal, the DXE motif, has been found in the C-terminal region of the vesicular stomatitis viral glycoprotein (VSVG), the potassium channel Kir2.1 and the cystic fibrosis transmembrane conductance regulator (CFTR) (Nishimura and Balch, 1997; Stockklausner *et al.*, 2001; Wang *et al.*, 2004). Mutations in the DXE motif (e.g. AXA) in VSVG allow VSVG to assemble correctly; however, the rate at which VSVG exits the ER is significantly reduced (Nishimura and Balch, 1997; Nishimura *et al.*, 1999), indicating that the DXE motif plays a role in enhancing the exit of cargo proteins from the ER. Other studies have indicated that the DXE motif only partially accounts for efficient ER exit of VSVG, and Sevier et al (2000) demonstrate that efficient export of VSVG from ER requires signals in the cytoplasmic tail that include both tyrosine-based and DXE motifs (Sevier *et al.*, 2000).

Interestingly, the DXE motif has also been found in the yeast membrane proteins such as the amino acid permease (Gap1p) and Sys1p (Votsmeier and Gallwitz, 2001; Malkus *et al.*, 2002), and this motif is involved in the interaction with Sar1 and the Sec23/24 complex. This di-acidic motif has been shown to facilitate efficient ER export for both Gap1p and Sys1p. A mutation that results in loss of DXE in the C-terminal

cytosolic domain of Gap1p leads to elimination of the concentrative sorting of this protein (Malkus *et al.*, 2002).

Based on mutagenesis studies of the GPCRs, the C-terminal tail of GPCRs is required for ER export of some receptors such as the dopamine D1 receptor (Bermak *et al.*, 2001), vasopressin V2 ($V_2R$) (Oksche *et al.*, 1998), adenosine A1 receptor (Pankevych *et al.*, 2003), angiotensin II type 1 (A1AR) (Gaborik *et al.*, 1998), $\alpha_{2B}$-adrenergic ($\alpha_{2B}$-AR) (Duvernay *et al.*, 2004) and melanin-concentrating hormone receptor I (Tetsuka *et al.*, 2004). A triple phenylalanine motif (FxxxFxxxF) in the C-terminal domain of dopamine D1 (Bermak *et al.*, 2001) is important for proper cell surface targeting. Mutations affecting the motif cause the receptors to be retained in the ER. Several motifs have been identified to be essential for ER export of GPCRs. The ExxxLL motif in the C-terminal domain of vasopressin V2 receptor has been found to be essential for transport to the cell surface (Schulein *et al.*, 1998). The similar motif FNxxLLxxxL has been found to mediate ER export of the human vasopressin V1b/V3 (Robert *et al.*, 2005). The $F(X)_6LL$ motif in the C-terminal tail of AT1R and $\alpha_{2B}$-AR is required for ER export, and disruption of this motif results in ER retention of these receptors (Duvernay *et al.*, 2004). The conserved NPXXY motif is also shown to play a role in endocytic trafficking of GPCRs such as N-formyl peptide receptor (Gripentrog *et al.*, 2000), V2 vasopressin (Bouley *et al.*, 2003) and B2 bradykinin receptor (Kalatskaya *et al.*, 2004). However, sequence analysis of Ste2 suggests that the motifs identified in GPCRs are not present in Ste2.

Although the motifs described above are required for the export of their respective GPCRs, the molecular mechanism by which they function is not understood. Unlike the DXE and FF motifs that directly associate with COPII vesicleproteins, no evidence has been reported indicating that the motifs in GPCRs can directly interact with the components of COPII vesicles. Whether these motifs mediate correct receptor conformation in the ER or dimerization remains to be determined. Interestingly, a few studies have suggested that exit of GPCRs from the Golgi apparatus to cell surface is also regulated (Gimelbrant *et al.*, 2001; Zhu *et al.*, 2006), but the specific sequences controlling this process have not been clearly elucidated. However, a motif containing a tyrosine and a serine (YS) has been shown to be crucial for $\alpha_2$-AR to be exported from the Golgi in that substitution of the YS motif leads to Golgi retention of the receptor (Dong and Wu, 2006).

In this study, two DXE motifs in the C-terminal domain of Ste2 have been identified as an ER export signal. Disruption of both DXE motifs results in ER retention in certain full-length Ste2 mutants. These results are presented in the chapters IV and V.

**ER retention motifs in GPCRs**

Certain GPCRs contain ER retention signals. The motif RSRR is present in the C-terminal domain of GABAb R1 (Margeta-Mitrovic *et al.*, 2000). The RxR motif was first identified in the plasma membrane K (ATP) channels as an ER retention signal (Zerangue *et al.*, 1999). GABAb R1 is retained in the ER when expressed alone due to the exposure of the ER retention motif. As discussed above, it is believed that

coexpression of GABAb R1 and GABAb R2 masks the motif by formation of a coil-coil domain between their C-terminal tails. In the metabotropic glutamate receptor (mGluR), Chan et al. (2001) found that the sequence RRKK within the C-termini of mGluR 1a and 1b functions as an ER retention signal. Removal of the sequence in increases the cell-surface expression of mGluR1b. However, the ER retention effect of this signal in mGluR 1a is overcome by a mGluR1a specific sequence in the C-terminus which results in normal plasma membrane expression (Chan *et al.*, 2001).

**GPCR folding and ER quality control**

The ability of proteins to perform their function relies on folding into a correct conformation. Thus, mutations that prevent proteins from achieving their native conformation lead to loss of protein function and eventual degradation. In eukaryotic cells, membrane and secretory proteins enter the secretory pathway at the endoplasmic reticulum (ER). Quality control mechanisms in the ER recognize the non-native or misfolded proteins and retain them as defective proteins in the ER and thereby prevent these misfolded proteins from escaping this organelle. The quality control system allows only correctly folded proteins to pass the checkpoints and be transported to their final destination ensuring proper function in the cell (Ellgaard and Helenius, 2003). Molecular chaperones in the ER function as sensors to recognize improperly folded proteins. Proteins failing to pass the final ER checkpoints are retained in the ER and undergo a process called ER-associated degradation (ERAD) which involves retro-translocation of

the misfolded proteins from the ER into the cytosol, polyubiquitination and degradation by the proteasome (Brodsky and McCracken, 1999; Tsai and Rapoport, 2002).

**Chaperones in GPCR export and maturation**

Protein chaperones play a role in GPCR ER trafficking and maturation. Receptor activity-modifying proteins (RAMPs) form hetero-complexes with the calcitonin receptor-like receptor (CRLR). These RAMPs assist in CRLR export and alter the response of the receptor to the ligand (McLatchie *et al.*, 1998). Other proteins such as NinaA and the HSJ1b have been shown to mediate proper trafficking of rhodopsin to the plasma membrane (Baker *et al.*, 1994; Chapple and Cheetham, 2003). The ER-associated protein, dopamine receptor interacting protein 78 (DRi78), has been found to play a crucial role in regulating the proper cell-surface expression of mammalian dopamine D1 receptor (Bermak *et al.*, 2001). In *Caenorhabditis elegans*, ODR-4 is found to regulate the ER exit and proper targeting of the olfactory receptor to the sensory organs (Dwyer *et al.*, 1998; Gimelbrant *et al.*, 2001). The chaperone protein 14-3-3 is involved in probing the assembly status of multimeric membrane proteins (Yuan *et al.*, 2003). GPCRs such as $\alpha_2$-adrenergic receptor subtypes, GABA receptors and parathyroid hormone receptors have been shown to interact with 14-3-3 (Prezeau *et al.*, 1999; Couve *et al.*, 2001; Tazawa *et al.*, 2003). However, the functional significance of protein-protein interactions between GPCRs and the 14-3-3 protein remains unclear.

Recently, proteins interacting with GPCRs and modulating their trafficking have been reviewed (Dong *et al.*, 2007). These proteins show interaction either with the

C-terminal tails of GPCRs or with the third intracellular loops of GPCRs. In addition, binding domains for some GPCR-interacting proteins remain to be revealed. How the GPCR-interacting proteins positively or negatively affect GPCR expression on cell surface varies among the different GPCRs. Although chaperone proteins are known to be involved in ER export and maturation of some GPCRs, currently it is unclear whether GPCR dimerization is required or regulated by interactions with these chaperone proteins.

**Endocytosis of GPCRs**

There are two major families of proteins, the GPCR kinases (GRKs) and the β-arrestins, involved in removal of some GPCRs from the cell surface. Endocytosis of these GPCRs is mediated by phosphorylation at the serine or threonine residues and internalization of GPCRs is associated with the binding of arrestins. The serine/threonine-specific GPCR kinases (GRKs) are recruited to the cytoplasmic surface of the agonist-activated receptors and mediate receptor phosphorylation (Krupnick and Benovic, 1998). β-arrestins are involved in both desensitization and down regulation of the receptors. The β-arrestins also physically couple the GPCRs to the endocytosis machinery. In addition, the β-arrestins have been shown to interact directly with the adaptor protein complex (AP-2), a crucial component of the clathrin-mediated endocytosis machinery (Laporte *et al.*, 1999).

Besides GRK and β-arrestins, other components have been shown to play a role in the endocytosis process. At the plasma membrane, it is thought that clathrin-coated pits

(CCPs) enriched in PIP2 (phosphatidylinositol (4, 5)-biphosphate) serve as the major pathway for GPCR internalization and several proteins are involved in this process (Marchese *et al.*, 2008). A large GTPase, dynamin has been proposed to pinch off the endocytic vesicle from the cell surface (McNiven, 1998). The small GTP-binding protein ADP-ribosylation factor (ARF6) plays a role in vesicular trafficking events. The ARF6 mutant incapable of binding or hydrolyzing GTP inhibits the agonist-induced internalization of the β-adrenergic receptor (Claing *et al.*, 2001).

In addition, linear peptide sequences in C-terminal domain of GPCRs, including tyrosine-based and dileucine-based motifs and PDZ ligands, are recognized by different endocytic adaptor proteins and play roles in mediating endosomal sorting and internalization of GPCRs (Marchese *et al.*, 2008). Previously, functional roles for PDZ domains in proteins have been associated with localization and assembly of signaling complexes. Based on bioinformatics searches, the data indicate most GPCRs have these types of sorting signals in their C-terminal domains (Marchese *et al.*, 2008).

**Ubiquitination of plasma membrane proteins in yeast and animal cells**

Three enzymes are required for conjugating the ubiquitin to the protein substrates in this three-step cascade mechanism. The ubiquitin activating enzyme (E1) activates ubiquitin in an ATP dependent reaction, the ubiquitin conjugating enzyme (E2) catalyzes ubiquitin transfer to the cytseine of E2 and the ubiquitin protein ligase (E3) catalyzes ubiquitin transfer from E2 to the target substrate (Hochstrasser, 1996; Dupre *et al.*, 2004). The function of ubiquitin was originally identified as a signal that leads to degradation of

the target proteins by 26S proteasome (Hochstrasser, 1996). Lysine residues are modified with a single ubiquitin or with multiple polyubiquitin chains and each uniquitin monomer is linked through isopeptide bonds at the residue Lys29, Lys48 or Lys63 of ubiquitin (Arnason and Ellison, 1994; Terrell *et al.*, 1998; Hicke, 2001). The position of the linkage determines the fate of the targeted proteins. For example, proteins that have Lys48 linked poly-ubiquitin are degraded by the proteasome degradation. The efficient recognition of proteins by the proteasome requires at least four ubiquitins linked via Lys48 (Hicke, 2001; Glickman and Ciechanover, 2002). Polyubiquitin linked through either Lys48 or Lys29 signals proteasomal degradation of misfolded and short-lived protein (Hicke, 2001; Glickman and Ciechanover, 2002). Terrell et al (1998) first showed that monoubiquitination on multiple lysine residues in Ste2 is sufficient for endocytosis of the α-factor receptor.

Monoubiquitination plays a role in endocytosis of plasma membrane proteins of yeast cells including the pheromone receptors, Ste2 and Ste3 (Hicke and Riezman, 1996; Roth and Davis, 1996); the multidrug transporter, Pdr5 (Egner and Kuchler, 1996); the ABC-transporter, Ste6 (Kolling and Hollenberg, 1994); the zinc transport protein, Ztr1p (Gitan and Eide, 2000); the general amino acid permease, Gap1 (Springael and Andre, 1998); the Uracil permease, Fur4 (Galan *et al.*, 1996), the maltose permease, Mal61 (Medintz *et al.*, 2000); and galactose transporter, Gal2 (Horak and Wolf, 2001).

**Differences between yeast cells and mammalian cells in endocytosis**

It should be pointed out that there are differences between endocytosis in mammalian cells and yeast cells. In yeast cells, the plasma membrane proteins lack the classical tyrosine-based or di-leucine-based internalization signals that are recognized by AP2 in mammalian cells. Since yeast cells lack the involvement of Ap2-like adaptors in endocytosis, it is thought that for most yeast plasma membrane proteins, post-translational modification by ubiquitin serves as an endocytic signal (Hicke and Dunn, 2003; Horak, 2003). Ent1, Ent2 and Ede1 recognize the ubiquitinated Ste2 receptor through the ubiquitin-binding domains (UBDs) and regulate receptor internalization (Shih *et al.*, 2003). Instead of being degraded by the proteasome, ubiquitinated yeast plasma membrane proteins are degraded in the vacuole/lysosome following endocytosis. In mammalian cells, ubiquitin also plays a crucial role in the endocytosis of the growth hormone receptor (Strous *et al.*, 1996; Govers *et al.*, 1997).

Although clathrin heavy and light chains are important for endocytic internalization in mammalian cells, they are not required for endocytosis in yeast. The mutant strains carrying deletion of either the *CHC1* or *CLC1* genes (encoding clathrin heavy and light chains, respectively) are capable of undergoing internalization, albeit at a slower kinetic rate (Payne *et al.*, 1988; Chu *et al.*, 1996). Kaksonen et al (2005) showed that clathrin facilitates the initiation of endocytic-site assembly and the assembly of the actin-mediated internalization machinery. The early endocytosis proteins such as Las17p and Sla1p still localize to the cortical patch but the number of patches is remarkably reduced either in the *clc1* mutant or *chc1* mutant (Kaksonen *et al.*, 2005). Therefore in

yeast, clathrin is not required for membrane invagination or vesicle formation since endocysosis can occur in the absence of clathrin (Kaksonen *et al.*, 2005).

In yeast cells, however, recent discovees have identified a family of proteins, arrestin-related trafficking adaptors (ARTs) that function by targeting certain plasma membrane proteins such as amino acid transporters to the endocytic system. Nine ART family members have been revealed based on the sequence analysis (Lin *et al.*, 2008). So far, only two ARTs have been characterized. Art1p is required for endocytosis of argnine transporter Can1p and methionine transporter Mup1 (Lin *et al.*, 2008). Either Art1p or Art2p is required for the down-regulation of the lysine transporter, Lyp1p (Lin *et al.*, 2008). The ubiquitin ligase, Rsp5p, is recruited to modify cargo proteins and ARTs through the PY motifs of the ARTs, and the ubiquitinated cargo proteins are internalized and degraded in the vacuole (Lin *et al.*, 2008).

**Endocytosis mutants in yeast**

The budding yeast *S. cerevisiae* is becoming a widely used model organism for studying clathrin/actin mediated endocytosis. Many features of this pathway are conserved evolutionarily from yeast to mammals, and the functions of the actin cytoskeleton in endocytosis have been extensively studied (Engqvist-Goldstein and Drubin, 2003; Kaksonen *et al.*, 2003; Kaksonen *et al.*, 2005, 2006). Endocytosis can be classified as either fluid-phase or receptor-mediated. Previously, the membrane-impermeant fluorescent dye Lucifer yellow carbohydrazide (LY) has been used to identify mutants in fluid-phase endocytosis (Riezman, 1985; Dulic *et al.*, 1991).

Two mutants, *end3* and *end4*, have been identified that are defective in both fluid-phase and receptor-mediated endocytosis in budding yeast (Raths *et al.*, 1993). Extensive work of Riezman and colleagues (D'Hondt *et al.*, 2000; Munn, 2001) has identified several *end* mutants that are defective in receptor-medicated endocytosis. Molecular genetic studies of internalization in yeast reveal a striking correlation between endocytosis and cytoskeletal proteins (Munn, 2001; Engqvist-Goldstein and Drubin, 2003). Most of the mutants defective for receptor endocytosis are important for polarization of the actin cytoskeleton. For example, the *END7* (*ACT1*) mutant results in loss of cortical actin patch polarization (Munn *et al.*, 1995). Mutations in *END4* (*SLA2*) that encodes an actin-binding protein also leads to delocalized cortical actin patches (Holtzman *et al.*, 1993).

In yeast, the $NPFX_{(1,2)}D$ motif, originally identified in Kex2p, provides a signal for receptor-mediated endocytosis (Tan *et al.*, 1996). This signal motif is found in the Ste3 receptor, and a similar motif (GPFAD) is found in the Ste2 receptor as well (Howard *et al.*, 2002). However, the GPFAD motif is not required for full-length Ste2p internalization (Howard *et al.*, 2002).

The ubiquitin-dependent pathway is the main receptor-mediated endocytosis pathway in yeast. Ubiquitinated permeases, transporters and G protein-coupled receptors (including Ste2) are subject to internalization from the cell surface (Munn, 2001). Knowledge of the sequential steps for receptor-mediated internalization is limited. However, Ste2 has been extensively studied with regard to its internalization process. Based on genetic epistasis and mutant phenotypes, several major steps have been put in

order including ligand binding, phosphorylation, ubiquitination, adaptor binding and actin assembly, and the proteins involved in this process have been described (Munn, 2001; Engqvist-Goldstein and Drubin, 2003; Toret and Drubin, 2006). Combining the recent live-cell imaging studies with genetic biochemical and tests of function, Toret and Drubin (2006) present a picture of our current understanding of endocytosis in the budding yeast. Pathways regulating endocytic coat disassembly in yeast for downstream trafficking have also been discussed (Toret *et al.*, 2008).

It is thought that ligand binding to the receptor triggers phosphorylation of several serine and threonine residues in the cytoplasmic tail of Ste2. Yck1p, and Yck2p and Akr1p (ankyrin-repeat protein) are likely to be involved in this step since temperature-sensitive mutants of Yck1p, and Yck2p block phosphorylation of Ste2 (Feng and Davis, 2000), and Akr1p is required for the recruitment of Yck2p (Feng and Davis, 2000). Akr1p is a palmitoyl transferase, and both kinasesYck1p and Yck2p require palmitoylation for proper plasma membrane localization (Feng and Davis, 2000; Roth *et al.*, 2002). In addition to phosphorylating Ste2 and Ste3, Yck1p and Yck2p are involved in phosphorylation of other proteins. Current data indicate that type-I casein kinases Yck1p and Yck2p are involved in regulating protein import by phosphorylating the N-recognin Ubr1 that recognizes proteins with destabilizing N-terminal residues (Hwang and Varshavsky, 2008). Local regulation of mRNA translation is affected by the membrane-associated kinase Yck1p (Paquin *et al.*, 2007). The yeast ASH1 mRNA translational repression is released due to the disruption of Khd1p-RNA complex which results from Khd1p phosphoyation by Yck1p (Paquin *et al.*, 2007).

In addition, ergosterol is important for endocytosis in yeast. Several *erg*Δ mutants lead to a strong internalization defect for Ste2p (Heese-Peck *et al.*, 2002). It is suggested that specific sterol structures are required for Ste2p hyperphosphorylation, a prerequisite for internalization, and *erg* mutants lead to defects in hyperphosphorylation and ubiquitination of the Ste2 receptor (Heese-Peck *et al.*, 2002). However, the lack of phosphorylation of Ste2 is not due to a defect in Ste2 localization or ligand-receptor interaction since Ste2 is present on the cell surface in *erg*Δ cells, and α-factor shows a similar binding affinity for Ste2 either in *erg*Δ cells or wild-type cells (Heese-Peck *et al.*, 2002).

An E3 ubiquitin ligase, RSP5, involved in mono-ubiquitination of the Ste2 receptor and is known to be important for receptor internalization. Mutations in *RSP5* leads to defects in Ste2 internalization (Dunn and Hicke, 2001). However, a Ste2p-ubiquitin chimera that does not require post-translational ubiquitination cannot be internalized in the temperature-sensitive *rsp5* mutant. In addition, a modified Ste2p with a NPFXD motif as its only internalization signal also fails to be internalized in *rsp5* mutant cells (Dunn and Hicke, 2001). Therefore, Rsp5p-dependent ubiquitination is required for internalization mediated by ubiquitin-dependent and ubiquitin-independent endocytosis signals (Dunn and Hicke, 2001).

**Proteins involved in endocytosis in yeast cells**

Several adaptor proteins are involved in binding to the ubiquitinated receptors. Ent1p and Ent2p containing ubiquitin-interacting motifs (UIM) can bind to

mono-ubiquitin *in vitro* (Shih *et al.*, 2000), and Ent1/2p interacts with the Arp2/3 activator, Pan1p (Duncan *et al.*, 2001). Another ubiquitin-binding protein Ede1p has been proposed to play a role in proper initiation of endocytic sites (Kaksonen *et al.*, 2006). Other proteins such Sla2p, Yap1801p and Yap1802p, although they do not contain ubiquitin-interacting domains, may function to recruit the endocytic complexes on the plasma membrane (Engqvist-Goldstein and Drubin, 2003). The Sla2p may be required for the linkage of actin cytoskeleton to the coat module (Kaksonen *et al.*, 2003; Newpher *et al.*, 2005). In the step of actin assembly, the machinery for actin polymerization is recruited to the endocytic sites through binding to adaptor proteins. Las17p (the yeast homolog to human Wiskott-Aldrich sybdrome protein, WASP) activates the Arp2/3 complex promoting actin assembly. Vrp1p (a Las17p-interacting protein) binds to the Las17p and Myo5p, a type I myosin motor protein, to promote actin assembly as required for internalization (Sun *et al.*, 2006). Two amphiphysins, Rvs161p and Rvs167p, may be involved in release of the forming vesicle (Kaksonen et al., 2005). Other proteins such as Abp1p, Sac6p, Cap1p and Cap2p are reported to be associated with the actin assembly meshwork dynamics (Kaksonen *et al.*, 2005; Sun *et al.*, 2006).

**Endocytosis of α-factor receptors (Ste2p)**

Constitutive endocytosis and ligand-stimulated endocytosis have been observed for the yeast α-factor receptors. Constitutive endocytosis of α-factor receptor takes place at a slow rate but endocytosis is increased 5-10 fold after α-factor binding. Ste2p is endocytosed and degraded rapidly in the presence of mating pheromone (Jenness and

Spatrick, 1986). This result indicates that internalization of Ste2p is regulated. It should be noted that although α-factor binding increases Ste2 internalization, the endocytosis process is not G-protein dependent (Jenness and Spatrick, 1986; Zanolari *et al.*, 1992). Schandel and Jenness (1994) provided direct evidence for α-factor induced internalization of cell surface Ste2 receptors based on cell fractionation and extracellular protease digestion analysis. In the presence of α-factor, the membranes containing the internalized Ste2p cofractionate with vacuolar membranes. Degradation of receptors is blocked in a *pep4* mutant deficient for vacuolar proteases (Schandel and Jenness, 1994). In addition, the Ste2-L236H mutant receptor is defective for α-factor response but capable of ligand-induced endocytosis indicating that signal transduction and internalization are independent events (Schandel and Jenness, 1994). The α-factor receptors transit the endocytic pathway from the plasma membrane to the vacuole by passing through two intermediates, the early and late endosomes (Hicke, 1997).

**Endocytosis signals in mating-factor receptors Ste2p and Ste3p**

There are at least two internalization motifs characterized in the yeast mating-factor receptors, Ste2p and Ste3p. Both endocytosis signals are located in the cytoplasmic tail domain (Rohrer *et al.*, 1993; Tan *et al.*, 1996). Through the mutational analysis of the partially truncated receptor Ste2-T345, an amino acid motif $^{331}$SINNDAKSS$^{339}$ in the C-terminus of Ste2 has been identified to be required for endocytic activity of Ste2-T345 (Rohrer *et al.*, 1993). The NPFXD in the cytoplasmic tail of Ste3 has also been shown to be sufficient to confer endocytosis (Tan *et al.*, 1996).

This sequence in the C-terminal domain of Ste2 has been shown to be essential for both basal and ligand-induced endocytosis. Although truncated receptors Ste2p or Ste3p lacking the entire cytoplasmic C-terminal domain are defective for endocytosis, full-length mutants that simply lack the $^{331}$SINNDAKSS$^{339}$ or the NPFXD motif in Ste2p and Ste3p, respectively, remain competent for endocytosis (Rohrer *et al.*, 1993; Tan *et al.*, 1996). These results indicate the presence of multiple independent internalization motifs in the cytoplasmic tail of mating receptors. Interestingly, the NPFXD-related signal sequence GPFAD residues 392-396 has been shown to be functional motif in endocytosis of full-length Ste2 (Howard *et al.*, 2002). The internalization of Ste2p is slowed but not completely blocked in a mutant receptor in which all eleven lysines in the C-terminal tail have been converted to arginine (Ste2p11KR) or in the same mutant lacking GPFAD (Ste2pKR-G392A) (Terrell *et al.*, 1998; Howard *et al.*, 2002).

A deletion strategy has been used to delineate the endocytic signals in the cytoplasmic tail of the Ste2p. Yesilaltay (2001) studied certain deletions in the Ste2 tail that lack the endocytosis motif $^{331}$SINNDAKSS$^{339}$. Ste2-Δ(297-360)-GFP is able to undergo constitutive and ligand-induced endocytosis. The result indicates that 71 amino acids at the C-terminal end of the Ste2 cytoplasmic tail from residues 360 to 431 including the NPFX$_{(1,2)}$D-like sequences GPFAD contain enough information for endocytosis. However, Ste2-Δ(297-391)-T391-GFP is unable to undergo endocytosis indicating that the residues 360-391 are critical for endocytosis of Ste2-Δ(297-391)-GFP or that they may be required for function of the GPFAD motif (Yesilaltay, 2001). However, the Ste2-Δ(297-360)-T399-GFP mutant also fails to undergo endocytosis

suggesting that C-terminal sequences of Ste2p beyond residue 399 are also important for the efficient endocytosis (Yesilaltay, 2000).

**Post-translational modifications of Ste2p**

Wild-type Ste2p undergoes several post-translational modifications including N-linked glycosylation, phosphorylation and monoubiquitin. The functional significance of these modifications is discussed below.

**Phosphorylation of Ste2**

Ste2 is phosphorylated at serine and threonine residues and hyperphosphorylated upon binding of α-factor resulting in slower migration on SDS gels (Reneke *et al.*, 1988; Hicke *et al.*, 1998). In truncated Ste2-T345, substituting serine residues with alanine in the $^{331}$SINNDAKSS$^{339}$ motif (residue 331, 338 and 339) impaired both endocytosis and the ligand induced mobility shift of the truncated mutant receptor (Hicke *et al.*, 1998). This truncated Ste2 mutant with S331A, S338A and S339A substitutions is not phosphorylated in the absence or in the presence of α-factor, and it is unable to be ubiquitinated or internalized (Hicke and Riezman, 1996; Hicke *et al.*, 1998). The results indicated that phosphorylation of the truncated Ste2p may be a prerequisite for ubiquitination. Two casein kinase I homologues, Yck1p and Yck2p, are thought to be involved in phosphorylating Ste2 since in *yck*$^{ts}$ cells the Ste2 receptors fail to be internalized and lack phosphorylation and ubiquitination (Hicke *et al.*, 1998; Feng and Davis, 2000). Phosphorylation at other sites has been shown to play a role in regulating

Ste2p function as well. Mutations affecting the four most distal serine and threonine residues in the C-terminal domain of the receptor (Ste2-4ala) result in increased sensitivity to α-factor and the alanine substitution mutations lead to decreased phosphorylation of Ste2p (Chen and Konopka, 1996). The ligand-binding assays with labeled α-factor suggest that phosphorylation of the C-terminal domain of the receptor does not alter ligand binding (Chen and Konopka, 1996). The doublet bands on the immunoblotting are due to the phosphorylation of the receptor in non-glycosylated Ste2p (Mentesana and Konopka, 2001).

**Ubiquitination of Ste2**

Ubiquitination has been demonstrated to play a role in endocytosis of plasma membrane proteins in yeast cells. Ubiquitination is required for endocytosis of Ste2. Hicke and Riezman (1996) showed that *end4* Δ strain has a defect in endocytosis of plasma membrane proteins including Ste2 and accumulates a high molecular weight form of consistent with ubiquitinated Ste2p (Hicke and Riezman, 1996). Ubiquitin conjugating enzymes have been shown to be required for efficient internalization. Mutants that lack multiple ubiquitin conjugating enzymes such as *ubc1 ubc4 and ubc4 ubc5* display much slower internalization rates for stimulated endocytosis of Ste2p (Hicke and Riezman, 1996). Endocytosis of Ste2 is associated with phosphorylation and ubiquitination of the cytoplasmic C-terminal domain of the receptor (Hicke and Riezman, 1996; Hicke, 1997). The non-classical signal $^{331}$SINNDAKSS$^{339}$ located in the C-terminal domain has been shown to contain the ubiqutination and phosphorylation sites

that participate in endocytosis (Hicke and Riezman, 1996; Hicke *et al.*, 1998). The lysine at residue 337 within this $^{331}$SINNDAKSS$^{339}$ motif sequence is crucial for mediating ubiquitination of truncated Ste2-T345 (Hicke and Riezman, 1996). Substitution of the lysine residue on 337 (K to R) disrupts both ligand-induced ubquitinnation and internalization of this truncated Ste2p (Hicke and Riezman, 1996). Although the $^{331}$SINNDAKSS$^{339}$ motif is sufficient for Ste2 internalization, it is not required in full length Ste2p (Rohrer *et al.*, 1993).

To test whether polyubiquitin chain formation through Lys48 is required for ubiquitin to serve as an internalization signal in Ste2p, double mutation in the ubiquitin molecule Ub-K48R/G76A have been introduced. The lysine to arginine change at position 48 is used to block poly-ubiquitin chain formation in the substrate and the glycine to alanine change at the C-terminus of Ub results in inhibition of de-ubiquitination of the substrate. The data indicate that formation of polyubiquitin chains is not required for $\alpha$-factor receptor internalization (Terrell et al., 1998). This monoubiquitination of Ste2p is sufficient for ligand-induced endocytosis of Ste2p, and monoubiquitination serves as a sorting signal in yeast (Terrell *et al.*, 1998).

It has been reported that Lys337 of the $^{331}$SINNDAKSS$^{339}$ sequence is the most frequently ubiquitinated lysine in the Ste2p (Terrell *et al.*, 1998). Whether other lysine residues in the cytoplasmic C-terminal domain of Ste2 are also ubiquitinated and involved in the Ste2 internalization has been discussed (Yesilaltay, 2001). Ste2-$\Delta$(297-391)-GFP mutant is defective in endocytosis (Yesilaltay, 2001), indicating that neither the GPFAD motif nor the two most distal lysine residues are not sufficient for

endocytosis. In contrast, the Ste2-Δ(297-360)-GFP mutant shows a significant rate of endocytosis, but slower than the wild-type. Therefore, the sequence from 360 to 391 contains residues that are critical for endocytosis of Ste2-Δ(297-360)-GFP. Lys374 and Lys387 are contained in this region. Loss of Lys387 or Lys374 plus Lys387 leads to a further reduction in the rate of receptor removal from the cell surface compared to the Ste2-Δ(297-360)-GFP mutant that contains no lysine substitutions. Therefore, Lys387 is essential for a redundant endocytosis signal and may provide an additional ubiquitination site outside of the $^{331}$SINNDAKSS$^{339}$ sequence.

**Glycosylation of α-factor receptor**

Post-translational modifications such as phosphorylation and ubiquitination have been shown to regulate signaling activity and membrane trafficking. Therefore glycosylation of wild-type Ste2 has also been investigated. Mutations affecting two sites in the receptor N-terminal domain (N25Q and N32Q) eliminate detectable N-linked glycosylation of the receptor, and the unglycosylated receptor retains normal function and subcellular location. However, elimination of glycosylation sites in the temperature-sensitive Ste2-3 mutant receptor leads to increased plasma membrane localization for the mutant receptors at the non-permissive temperature. The mutant receptors containing glycosylation sites would otherwise have been retained intracellularly. This result suggests that N-linked glycosylation of Ste2 receptors plays a role in a sorting process for misfolded Ste2 proteins (Mentesana and Konopka, 2001).

Heterogeneity of wild-type Ste2, as detected by SDS gel electrophoresis and western blotting, results from oncomplete modification of the N-linked glycosylation sites.

**Degradation of α-factor receptors**

Vacuolar hydrolases are required for the efficient degradation of Ste2p (Schandel and Jenness, 1994), indicating that degradation of Ste2 occurs in the vacuole and is not mediated by the proteasome. The *pre1pre2* double mutant lacks the two essential β-tsubunits that are required for proteasome activity. In this double mutant, ligand-induced degradation of Ste2p occurs at a similar rate when compared with wild-type cells. In contrast, in the mutant *pep4 prb1* that lacks the vacuolar proteases A and B, receptor degradation is blocked. Both experiments confirm that degradation of Ste2p occurs in vacuole but is not mediated by the proteasomal degradation pathway (Hicke and Riezman, 1996). Li et al (1999) also demonstrated the similar result that the degradation of full-length Ste2-GFP occurs in a Pep4 dependent manner. Disruption of *PEP4* gene results in stabilization of full-length Ste2-GFP in vacuole, whereas free GFP accumulates in the vacuole of wild-type cells (Li *et al.*, 1999).

**Rationale for this work**

The structure of Ste2p is depicted in Fig. 1-1. The endocytosis motif sequence and the positions of the mutations used in this study are shown. Several results indicated that Ste2 receptors form either dimers or higher oligomeric complexes (Overton and Blumer, 2000; Yesilaltay and Jenness, 2000). Although the receptors are in an oligomeric

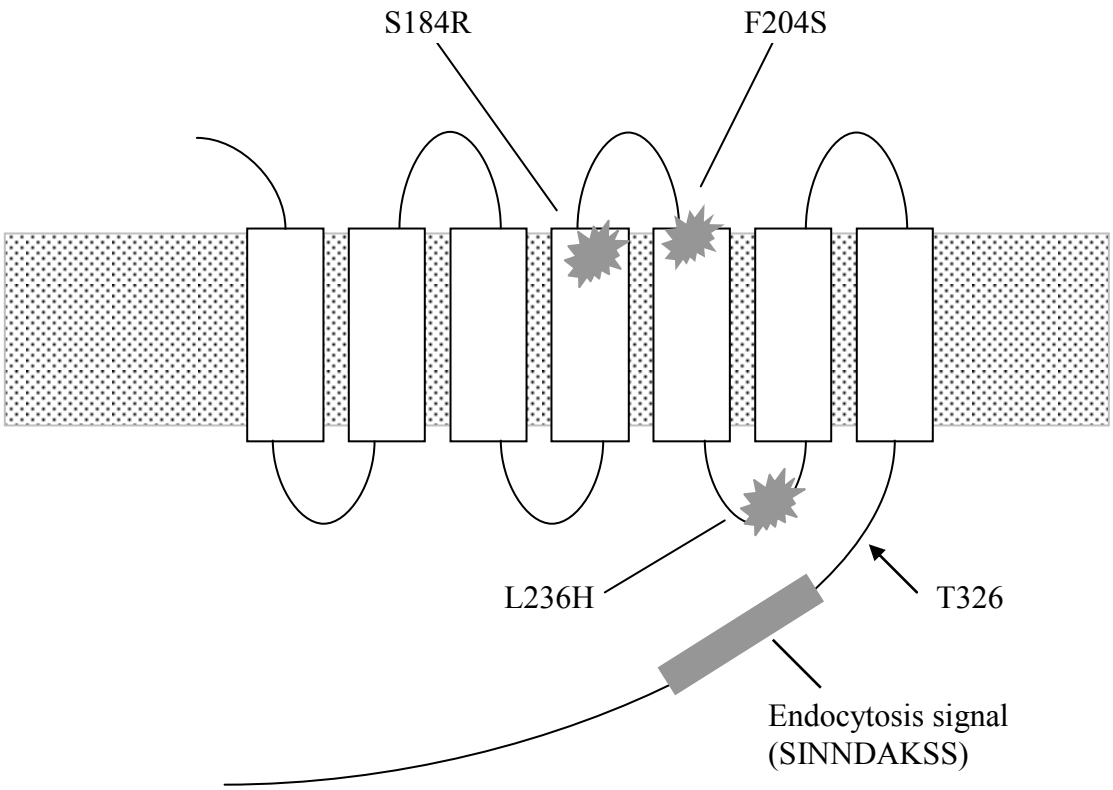


**Figure 1-1.** The secondary structure of the α-factor receptor. The positions of the mutations used in this study are shown. Ste-S184R and Ste2-F204S are binding defective mutants. Ste2-L236G is a G-protein coupling defective mutant. The endocytosis motif SINNDAKSS sequence is denoted in gray box. The residue 326 is marked with an arrow.

state when they are endocytosed, whether oligomerization of Ste2p is required for ligand-induced endocytosis remained unclear. Despite the proposal that $^{56}$GxxxG$^{60}$ motif in the TM1 of Ste2p plays a role of forming the interface between Ste2p subunits (Chinault *et al.*, 2004), it is not clear whether other transmembrane domains or segments are also involved in the oligomer interface(s). In addition, full-length *ste2* mutants defective in $^{56}$GxxxG$^{60}$ show a different cytoplasmic location than tailless *ste2* mutants containing the same residue substitution, suggesting that the C-terminal domain of Ste2p plays a role in ER exit. Based on these observations several questions are addressed in this thesis:

1) What is the functional impact of oligomerization on conformational changes? Can the ligand-activated Ste2 subunit affect neighboring Ste2 units that cannot bind the ligand?
2) What is the role of the endocytosis motif in the endocytosis of oligomers? Must the endocytosis motif undergo a conformational change in order to be recognized by the endocytic machinery or does it play a passive role for recognition?
3) What is the interface for Ste2p oligomerization? Can a single residue substitution of Ste2p disrupt the interface contact site for oligomer of the Ste2 oligomer?
4) What are the functional requirements for ER exit of Ste2p? Is oligomerization of Ste2p a prerequisite? Do specific ER export signals exist in the C-terminal domain Ste2p?
5) Is the oligomerization of Ste2 required for the signal transduction?

In this thesis, results are presented based on the *in vitro* and *in vivo* experiments that extend and explore the understanding of the functional significance of Ste2p oligomerization.

# CHAPTER II

# MATERIALS AND METHODS

**Primers.** All primers used in this study are listed in Table 2-1.

**Plasmids.** Plasmids used in this study are listed in Table 2-2. Single mutations in the *STE2* gene were confirmed by DNA sequencing. The integrating plasmid pDJ637 contains TRP1 and GPD-*ste2-T58* in which GPD (glyceraldehyde-3 phosphate dehydrogenase) promoter has been fused to the first 58 codons from the *STE2* gene. It was constructed by ligating *Xho*I/*Spe*I (New England Biolabs Inc., Beverly, MA) fragment from pDJ432 with *Xho*I/*Spe*I cut pDJ429 containing the *TRP1*gene. pDJ654 that contains the wild-type *STE2* gene fused with the sequence encoding the T7 epitope was created in two steps. The first PCR product was obtained by using primer pairs PO-515 and PO-516 and used plasmid pDJ135 as a template. The second PCR product was obtained by using primer pairs PO-517 and PO-210 and used plasmid pDJ437 as a template. Both PCR products were gel purified and used as template in the final PCR reaction using primers PO-515 and PO-210. The product was digested by *Mlu*I/*Hpa*I (New England Biolabs Inc., Beverly, MA) and cloned into the *Mlu*I/*Hpa*I fragment of pDJ135. Plasmid pDJ655 contains the T7 epitope-tagged version of *STE2* with a mutation at codon 204 (F204S). Primers PO-587 and PO-588 were used to construct the

TABLE 2-1. Primers used in this study.

| Primer | Sequence |
|---|---|
| PO-171 | GATGTTAGTGCCACCCAAG |
| PO-210 | GGAATTCCCAACCATGTGGTCTGACACCAAACATAATGG |
| PO-211 | CGGGACTAGTCATAAAATGTCTGATGCGGCTCCTTCAT |
| PO-478 | GCCGAAAATCAAGACGGAGC |
| PO-479 | GATGAAGTCTACGCTTTTGCATG |
| PO-515 | ATTCCAGATATGCGTTATAACCT |
| PO-516 | ACCACCAGTCATAGAAGCCATTTTTGATTCTTGGATATGGTT |
| PO-517 | ATGGCTTCTATGACTGGTGGT |
| PO-522 | GCATTGAGCTCGTTATCCAATGCCTGCCAA |
| PO-587 | CAATACACTTCCATATATGGGCAAGGATCTACCATCACTTTCGATGA |
| PO-588 | TTGCCCATATATGGAAGTGTATTGAATGGTGCTTTGACCAGGATTATA |
| PO-605 | GAACCACGCGTGACTCACTATAGGGCGAATTG |
| PO-604 | CTTGGGTGGCACTAACATC |
| PO-646 | AGAGAAAGTAGTGACAAGTGTTG |
| PO-652 | AAGGTTTAATAGACGATAAATTTCCATA |
| PO-654 | GTAGCGCGTATGACTCTTAATC |
| PO-655 | ACATTCTCGCATAATAATAGTAACA |
| PO-656 | AGTAGAGGTGACGTTCATGTTTA |
| PO-657 | TAAACATGAACGTCACCTCTACT |
| PO-658 | TACGCACCTGCAGATGCTATAGAGAAAAATCAGTTTTATCAG |
| PO-659 | GATACGGCAGCTGCTGAGGAAGCCAGAAAGTTCTG |

TABLE 2-1 continued.

| Primer | Sequence |
|---|---|
| PO-660 | TGGCTTCCTCAGCAGCTGCCGTATCGGGAGTG |
| PO-661 | GCGCGGCCGTCTAGATTATTTGTATAGTTCATCCATGCCA |
| PO-669 | ATGTTTGGTGTCAGAGCAGGTGCAGCTGCTTTGACTTTG |
| PO-670 | CAAAGCAGCTGCACCTGCTCTGACACCAAACATAATGGC |
| PO-671 | TTTTTAATCATTTTGGCATCTGCACTCTATTTTAAATATTTA |
| PO-672 | ATAGAGTGCAGATGCCAAAATGATTAAAAACAATGAAAC |
| PO-673 | TTACTGTCTAATTGTTCTTCAGTGACTTACGCTC |
| PO-674 | GTAAGTCACTGAAGAACAATTAGACAGTAAATATTTAAAATA GAG |
| PO-675 | TTTTTAATCATTTTGCCATCTGCACTCTATTTTAAATATTTA |
| PO-676 | ATAGAGTGCAGATGGCAAAATGATTAAAAACAATGAAAC |

TABLE 2-2. Plasmids used in this study

| Plasmid | Description |
|---|---|
| pDJ124 | Centromeric plasmid containing LEU2 gene as a control vector |
| pDJ125 | 2μ plasmid containing LEU2 gene as a control vector |
| pDJ135 | Centromeric plasmid containing URA3 gene and *STE2* |
| pDJ203 | Centromeric plasmid containing URA3 gene and *Fus1-lacZ* |
| pDJ303 | Centromeric plasmid containing URA3 gene as a control vector |
| pDJ304 | Centromeric plasmid containing URA3 gene and *STE2* |
| pDJ429 | Integrating plasmid containing URA3 gene and GPD promoter with N-terminal Ste2 |
| pDJ432 | Integrating plasmid containing TRP1 gene and GPD promoter |
| pDJ437 | Integrating plasmid containing URA3 gene and T7 tag with N-terminal Ste2 |
| pDJ451 | 2μ plasmid containing URA3 gene and *Ste2-F204S* |
| pDJ469 | Centromeric plasmid containing URA3 gene and *Ste2-T326-GFP* |
| pDJ481 | Centromeric plasmid containing LEU2 gene with triple HA tag |
| pDJ637 | Integrating plasmid containing TRP1 gene and GPD promoter with N-terminal Ste2 |
| pDJ638 | Centromeric plasmid containing URA3 gene and *Ste2-S141P,R161G-T326-GFP* |
| pDJ639 | Centromeric plasmid containing URA3 gene and *Ste2-F55L,S145P-T326-GFP* |

| | |
|---|---|
| pDJ640 | Centromeric plasmid containing URA3 gene and *Ste2-C59R,R122G,Y193C, N216H,S310 F312T-T326-GFP* |
| pDJ641 | Centromeric plasmid containing URA3 gene and *Ste2-H94,F116,Q240R, N300Q-T326-GFP* |
| pDJ642 | Centromeric plasmid containing URA3 gene and *Ste2-R12,Y19,N216H, S31,F312T-T326-GFP* |
| pDJ643 | Centromeric plasmid containing URA3 gene and *Ste2-F116,Q240R,N300Q-T326-GFP* |
| pDJ644 | Centromeric plasmid containing URA3 gene and *Ste2-F55L-T326GFP* |
| pDJ645 | Centromeric plasmid containing URA3 gene and *Ste2-R161G-T326-GFP* |
| pDJ646 | Centromeric plasmid containing URA3 gene and *Ste2-G56L-T326-GFP* |
| pDJ647 | Centromeric plasmid containing URA3 gene and *Ste2-C59R-T326-GFP* |
| pDJ648 | Centromeric plasmid containing URA3 gene and *Ste2-H94P-T326-GFP* |
| pDJ649 | Centromeric plasmid containing URA3 gene and *Ste2-S141P-T326-GFP* |
| pDJ650 | Centromeric plasmid containing URA3 gene and *Ste2-S145P-T326-GFP* |
| pDJ651 | Centromeric plasmid containing URA3 gene and *Ste2-F204S-T326-GFP* |
| pDJ652 | Centromeric plasmid containing URA3 gene and *Ste2-C59A-T326-GFP* |
| pDJ653 | Centromeric plasmid containing URA3 gene and *Ste2-H94A -T326-GFP* |
| pDJ654 | Centromeric plasmid containing URA3 gene and T7 epitope -tagged *STE2* |
| pDJ655 | Centromeric plasmid containing URA3 gene and T7 epitope -tagged *Ste2-F204S* |
| pDJ656 | Derived from pDJ654 with N25Q/N32Q substitution on *STE2* |

| | |
|---|---|
| pDJ657 | Derived from pDJ655 with N25Q/N32Q substitution on *Ste2-F204S* |
| pDJ658 | Centromeric plasmid containing URA3 gene and *STE2-GFP* |
| pDJ659 | Centromeric plasmid containing URA3 gene and *Ste2-G56L-GFP* |
| pDJ660 | Centromeric plasmid containing URA3 gene and *Ste2-C59R-GFP* |
| pDJ661 | Centromeric plasmid containing URA3 gene and *Ste2-H94P-GFP* |
| pDJ662 | Centromeric plasmid containing URA3 gene and *Ste2-S141P-GFP* |
| pDJ663 | Centromeric plasmid containing URA3 gene and *Ste2-S145P-GFP* |
| pDJ664 | Centromeric plasmid containing URA3 gene and *Ste2-H94A-GFP* |
| pDJ665 | Centromeric plasmid containing URA3 gene and *STE2-AXE-GFP* |
| pDJ666 | Centromeric plasmid containing URA3 gene and *Ste2-G56L-AXE-GFP* |
| pDJ667 | Centromeric plasmid containing URA3 gene and *Ste2-C59R-AXE-GFP* |
| pDJ668 | Centromeric plasmid containing URA3 gene and *Ste2-H94P-AXE-GFP* |
| pDJ669 | Centromeric plasmid containing URA3 gene and *Ste2-S141P-AXE-GFP* |
| pDJ670 | Centromeric plasmid containing URA3 gene and *Ste2-S145P-AXE-GFP* |
| pDJ671 | Centromeric plasmid containing URA3 gene and *Ste2-H94A-AXE-GFP* |
| pDJ672 | Centromeric plasmid containing URA3 gene and *GPD-STE2- T326-GFP* |
| pDJ673 | Centromeric plasmid containing URA3 gene and *GPD -Ste2-G56L-T326-GFP* |
| pDJ674 | Centromeric plasmid containing URA3 gene and *GPD -Ste2-C59R- T326-GFP* |
| pDJ675 | Centromeric plasmid containing URA3 gene and *GPD -Ste2-H94P-T326-GFP* |

| | |
|---|---|
| pDJ676 | Centromeric plasmid containing URA3 gene and *GPD -Ste2-S141P-T326-GFP* |
| pDJ677 | Centromeric plasmid containing URA3 gene and *GPD -Ste2-S145P- T326-GFP* |
| pDJ678 | Centromeric plasmid containing URA3 gene and *GPD -Ste2-F204S-T326-GFP* |
| pDJ679 | Centromeric plasmid containing LEU2 gene and *GPD -Ste2-F204S-T326-HA* |
| pDJ680 | Centromeric plasmid containing LEU2 gene and *Ste2-T326-HA* |
| pDJ681 | Centromeric plasmid containing URA3 gene and *Ste2-Y106C* |
| pDJ682 | Centromeric plasmid containing URA3 gene and *Ste2-Y106C, F204S* |
| pDJ683 | Centromeric plasmid containing LEU2 gene and *Ste2-Y106C-HA* |
| pDJ684 | Centromeric plasmid containing LEU2 gene and *Ste2-Y106C, F204S-HA* |
| pDJ685 | Centromeric plasmid containing LEU2 gene and GPD-*Ste2-HA* |
| pDJ686 | Centromeric plasmid containing LEU2 gene and GPD-*Ste2-G56L-HA* |
| pDJ687 | Centromeric plasmid containing LEU2 gene and GPD-*Ste2-C59R-HA* |
| pDJ688 | Centromeric plasmid containing LEU2 gene and GPD-*Ste2-H94P-HA* |
| pDJ689 | Centromeric plasmid containing LEU2 gene and GPD-*Ste2-S141P-HA* |
| pDJ690 | Centromeric plasmid containing LEU2 gene and GPD-*Ste2-S145P-HA* |
| pDJ691 | Centromeric plasmid containing LEU2 gene and *Ste2-F204S-T326-HA* |
| pDJ695 | Centromeric plasmid containing LEU2 gene and GPD-*Ste2-H94P-T326-HA* |
| pDJ696 | 2μ plasmid containing LEU2 gene and *Ste2-S184R* |

| | |
|---|---|
| pDJ697 | Centromeric plasmid containing URA3 gene and *Ste2-Q85,F116L-T326-GFP* |
| pDJ698 | Centromeric plasmid containing URA3 gene and *Ste2-V45A,R122G,L210S-T326-GFP* |
| pDJ699 | Centromeric plasmid containing URA3 gene and *Ste2-T114I,D210G I249L, T278S-T326-GFP* |
| pDJ700 | Centromeric plasmid containing URA3 gene and *Ste2-Q85H-T326-GFP* |
| pDJ701 | Centromeric plasmid containing URA3 gene and *Ste2-F116L-T326-GFP* |
| pDJ702 | Centromeric plasmid containing URA3 gene and *Ste2-V45A, R122G-T326-GFP* |
| pDJ703 | Centromeric plasmid containing URA3 gene and *Ste2-L210S-T326-GFP* |
| pDJ704 | Centromeric plasmid containing URA3 gene and *Ste2-T114I, D210G, I249L-T326-GFP* |
| pDJ705 | Centromeric plasmid containing URA3 gene and *Ste2-T278S-T326-GFP* |
| pDJ706 | Centromeric plasmid containing URA3 gene and *Ste2-R122G-T326-GFP* |

plasmid pDJ656 and pDJ657 that contained either T7 epitope-tagged *STE2* or *STE2*-F204S gene and both plasmids contained mutations at amino acid position 25 and 32 (N25Q, N32Q). Plasmid pDJ658 containing full length *STE2-GFP* fused gene and the *URA3* gene was constructed by ligating the *Pst*I/*Xba*I fragment of pDJ338 with the *Pst*I/*Xba*I pDJ304 vector. Plasmids pDJ646 through pDJ653 encoded the tailless Ste2 receptor with the single residue substitution indicated in Table 2. DNA fragments with single mutation in the *STE2-T326* gene were constructed with two-step PCR. Primers PO-539 and PO-540 were used to construct pDJ646, pDJ647, pDJ650 and pDJ651. Primers PO-541 and PO542 is used to construct pDJ649. Primers PO-669 and PO-670 were used for pDJ652. Primers PO-671 and PO-672 were used for pDJ653. Primers PO-675 and PO-676 were used for pDJ648. PCR fragments were digested with *Mlu*I/*Cla*I cloned into *Mlu*I/*Cla*I digested vector plasmid pDJ469. Similar approach was applied on the plasmids pDJ659 through pDJ664 containing single codon mutations in the *STE2* gene encoding the full-length receptor. Plasmid pDJ665 containing the *STE2-AXE-GFP* gene was constructed with two-step PCR. Both PCR fragments used pDJ658 as a template. One PCR fragment was synthesized using primers PO-658 and PO-660, and the other PCR fragment was synthesized using primers PO-659 and PO-646. Both PCR products were gel purified and served as the template for the final PCR using primers PO-658 and PO-646. PCR products were digested with *Pst*I and *Sac*II and cloned into pDJ658 digested with the same enzymes. Other plasmids pDJ666 through pDJ671 encoding defined mutant Ste2 receptors containing AXE substitution were constructed by subcloning the *Pst*I/*Sac*II fragment from pDJ665 into *Pst*I/*Sac*II cut

pDJ659 through pDJ664. Plasmids pDJ672 through pDJ678 were constructed by replacing the endogenous Ste2 promoter by the GPD promoter. PCR products containing GPD promoter DNA was obtained by using PCR with primer pair PO-605 and PO-210 and using pDJ637 as a template. PCR products were digested with *Mlu*I/*Hpa*I and cloned into *Mlu*I/*Hpa*I cut pDJ646 through pDJ653. Two PCR products from primer pair PO-646 and PO-673 and primer pair PO-211 and PO-674 were used with template pDJ304 or pDJ451for the second PCR products containing the Y106C or Y106C, F204S codon, respectively. This product was digested with *Hpa*I/ *Cla*I and cloned into plasmid pDJ304 treated with the same enzymes to produce plasmids pDJ681 and pDJ682. Plasmids pDJ683 and pDJ684 were constructed by using a two-step PCR and cloning strategy. Plasmids pDJ681 (containing Y106C) or pDJ682 (containing Y106C, F204S) were used as the templates primer pair PO-515 and PO-604 to construct two PCR products (A1 and A2), and primer pair PO-171 and PO-646 with template plasmid pDJ658 were used for another PCR product (B). The A1 and B PCR products and the A2 and B PCR products were combined and used as template together with primer pair PO-522 and PO-604 to synthesize the PCR products containing the either full-length Y106C and Y106C, F204, respectively. These PCR products were digested with *Sac*I/ *Sal*I and cloned into the plasmid pDJ481 treated with the same enzymes to produce plasmids pDJ683 and pDJ684, respectively, that carried the *LEU2* selectable marker and encoded receptors with the HA tag fused to the C-terminus. Plasmids encoding either the wild-type or mutant Ste2-HA fusion protein under control of the GPD promoter were constructed by replacing the native promoter of Ste2 in a two-step PCR strategy using

plasmids pDJ672 through pDJ678 as template with primer pair PO-605 and PO-604, and using pDJ658 as template with primer pair PO-171 and PO-646. Each of the PCR products that used pDJ672 through pDJ678 as template were combined with PCR product that use pDJ658 as template for the final PCR reaction with primer pair PO-605 and PO-646. These PCR products from defined wild-type or mutant Ste2 were digested with *Sac*I/ *Sal*I and cloned into the plasmid pDJ481 treated with the same enzymes to produce plasmids from pDJ685 through pDJ690. pDJ679 was constructed by cloning *Sac*I/ *Sal*I treated DNA fragment containing GPD-Ste2-F204S from pDJ678 into pDJ481 treated with the same enzymes. pDJ691 was constructed by cloning the *Mlu*I/ *Cla*I treated DNA fragment containing Ste2-F204S from pDJ451 into pDJ469 treated with the same enzymes.

**Yeast strains.** Yeast strains listed in Table 2-3 are congenic to stain 381G. Yeast strains were transformed with plasmids by using standard techniques (Soni et al., 1993). Strain DJ147-1-2*pep4*Δ::*ura3* was described previously (Li *et al.*, 1999). Strain DJ482-1 was derived from Strain AY6. The *Mlu*I/EcoRI fragment of pDJ451 containing *STE2*-F204S gene was gel purified before transformation into AY6 to target the *URA3* gene locus replacement. The helper plasmid with leucine marker was cotransformed with the purified DNA fragment. Yeast cells were grown on plate without leucine for 2 days and colonies were transferred into new YEPD plates and replicated into FOA plates and grew for two days. Colonies from FOA plates indicating *URA3* gene replacement were further

TABLE 2-3. Yeast strains used in this study

| Strains[a] | Genotype[b] |
|---|---|
| 381G | *MAT**a** cry1 ade-2 his4-580 lys2 trp1 tyr1 SUP4-3$^{ts}$* |
| DJ147-1-2 | 381G *leu2 ura3 TYR1 pep4*Δ::*ura3* |
| *pep4*Δ::*ura3* | |
| DJ211-5-3 | 381G *bar1-1 leu2 ura3* |
| DJ213-7-3 | 381G *bar1-1 leu2 ura3 ste2-10::LEU2* |
| DJ1378-A-1 | 381G *bar1-1 leu2 ura3 ste2Δ* |
| DJ901-A-1 | 381G *bar1-1 leu2 ura3 ste2-L236H* |
| AY6 | 381G *bar1-1 leu2 ura3 ste2Δ*::*URA3* |
| DJ482-1 | 381G *bar1-1 leu2 ura3 ste2-F204S* |
| DJ483-1 | 381G *bar1-1 ADE2$^{+}$ HIS4$^{+}$ LYS2$^{+}$ TYR1$^{+}$ ura3 STE2*::pDJ637 |
| DJ484-1 | 381G *bar1-1 leu2 ura3 STE2*::pDJ637 |
| DJ485-1 | 381G *bar1-1 leu2 ura3 ste2-F204S*::pDJ637 |
| DJ486-1 | 381G *bar1-1 leu2 ura3 ste2-L236H*::pDJ637 |
| DJ487-1 | 381G *bar1-1 leu2 ura3 der3*::*KAN* |
| DJ488-1 | 381G *bar1-1 leu2 ura3 ste2-10::LEU2 der3*::*KAN* |
| DJ489-1 | 381G *bar1-1 leu2 ura3 ste2Δ der3*::*KAN* |

[a]All strains are congenic with strain 381G (Hartwell, 1980).

[b]Mutation *bar1-1* inhibits α-factor degradation (Sprague and Herskowitz, 1981). Temperature-sensitive mutation *SUP4-3* suppresses amber mutations *his4-580* and *trp1* at 22°C but not at 34°C. Mutation *pep4*Δ::*ura3 (Li et al., 1999)* is a Ura$^{-}$ derivative of the

*pep4*Δ::*URA3* allele (Rothman *et al.*, 1986) and results in a loss of protease A and other vacuolar proteases. *STE2*::pDJ637, *ste2-F204S*::pDJ637 and *ste2-L236H*::pDJ637 result in the constitutive overproduction of wild-type Ste2, mutant Ste2-F204S and mutant Ste2-L236H, respectively. Mutation *ste2Δ* in strains DJ1378-A-1 and DJ489-1 removes an internal fragment of the *STE2* coding sequence from codon 101 to codon 261. Mutation *ste2-10::LEU2* replaces the promoter and the first 407 codons of *STE2* with the *LEU2* gene. Mutation *ste2Δ*::*URA3* replaces the entire *STE2* coding sequence with the *URA3* gene.

confirmed by PCR sequencing. Production of Ste2 protein was confirmed by western blotting. Strain DJ483-1 was derived from DJ1205-6-3 and the wild-type Ste2 was under control of GPD promoter by replacing the native promoter of Ste2. Strain DJ484-1 was derived from DJ211-5-3 and the wild-type Ste2 was under control of GPD promoter by replacing the native promoter of Ste2. Strain DJ485-1 was derived from DJ482-1 that native promoter of *STE2*-F204S gene was replaced by GPD promoter as described below. Strain DJ486-1 was derived from DJ901-A-1 that native promoter of *STE2*-L236H gene was replaced by GPD promoter as described above by integration. Disruption of *Der3* gene in the strains DJ487-1, DJ489-1 and DJ488-1 was performed by gene replacement. Genomic DNA was isolated from Euroscarf stain 1217-10 which *Der3* gene has been replaced by kanamycin gene. PCR products containing the *der3::KAN* gene were synthesized by using primers PO-652 and PO-653, and then used to transform the recipient strains. Yeast cells were transformed and cultured on a YEPD plate for 1 day and then replicated onto YEPD plate that contained 200μg/ml G418. Each single colony was picked up for genomic DNA preparation and PCR products from the genomic DNA were sequenced to confirm that the gene replacement was correct.

**Integration of GPD promoter into the chromosomal *STE2* locus.** Cleavage of pDJ637 with *HpaI* followed by transformation and selection on -Trp medium results in integration at the chromosomal *STE2* locus and the replacement of native promoter of the *STE2* gene with GPD promoter. The GPD (glyceraldehyde-3 phosphate dehydrogenase) promoter, which is a strong constitutive promoter, was introduced into the untagged

chromosomal wild-type *STE2* gene. The yeast cells were transformed using the standard protocol as described and a single integration event was confirmed by PCR and sequencing.

**PCR mutagenesis.** The forced mutagenic PCR method (Fromant *et al.*, 1995) was used to generate random mutations in the *STE2* gene. Four different forced dNTP mixtures, designated forced A mixture, forced T mixture, forced C mixture and forced G mixture, were prepared for the mutagenic PCR reaction and diluted to the final concentration, forced A mixture (3.4 mM dATP, 200 μM dTTP, 200 μM dCTP, 200 μM dGTP), forced T mixture (200 μM dATP, 3.4 mM dTTP, 200 μM dCTP, 200 μM dGTP), forced C mixture (200 μM dATP, 200 μM dTTP, 3.4 mM dCTP, 200 μM dGTP) and forced G mixture (200 μM dATP, 200 μM dTTP, 200 μM dCTP, 3.4 mM dGTP). Forced A mixture was eliminated due to a technical difficulty. The final contraction of $MgCl_2$ was 4.7 mM. The primers were PO-211 and PO-646 (1 μM each). The reaction contained1ng pDJ469 DNA template, 1X Mg-free reaction buffer, and 0.5 μl Taq DNA polymerase (Promega, Madison, WI) and water was added to adjust the volume to 100 μl. The PCR products from forced T, force C and forced G mixture were cut with *Hpa*I and *Sac*II (New England Biolabs Inc., Beverly, MA) and the 0.85 kb *Hpa*I/ *Sac*II digestion product of mutated PCR fragment was cloned into the *Hpa*I/ *Sac*II fragment of plasmid pDJ469. Plasmids were transformed into the DH5α bacterial strain. Colonies collected from mutation pools, forced T mixture, forced C mixture and forced G mixture were designated pool T, pool C and pool G. Each pool represented approximately 850-900

single colonies. Five colonies were randomly picked from each mutation pools. Plasmids were recovered and sequenced. Mutation frequency was calculated and averaged by counting the mutation sites on the Ste2 DNA sequence between the *Hpa*I/ *Sac*II sites. The average mutation frequency was approximately 8, 5 and 3 mutations in the 0.85 kb DNA containing Ste2 sequence for pool T, pool C and pool G, respectively.

**Fluorescence microscopy.** Procedures for fluorescence microscopy were carried out as describedpreviously (Yesilaltay and Jenness, 2000) with minor modifications. Yeast cells were grown overnight to a density of $10^7$ cells /ml in selective medium. Cells received cycloheximide (10 μg/ml) for 5 minutes before addition of α-factor ($10^{-7}$M). In the parallel experiment, no α-factor was added to the culture. Cultures were incubated at 30° C for 20 minutes and terminated by the addition of the metabolic poisons, $NaN_3$ (10 mM) and KF (10 mM) and chilled on ice. Cells were then collected by centrifugation and suspended in ice-cold water. Epifluorescent images were obtained with a Nikon microscope equipped with a Plan Apo 100x/1.40 oil objective, a FITC-HYQ filter set and a cooled CCD camera (model ST-8I, SBIG Astronomical Instruments, Santa Barbara, CA).

**Endocytosis mutant screening method.** Mutagenized plasmid pDJ469 from the different pools were transformed into yeast cells (strain DJ-483-1). Colonies were cultures in liquid selective medium, treated with $10^{-7}$ M α-factor for 20 minutes at 30° C and viewed with the fluorescence microscope. Cells that retained fluorescence on the

plasma membrane in the presence of α-factor were expected as candidates for loss of oligomerization.

**ER retention mutant screening method.** Mutagenized plasmid pDJ469 from the different pools were transformed into yeast cells (strain DJ485-1). Transformant colonies were processed as described above for the endocytosis mutant screening method. Isolates showing ER retention fluorescence judged by a perinuclear GFP signal were selected. Plasmids were recovered and retransformed into the same host strain for confirmation. The mutagenized portion of the plasmid was then be sequenced.

**Complementation mutant screening method.** Mutagenized plasmid pDJ469 from the different pools were transformed into yeast cells (strain DJ1378-A-1) containing plasmid pDJ696). Double transformants were first cultured on double selective plates lacking leucine and uracil for two days at 30° C. Each single colony was picked and transferred to another plate lacking leucine and uracil and incubated for one day and then replica-plated to two different plates containing α-factor ($5x10^{-5}$ M). One plate contained leucine and lacked uracil, and the other plate lacked both leucine and uracil. Mutants were selected that were sensitive to α-factor under selection for the YEp *LEU2 ste2-S184R* plasmid but resistant to α-factor on plates containing leucine where the cells were allowed to lose the plasmid. Plasmids were recovered and retransformed into the same host strain for confirmation. The mutagenized portion of the plasmid was then be sequenced.

**Culture media.** Liquid and solid media were prepared as previously described (Hasson *et al.*, 1994; Jenness *et al.*, 1997). YM-1 is a reach liquid medium. Minimal medium was yeast nitrogen base (without amino acids; Difco Laboratories) supplemented with ammonium sulfate (1 mg/ml) as the nitrogen source and glucose (2%) as the carbon source Minimal medium was supplemented with amino acids (40 μg/ml), uracil (20 μg/ml) or adenine (20 μg/ml) as need. -Ura, -Leu, -Ura-Leu, -Leu-Trp and -Ura-Trp media were from complete medium lacking uracil, lacking leucine, lacking both uracil and leucine, lacking both leucine and tryptophan or lacking uracil and tryptophan, respectively. Both -Ura and -Ura-Trp were supplemented with 0.1% Casamino Acids (Difco).

**Antisera and reagents**. Rabbit polyclonal antisera were specific for the carboxy-terminal portion of Ste2 (Konopka *et al.*, 1988). A mouse monoclonal antibody (Anti-HA-3F10) conjugated to horseradish peroxidase (HRP) that recognizes the *influenza* hemagglutinin epitope were from Roche, Mannheim, Germany. Mouse monoclonal antibodies against T7 and conjugated to horseradish peroxidase (HRP) were from Novagen, Madison, WI. Mixtures of mouse monoclonal antibodies (Clones 7.1 and 13.1) that recognize the Green Fluorescent Protein (GFP) were from Roche, Mannheim, Germany. Peroxidase-conjugated goat anti-mouse secondary antibodies were from Sigma Chemical Co., St. Louis, MO. The antibodies were used at the concentrations recommended by the supplier. The bovine serum albumin (BSA), chemiluminescence kit Super Signal and UltraLink Immobilixed Streptavidin Plus beads were from Pierce

Chemical Co., Rockford, IL. MTSEA-biotin (2-[(biotinoyl) amino] ethyl methanethiousulfonate) was purchased from Biotium Co., Hayward, CA)

**Genomic DNA preparation.** Genomic DNA was isolated from yeast cells using a DNA isolation kit (Gentra Systems Inc.) with some modifications. 1 ml of an overnight cell suspension in a1.5 ml microfuge tube was spun down at 13000x g for 5 seconds and 300 μl of the cell suspension solution was added to the cell pellet. 5 μl oxalyticase (5 mg/ml) and 5 μl β-mercaptoethanol were added and incubated at 37° C for 30 minutes. Cells were centrifuged at top speed for 1 minute to pellet the cells. Supernatant was removed before adding 300 μl cell lysis solution. 100 μl protein precipitation solution was added to the cell lysate and shaken at high speed for 20 second, and the resulting cell lysate was centrifuged at 13000g for 3 minutes. The supernatant was transferred to a clean 1.5 ml microfuge tube with 300 μl isopropanol. The sample was mixed by inverting gently 50 times and centrifuged at 13000 x g for 1 minute. The supernatant was removed and 300 μl of 70% ethanol was added to wash the DNA pellet. The DNA pellet was collected by centrifugation for 1minute at 13000 x g and air dried for 10 minutes. 50 μl of DNA hydration solution and 1.5 μl RNase were added to the purified DNA sample. DNA was incubated at 37°C for 1 hr and rehydrated at 65°C for one hour.

**Renografin density gradients and purification of plasma membranes.** Yeast cells were grown in selective medium. Membranes were then resolved in renografin density gradients as previously described (Schandel and Jenness, 1994) as modified below.

Renografin-60 was used to replace Renografin-76. Floating gradients were prepared by successively layering 2.05 ml of 34, 30, 26, 22% Renografin solutions that had been prepared by diluting Renografin-60. The gradients were centrifuged for 20h in an SW41 rotor at 30 krpm at 4°C. Fractions containing Pma1p were identified by resolving the proteins by SDS PAGE and staining gels with Commassie Blue. Membranes from the pooled fractions were collected by centrifugation for 90 minutes in the Ti 60 rotor at 50 krpm at 4°C. Membrane pellets were suspended in 300 μl TE50 buffer (50 mM TrisHCl, pH 7.5, 1 mM EDTA) and dispersed with a Dounce homogenizer. The bicinchoninic acid assay (BCA ) was performed to determine the protein concentration.

**Limited trypsin digestion.** The assay was a modification of the method of Bukusoglu and Jenness (1996). Tosylsulfonyl phenylalanyl chloromethyl ketone (TPCK) treated trypsin wass from Sigma. Reaction buffer for trypsin digestion assay contained 1mM magnesium acetate, 0.1 mM dithiothreitol (DTT), 0.1 mM EDTA, 7.6% glycerol and 10 mM morpholinepropanesulfonic acid (MOPS, pH 7.0). The different time points were from separate tubes containing aliquots (2 μg) of membrane protein. Duplicate tubes contained α-factor (final concentration$10^{-8}$ M to 5 x $10^{-6}$ M depending on the experiment). The reaction was started by adding trypsin (final concentration 2 μg/ml). The reaction was performed at 30°C and terminated by adding 15 μl 1 N HCl. Membranes were collected by centrifugation with the Beckman Airfuge at 28 Psi for 20 minutes. Membranes were then suspended at 10 μl denaturation buffer (0.5% sodium dodecyl sulfate (SDS) and 1% β-mercaptoethanol) at 42°C for 20 minutes. 10 μl

endoglycosidase H mix was added to the samples and incubated at 37°C for 45 minutes. Proteins were denatured with SDS sample buffer at 37°C for 10 minutes and resolved on 12% SDS-PAGE and electrophoretically transferred to a polyvinylidene difluoride (PVDF) membrane (Millipore Crop, Bedford Mass). The membrane was probed with horseradish peroxidase (HRP) conjugated monoclonal antibody against the T7 or the HA epitope and visualized by using the chemiluminescence kit (Pierce Chemical Co., Rockford, IL). Trypsin digestion assays using plasma membranes from cells expressing the glycosylation-defective mutant receptors were preformed in a same way except that the endoglycosidase H digestion steps were omitted. At the end of the reaction, membranes were collected by centrifugation, suspended directly in the SDS sample and loaded on SDS-PAGE.

***Fus1-LacZ* assay (β-galactosidase assay).** Yeast cells were grown to exponential phase overnight in the selective medium. The density of the culture was estimated spectrophotometrically. The cultures were diluted to the $10^7$ cells/ml, and then 1 ml of a cells suspension was treated with α-factor (0, $10^{-9}$ M and $10^{-7}$ M) for 2 hours at 30° C. Each reaction was performed in duplicate. Inductions were terminated by the addition of 10 μl 10 mg/ml cycloheximide. Cells were collected by centrifugation, and the pelleted cells were suspended in 4 ml Z buffer (10 mM KCL, 1 mM $MgSO_4$, 0.1 M sodium phosphate, pH 7) with 1.5 ml of the cell suspension was added to 750 μl ZSB buffer (Z buffer with 50 mM β-mercaptoethanol and 0.01% SDS). Cells were permeabilized and votexed vigorously by adding 60 μl chloroform. 200 μl of 4 mg/ml colorimetric

substrate, *0*-nitrophenol-β-galactropyranoside (ONPG), was added to the permeabilized cells and incubated at 28° C for 30 minutes. Reactions were terminated by adding 500 μl 1M sodium carbonate. Cell debris was removed by centrifugationat 2 krpm for 10 minutes. The supernatant was transferred to a new tube to measure $A_{420}$. Units of activity were calculated by using the formula of (1000 x $A_{420}$ of reaction) ÷ ($A_{600}$ of culture x volume [in ml] of culture used x time of reaction [in min]). Units of activity were ($A_{420}$ x1000)÷ ($A_{600}$ x 1.5 ml x 30 min) = $A_{420}$ x 22.2÷$A_{600}$.

**α-Factor sensitivity (Halo) assay.** Yeast cells were grown in exponential phase overnight in the selective medium. Cell density was estimated spectrophotometrically as $A_{650}$. 5 x $10^6$ cells were added to 4 ml of 0.7% melting soft agar at about 42° C and then spread onto solid selective medium. Four different concentrations of α-factor 5 x $10^{-5}$, 2.5 x $10^{-5}$, 1.25 x $10^{-5}$ and 0.625 x $10^{-5}$ M were used for each strains to be tested. 20 μl of α-factor at the different concentrations was added to the sterile filter discs, and the saturated discs were immediately placed on the surface of the agar plates. The plates were incubated at 30°C for two days.

**Quick screen for Ste2.** This method was developed as a rapid and convenient way to detect the Ste2 protein. Cells were grown in selective media overnight. The saturated culture was diluted ten fold with fresh medium and cultured for an additional 4 hours. The cell culture density was determined at $A_{650}$, and 2.5 x $10^7$ cells were collected. Cell pellets were suspended in ice-cold membrane buffer (50 mM Tris HCl, 1 mM EDTA,

10 mM $NaN_3$ and 10 mM KF). Cells were spun down and supernatant were removed completely. 200 μl of sample buffer (Schandel and Jenness, 1994) was added to the pellet. Glass beads were added to the cells, and tubes containing cells were homogenized by vortexing at high-speed for 10 minutes. The samples were resolved by 12% SDS-PAGE and transferred to a PVDF membrane (Millipore Crop, Bedford Mass). The membrane was probed with anti-Ste2-carboxy-terminal antisera and then probed with HRP goat anti-mouse antibody. Results were visualized by the chemiluminescence kit from Pierce Chemical Co., Rockford, IL.

**MTSEA-labeling, immobilization, membrane preparation and immunoblots.** Whole-cell MTSEA-labeling in this study was based on the method of Hauser et al (Hauser et al., 2007) with some modifications. Plasmids encoding constructs such as Ste2-Y106C-HA and Ste2-Y106C, F204S-HA were transformed into yeast strains DJ213-7-3, DJ484-1 and DJ485-1. The chromosomal *STE2* locus in yeast strains DJ484-1 and DJ485-1 was under the control of the constitutive *GPD* promoter. Cells were cultured in selective media overnight at 30° C (strain DJ213-7-3) or 34° C (strains DJ484-1 and DJ485-1). Cells were harvested at mid-log phase, washed once and suspended in phosphate-buffered saline (PBS; 10 mM $Na_2HPO_4$, 1.5 mM $KH_2PO_4$, 3 mM, 150 mM NaCl, pH 7.4). The cells were suspended and the optical density ($OD_{600}$) was adjusted to 20-30 OD units in the final volume of 1ml. Following a 30 min incubation on ice in the presence or absence of α-factor, cells were warmed to room temperature. Cells were labeled with MTSEA-biotin (2-[(biotinoyl) amino] ethyl

methanethiousulfonate; Biotium, Hayward, CA) at a final concentration of 0.1 mM. The reaction was stopped after 2 minutes by the addition of 1 M HCl to a final concentration of 10 mM and incubated on ice for 5 minutes. MTSEA-biotin treated cells were pelleted, suspended in 400 μl of PBS and lysed with glass beads. The supernatant was transferred to a new microfuge tube and followed by a low speed spin (700 x g, 5 min). The resulting supernatant was transferred to another tube and centrifuged at high speed (15000 x g, 30 min). The supernatant was removed and membrane pellet was suspended in 300 μl of PBS buffer. Protein concentration was determined using the Bio-Rad Protein assay (Bio-Rad Laboratories, Hercules, CA). Membranes were solubilized in RIPA buffer (0.1% SDS, 1% Triton X-100, 0.5% deoxycholic acid, 1 mM EDTA in 1X PBS, pH 7.4) incubated at room temperature for 1 hour with end-over-end mixing. Following a high-speed spin (15000 x g, 15 min), the solubilized biotinylated proteins were transferred to a fresh microfuge tube and adsorbed to UltraLink Immobilixed Streptavidin Plus beads (Piece, Rockford, IL) by overnight incubation at 4° C with end-over-end mixing. The beads were washed four times with ice cold RIPA buffer, once with 2% SDS in PBS at room temperature, and followed by a final wash with RIPA buffer. During each wash, the beads were suspended and settled by gravity for 20 minutes. Bound proteins were extracted from beads using SDS sample buffer (10% glycerol, 1% SDS, 0.03% bromophenol blue, 62.5 mM TrisHCl, pH6.8, 5% 2-mercaptoethanol). Following 5-minute incubation at 55° C, The solubilized proteins were resolved by 10% acrylamide SDS-PAGE and transferred to Immobilon™-p membrane (Millipore Corporation, Bedford, MA). The blot was then probed with anti-Ste2-C-terminus or

anti-HA antibodies depending on the experiment. The receptors were detected by developing the blot with the West Pico chemiluminescent detection system (Pierce Biotechnology, Inc., Rockford, IL).

# CHAPTER III

# RECEPTOR INTERACTION DURING LIGAND-INDUCED ENDOCYTOSIS

In the past decade, it has become a common theme that GPCRs exist as homo-oligomeric complexes. Early examples of GPCRs that form oligomers include β2-adrenergic (Hebert et al., 1996), dopamine receptor (Ng et al., 1996; George et al., 2000), opioid receptor (Cvejic and Devi, 1997; Jordan and Devi, 1999), $Ca2^{+}$-sensing receptor (Bai et al., 1997; Bai et al., 1998), GABA receptor (Jones el al., 1998;White et al., 1998), M3 muscarinic receptor (Zhu and Wess, 1998), β2-adrenergic receptor (Hebert et al., 1996), α-factor receptor (Yesilaltay and Jenness, 2000) and somatotatin receptor (Rocheville et al., 2000). The evidence suggesting oligomerization of GPCRs is based on the results of western blot analysis and co-immunoprecipitation assays. Fluorescence resonance energy transfer (FRET) techniques have also been employed to detect associations of GPCR subunits in *vivo* for the β2-adrenergic receptor (Anger et al., 2000) and for the α-factor receptor (Overton and Blumer 2000). The recent evidence showing thatrhodopsin can form two-dimensional arrays of dimers is supported by atomic force microscopy analysis (Fotiadis et al., 2003; Liang et al., 2003). The α-factor pheromone receptor is a member of the G-protein-coupled receptor (GPCR) family. In yeast, binding of α-factor pheromone to its receptor initiates a signal transduction pathway that is

mediated by the action of a heterotrimeric G protein that triggers a protein kinase cascade and ultimately causes cell division arrest in the $G_1$ phase of the cell cycle.

**Endocytosis of the α-factor receptor (Ste2p)**

In the yeast cell, constitutive endocytosis of α-factor receptor takes place at a slow rate but is increased 5-10 fold after α-factor binding during ligand-induced endocytosis. Ste2p is endocytosed and degraded rapidly in the presence of mating pheromone (Jenness and Spatrick, 1986). An amino acid motif SINNDAKSS in the truncated receptor Ste2-T345 has been identified to be required for endocytic activity of Ste2-T345 (Rohrer et al., 1993). The signal SINNDAKSS located in the C-terminal domain has been shown to contain ubiqutination and phosphorylation sites necessary for endocytosis (Hicke and Riezman, 1996; Hicke et al., 1998). Ste2p is ubiquitinated on the lysine residue with a single ubiquitin molecule (Terrell et al., 1998) and this monoubiquitination of Ste2p is sufficient for ligand-induced endocytosis of Ste2p (Terrell et al., 1998). The phosphorylation of Ste2 may be a prerequisite for ubiquitination of Ste2 since a truncated Ste2 mutant with serine to alanine is not ubiquitinated and internalized in the absence or in the presence of α-factor (Hicke and Riezman, 1996; Hicke *et al.*, 1998).

# Results

## Endocytosis complementation between two Ste2 subunits

Previous results from our lab have shown α-factor receptor lacking the endocytosis signal sequence and tagged with GFP (Ste2-T326-GFP) or with the HA epitope (Ste2-T326-HA) undergo internalization when coexpressed with full-length wild-type receptors (Ste2) (Yesilaltay and Jenness, 2000). Likewise, tagged forms of mutant receptors Ste2-S184R, defective in ligand binding, undergo ligand-mediated endocytosis when they are expressed with wild-type receptors (Yesilaltay and Jenness, 2000). In both cases, the co-internalization of mutants and wild-type receptors indicates that oligomeric receptor complexes exist during endocytosis and suggests the possibility that oligomerization of receptors plays a role in endocytosis. My first objective was to test whether oligomeric receptor complexes are endocytosed when the α-factor binding site and the endocytosis signal sequence are contained in the different subunits. For my studies, I used the mutation Ste2-F204S mutant instead of the Ste2-S184R to block α-factor binding because Ste2-F204S leads to a more pronounced defect in the α-factor response as measured by α-factor binding to whole cells (Dosil et al, 2000 and our unpublished observations). The Ste2-T326 truncation mutant (Rohrer et al., 1993) was used to express a Ste2 receptor that lacks the endocytosis signal sequence. Tailless receptor (Ste2-T326) is truncated at residue 326 in the C-terminal cytoplasmic domain (residues 301 through 326). This mutant receptor lacks the SINDAKSS sequence (residues 331 through 339) (Rohrer et al., 1993; Hicke et al., 1998) as well as the other

endocytosis signal sequences present in the C-terminal cytoplasmic domain (Yesilaltay, 2001; Howard *et al.*, 2002). GFP was fused to the C-terminus of one of the mutant receptors in order to monitor its endocytosis when a different untagged receptor is present.

As depicted in Fig. 3-1, fluorescence microscopy was used to monitor the internalization of tailless defective Ste2-T326 and mutant Ste2-F204S-T326 receptors that are tagged with GFP (Ste2-T326-GFP and Ste2-F204S-T326-GFP, respectively). Yeast cells coexpressing tailless Ste2-F204S-GFP and full-length Ste2-F204S served as a negative control (Fig. 3-1, top row). In the absence and presence of α-factor, cells exhibited similar fluorescence both at the plasma membrane and in the vacuole. Fluorescence in the vacuole reflects the slow basal rate of constitutive endocytosis; free GFP remains intact in the vacuole after the Ste2-GFP fusion proteins have been endocytosed and the Ste2 portion of the fusion proteins have been degraded (Li, et al., 1999).

Yeast cells coexpressing tagged tailless Ste-T326-GFP and full-length wild-type Ste2 served as a positive control (Fig. 3-1, second row). Yeast cells coexpressing tagged tailless Ste2-F204S-T326-GFP and wild-type Ste2 served as a second positive control (Fig. 3-1 third row). In the absence of α-factor, both positive control strains showed very similar fluorescence location. In the presence of α-factor, unlike the negative control strain, both strains showed that the fluorescence on the plasma membrane had been reduced significantly and that the fluorescence mostly appeared in internal punctate

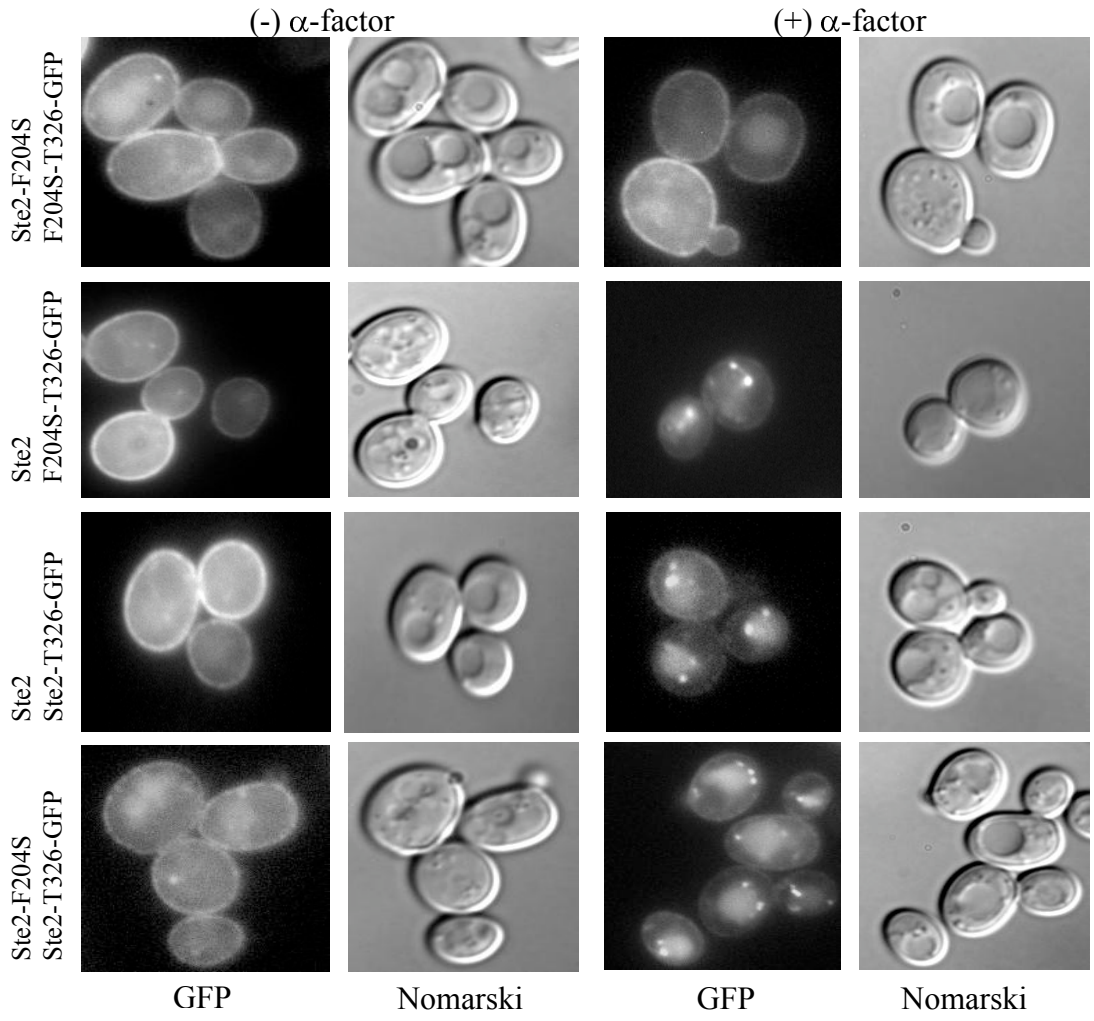


**Figure 3-1**. Ligand-induced internalization of GFP-tagged endocytosis-defective receptors depends on the presence of full-length binding-defective receptors Ste2-F204S or full-length wild-type receptors Ste2. Cultures were treated with cyclohexmide and α-factor for 15 minutes at 30°C. GFP fluorescence images and Nomarski images are indicated below each column; first two columns are cultures lacking α-factor; the last two columns are cultures treated with α-factor. The first row, cells expressed both untagged Ste2-F204S and Ste2-F204S-T326-GFP (strain DJ482-1 containing plasmid pDJ691). The second row, cells expressed both untagged Ste2 and F204S-T326-GFP (strain DJ484-1 containing plasmid pDJ691). The third row, cells expressed both untagged Ste2 and Ste2-T326-GFP (strain DJ484-1 containing plasmid pDJ469). Bottom row, cells expressed both untagged Ste2-F204S and Ste2-T326-GFP (strain DJ482-1 containing plasmid pDJ469).

structures. In the presence of cycloheximide, endocytosed Ste2 is trapped in endocytic compartments that appear as punctate structures.

Interesting, cells coexpressing both tailless Ste2-T326-GFP and the full-length binding-defective mutant Ste2-F204S (Fig. 3-1 bottom row) showed a pattern that was indistinguishable from the positive controls in that the GFP was significantly decreased on the plasma membrane and mostly appeared in the internal punctate structures when α-factor was present. I analyzed the data quantitatively in Table3-1. For cells expressing both Ste2-F204S-T326-GFP and full-length Ste2-F204S, α-factor did not affect the appearance of fluorescence foci, consistent with the inability of either receptor to bind α-factor. In contrast, cells coexpressing both Ste2-T326-GFP and Ste2-F204S over 80% of cells showed more than one focus after α-factor treatment. Similar results were observed for both of the positive controls (Ste2 expressed with Ste2-F204S-T326-GFP and Ste2-F204S expressed with Ste2-F204S-T326-GFP).

This endocytosis complementation results indicated that two mutant subunits in a receptor complex can cooperate during endocytosis if one subunit provides the α-factor binding site (Ste2-T326-GFP) and the other subunit provides the endocytosis signal sequence (Ste2-F204S). Two models are consistent with these results. In one model the ligand-induced change in one subunit is communicated to the neighboring subunit, activating its endocytosis signal sequence. In the other model, the ligand-induced conformational change and the endocytosis signal are recognized independently by the endocytosis machinery. In the first model, the endocytosis signal plays an active role in ligand-induced endocytosis, whereas in the second model the endocytosis signal plays a

Table 3-1. Quantitative summary of fluorescent foci induced by α-factor in the endocytosis complementation assay

| | | Percentage of cells [a] | |
|---|---|---|---|
| Ste2 forms expressed [b] | α-factor | n≥1 | n≥3 |
| Ste2-F204S and Ste2-F204S-T326-GFP | - | 3±2 | 0 |
| Ste2-F204S and Ste2-F204S-T326-GFP | + | 5±3 | 0 |
| Ste2 and Ste2-F204S-T326-GFP | - | 4±3 | 1±1 |
| Ste2 and Ste2-F204S-T326-GFP | + | 77±5 | 16±6 |
| Ste2 and Ste2-T326-GFP | - | 5±4 | 1±1 |
| Ste2 and Ste2-T326-GFP | + | 85±5 | 18±5 |
| Ste2-F204S and Ste2-T326-GFP | - | 4±2 | 1±1 |
| Ste2-F204S and Ste2-T326-GFP | + | 82±4 | 18±3 |

[a] Fluorescent foci were counted based on GFP images of cells. Cells were treated with cycloheximide for 5 minutes and then cultured for 15 minutes in the absence or presence of α-factor. The percentage of cells with one or more fluorescent foci (n≥1) and the percentage of cells with three or more fluorescent foci (n≥3) are indicated on the last two columns. More than 100 cells were examined for each entry. Each entry has been performed twice from two independent experiments, and the error indicates the standard deviation.

[b] The forms of Ste2 expressing in each strain are shown. Strains used are DJ482-1 containing plasmid pDJ691 (rows 1, 2), DJ484-1 containing plasmid pDJ691 (rows 3, 4), DJ484-1 containing plasmid pDJ469 (rows 5, 6) and DJ482-1 containing plasmid pDJ469 (rows 7, 8).
Untagged Ste2 or Ste2-F204S is encoded by a chromosomal allele and GFP-tagged endocytosis-defective Ste2-T326-GFP or Ste2-F204S-T326-GFP is encoded by the low copy number plasmid.

passive role. In order to distinguish between these two models, I investigated whether α-factor binding to one receptor subunit influences the conformational state of other subunits in the receptor complex. To this end, I employed three methods to detect α-factor induced conformational changes in binding-defective receptors when they are coexpressed with binding-competent receptors.

**Conformation changes between two subunits of α-factor receptors**

The α-factor-induced conformational changes can be detected in vitro by subjecting purified plasma membranes to limited trypsin digestion in the presence and absence of α-factor (Bukusoglu, and Jenness, 1996). The influence of α-factor on the rate of specific cleavages can be monitored by using a western blotting assay. Conformational differences in occupied and unoccupied receptors reflect ligand-mediated changes in both the third intracellular loop and in the C-terminal domain. When two different forms of the receptor are expressed simultaneously, it is possible to selectively monitor the one of the two forms of Ste2p by using an N-terminal epitope tag. Previous data have shown that the third intracellular loop is more accessible to trypsin cleavage in the ligand occupied receptor, whereas sites in the C-terminal domain of Ste2 are more sensitive to the trypsin cleavage in the unoccupied receptors (Bukusoglu, and Jenness, 1996).

Fig. 3-2A depicts the trypsin accessibility assay as described by Bukusoglu, and Jenness (1996) except that receptors contained the T7 epitope that had been fused to the N-terminus of the receptor. Plasma membranes that had been purified from yeast cells

producing epitope-tagged receptors were digested with trypsin in the presence and absence of $10^{-8}$ M $\alpha$-factor. At the time points indicated samples were withdrawn, treated with endoglycoside H to remove N-linked carbohydrates and then resolved by using SDS-PAGE. Cleavage products containing the T7 epitope were detected by using western blotting methods. At the initial time point, the undigested membrane preparations contained two electrophoretic species corresponding to full-length receptor (approximately 43 kDa) and a smaller fragment (35 kDa) that apparently resulted from cleavage during membrane preparation. Three trypsin cleavage products were detected during the time course of the reaction. The F2 cleavage product results from cleavage in the C-terminal cytoplasmic domain at a site near the SINNDAKSS endocytosis signal (Bukusoglu, and Jenness, 1996), and the F1 fragment results from cleavage at a distal site in the C-terminal cytoplasmic domain. The F3 fragment results from cleavage in the third intracellular loop of the receptor (Bukusoglu, and Jenness, 1996). Consistent with previous observation (Bukusoglu, and Jenness, 1996), the rate of cleavage at the site near SINNDAKSS sequence was reduced when $\alpha$-factor was present as judged by the slower appearance of the F2 fragment. The rate of cleavage in the third intracellular loop of the receptor was increased when $\alpha$-factor was present, as judged by faster accumulation of the F3 fragment. Similar results were obtained when the membranes contained receptors that were defective for both of the N-linked glycosylation sites at positions N25 and N32 in wild-type receptors in wild-type receptors (Fig. 3-2B). As previously reported (Mentesana and Konopka, 2001) the full-length unglycosylated receptor appears as a doublet band on SDS-PAGE due to a greater level of phosphorylation. It has also been

A

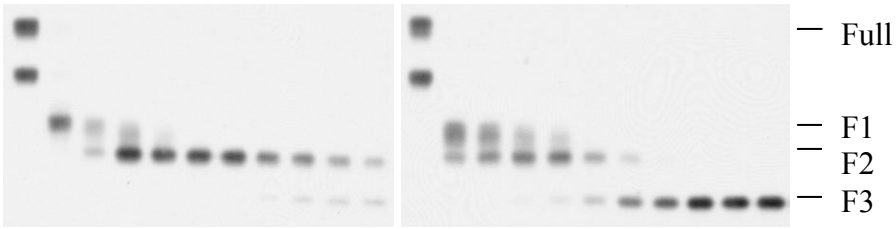
Full
F1
F2
F3
Time(mins) 0 0.5 1 2 4 10 20 30 40 60 90 0 0.5 1 2 4 10 20 30 40 60 90

B

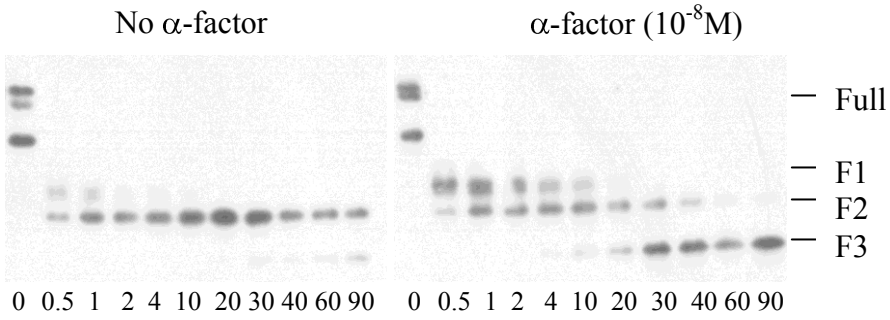
No α-factor
α-factor (10-8M)
Full
F1
F2
F3
Time(mins) 0 0.5 1 2 4 10 20 30 40 60 90 0 0.5 1 2 4 10 20 30 40 60 90

C

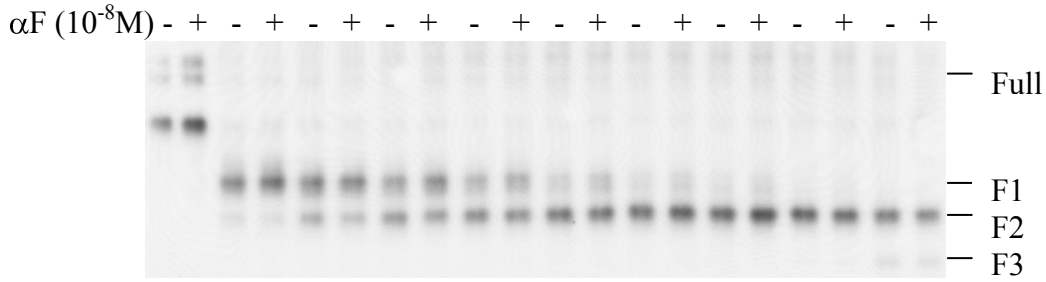
αF (10-8M) - + - + - + - + - + - + - + - + - + - + - +
Full
F1
F2
F3

D

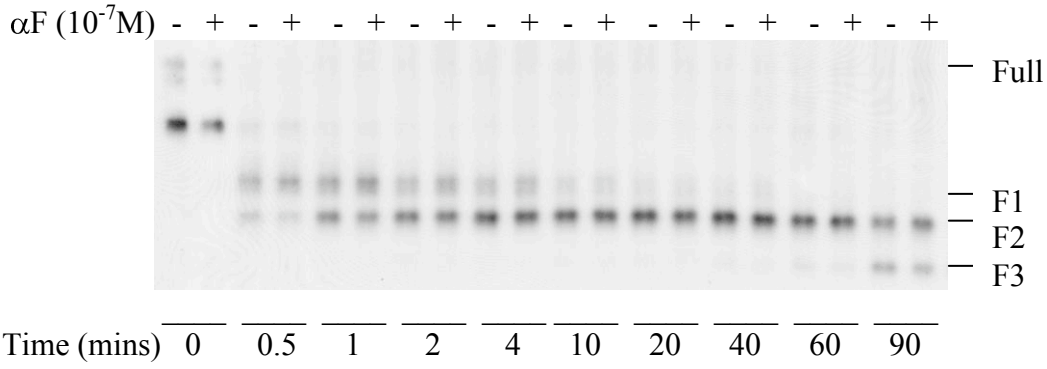
αF (10-7M) - + - + - + - + - + - + - + - + - + - + - +
Full
F1
F2
F3
Time (mins) 0 0.5 1 2 4 10 20 40 60 90

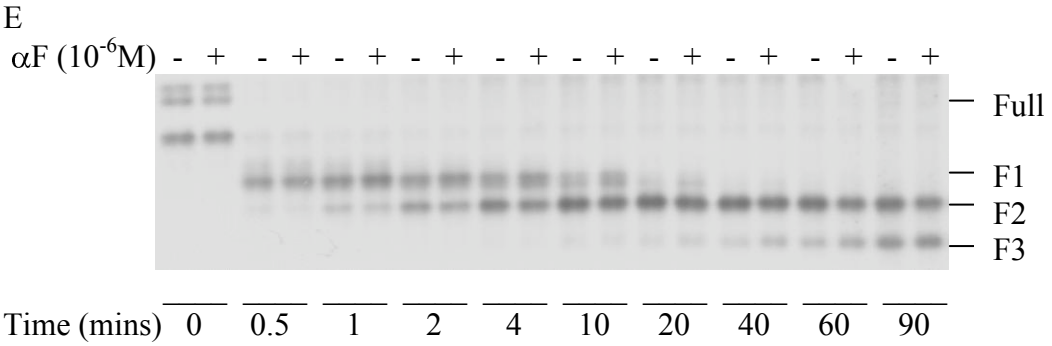


**Figure 3-2.** Limited trypsin digestion assay time course for wild-type and Ste2-F204S mutant receptors. Purified plasma membranes were incubated with trypsin in the absence (-) or presence (+) of α-factor. The resulting cleavage products are analyzed by SDS-polyacrylamide gel electrophoresis (SDS-PAGE) and immunoblotting. The antiserum is against the T7-epitope tag fused to the N-terminus of the receptor.
(A) Membranes were from the strain expressing the wild-type T7-tagged receptor (strain DJ213-7-3 containing plasmid pDJ654. Membranes were treated with endoglycosidase H before SDS-PAGE. (B) Membranes were from the stain expressing wild-type T7-tagged receptors that lacked glycosylation site positions 25 and 32 (T7-Ste2-N25Q,N32Q) (strain DJ213-7-3 containing plasmid pDJ656). (C), (D) and (E) Membranes were from the strain DJ213-7-3 with T7-tagged Ste2-F204S that lacked both glycosylation sites (T7-Ste2-N25Q,N32Q,F204S) (strain DJ213-7-3 containing plasmid pDJ657). Concentrations of α-factor are indicated at the left. Full-length receptor and three major cleavage products (F1, F2 and F3) are indicated at the right. Time points for treatment with trypsin are indicated on the bottom.

shown that mutations affecting the two sites near the receptor N-terminus of Ste2 (N25Q and N32Q) eliminated detectable N-glycosylation of receptors, and the non-glycosylated receptors retain normal function and sub-cellular location (Mentesana and Konopka, 2001).

Ste2-F204S exhibits a strong defect in α-factor binding ($K_D$>$10^{-6}$ M), and it shows a normal subcellular localization and the mutant receptors do not alter the subcellular localization of co-expressed wild-type Ste2 receptors (Dosil et al., 2000). For the Ste2-F204S mutant to be useful, it must be capable of attaining the conformational state that is induced by α-factor. Consistent with this property, Dosil et al (2000) found that the Ste2-F204S mutant cells were responsive to a high α-factor concentration in a cell division arrest (halo) assay and in α-factor induced transcription assays. I tested whether high α-factor concentration ($5x10^{-6}$ M) leads to the altered trypsin digestion pattern that is associated with binding of α-factor to the wild-type receptor. To simplify the analysis, I tested the Ste2-F204S mutant receptors and the binding competent control receptors that lacked both N-linked glycosylation sites and contained the N-terminal T7 epitope tag. After 2 minutes in trypsin, both the Ste2-F204S mutant and the control membrane preparation showed a reduced accumulation of the F2 cleavage product relative to the F1 cleavage products (Fig. 3-3). After 20 minutes in trypsin, both membrane preparations showed increased accumulation of the F3 cleavage product relative to F2 when α-factor was present. These results indicate that Ste2-F204S receptor undergoes ligand-induced conformational changes when the ligand-binding site is occupied at $5x10^{-6}$ M α-factor. At an α-factor concentration less than $5x10^{-6}$ M,

conformational changes in Ste2-F204S were not detected (Fig. 3-2C-E). At the concentration range of α-factor $1x10^{-8}$ M to $10^{-6}$ M, α-factor caused no obvious change in the rate of appearance of the F1, F2 and F3 fragments of T7-tagged unglycosylated Ste2-F204S. In contrast, the ligand induced conformational changes were observed on the T7-tagged unglycosylated wild-type control at the concentration of α-factor as low as $10^{-8}$ M (Fig. 3-2B).

When plasma membranes from cell expressing both wild-type receptors and T7-tagged Ste2-F204S mutant receptors were subjected to the limited trypsin digestion assay, the binding of α-factor to the wild-type receptor was unable to influence the cleavage rates of the trypsin sites in the mutant receptor. Fig. 3-4 compares the results obtained with two different plasma membrane preparations. One preparation was from cells that expressed a normal level of the T7-tagged Ste2-F204S receptors (Fig. 3-4A and 3-4C), and the other preparation was from cells that expressed a normal level of T7-tagged Ste2-F204S receptors and over-expressed wild-type receptors (Fig. 3-4B and 3-4D). As a positive internal control, plasma membranes from cells expressing HA-tagged wild-type receptors were added to both preparations. Each of the two preparations was digested with trypsin in the presence and absence of $10^{-8}$ M α-factor. In Fig. 3-4, this α-factor concentration induced conformational changes in wild-type Ste2 but did not induce conformational changes in Ste2-F204S. Cell membranes containing T7-tagged Ste2-F204S (Fig. 3-4A) alone and for the membranes containing both T7-tagged Ste2-F204S and overexpressed untagged wild-type Ste2 (Fig. 3-4B) resulted in trypsin cleavage patterns that were

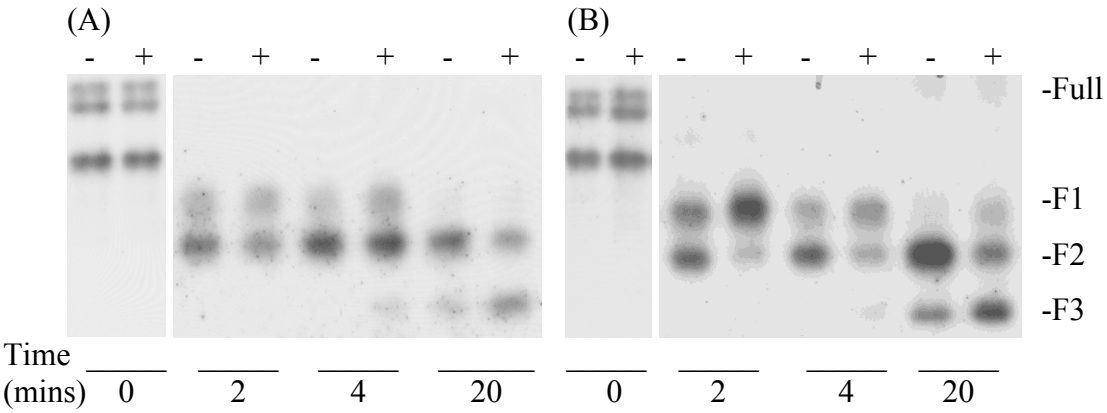


**Figure 3-3.** Binding-defective receptors Ste2-F204S undergo conformational changes in high concentration of α-factor. Purified plasma membranes were incubated with trypsin for the number of minutes in the absence (-) or in the presence (+) of $5x10^{-6}$M α-factor. The resulting cleavage products were analyzed by SDS-PAGE and immunoblotting. The antiserum is against the T7-tag epitope fused to the N-terminus of the receptors. (A) Membranes with T7-tagged binding-defective Ste2-F204S receptors (T7-Ste2-N25Q,N32Q,F204S; strain DJ213-7-3 containing plasmid pDJ657). (B) Membranes with binding-competent T7-tagged receptors (T7-Ste2-N25Q,N32Q; strain DJ213-7-3 containing plasmid pDJ656). Full length and three major cleavage products (F1, F2. and F3) are indicated at the right. The absence (-) and the presence (+) of $5x10^{-6}$ M α-factor are indicated on the top. Time points for treatment of trypsin are indicated on the bottom.

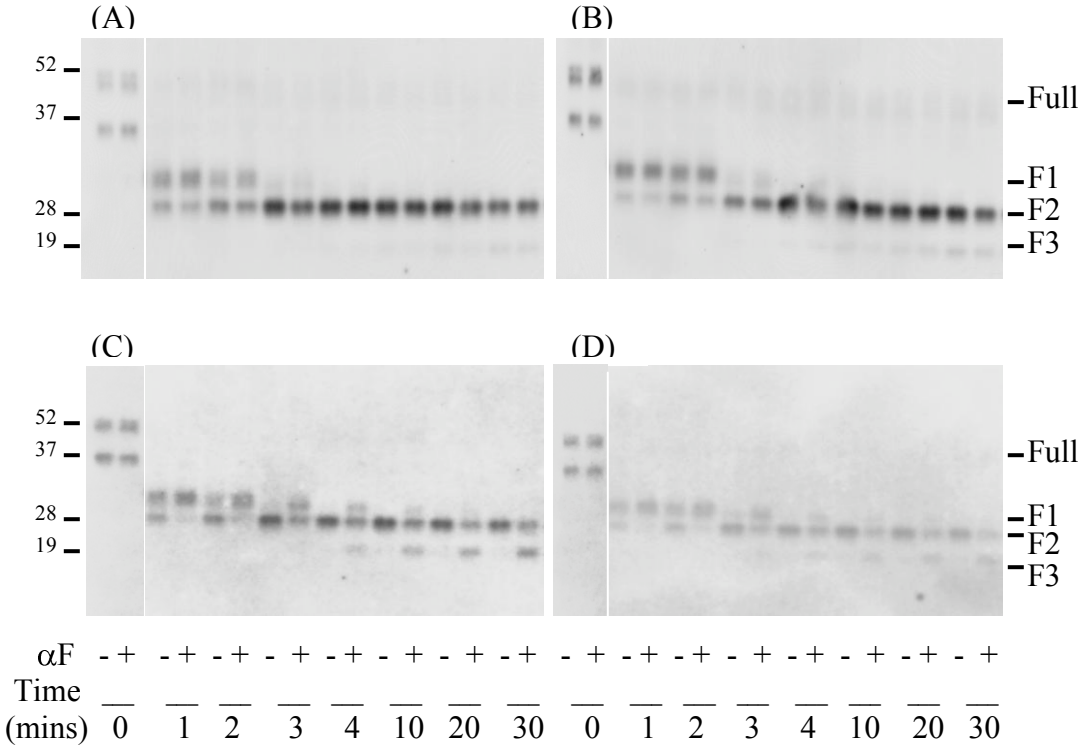


**Figure 3-4.** Limited trypsin digestion time course for co-expressed wild-type and T7-Ste2-F204S mutant receptors. Purified plasma membranes were incubated with trypsin in the absence (-) or presence (+) of α-factor (αF). The resulting cleavage products were analyzed by SDS-PAGE and immoblotting. Digestion reaction I contained membranes from strain DJ213-7-3 expressing T7-Ste2-F204S; DJ213-7-3 containing plasmid pDJ655. Digestion reaction II contained membranes from strain DJ484-1 expressing T7-Ste2-F204S and over-produced wild-type Ste2; DJ484-1containing plasmid pDJ655. Membranes from strain DJ2519 expressing HA-Ste2 were added to both digestion reactions as an internal control. (A) Digestion reaction I probed with anti-T7 antiserum. (B) Digestion reaction II probed with anti-T7 antiserum. (C) Digestion reaction I probed with anti-HA antiserum. (D) Digestion reaction II probed with anti-HA antiserum.

unaffected by α-factor for 30 minute duration of the assay even though the internal control membranes containing HA-tagged wild-type receptors resulted in trypsin cleavage patterns that were altered by the presence of α-factor (Fig. 3-4C and 3-4D). These results suggest that α-factor binding to wild-type Ste2 influences the conformational state; however, these ligand-induced conformational changes do not affect the conformational state of the neighboring subunits in the multimeric complex which can not bind α-factor. It has been shown Ste2-F204S is a dominant-negative mutant that interferes with the functions of the wild-type Ste2 in a dose-dependant manner (Dosil et al., 2000). Therefore, I considered the possibility that Ste2-F204S may interfere with ligand-induced conformational changes in wild-type Ste2 when Ste2-F204S and Ste2 are co-expressed. Fig. 3-5 summarizes reciprocal tests for interactions between mutant and wild-type receptors in the trypsin digestion assay. Membrane from cells expressing untagged wild-type Ste2 and T7-tagged Ste2 (Fig. 3-5A) and from cells expressing untagged Ste2 and T7-tagged binding-defective mutant Ste2$^{-}$F204S (Fig. 3-5B) showed tryptic digestion pattern that were consistent with the results in Figure 3-4 suggesting that ligand-induced conformational changes in wild-type receptors do not influence the conformational state of co-expressed mutant receptors. Membranes from cells expressing untagged Ste2-F204S receptors and tagged receptors (Fig. 3-5D) resulted in ligand-induced changes in the trypsin digestion pattern that were indistinguishable from the results obtained with control membranes from cells expressing only wild-type receptors (Fig. 3-5A). This result indicates that Ste2-F204S does not interfere with ligand-induced conformational changes in wild-type Ste2.

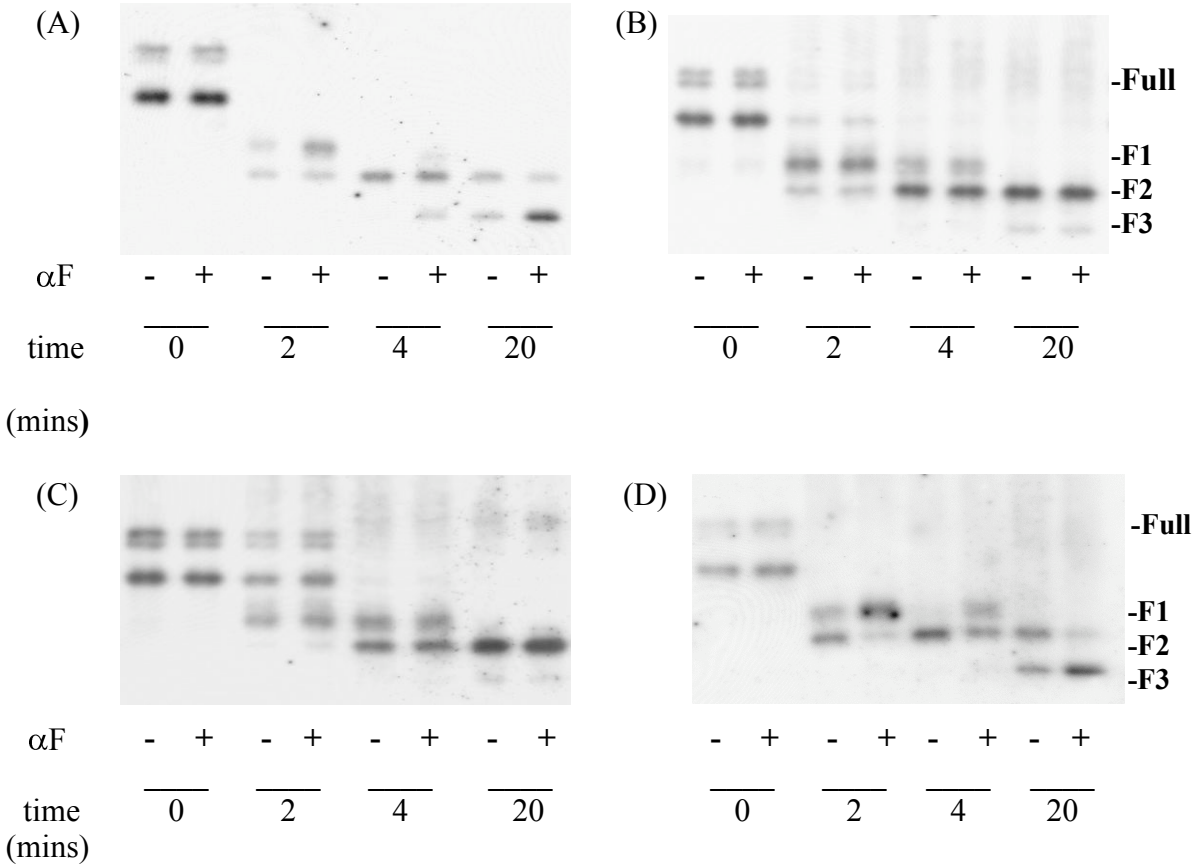


**Figure 3-5.** Conformational changes between two subunits of α-factor receptors on the trypsin cleavage pattern. Membranes were incubated with trypsin in the absence (-) or presence (+) of α-factor (αF). The antiserum was against the T7 epitope-tag fused to the N-terminus of the receptors. Two major glycosylation sites (position on 25 and 32) on T7-tagged Ste2 have been removed by genetic manipulation for experimental convenience. (A) Membranes were from the strain expressing untagged wild-type Ste2 and T7-tagged Ste2-N25Q,N32Q; strain DJ213-7-3 containing plasmid pDJ656. (B) Membranes were from the stain expressing untagged wild-type Ste2 and T7-tagged Ste2-F204S-N25Q,N32Q; strain DJ484-1containing plasmid pDJ657. (C) Membranes were from the strain expressing T7-tagged Ste2-F204S-N25Q,N32Q; strain DJ213-7-3 containing plasmid pDJ657). (D) Membranes were from the strain expressing untagged Ste2-F204S and T7-tagged Ste2-N25Q,N32Q; strain DJ482-1 containing plasmid pDJ656. The resulting cleavage products were analyzed by SDS-PAGE and immunoblotting using anti-T7 antiserum. Three major cleavage products (F1, F2. and F3) are indicated at the right. Time points for treatment of trypsin are indicated on the bottom. All untagged receptors were synthesized under the direction of the GPD transcriptional promoter.

**Signal complementation between Ste2 subunits**

As a functional test for cooperative interactions between α-factor receptors *in vivo*, I tested whether α-factor responsiveness is restored to cells that co-express Ste2-F204S receptors and receptors that fail to couple to the heterotrimeric G-protein. The *ste2-L236H* mutation affects the third intracellular loop of the α-factor receptor. The mutant receptors are partially impaired in signal transduction activity, but they retain the ability to undergo α-factor induced conformational changes and the ability to undergo ligand-induced endocytosis (Weiner *et al.*, 1993; Schandel and Jenness, 1994; Bukusoglu and Jenness, 1996). The *ste2-F204S-T326-GFP* allele was used instead of *ste2-F204S* to avoid the dominant negative phenotype of Ste2-F204S (Dosil *et al.*, 2000). The ability of α-factor to cause cell division arrest was judged by the α-factor halo test (Fig. 3-6). In the assay, a clear zone (halo) in a lawn of **a** cells forms surrounding the α-factor source, due to α-factor-induced cell-division arrest. Larger halos reflect greater α-factor sensitivity. The Ste2-F204S-T326-GFP mutant (Fig. 3-6A) and the Ste2-L236H (Fig. 3-6B) produced halos that were much smaller than the wild-type control strain (Fig. 3-6C). The strain expressing both Ste2-F204S-T326-GFP and Ste2-L236H (Fig. 3-6D) produced halos that were no larger than the strains expressing the single alleles. As judged by this assay, the binding of α-factor to Ste2-L236H receptors was unable to cause significant G protein coupling in the co-expressed Ste2-F204S-T326-GFP receptors. To determine whether ligand-induced changes in Ste2-L236H are propagated to Ste2-F204S-T326-GFP in a shorter term assay, I introduced a plasmid-borne, pheromone-inducible gene, *FUS1-LacZ* gene, into each of the four strains depicted in Fig. 3-6 and then tested for

β-galactosidase after a 60 min α-factor exposure. Table 3-2 indicates that the strain expressing both ste2-F204S-T326-GFP and Ste2-L236H was no more responsive to α-factor than the strains expressing either of the single alleles.

**Detection of conformational changes by substituted cysteine accessibility method**

Whole-cell MTSEA biotin labeling provides an independent assay to test whether ligand-induced conformational changes are propagated to neighboring receptor subunits. Hauser et al (Hauser *et al.*, 2007) first used MTSEA biotin labeling to show that the first extracellular loop of Ste2 undergoes a conformational change upon α-factor binding. They showed that single cysteine residues placed at position 101 or 106 are readily accessible to solvent in the absence but not in the presence of α-factor. The decrease in solvent accessibility is not due to direct steric hindrance by the ligand since the antagonist, desTrp,Ala3-α-factor, does not significantly alter reactivity of cysteine residues at either position (Hauser *et al.*, 2007). Our laboratory has shown that desTrp,Ala3-α-factor binding does not cause the α-factor-induced conformational changes in the receptor that are detected by limited trypsin digestion (Bukusoglu and Jenness, 1996). To determine whether α-factor binding to one receptor affects the accessibility of a cysteine residue at position 106 in an adjoining receptor, I tested whether the HA-tagged binding-defective mutant receptor, Ste2-Y106C, F204S-HA, undergoes α-factor-induced conformational changes when over-produced wild-type Ste2 is present in the same cell. In control experiments, I showed that cysteine accessibility of the binding-proficient Ste2-Y106C-HA receptor was sensitive to α-factor, whereas

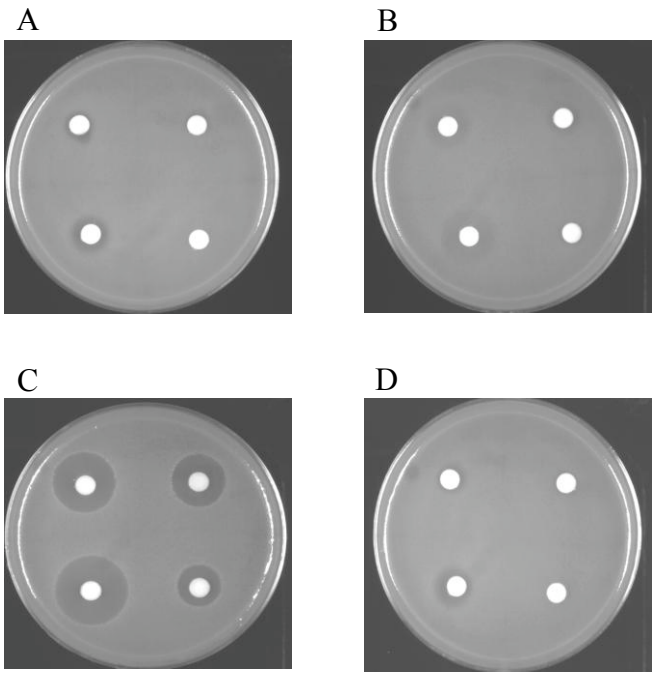


**Figure 3-6.** Complementation test for the Ste2-L236H and Ste2-F204S-T326-GFP alleles in cell division arrest assay. Each filter disk containing different amount of α-factor (1, 0.5, 0.25 and 0.125 nmol, proceeding clockwise from bottom left) were placed on a lawn of indicated yeast cells and incubated for 2 days at 30°C. (A) Strain DJ213-7-3 containing plasmid pDJ691 (Ste2-F204S-T326-GFP). (B) Strain DJ901-A-1 containing plasmid pDJ303 (Ste2-L236H). (C) Strain 211-5-3 containing plasmid pDJ303 (wild-type Ste2). (D) Strain DJ901-A-1 containing plasmid pDJ691 (Ste2-L236H/Ste2-F204S-T326-GFP).

Table 2-2. Signal complementation between different subunits of Ste2 receptors in the α-factor induced *Fus1-LacZ* assay.

| | β-galactosidase activity units[a] | |
|---|---|---|
| Ste2 receptor[b] | No α-factor | $10^{-8}$M α-factor |
| STE2 | 1.09±0.09 | 42.95±3.18 |
| Ste2-L236H | 1.08±0.07 | 2.06±1.42 |
| Ste2-F204S | 1.15±0.09 | 1.22±0.01 |
| Ste2-L236H/ Ste2-F204S-T326-GFP | 1.10±0.02 | 1.10±0.04 |

[a] The measurement of β-galactosidase activity units was described in the materials and methods. Duplicate assay measured β-galactosidase activity in permeabilized cells in two independent experiments. The average activity and the standard deviation are shown.

[b] Strains are DJ211-5-3 containing plasmid pDJ124 and pDJ203 (wild-type Ste2), DJ901-A-1containing plasmids pDJ124 and pDJ203 (Ste2-L236H/ Ste2-F204S-T326-GFP), DJ1378-A-1 containing plasmid pDJ203 and pDJ691 (Ste2-F204S-T326-GFP) and DJ1378-A-1 containing pDJ203 and pDJ491 (Ste2-F204S-T326-GFP).

cysteine accessibility of the Ste2-Y106C, F204S-HA was not sensitive to α-factor when it was expressed alone (Fig. 3-7A). Cysteine accessibility of the Ste2-Y106C-HA receptor remained sensitive to α-factor when Ste2 or Ste2-F204S were over-expressed in the same cell (Fig. 3-7B). However, cysteine accessibility of the Ste2-Y106C,F204S-HA receptors was not influenced by α-factor when either Ste2 or Ste2-F204S were over-expressed (Fig. 3-7B). These results are consistent with the trypsin digestion assay (Fig. 3-4 and Fig. 3-5), indicating that binding-defective Ste2-F204S receptors do not undergo ligand-induced conformational changes when they are allowed to form oligomers with wild-type Ste2 receptors. In addition, the failure of Ste2-F204S to impart a dominant-negative effect on ligand-induced changes in Ste2-Y106C (Fig. 3-7, lanes 5 and 6) is consistent with the results from the limited trypsin digestion assay (Fig. 3-5), supporting the view that the dominant-negative phenotype of the Ste2-F204S mutation results from G protein competition and not from direct interaction of mutant and wild-type receptors (Dosil *et al.*, 2000).

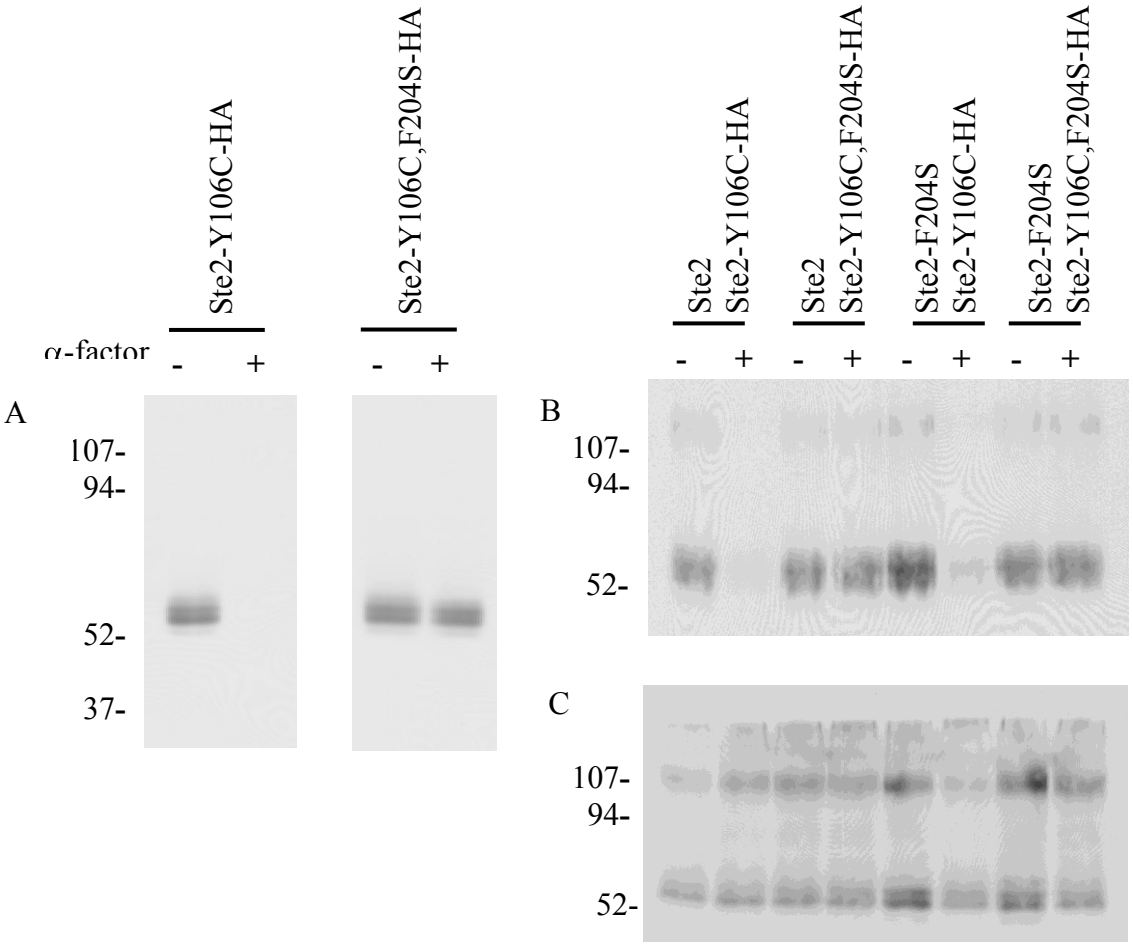


**Figure 3-7.** Whole-cell MTSEA-labeling of receptors containing cysteine at position 106. Cells were labeled with MTSEA in the absence (-) or presence (+) of $10^{-5}$M α-factor. Detergent solubilized receptors that had been labeled with MTSEA were collected on avidin beads and analyzed by SDS-PAGE and immunoblotting with anti-HA antiserum. (A) Strains were DJ213-7-3 containing plasmid pDJ683 (Ste2-Y106C-HA) and strain DJ213-7-3 containing plasmid pDJ684 (Ste2-Y106C,F204S-HA). (B) Plasmids encoding Ste2-Y106C-HA or Ste2-Y106C, F204S-HA were intrdouced into the strains expressing wild-type or Ste2-F204S under the direction of the *GPD* transcriptional promoter. Strains were DJ484-1 containing plasmid pDJ 683 (Ste2/Ste2-Y106C-HA), DJ484-1 containing plasmid pDJ684 (Ste2/Ste2-Y106C, F204S-HA), DJ482-1 containing plasmid pDJ683 (Ste2-F204S/Ste2-Y106C-HA), and DJ482-1 containing plasmid pDJ684 (Ste2-F204S/Ste2-Y106C,F204S-HA). (C) Total protein control for (B) Total detergent solubilized receptors were analyzed before the avidin purification step. Immunoblots are developed with anti-HA antiserum. Molecular weights of the marker are indicated in kDa at the left.

## Discussion

The ligand-induced conformational change and the endocytosis signal are required for efficient receptor internalization. In this study, I showed that the receptor lacking the endocytosis signal sequence (Ste2-T326-GFP) was endocytosed when expressed with a ligand-binding-defective receptor (Ste2-F204S) containing an endocytosis signal sequence. The result suggests that the endocytosis signal can be recognized *in trans* in the heterooligomers. In addition lack of conformational coupling between subunits of Ste2 suggests that the endocytosis signal plays a passive role in ligand-mediated endocytosis.

Previously, the coimmunoprecipitation data from our lab (Yesilaltay and Jenness, 2000) and the FRET assay data from others (Overton and Blumer, 2000) indicated that homo-oligomeric complexes of Ste2p are subject to ligand-induced endocytosis. In this study, I first explore the functional significance of oligomeric α-factor receptor complexes in the budding yeast *Saccharomyces cerevisiae*. Results from my endocytosis complementation assay indicated that the subunits of the α-factor receptor cooperate during ligand-mediated endocytosis. I showed that receptors that lack the endocytosis signal sequence (Ste2-T326-GFP) were endocytosed when coexpressed with a ligand-binding-defective receptor (Ste2-F204S) that contains the endocytosis signal sequence. Several approaches were applied to determine whether α-factor binding to one subunit influences the conformational state and activity of neighboring subunits that cannot bind α-factor. *In vitro* limited trypsin digestion assays and substituted cysteine

accessibility assays showed that α-factor binding does not influence the conformational state of neighboring subunits that are unable to bind α-factor. The *in vivo* signal complementation test also showed that the receptor mutant (Ste2-L236H) that cannot couple to the G protein failed to complement the α-factor binding mutant receptor Ste2-F204S-T326-GFP. In the present study, I show that the endocytosis signal sequence and the α-factor binding site participate in ligand-induced endocytosis when they are located in different subunits of the receptor complex, and I present evidence indicating that α-factor binding to one subunit fails to affect the conformational state of other subunits in the receptor complex. I conclude that the ligand-induced endocytosis machinery recognizes at least two parts of Ste2 for efficient endocytosis. In one part of the receptor (the transmembrane domain), the α-factor induced conformational change is detected by the endocytosis machinery. In the C-terminal cytoplasmic domain, the endocytosis signal sequence plays an essential role in endocytosis without undergoing a ligand-medicated change in conformation. Taken together, the results indicate that the endocytosis signal promotes endocytosis of mixed receptor complexes even when the receptor containing the endocytosis signal does not undergo a ligand-induced conformational change. Therefore the endocytosis signal sequence apparently plays a passive role in endocytosis. My results are consistent with a model in which the ligand-induced endocytosis machinery recognizes at least two parts of Ste2 for efficient internalization: a) an α-factor induced conformational change in at least one subunit of a receptor complex and b) the presence of an endocytosis signal sequence in at least one subunit. The ability of the endocytosis signal to act in *trans* indicates that recognition of

signal and the recognition of the ligand-induced conformational change are likely to be independent events.

Dominant-negative mutants such as Ste2-F204S interfere with the functions of the wild-type Ste2 in a dose-dependant manner and may be a general feature of mutant receptors that cannot bind α-factor (Dosil *et al.*, 1998; Leavitt *et al.*, 1999). The dominant-negative effect is associated with its C-terminal domain since removal of C-terminal domain of the receptor diminishes the dominant-negative effect (Dosil *et al.*, 2000). The dominant-negative effect is consistent with the sequestration of G-protein by the mutant receptors since it can be reversed by coordinately overexpressing the G protein subunits. As yet, no published study has tested whether the domiant-negative receptors exert the negative influence directly among subunits in the oligomeric receptor complex. Results from the limited trypsin digestion assay (Fig. 3-5) argue against the possibility that Ste2-F204S negatively influences the activity of wild-type Ste2 since no obvious changes in the trypsin digestion pattern of wild-type Ste2 were observed when Ste2-F204S was also present.

Two assays were used test whether ligand-induced conformational changes are propogated from occupied receptors to unoccupied receptors. Together, the two assays probe three different sites on the receptors and each of the assays has distinct advantages. The trypsin digestion provides informative data for detecting changes in protein conformation *in vitro* (Bukusoglu and Jenness, 1996). It has the advantage that it probes functionally significant sites that have been implicated in G-protein coupling (intracellular loop 3) and endocytosis (sites near the SINNDAKS sequence). The

substituted cysteine accessibility assay has the advantage that it detects receptor changes in whole cells and is not subject to potential problems arising from the cell-free assay. However, this assay monitors receptor changes that occur on the external face of the membrane.

In contrast to my results, complexes of the G protein coupled receptor BLT1 have been shown to undergo cross-conformational changes induced by agonist binding. Damien et al (2008) produced heterodimeric receptor complexes with wild-type BLT1 and a BLT1/ALXR chimera, where the BLT1 subunit is activated by the BLT4 ligand and the BLT1/ALXR chimera is activated by ALXR agonists. They detected a BLT4-induced conformational changes in BLT1/ALXR as increased fluorescence of sole tryptophanyl residue located in the sixth transmembrane domain of the chimeric subunit. Despite the cross-conformational change, BLT4 was unable to promote G-protein coupling to the chimeric subunit when the coupling defective mutant receptor ($BLT_{i3\text{-}1}$) replaced BLT in the heterodimeric complex. Therefore, although agonist binding to one of the receptor subunits leads to a conformational change in the other subunit, this conformational change in the agonist-free protomer is not associated with G protein activation (Damian *et al.*, 2008).

Chinault et al (2004) used a very similar approach in the signal complementation assay by co-expressing the G protein coupling-defective Ste2-L236R and the truncated tailless ligand binding-defective mutant Ste2-S184R. No complementation between two subunits was detected. This result is also consistent with the view that each subunit is activated independently in the Ste2 oligomeric complex. The Ste2-S184R is also a

dominant-negative Ste2 mutant and the ligand-binding defect is less characterized. Significantly, S184R substitution does not appear directly reduce α-factor binding since I have found that Ste2-S184R still shows ligand-induced conformational changes dected by trypsin digestion of α-factor concentrations is as low as $10^{-8}$M (data not shown). Therefore the S184R may result in conformational constraints in the receptor that are relieved in the isolated membranes. The Ste2-F204S receptors show a stronger α-factor binding defect and resist α-factor induced changes in isolated membranes (see Chapter 3). My results showing that Ste2-L236H fails to promote trans-activation of Ste2-F204S in the signal complementation assay are consistent with the results of Chinault et al (2004).

Interestingly, Chinault et al (2004) observed partial *trans* signal complementation when cells co-expressed two mutants affecting the intercellular loop 1 and 3. The L236R mutant affects loop3, the ic1A mutant substitutes almost all the amino residues in intercellular loop 1 with alanine and the 80-2A mutant replaces three amino acids with alanine residues in the cytoplasmic-proximal portions of TMII (Chinault *et al.*, 2004). The results indicated that complementation occurred between the L236R and ic1A mutants as well as between the L236R and the 80-2A mutants. However the mechanism for the partial complementation remains unclear. Chinault et al (2004) suggests that one G-protein binds to a receptor dimer. Unfortunately, Chinault et al do not address the mislocalization of both the Ste2-ic1A and the Ste2-80-2A mutants that accumulate in the ER and vacuole respectively. It is possible that partial signal complementation may be due to improved cell surface targeting of hetero-oligomers.

Taken together, my results are consistent with a model in which conformational changes and recognition of the endocytosis signal sequence are independent events. Fig. 3-8A depicts a simple alternative model where ligand-induced changes in the receptor are directly linked to changes in the endocytosis signal. For this model to explain the endocytosis complementation reports (Fig. 3-1), conformational signals that result from α-factor binding to one subunit must be propagated to the neighboring subunit (Fig. 3-8B). However results from the limited trypsin digestion assay and the substituted cysteine accessibility assay indicate that no cross-conformational changes occur within the dimeric complex. I conclude that the ligand-induced conformational changes among subunits in the oligomeric complex are likely to occur as independent events and that the endocytosis signal sequence plays a passive role in the process. The endocytosis machinery must recognize both signals in the Ste2 oligomeric complexes for the efficient ligand-induced internalization. Therefore, I rule out the model depicted in Fig. 3-8A and 3-8B. An example of a model that is consistent with my results is shown in Fig. 3-8C. In this model, truncated Ste2-T326 is activated upon α-factor exposure and the conformational changes are recognized by elements of the endocytic machinery. The protein kinase is recruited in this complex and leads to the phosphorylation of the endocytosis signal sequence in Ste2-F204S. The phosphorylated Ste2-F204S is thought to lead ubiquitination of the signal sequence and to subsequent steps in endocytosis. It is also possible that recognition by the endocytic machinery causes the receptors to move to another location in the cell where phosphorylation and ubiquitination occur.

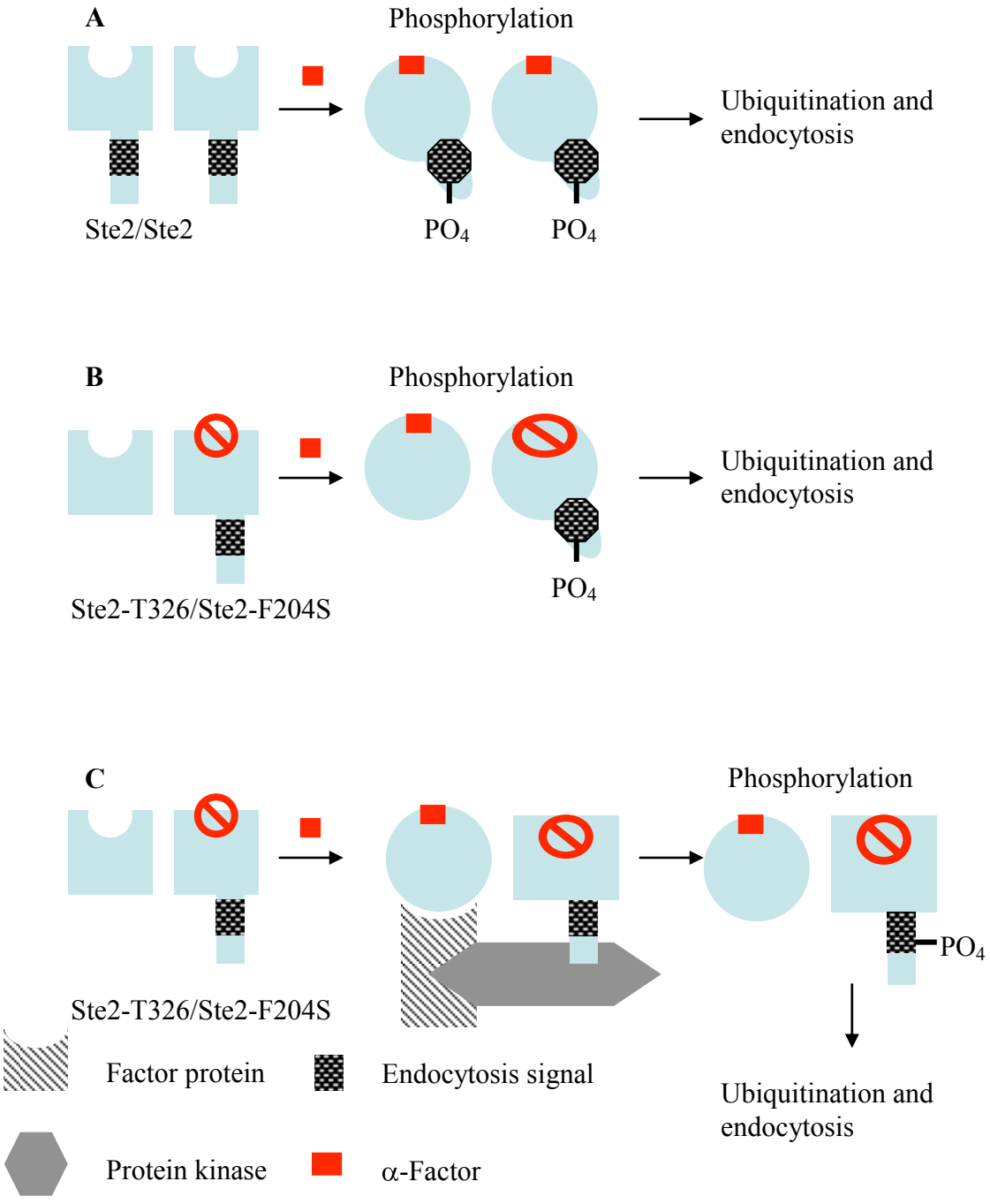
A
Phosphorylation
Ubiquitination and endocytosis
Ste2/Ste2
PO4
PO4
B
Phosphorylation
Ubiquitination and endocytosis
Ste2-T326/Ste2-F204S
PO4
C
Phosphorylation
PO4
Ste2-T326/Ste2-F204S
Ubiquitination and endocytosis
Factor protein
Endocytosis signal
Protein kinase
α-Factor

**Figure 3-8.** Models for the ligand-induced endocytosis between Ste2 subunits. (A) In the presence of α-factor, wild-type Ste2 receptors undergo conformational changes that lead to the phosphorylation in the C-terminus by recruiting the factor protein and the protein kinase. The phosphorylated Ste2 receptors are ubiquitinated and subject to the ligand-induced endocytosis. (B) In the presence of α-factor, the cross-conformational changes occur between truncated wild-type Ste2 and full-length binding-defective Ste2-F204S, which allows Ste2-F204S become active for subsequent phosphorylation and ubiquitination. Therefore, the heterooligomers of truncated Ste2 and Ste2-F204S are subject to the ligand-induced endocytosis. (C) In the presence of α-factor, there are no cross-conformational changes occur between truncated wild-type Ste2 and full-length binding-defective Ste2-F204S. Instead, the factor protein recognizes the conformational changes upon the α-factor exposure on the truncated Ste2. The protein kinase is recruited and phosphorylates the neighboring Ste2-F204S subunit that leads to its ubiquitination and endocytosis. Both the truncated Ste2 and Ste2-F204S are internalized by forming heterooligomeric complexes. The factor protein, protein kinase, endocytosis signal and α-factor are shown.

# CHAPTER IV

# ISOLATION OF ER EXPORT-DEFECTIVE MUTANTS AND REQUIREMENTS FOR STE2 ER EXIT

New *ste2* mutants were isolated in order to explore the factors that contribute to receptor oligomerization and the exit of newly synthesized α-factor receptors from the ER. α-factor receptors form homo-oligomeric complexes that are the functional units of endocytosis based on co-internalization, co-immunoprecipitation and the fluorescence energy transfer (FRET) (Overton and Blumer, 2000; Yesilaltay and Jenness, 2000). Treatment of cultures with α-factor has little effect on the extent of oligomerization based on the efficiency of co-immunoprecipitation and sedimentation behavior of the receptor complexes (Yesilaltay and Jenness, 2000). The C-terminal cytoplasmic tail of Ste2 is not required for oligomerization since truncated Ste2 still forms dimers as judged by co-immunoprecipitation experiments. However, the functional significance of oligomerization in α-factor receptors remains unclear. In addition, no satisfactory methods exist for blocking oligomerization in *vivo*. In order to further our understanding of the biological significance of Ste2 oligomerization, I applied several approaches to identify mutant receptors that are likely to be defective in oligomer formation. Oligomerization-defective mutants were sought by screening for random mutations of the *STE2* gene. Potential relationships between ER retention and oligomerization of Ste2

were investigated by screening for ER retention mutants and complementation-defective mutants.

# Results

## Construction of a pool of random mutations in *STE2* coding sequence

All of the mutant isolation procedures performed in this study involved screening strains expressing mutant variants of the truncated receptor, Ste2-T326-GFP. When expressed alone, most of the Ste2-T326-GFP receptors accumulate in the plasma membrane due the lack of an endocytosis signal sequence, and a smaller portion of the Ste2-T326-GFP receptors are retained, at least transiently, in the ER (Yesilaltay, 2001). The cellular localization of Ste2-T326-GFP receptor is unaffected by the presence of α-factor in the culture. When Ste2-T326-GFP receptor is coexpressed with the untagged wild-type receptor, they exit the ER efficiently, and they are subject to ligand-mediated endocytosis when they reach the plasma membrane (Yesilaltay, 2001). Random mutations were introduced into the *ste2-T326* gene by using mutagenic PCR, the open reading frame from codon 47 through codon 326 was cloned into a yeast centromeric plasmid pDJ469 that encodes Ste2-T326-GFP, and pools of *E. coli* transformants were obtained. The mutation frequency was determined by DNA nucleotide sequencing of representative transformants. Pools containing different substitution rates were constructed to increase the chance of obtaining potentially rare oligomer-defective mutants.

**Endocytosis mutant screening**

For the endocytosis mutant-screening strategy, cells that over-express wild-type untagged receptors were transformed with a pool of plasmids expressing mutant Ste2-T326-GFP receptors, and the transformants were screened for failure of the Ste2-T326-GFP receptors to undergo ligand-mediated endocytosis. The desired mutant cells were expected to retain fluorescence on the plasma membrane suggesting a loss in the ability of Ste2-T326-GFP to form oligomers with wild-type receptors. This screening strategy was based on two assumptions. First, oligomerization of Ste2 is not required for ER export. Second, the failure to internalize is due to a failure to form heterodimers with wild-type Ste2 and not to a dominant defect that blocks endocytosis of the heteromeric complex. Plasmids containing the mutagenized *ste2-T326* gene were introduced into yeast cells that over-produced wild-type Ste2 due to the insertion of the *GPD1* transcription promoter at the chromosomal *STE2* locus. The transformant colonies were incubated in the liquid medium overnight and then exposed to α-factor. More than 3000 isolates were tested and none satisfied the criterion described above. The result indicated that either one or both of the assumptions were incorrect or that specific oligomerization mutants are very rare, possibly requiring multiple mutations in the *STE2* gene.

**Relationship between Ste2 dimerization and endoplasmic reticulum export**

Previous observations have indicated that the export of Ste2 from the ER is potentially related to the C-terminal cytoplasmic domain of the receptor and to receptor oligomerization. Fluorescence microscopy has shown that the truncated Ste2-T326-GFP

receptor exhibit trace peri-nuclear localization (i. e., ER localization) when expressed alone, but the peri-nuclear GFP signal disappears when the cells express both Ste2-T326-GFP and full-length Ste2 (Yesilaltay and Jenness, 2000). *STE2* mutations that affect a suspected dimerization motif ($^{56}$GxxxG$^{60}$) in TM1 cause reduced receptor oligomerization as judged by the FRET assay, and they cause truncated receptors to be retained in the ER to a greater extent than the wild-type truncated receptors (Overton and Blumer, 2002; Overton *et al.*, 2003). Full-length receptor mutants exit the ER and appear in the vacuole or on the cell surface, even though they contain defects in the $^{56}$GxxxG$^{60}$ motif.

These observations raised an intriguing possibility that at least two independent signals promote the export of Ste2 receptors from the ER. First, the C-terminal domain of Ste2 may serve as one signal in facilitating proper cell surface expression of the Ste2 protein. Second, since tailless wild-type Ste2p reaches the cell surface, the proper conformation of the main body of Ste2 may also provide a signal for receptor trafficking. In order to investigate the correlation between Ste2 dimerization and ER trafficking, I applied two different mutant isolation strategies depicted in Fig. 4-1: the ER retention mutant screening method and the complementation mutant screening method.

**Complementation mutant screening**

The Ste2-S184R muntant was employed in the complementation screening strategy. This allele encodes a full-length receptor that is specifically defective in

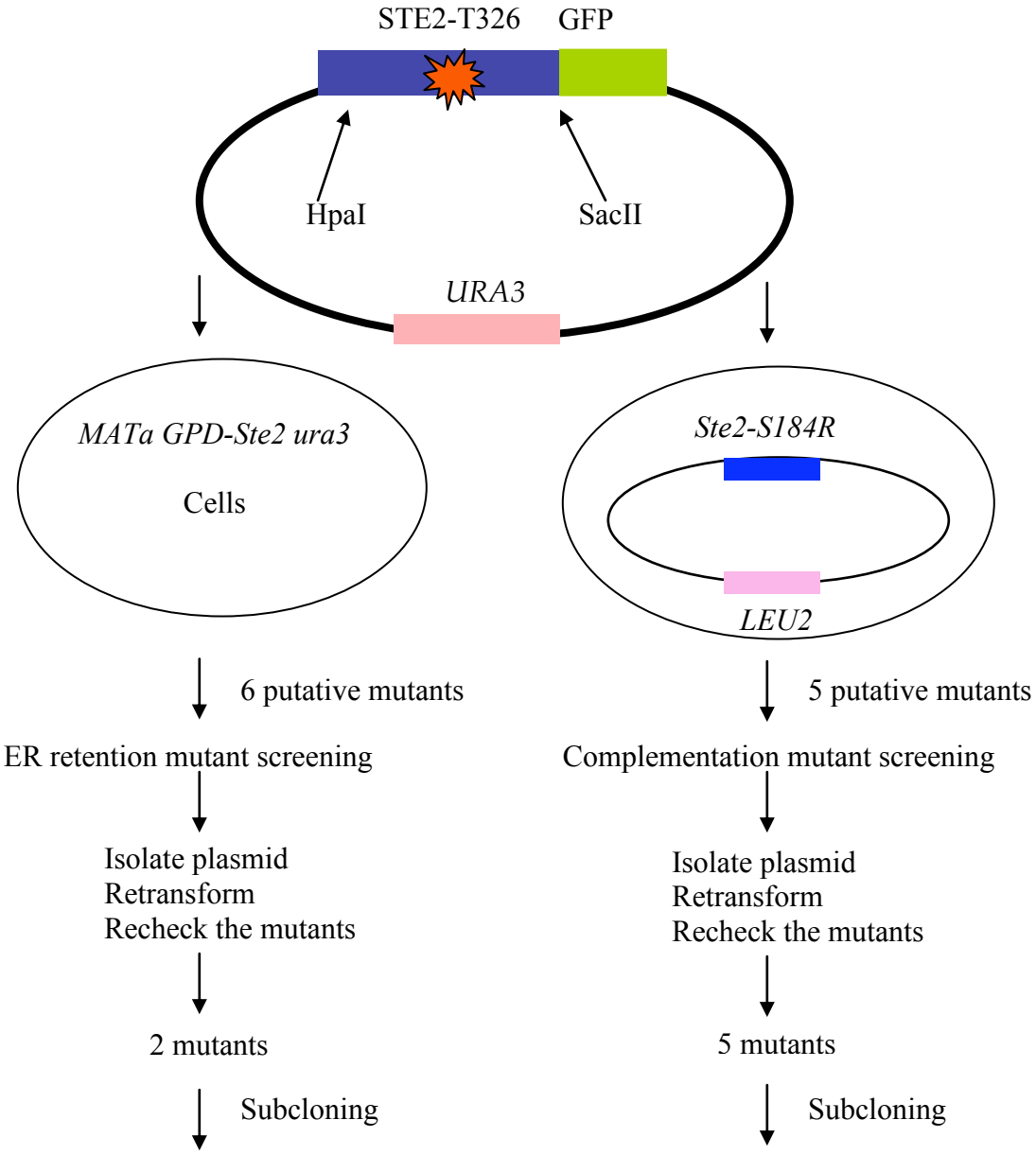


Figure 4-1. Two strategies for ER trafficking mutant screening. PCR-based mutagenesis of the plasmid encoding Ste2-T326-GFP is depicted at the top. The ER retention mutant screening method is shown on the left. The complementation mutant screening method is shown on the right. In this method *ste2*Δ cells contain two plasmids encoding different receptors.

α-factor binding. My objective was to identify mutated forms of Ste2-T326-GFP that cannot form homo-oligomers but can still form heterooligomers with Ste2-S184R. I also reasoned that if oligomerization is essential for Ste2-T326-GFP to function, then cells expressing both the mutated Ste2-T326-GFP and Ste2-S184R would be sensitive to α-factor, whereas cells expressing the mutated Ste2-T326-GFP alone would be resistant to α-factor. Functions of monomeric Ste2-T326-GFP that could potentially be impaired include proper plasma membrane location, α-factor binding activity and signal transduction activities. For the complementation screening strategy, genes encoding Ste2-S184R and mutated Ste2-T326-GFP were present on two different plasmids. The plasmid encoding Ste2-S184R contained the *LEU2* marker, and the plasmid encoding mutated Ste2-T326-GFP contained the *URA3* marker. Double transformants of a *ste2Δ* strain were first cultured on double selection plates lacking leucine and uracil and then replica-plated onto two different plates containing α-factor. One plate contained leucine and lacked uracil, and the other plate lacked both leucine and uracil. I screened for mutants that were sensitive to α-factor under selection for the YEp *LEU2 ste2-S184R* plasmid but were resistant to α-factor when the cells were allowed to lose the plasmid.

Two thousand single colonies were screened and five putative mutants were identified. The YCp *URA3* plasmids were recovered from each of the five isolates and designated MutJ, Mut8, Mut9, Mut12 and Mut14. DNA sequencing indicated that all five mutant isolates resulted in multiple amino acid substitutions in the α-factor receptor: MutJ (Ste2-S141P,R161G-T326-GFP), Mut8 (Ste2-F55L,S145P-T326-GFP), Mut9 (Ste2-Q85H,F116L-T326-GFP), Mut12 (Ste2-V45A,R122G,L210S-T326-GFP) and

Mut14 (Ste2-T114I,D201G,I249L,T278S-T326-GFP). Each mutant plasmid was reintroduced into the *ste2Δ* strain and into the *ste2Δ* strain containing the YEp *LEU2 ste2-S184R*, and the transformants were tested for α-factor sensitivity to confirm the original phenotype. The transformant expressing Ste2-S184R alone (Fig. 4-2C) served as a negative control, and the transformant expressing Ste2-S184R and Ste2-T326-GFP as the positive control (Fig. 4-2D). Transformants containing MutJ, Mut8, Mut9, Mut12 and Mut14 alone (Fig. 4-2E, G, I, K and N) showed no detectible sensitivity to α-factor, whereas transformants containing MutJ, Mut8, Mut9, Mut12 and Mut14 together with the YEp *LEU2 ste2-S184R* (Fig. 4-2F, H, J, M and O) showed α-factor sensitivity that approximated the positive control (Fig. 4-2D). Note the positive control (Fig. 4-2D) was not as sensitive to α-factor as the control strains expressing Ste2 (Fig. 4-2A) or Ste2-T326-GFP (Fig. 4-2B) alone because of the partial dominant-negative phenotype associated with *ste2-S184R*.

In order to identify the mutations that were responsible for the mutant phenotype, I constructed recombinant plasmids that replaced wild-type sequences from the *ste2-T326-GFP* gene with mutant sequences from the MutJ, Mut8, Mut9, Mut12 and Mut14 plasmids. The recombinant plasmids were introduced into the *ste2Δ* strain (DJ2616), and the transformants were tested for α-factor sensitivity (Fig. 4-3). Results for the positive control cells carrying wild-type Ste2-T326-GFP are shown in Fig. 4-3A, and results for cells carrying the recombinant plasmids are shown in Fig. 4-3B-L. S141P was assigned as the relevant codon substitution in plasmid MutJ since cells expressing Ste2-S141P-T326-GFP (Fig. 4-3C) were α-factor resistant and cells expressing

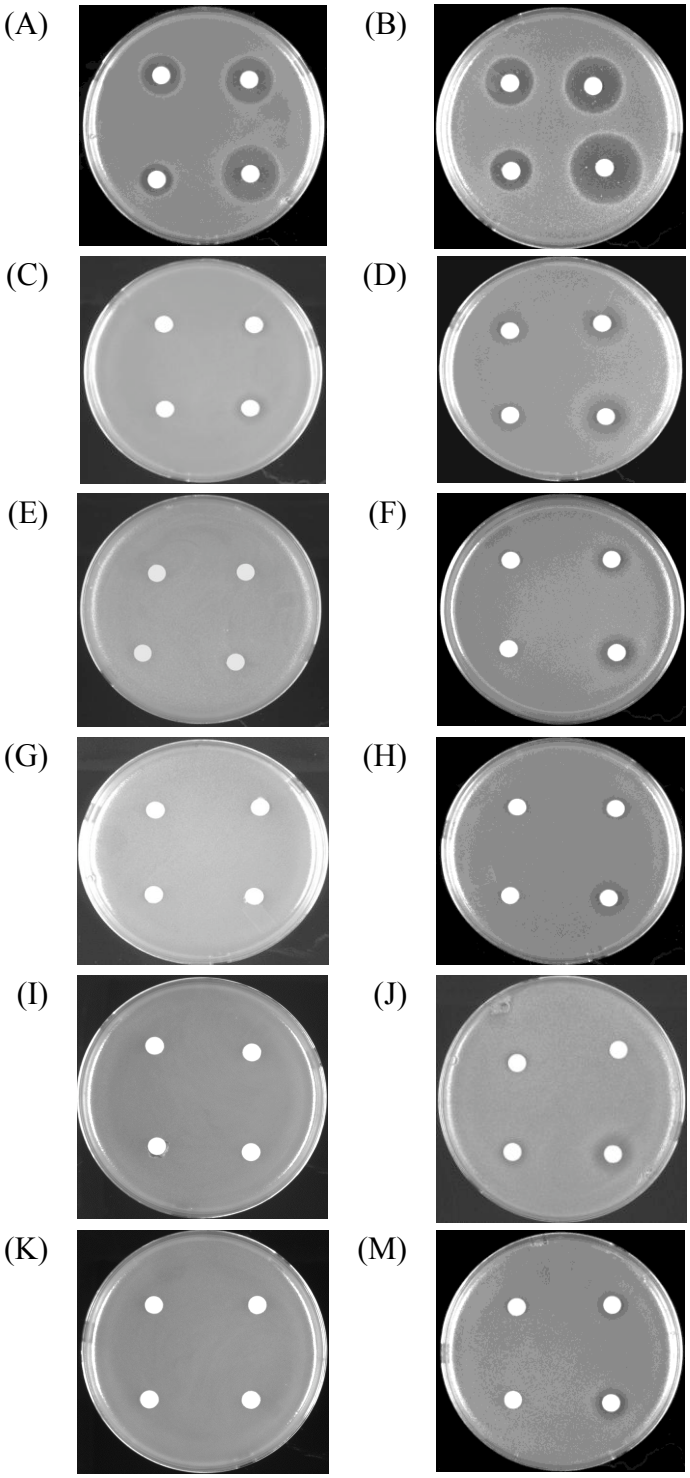
(A)
(B)
(C)
(D)
(E)
(F)
(G)
(H)
(I)
(J)
(K)
(M)

(N) 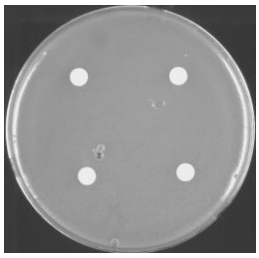 (O) 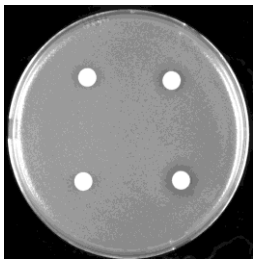

**Figure** 4-**2**. Retesting mutants from the complementation screen. Each filter disk contained α-factor (1, 0.5, 0.25 and 0.125 nmole, proceeding counter-clockwise from bottom right) and was placed on a lawn of yeast cells (strain DJ1378-A-1) containing plasmid expressing the indicated receptors. (A) Cells expressed only full-length wild-type receptors. (B) Cells expressed only truncated wild-type Ste2-T326-GFP. (C) Cells expressed only full-length Ste2-S184R. (D) Cells expressed both truncated wild-type Ste2-T326-GFP and full-length Ste2-S184R. (E), (G), (I), (K) and (N) Cells expressed truncated Ste2-T326-GFP mutants, MutJ, Mut8, Mut9, Mut12 and Mut14, respectively. (F), (H), (J), (M) and (O) Cells expressed full-length Ste2-S184R as well as truncated Ste2-T326-GFP mutants, MutJ, Mut8, Mut9, Mut12 and Mut14, respectively. Plasmids were pDJ469 (Ste2-T326-GFP), pDJ658 (Ste2-GFP), pDJ696 (Ste2-S184R), pDJ638 (MutJ), pDJ639 (Mut8), pDJ697 (Mut9), pDJ698 (Mut12) and pDJ699 (Mut14). Cells depicted in panel C also contained the *URA3* vector plasmid, pDJ303. Cells depicted in panels A, B, E. G. I, K and N also contained the *LEU2* vector plasmid pDJ125. -Leu -Ura growth medium was used. Plates were incubated for 2 days at 30° C.

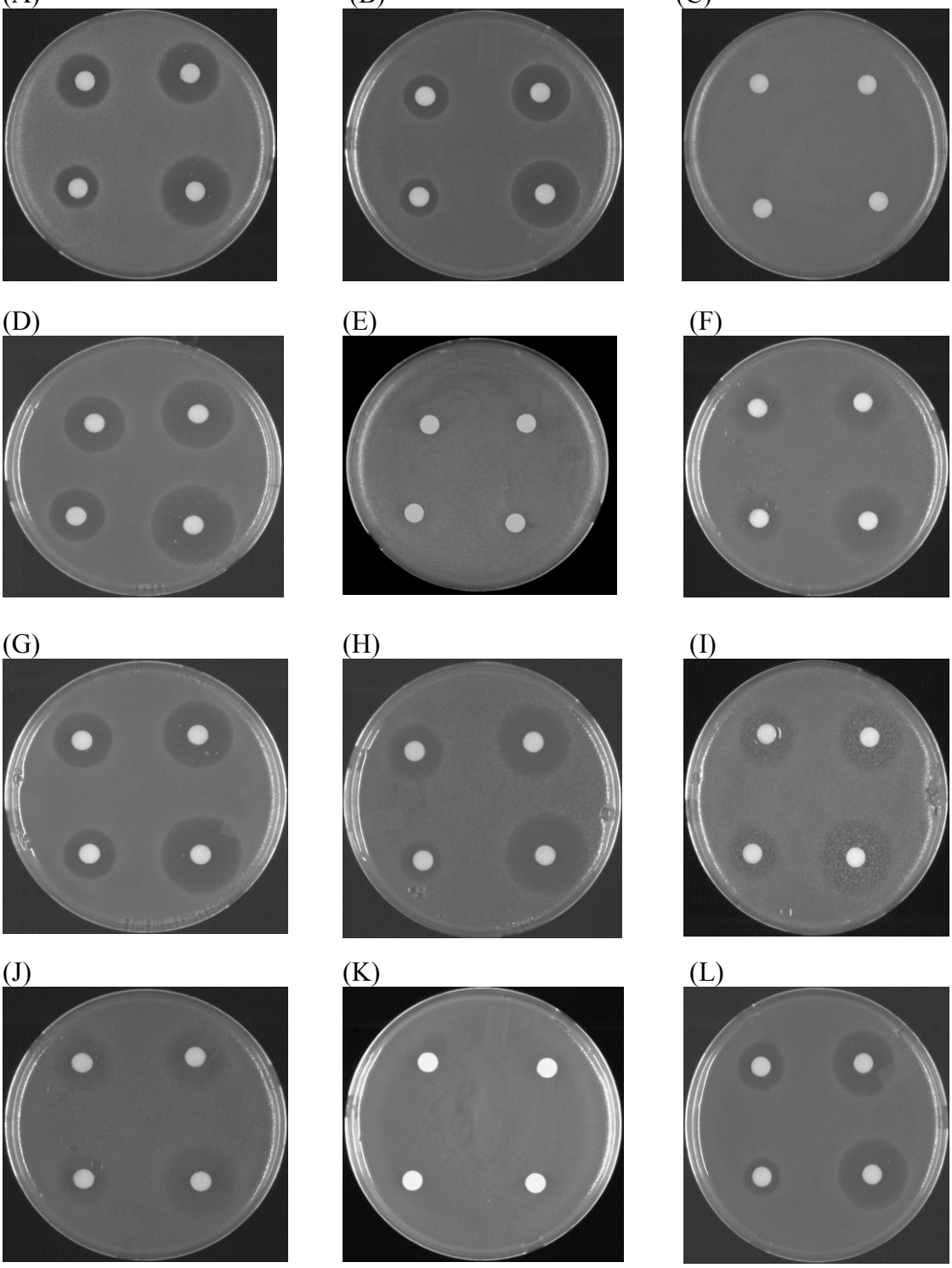
(A)
(B)
(C)
(D)
(E)
(F)
(G)
(H)
(I)
(J)
(K)
(L)

**Figure 4-3.** α-factor sensitivity test for subcloned mutants. Each filter disk contained α-factor (1, 0.5, 0,25 and 0,125 nmol, proceeding counter-clockwise from bottom right) and was placed on a lawn of yeast cells. Yeast cells (strain DJ213-7-3) expressed truncated mutant receptor from the various subcloned plasmids.
(A) Cells expressed truncated wild-type Ste2-T326-GFP (plasmid pDJ469). (B) Cells expressed truncated Ste2-F55L-T326-GFP (plasmid pDJ644). (C) Cells expressed truncated Ste2-S141P-T326-GFP (plasmid pDJ649). (D) Cells expressed truncated Ste2-R161G-T326-GFP (plasmid pDJ645). (E) Cells expressed truncated Ste2-S145P-T326-GFP (plasmid pDJ650). (F) Cells expressed truncated Ste2-V45A, R122G-T326-GFP (plasmid pDJ702). (G) Cells expressed truncated Ste2-R122G-T326-GFP (plasmid pDJ706). (H) Cells expressed truncated Ste2-L210S-T326-GFP (plasmid pDJ703). (I) Cells expressed truncated Ste2-Q85H-T326-GFP (plasmid pDJ700). (J) Cells expressed truncated Ste2-F116L-T326-GFP (plasmid pDJ701). (K) Cells expressed truncated Ste2-T114I, D210G, I249L-T326-GFP (plasmid pDJ704). (L) Cells expressed truncated Ste2-T278S-T326-GFP (plasmid pDJ705). –Ura+CAA growth medium was used. Plates were incubated for 2 days at 30° C.

Ste2-R161G-T326-GFP (Fig. 4-3D) were sensitive. Similarly, S145P was assigned as the relevant codon substitution in plasmid MutJ since cells expressing Ste2-S145P-T326-GFP (Fig. 4-3E) were α-factor resistant and cells expressing Ste2-F55L-T326-GFP (Fig. 4-3B) were sensitive. Neither single codon substitution in plasmid Mut9 (Fig. 4-3I and Fig.4-3J) resulted in α-factor sensitivity indicating a synthetic phenotype. Similarly, Mut12 showed a synthetic phenotype since cells expressing Ste2-V45A,R122G-T326-GFP (Fig. 4-3F), Ste2-R122G-T326-GFP (Fig. 4-3G) and Ste2-L210S-T326-GFP (Fig. 4-3H) were α-factor sensitive. Plasmids Mut9 and Mut12 were not pursued further. Cells expressing Ste2-T278S-T326-GFP (Fig. 4-3L) were α-factor sensitive although cells expressing Ste2-T114I, D201G, I249L-T326-GFP (Fig. 4-3K) remained α-factor resistant; due to its complexity, the quadruply mutant Mut14 plasmid was not investigated further.

Single mutation *ste2-S141P-T326-GFP* and *ste2-S145P-T326-GFP* that resulted in α-factor resistance were tested for complementation with mutation *ste2-S184R* (Fig. 4-4). Cells expressing both Ste2-S141P-T326-GFP and Ste2-S184R were more α-factor sensitive than cells expressing either Ste2-S141P-T326-GFP or Ste2-S184R alone, although they were somewhat less sensitive than the positive control cells expressing Ste2-T326-GFP and Ste2-S184R. Thus *ste2-S141P-T326-GFP* mutation satisfies the criteria established for the complementation strategy. In contrast, cells that express both Ste2-S145P-T326-GFP and Ste2-S184R were not significantly more sensitive than the cells expressing Ste2-S184R alone. Since mutation *ste2-F55L,S145P-T326-GFP* was complemented by mutation *ste2-S184R* (Fig. 4-2H),

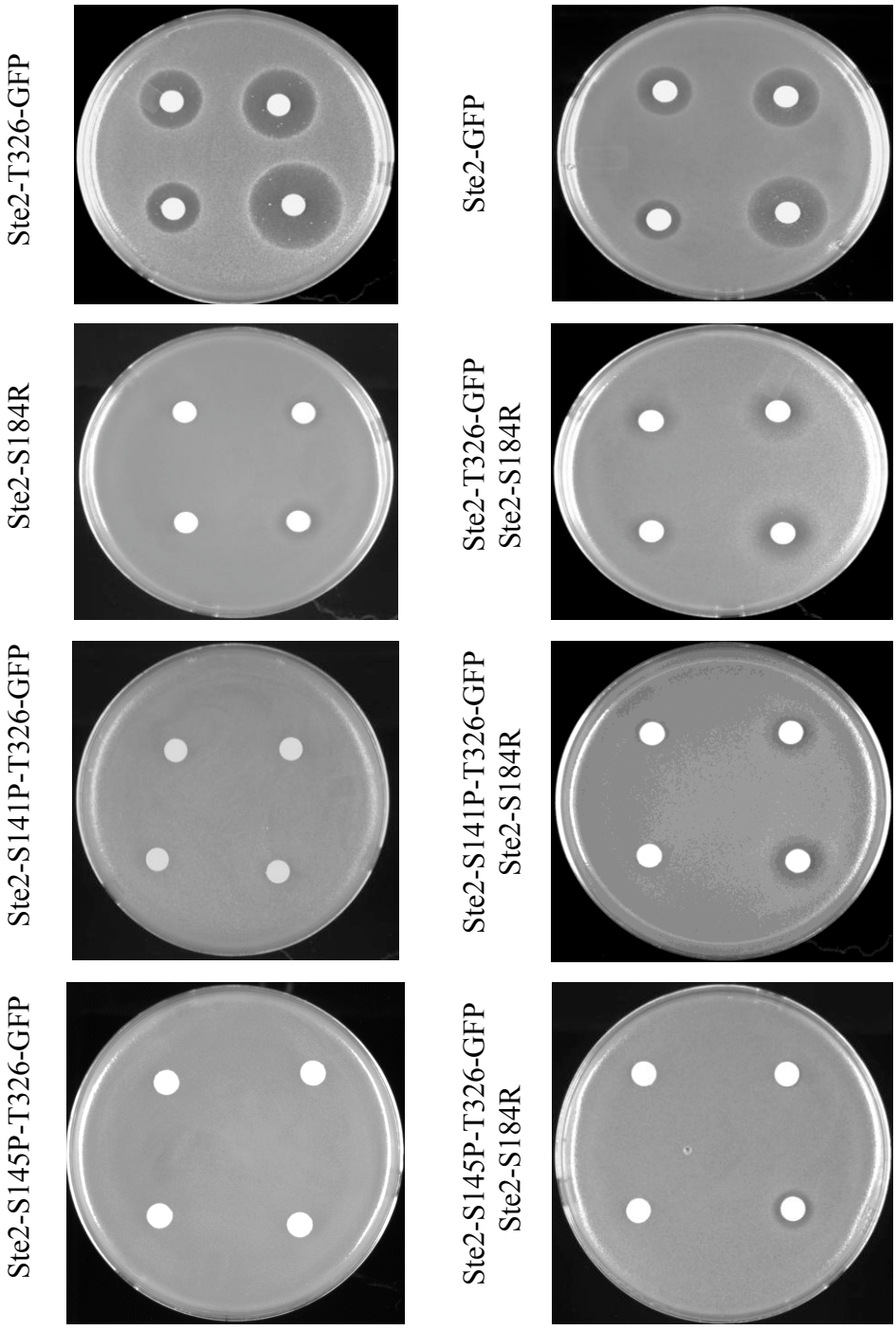
Ste2-T326-GFP
Ste2-S184R
Ste2-S141P-T326-GFP
Ste2-S145P-T326-GFP
Ste2-GFP
Ste2-T326-GFP
Ste2-S184R
Ste2-S141P-T326-GFP
Ste2-S184R
Ste2-S145P-T326-GFP
Ste2-S184R

**Figure 4-4.** Complementation tests of Ste2-S184R with Ste2-S141P-GFP and Ste2-S145P-GFP. Each filter disk contained α-factor (1, 0.5, 0.25 and 0.125 nmole, proceeding counter-clockwise from bottom right) and was placed on a lawn of yeast cells (strain DJ1378-A-1) containing plasmid expressing the indicated receptors. Cells expressed Ste2-T326 (top left) and Ste2-GFP (top right). Positive control cells expressed Ste2-S184P and Ste2-T326-GFP (second row, right). Negative control cells expressed Ste2-S184R (second row, left), Ste2-S141P-T326-GFP (third row, left), or Ste2-S145P-T326-GFP (fourth row, left). The zone of inhibition for the positive control is smaller than for the cells expressing wild-type receptors because Ste2-S184R receptors result in a dominant negative phenotype. Plasmids were pDJ469 (Ste2-T326-GFP), pDJ658 (Ste2-GFP), pDJ696 (Ste2-S184R), pDJ676 (Ste2-S141PT326-GFP), pDJ677 (Ste2-S145P-T326-GFP), pDJ124 (*LEU2* vector) and pDJ303 (*URA3* vector). –Leu -Ura growth medium was used. Plates were incubated for 2 days at 30° C.

I conclude that the F55L amino acid substitution was necessary for the activity of receptor complexes containing Ste2-S145P-T326-GFP and Ste2-S184R. In principle, F55L may correct one or more defects in Ste2-S145P-T326-GFP that are not corrected by interaction with Ste2-S184R. The role of F55L is addressed below and in Chapter 5.

**The ER retention mutant screening**

As discussed above, *ste2* mutations that affect the $^{56}$GxxxG$^{60}$ motif in transmembrane domain I are believed to cause a reduction in the extent of receptor oligomerization and to cause truncated tailless receptors to be retained in the ER (Overton *et al.*, 2003). My ER retention mutant screening strategy was set up based on this result. I reasoned that if truncated oligomerization-defective mutants are retained in the ER then any new mutant receptor that cannot form hetero-oligomers with full-length wild-type receptors will accumulate in the ER. In my screening procedure, plasmids from the mutagenized pool that expressed Ste2-T326-GFP under the control of the native promoter were introduced into strain DJ483-1 that expressed wild-type Ste2 under the control of GPD promoter in order to maximize the ratio of heterodimers. To confirm that the expression level of wild-type Ste2 was sufficient to promote hetero-oligomers, I exposed each transformant colony to α-factor pheromone to promte endocytosis of cell surface recetors. The α-factor treatment also avoided potential confusion between cortical ER and plasma membrane straining. I used fluorescence microscopy to screen the individual transformants for ER retention of Ste2-T326-GFP as judged by the accumulation of GFP signal in the perinuclear region. Isolates that formed

hetero-oligomers were expected to accumulate Ste2-T326-GFP in the vacuole and endocytic compartments as described in chapter 3. I screened over 1700 transformant colonies. Two positive mutants, Mut71 and Mut136, were isolated. The plasmids were recovered from the cells and reintroduced into strain DJ483-1 to confirm that the ER retention phenotype was linked to the plasmid. DNA sequencing results indicated that Mut71 contained six substitutions (C59R, R122G, Y193C, N216H, S310T, F312T) in the Ste2 gene and that Mut136 contained four substitutions (H94P, F116V, Q240R, N300Q). When viewed in the fluorescence microscope, both mutant receptors were found to accumulate in the ER as judged by the perinuclear localization of the GFP fluorescence. In order to determine whether the ER retention was due to a single amino acid change or to a combination of multiple residue alterations, I constructed recombinant plasmids that contained subsets of the codon substitutions present in Mut71 and Mut136; the recombinant plasmids were introduced into strain DJ483-1. After the α-factor treatment, most of the GFP signal in cells containing wild-type Ste2-T326-GFP receptors accumulated in the vacuole and endosomes (Fig. 4-5A), whereas the GFP signal was retained in the ER in cells containing Mut71 Fig. (Fig. 4-5B) and Mut136 (Fig. 4-5C). Ste2-C59R-T326-GFP (Fig. 4-5D) accumulated in the ER, whereas Ste2-R122G,Y193C, N216H,S310T, F312T-T326-GFP (Fig. 4-5E) accumulated in the vacuole and endosomes, indicating that the C59R substitution was responsible for the mutant phenotype associated with Mut71. Similarly, Ste2-H94P-T326-GFP (Fig. 4-5F) was retained in the ER, and Ste2-F116V,Q240R,N300Q-T326-GFP (Fig. 4-5G) was present

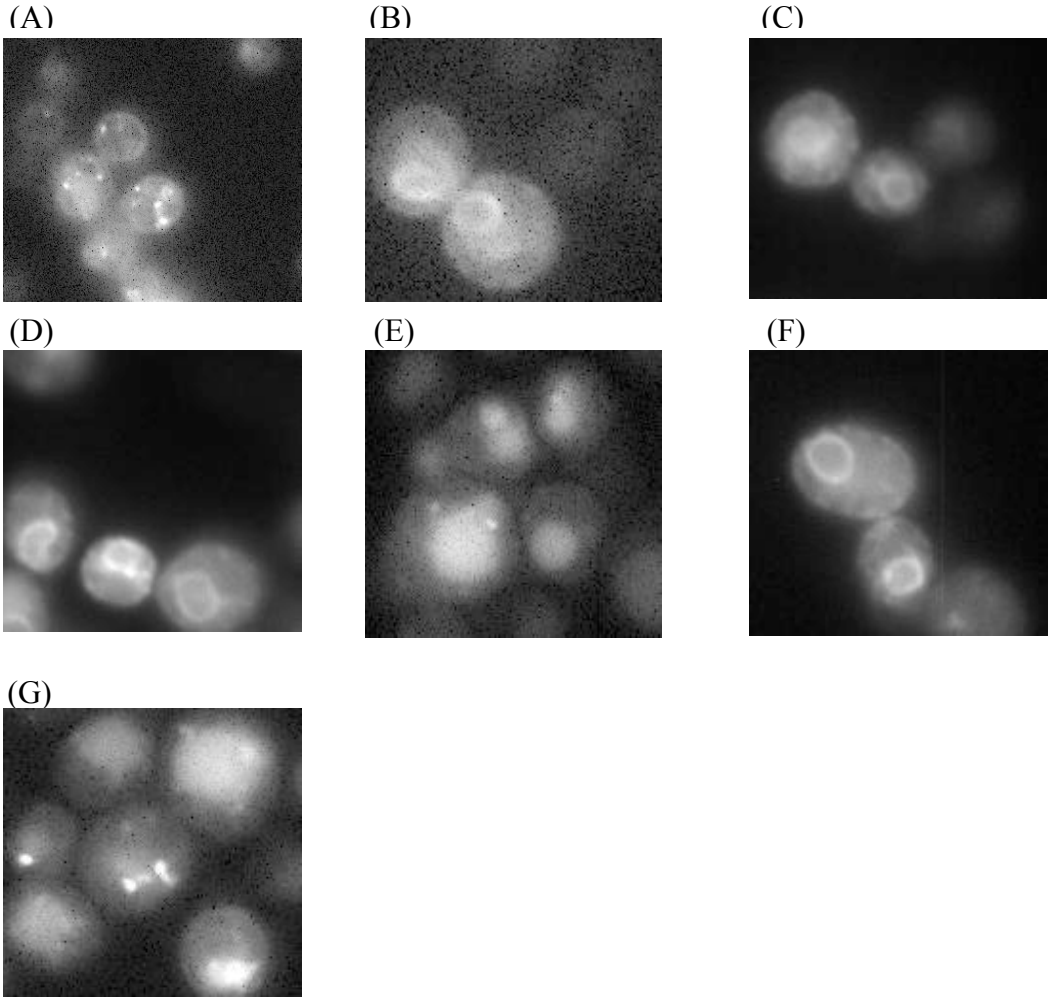


**Figure 4-5.** ER retention mutant screening and subcloning. Plasmids encoded either truncated wild-type Ste2-T326-GFP or truncated mutant receptors were introduced into yeast cells (strain DJ483-1) that over-expressed full-length Ste2 under the control of the *GPD* transcriptional promoter. Cultures were treated with α-factor. (A), (B) and (C) Cells expressed wild-type Ste2-T326-GFP (plasmid pDJ469), Mut71 (plasmid pDJ640) or Mut136 (plasmid pDJ641), respectively. (D) and (E) Subcloned mutants from Mut71 expressed Ste2-C59R-T326-GFP (plasmid pDJ647) and Ste2-R122G,Y193C,N216H,S310T,F312T-T326-GFP (plasmid pDJ642), respectively. (F) and (G) Subcloned mutants from Mut136 expressed Ste2-H94P-T326-GFP (plasmid pDJ648) and Ste2-F116V,Q240R,N300Q-T326-GFP (plasmid pDJ643), respectively. The result indicated that C59R and H94P mutations in Ste2-T326-GFP are responsible for the ER retention phenotype in Mut71 and Mut136, respectively.

in the vacuole and endosomes, indicating that the H94P substitution was responsible for the mutant phenotype in Mut136.

**Comparison of mutants identified in the two mutant screening strategies**

My results identified two different groups of ER retention mutants affecting α-factor receptors. Mutants isolated using one of the two strategies were not recovered using the other strategy. One group of mutant receptors consisting of Ste2-S141P-T326-GFP and Ste2-S145P-T326-GFP were identified using the complementation screening strategy. The other group of mutants consisting of Ste2-C59R-T326-GFP and Ste2-H94P-T326-GFP were identified in the ER retention screening strategy. As a first test to clarify the distinction between the mutants identified in the two screens, I tested whether mutant receptors such as Ste2-C59R-T326-GFP and Ste2-H94P-T326-GFP can complement Ste2-S184R receptors in the cell division arrest assay. Ste2-G56L-T326-GFP (Overton *et al.*, 2003) was also included in this test. Plasmids encoding the Ste2-G56L-T326-GFP, Ste2-C59R-T326-GFP and Ste2-H94P-T326-GFP mutant receptors were each introduced into the yeast strain expressing binding-defective mutant Ste2-S184R. The test for complementation between mutant receptors is depicted in Fig. 4-6. Ste2-G56L-T326-GFP, Ste2-C59R-T326-GFP and Ste2-H94P-T326-GFP failed to complement Ste2-S184R in that the α-factor sensitivity of the cells was no greater than for the control cells that expressed only the Ste2-S184R mutant receptor. Thus, these mutants represent a mutant class that would not

have been uncovered using the complementation screening strategy. The result is consistent with the view that they are defective in oligomerization,

I broadened the complementation tests to include an additional receptor mutant with the aim of increasing the sensitivity of this assay. Although full-length Ste2-S184R is severely impaired in α-factor binding, the *ste2-S184R* mutant retains some degree of α-factor sensitivity in the α-factor halo assay (Fig. 4-6). In addition, the utility of the complementation test is limited by the dominant-negative phenotype of α-factor binding mutants (Dosil *et al.*, 2000). In order to increase sensitivity and to avoid the dominant-negative effect of Ste2-S184R, I tested the ER retention mutants for complementation with a mutant (Ste2-L236H) that is specifically defective for G protein coupling and retains α-factor binding activity (Weiner *et al.*, 1993; Schandel and Jenness, 1994). Ste2-L236H receptor was expressed under the control of the constitutive GPD promoter to optimize heterooligomer formation with Ste2-S141P-T326-GFP. Yeast cells coexpressing Ste2-L236H and Ste2-S141P-T326-GFP exhibited robust complementation in that α-factor responsiveness is almost as strong as the wild-type control (Fig. 4-7). I further tested whether the truncated Ste2-G56L-T326-GFP, Ste2-C59R-T326-GFP and Ste2-H94P-T326-GFP mutant receptors can complement signal defective mutant Ste2-L236H (Fig. 4-8). As expected, all of mutants show no increase in α-factor sensitivity when they were coexpressed with Ste2-L236H, consistent with an inability of ER retention mutants to form hetero-oligomers.

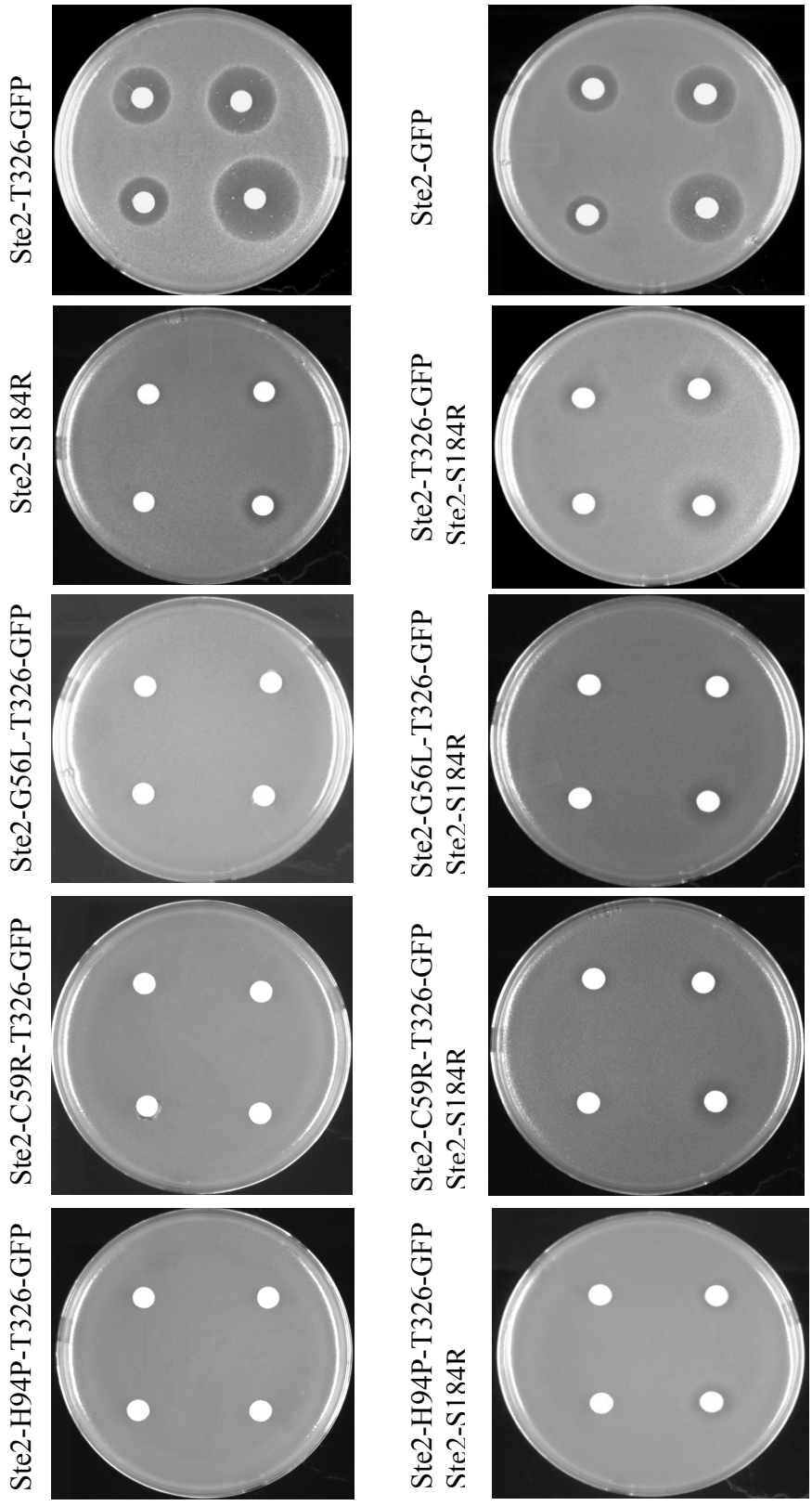
Ste2-H94P-T326-GFP
Ste2-C59R-T326-GFP
Ste2-G56L-T326-GFP
Ste2-S184R
Ste2-T326-GFP
Ste2-H94P-T326-GFP
Ste2-S184R
Ste2-C59R-T326-GFP
Ste2-S184R
Ste2-G56L-T326-GFP
Ste2-S184R
Ste2-T326-GFP
Ste2-S184R
Ste2-GFP

**Figure 4-6.** Complementation tests with mutants from the ER retention screening. Each filter disk contained α-factor (1, 0.5, 0.25 and 0.125 nmol, proceeding counter-clockwise from bottom right) and was placed on a lawn of yeast cells (strain DJ1378-A-1) containing plasmid expressing the indicated receptors. Cells expressed Ste2-T326 (top left) and Ste2-GFP (top right). Positive control cells expressed Ste2-S184P and Ste2-T326-GFP (second row, right). Negative control cells expressed Ste2-S184R (second row, left), Ste2-G56L-T326-GFP (third row, left), Ste2-C59R-T326-GFP (fourth row, left), or Ste2-H94P-T326-GFP (fifth row, left). Plasmids were pDJ469 (Ste2-T326-GFP), pDJ658 (Ste2-GFP), pDJ696 (Ste2-S184R), pDJ646 (Ste2-G56L-T326-GFP), pDJ647 (Ste2-C59R-T326-GFP) and pDJ648 (Ste2-H94P-T326-GFP). Cells also contained the *URA3* vector plasmid, pDJ303, or the *LEU2* vector plasmid pDJ125 when needed to provide the $Leu^+$ $Ura^+$ phenotype. -Leu -Ura growth medium was used. Plates were incubated for 2 days at 30° C.

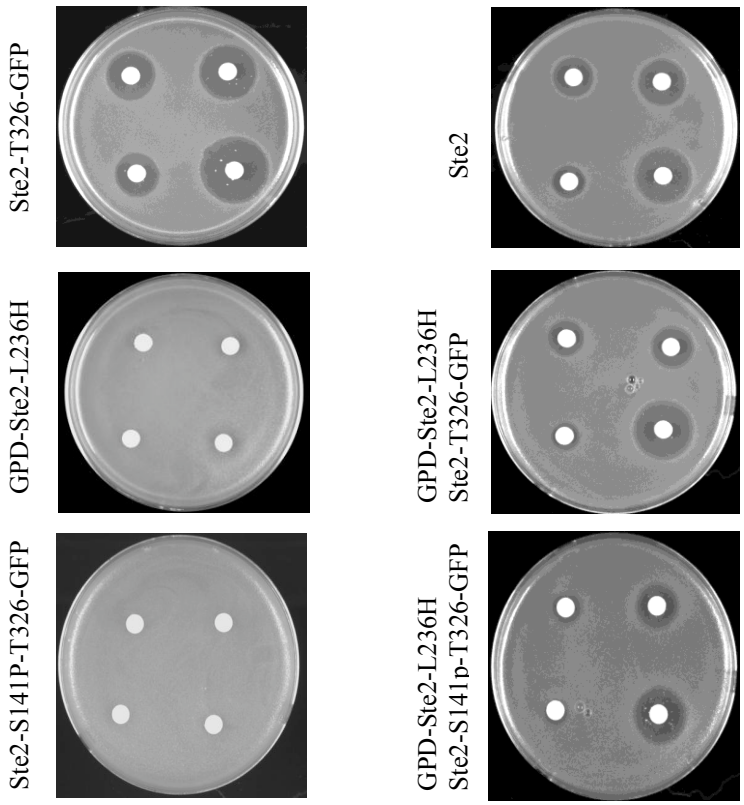


**Figure 4-7.** Signal complementation tests with Ste2-S141P and Ste2-L236H receptors. Each filter disk contained α-factor (1, 0.5, 0.25 and 0.125 nmol, proceeding counter-clockwise from bottom right) and was placed on a lawn of *ste2Δ* cells (strain 213-7-3) or cells that over-express Ste2-L236H (strain DJ486-1) containing a plasmid expressing the indicated receptor. Cells expressed Ste2-T326 (top left) and Ste2-GFP (top right). Positive control cells expressed Ste2-L236H and Ste2-T326-GFP (second row, right). Negative control cells expressed Ste2-L236H and the vector plasmid (second row, left) and Ste2-S141P-T326-GFP in a *ste2Δ* background (third row, left). Full complementation was observed for cells expressing Ste2-S141P-T326-GFP and Ste2-L236H (third row, right). Plasmids were pDJ469 (Ste2-T326-GFP), pDJ658 (Ste2-GFP), pDJ649 (Ste2-S141P-T326-GFP), and the pDJ303 (vector). –Ura+CAA growth medium was used. Plates were incubated for 2 days at 30° C.

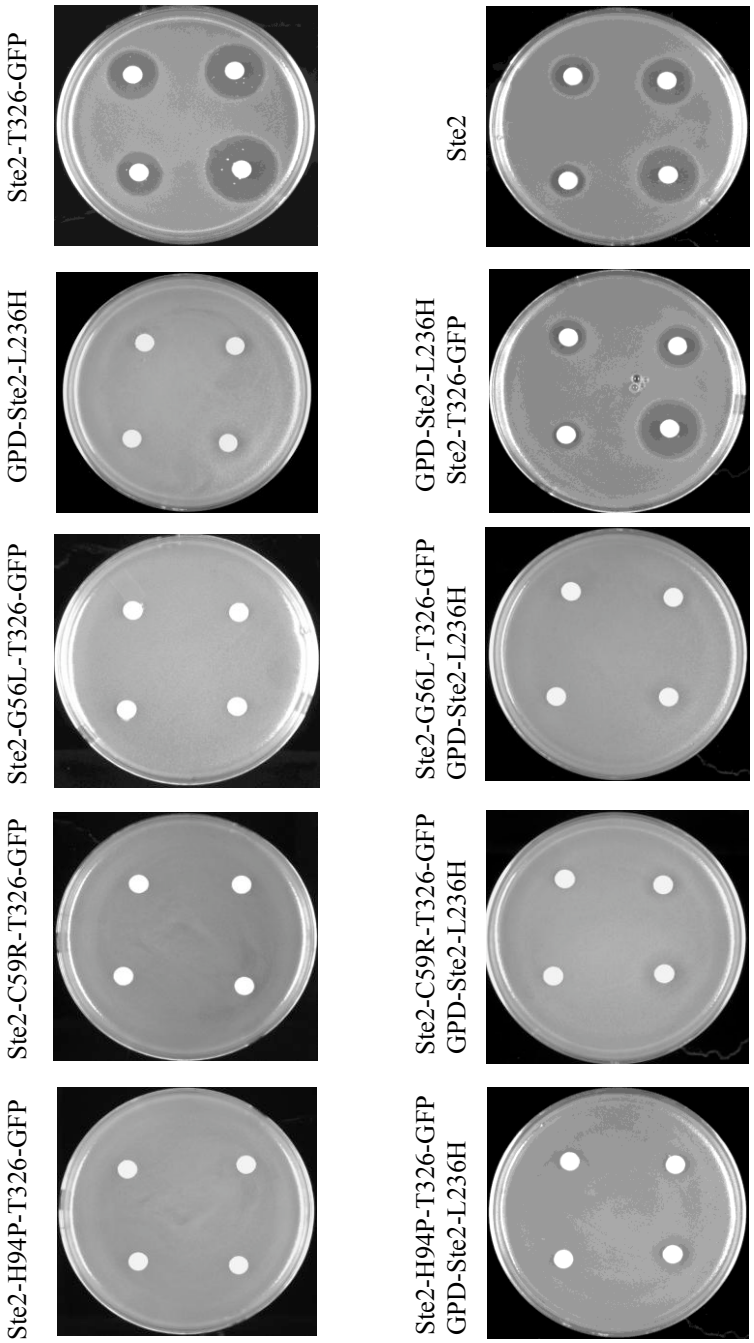
Ste2-H94P-T326-GFP
Ste2-C59R-T326-GFP
Ste2-G56L-T326-GFP
GPD-Ste2-L236H
Ste2-T326-GFP
Ste2-H94P-T326-GFP GPD-Ste2-L236H
Ste2-C59R-T326-GFP GPD-Ste2-L236H
Ste2-G56L-T326-GFP GPD-Ste2-L236H
GPD-Ste2-L236H Ste2-T326-GFP
Ste2

**Figure 4-8.** Tests for complementation of Ste2-L236H receptors with Ste2-G56L-GFP, Ste2-C59R-GFP and Ste2-H94P-GFP. Each filter disk contained α-factor (1, 0.5, 0.25 and 0.125 nmol, proceeding counter-clockwise from bottom right) and was placed on a lawn of *ste2Δ* cells (strain 213-7-3) or cells that over-express Ste2-L236H (strain 486-1) containing a plasmid expressing the indicated receptor. Cells expressed Ste2-T326 (top left) and Ste2-GFP (top right). Positive control cells expressed Ste2-L236H and Ste2-T326-GFP (second row, right). Negative control cells expressed Ste2-L236H and the vector plasmid (second row, left), Ste2-G56L-T326-GFP in a *ste2Δ* background (third row, left), Ste2-C59R-T326-GFP in a *ste2Δ* background (fourth row, left) and Ste2-H94P-T326-GFP in a *ste2Δ* background (fifth row, left). No complementation was observed for cells expressing Ste2-L236H together with Ste2-G56L-T326-GFP, Ste2-C59R-T326-GFP or Ste2-H94P-T326-GFP (third, fourth and fifth rows, right). Plasmids were pDJ469 (Ste2-T326-GFP), pDJ658 (Ste2-GFP), pDJ646 (Ste2-G56L-T326-GFP), pDJ647 (Ste2-C59R-T326-GFP), pDJ648 (Ste2-H94P-T326-GFP) and pDJ303 (vector). –Ura+CAA growth medium was used. Plates were incubated for 2 days at 30° C.

**Hetero-oligomer formation is sufficient to drive ER exit of Ste2-S141P-T326-GFP**

I tested whether truncated Ste2-S141P-T326-GFP receptors can reach the cell surface by forming hetero-oligomers with truncated Ste2-F204S-T326-HA receptors, even though both of the complementing receptors lack the ER exit signals contained in the C-terminal domain. The dominant-negative phenotype associated with the Ste2-F204S mutant (Dosil *et al.*, 2000) was eliminated by using the truncated receptor. In addition, the truncated Ste2-F204S-T326-HA mutant was expressed under the control GPD transcriptional promoter to facilitate the formation of hetero-oligomers with Ste2-S141P-T326-GFP. The cells expressing Ste2-S141P-T326-GFP or Ste2-F204S-T326-HA were resistant to α-factor, whereas the cells expressing both receptors showed full α-factor sensitivity (Fig. 4-9), suggesting the hetero-oligomer formation is sufficient to promote exit of Ste2-S141P-T326-GFP from the ER even in the absence of the C-terminal cytoplasmic domain.

**ER-retained α-factor receptor mutants are degraded by the ERAD pathway**

The relative abundance of the mutant receptors was evaluated by using immunoblotting methods. The genes encoding either the wild-type or mutant receptor fusion proteins were present in a single copy plasmid under the control of the native *STE2* promoter. Crude cell lysates containing GFP fusion proteins were subjected to immunoblot analysis using anti-GFP antiserum (Fig. 4-10A). The steady-state levels of mutant receptors Ste2- G56L-T326-GFP, Ste2-C59R-T326-GFP, Ste2-H94P-T326-GFP, Ste2-141P-T326-GFP and Ste2-S145P-T326-GFP were reduced significantly compared

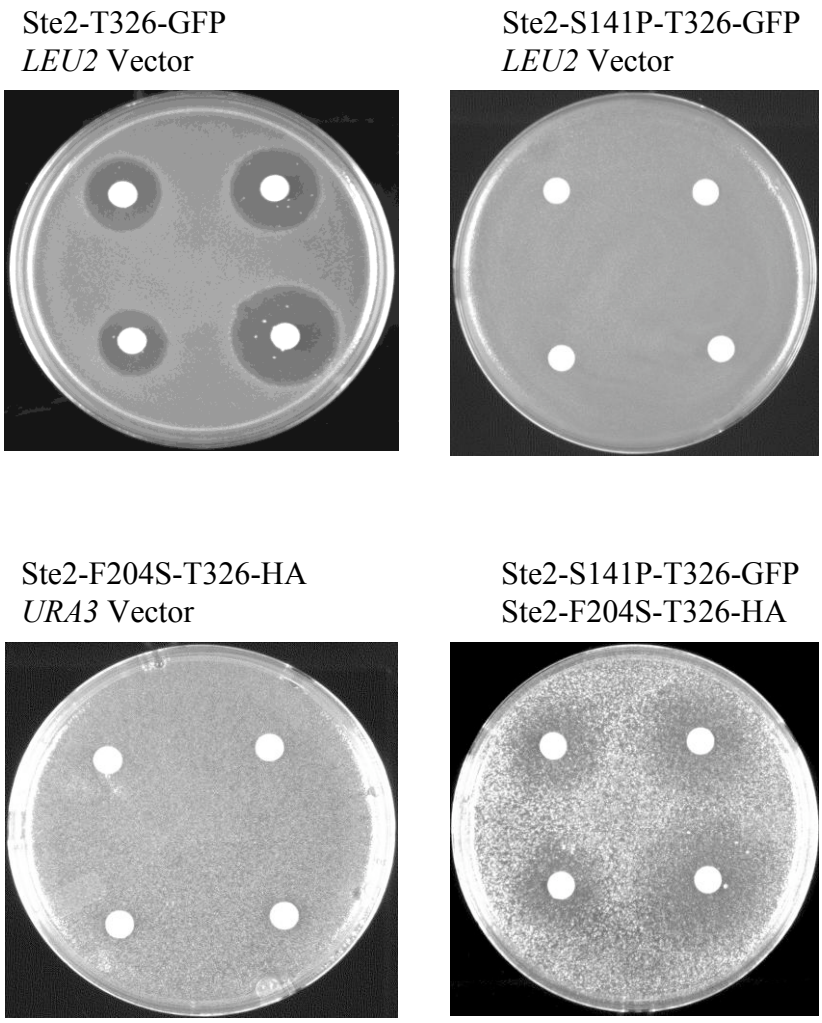


**Figure 4-9.** Complementation between Ste2-S141P-T326-GFP and Ste2-F204S-T326-HA receptors. Each filter disk contained α-factor (1, 0.5, 0.25 and 0.125 nmol, proceeding counter-clockwise from bottom right) and was placed on a lawn of *ste2Δ* cells (strain DJ1378-A-1) containing plasmids expressing the indicated receptors. Yeast cells expressed the receptors indicated at the top of each panel. Cells expressing Ste2-S141P-T326-GFP complemented over-expressed Ste2-F204S-T326-HA receptors. Plasmids were pDJ469 (Ste2-T326-GFP), pDJ649 (Ste2-S141P-T326-GFP), pDJ679 (Ste2-F204S-T326-GFP), pDJ124 (*LEU2* vector) and pDJ303 (*URA3* vector). -Leu -Ura growth medium was used. Plates were incubated for two days at 30° C.

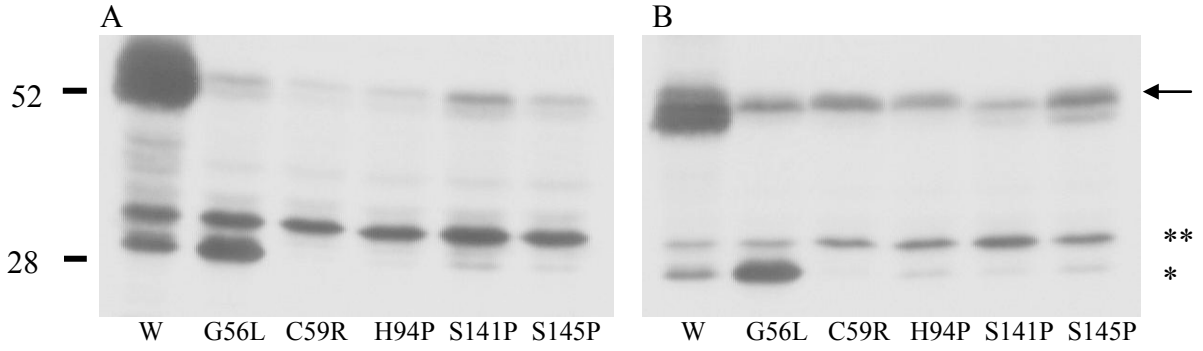


**Figure 4-10.** Expression of GFP-tagged mutant receptors in wild-type and *der3* cells. Crude lysates from cells expressing GFP-tagged truncated receptors were resolved by SDS PAGE, and the proteins were detected with anti-GFP antibodies. The cells had been transformed with plasmids encoding truncated wild-type receptors Ste2-T326-GFP (W), Ste2-G56L-GFP (G56L), Ste2-C59R-GFP (C59R), Ste2-H94P-GFP (H94P), Ste2-S141P-GFP (S141P) or Ste2-S145P-GFP (S145P). (A) The *ste2Δ* recipient strain DJ213-7-3. (B) The *ste2Δ der3* recipient strain DJ488-1. The arrow indicates the intact Ste2-T326-GFP fusion protein. Two degradation products containing GFP are labeled ** or *. Molecular weight (kDa) marker proteins are indicated at the left. Plasmids were pDJ469 (Ste2-T326-GFP), pDJ646 (Ste2-G56L-T326-GFP), pDJ647 (Ste2-C59R-T326-GFP), pDJ648 (Ste2-H94P-T326-GFP), pDJ649 (Ste2-S141P-T326-GFP) and pDJ650 (Ste2-S145P-T326-GFP).

with wild-type Ste2-T326-GFP, and two major degradation product containing GFP (indicated as "*" and "**") were present. Defective membrane proteins are retained in the ER and eventually transported into the cytosol and degraded by the endoplasmic reticulum-associated degradation (ERAD) pathway. This process represents the primary means of quality control within the secretory pathway (Meusser *et al.*, 2005). In *S. cerevisiae,* three different ERAD pathways ERAD-L, ERAD-M and ERAD-C have been identified based on their distinct ubiquitin-ligase complexes (Carvalho *et al.*, 2006). ERAD-L pathway recognizes substrates with misfolded ER lumenal domains. ERAD-M pathway recognizes substrates with a misfolded intramembrane domain. ERAD-C pathway recognizes substrates with a misfolded cytosolic domain (Carvalho *et al.*, 2006). Der3p (Hrd1p) is a ubiquitin ligase in the ERAD-L and ERAD-M pathways (Bordallo *et al.*, 1998; Bays *et al.*, 2001; Carvalho *et al.*, 2006). Since all of the mutant receptors were retained in the ER, I tested whether disruption of the Der3p gene would result in their stabilization. Plasmids encoding the mutant receptors (Fig. 4-10A) were introduced into the *der3Δ* mutant strain, and the GFP fusion proteins were detected with anti-GFP antiserum (Fig. 4-10B). All five mutants were increased in abundance relative to the Ste2-T326-GFP control, and the amount of the upper degradation product (**) was reduced relative to full-length fusion protein. The smaller degradation product (*) was observed in cells expressing Ste2-T326-GFP and Ste2-G56L-T326-GFP but not in the other mutants. To test whether this degradation product results from proteolysis in the vacuole, I introduced the plasmid encoding Ste2-G56L-T326-GFP gene into the *pep4* mutant strain. *PEP4* encodes proteinase A, which is required for the activity of the major

vacuolar proteases. Fig. 4-11 shows that smaller band (*) was absent in the *pep4*Δ strain. Taken together the results indicate that all of the mutants are subject to degradation by the ERAD pathway and that Ste2-G56L-T326-GFP is degraded in the vacuole as well.

**The C-terminal cytoplasmic domain of α-factor receptors facilitate ER exit**

As discussed above, the C-terminal cytoplasmic domain of the receptor contributes to the ER export of the wild-type receptor (Yesilaltay and Jenness, 2000) and mutant receptors containing defects in the $^{56}$GxxxG$^{60}$ motif (Overton *et al.*, 2003). I tested whether the C-terminal cytoplasmic domain also facilitates ER export of the mutant receptors identified in this study. Plasmids encoding full-length Ste2-G56L-GFP, Ste2-C59R-GFP, Ste2-H94P-GFP, Ste2-S141P-GFP and Ste2-S145P-GFP were constructed, and fluorescence microscopy was used to compare the cellular location of these full-length mutant proteins and the truncated mutants. An ER localization was indicated by the accumulation of fluorescence in the perinuclear ring, and the vacuole was visible in the Nomarski image. I first examined the mutants identified in the complementation screening strategy. The truncated mutants, Ste2-S141P-T326-GFP and Ste2-S145P-T326-GFP, were exclusively retained in the ER, while the truncated wild-type receptors Ste2-T326-GFP were only partially retained (Fig. 4-12). In contrast, the full-length Ste2-S141P-GFP showed significant GFP signal accumulation in the vacuole, similar to the phenotype of full-length wild-type Ste2-GFP. Full-length Ste2-S145P-GFP also exited the ER but not as efficiently as Ste2-S141P-GFP.

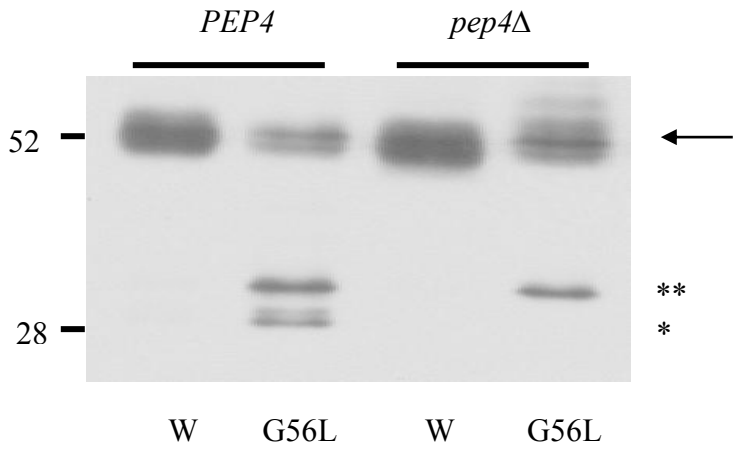


**Figure 4-11.** Expression of Ste2-G56L-GFP in wild-type and *pep4* cells. Crude lysates from cells expressing GFP-tagged truncated receptors were resolved by SDS-PAGE, and the proteins were detected with anti-GFP antibodies. The cells had been transformed with plasmids encoding truncated wild-type receptors Ste2-T326-GFP (W) and Ste2-G56L-GFP (G56L). (A) The wild-type recipient strain DJ213-5-3. (B) The *pep4* recipient strain DJ147-1-2. The arrow indicates the intact Ste2-T326-GFP fusion protein. Two degradation products containing GFP are labeled ** or *. Molecular weight (kDa) marker proteins are indicated at the left. Plasmids were pDJ469 (Ste2-T326-GFP) and pDJ646 (Ste2-G56L-T326-GFP). The presence of the *STE2*$^{+}$ allele at the chromosomal locus eliminates the partial accumulation of Ste2-G56L-T326-GFP in the ER (Yesilaltay and Jenness, 2000), and it resulted in the loss of both Ste2 -T326-GFP degradation products (compare Fig. 11, lane 1 to Fig. 10, lane 1) and resulted in a reduction of Ste2-G56L-T326-GFP degradation products (compare Fig. 11, lane 2 to Fig. 10, lane 2).

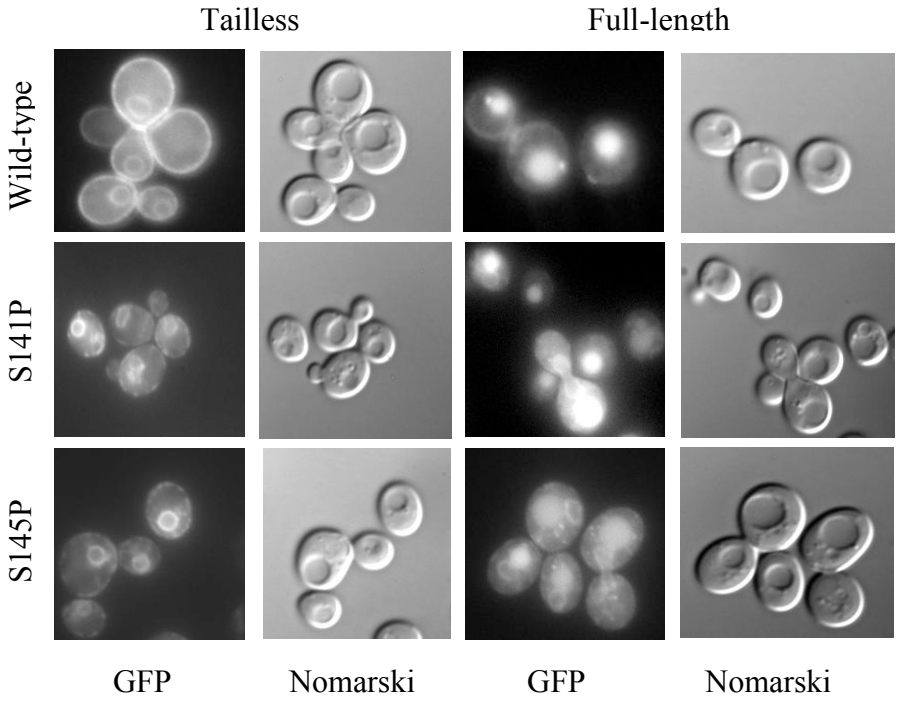


**Figure 4-12.** Role of the C-terminal domain in the localization of the Ste2-S141P-GFP and Ste2-S145P-GFP fusion proteins. GFP fluorescence images and Nomarski images are indicated below each column. Cells expressed receptors containing no amino acid substitution (wild-type) or containing the S141P or the S145P substitution as indicated at the left of each row. In the first two columns, cells expressed tailless Ste2-T326-GFP, Ste2-S141P-T326-GFP or Ste2-S145P-T326-GFP. In the last two columns, cells expressed full-length Ste2-GFP, Ste2-S141P-GFP or Ste2-S145P-GFP. Recipient strain was DJ489-1. Plasmids were Ste2-T326-GFP (pDJ469), Ste2-S141P-T326-GFP (pDJ649), Ste2-S145P-T326-GFP (pDJ650), Ste2-GFP (pDJ658), Ste2-S141P-GFP (pDJ662) and Ste2-S145P-GFP (pDJ663).

Previously Ste2-3, a temperature-sensitive mutant form of Ste2, was shown to transit directly to the vacuole without reaching the plasma membrane at the non-permissive temperature (Jenness *et al.*, 1997). Therefore, I further tested whether the Ste2-S141P-GFP and Ste2-S145P-GFP mutants reach the plasma membrane in an active form by testing for α-factor sensitivity. The full-length Ste2-S141P-GFP mutant showed an α-factor sensitivity that was similar to the full-length wild-type Ste2 receptors (Fig. 4-13), indicating that a significant number of receptors reach the plasma membrane in an active form before they are endocytosed and delivered to the vacuole. The full-length Ste2-S145P-GFP remained resistant to α-factor, however, as discussed above the S145P substitution results in inactive receptors unless the F55L substitution is also present.

The C-terminal cytoplasmic domain also facilitated export of the mutant receptors identified in the ER retention screen. Fluorescence microscopy showed that the truncated mutants (Ste2-C59R-T326-GFP and Ste2-H94P-T326-GFP) were retained exclusively in ER and that the Ste2-G56L-T326-GFP mutant accumulated in the ER and vacuole (Fig. 4-14). In contrast, the full-length mutants Ste2-G56L-GFP and Ste2-H94P-GFP were almost exclusively in the vacuole, and the full-length Ste2-C59R-GFP receptors were present in the ER and vacuole. Neither truncated or full-length Ste2-G56L-GFP, Ste2-C59R-GFP and Ste2-H94P-GFP receptors do not reach the plasma membrane in an active form as judged by the absence of α-factor sensitivity in the mutant cells (Fig. 4-15).

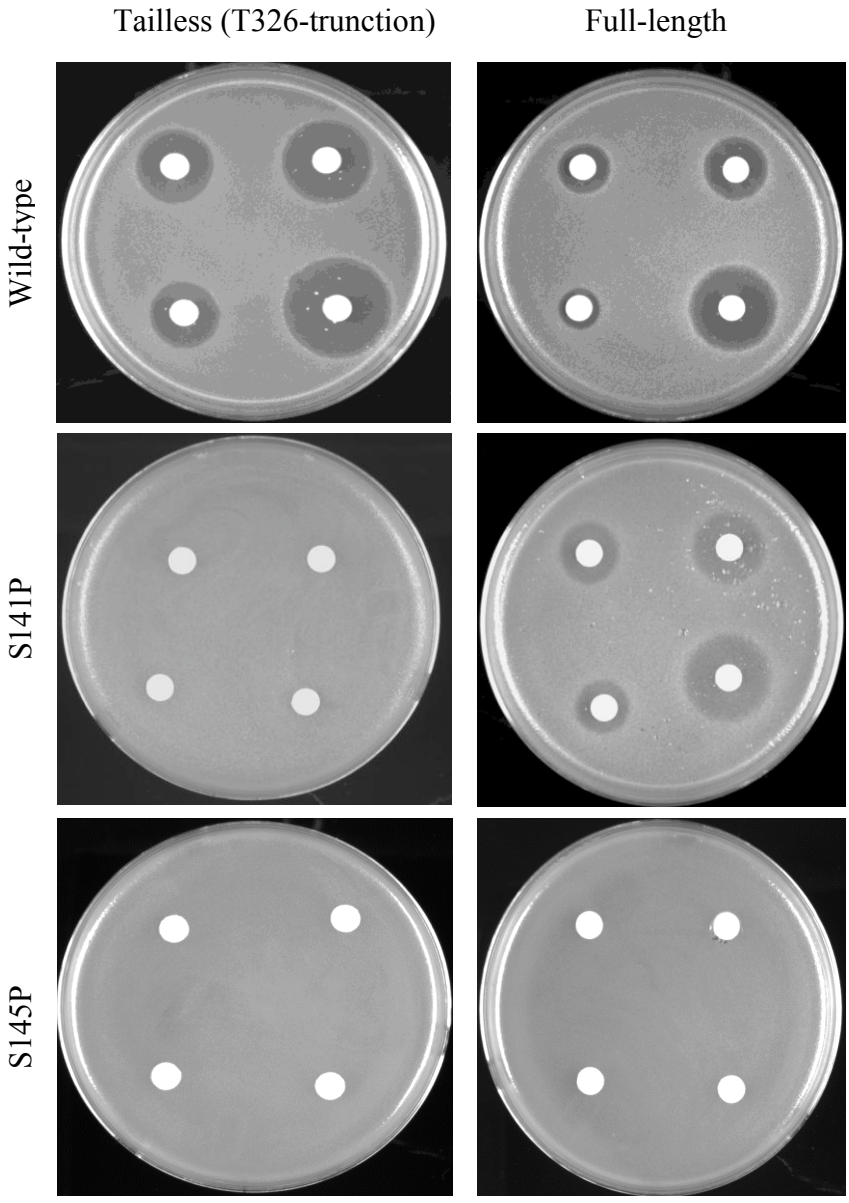
Tailless (T326-trunction)
Full-length
Wild-type
S141P
S145P

**Figure 4-13.** Full-length Ste2-S141P-GFP but not Ste2-S145P-GFP promotes α-factor sensitivity. Each filter disk contained α-factor (1, 0.5, 0.25 and 0.125 nmol, proceeding counter-clockwise from bottom right). Cells expressed receptors containing no amino acid substitution (wild-type) or containing the S141P or the S145P substitution as indicated at the left of each row. In the first column, cells expressed tailless Ste2-T326-GFP, Ste2-S141P-T326-GFP or Ste2-S145P-T326-GFP. In the second column, cells expressed full-length Ste2-GFP, Ste2-S141P-GFP or Ste2-S145P-GFP. Recipient strain was DJ1378-A-1. Plasmids were Ste2-T326-GFP (pDJ469), Ste2-S141P-T326-GFP (pDJ649), Ste2-S145P-T326-GFP (pDJ650), Ste2-GFP (pDJ658), Ste2-S141P-GFP (pDJ662) and Ste2-S145P-GFP (pDJ663). –Ura+CAA growth medium was used. Plates were incubated for two days at 30° C.

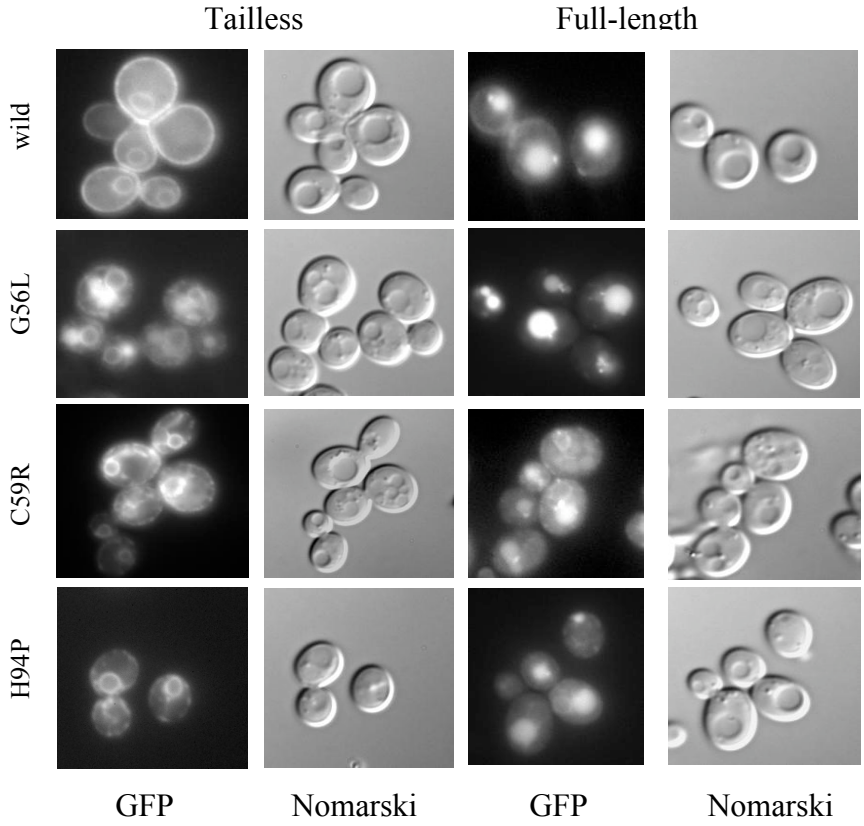


**Figure 4-14.** Role of the C-terminal domain in the localization of the Ste2-G56L-GFP, Ste2-C59R-GFP and Ste2-H94P-GFP fusion proteins. GFP fluorescence images and Nomarski images are indicated below each column. Cells expressed receptors containing no amino acid substitution (wild-type) or containing the G56L, the C59R or the H94P substitution as indicated at the left of each row. In the first two columns, cells expressed tailless Ste2-T326-GFP, Ste2-G56L-T326-GFP, Ste2-C59R-T326-GFP or Ste2-S145P-T326-GFP. In the last two columns, cells expressed full-length Ste2-GFP, Ste2-G56L -GFP, Ste2-C59R -GFP or Ste2-S145P -GFP. Recipient strain was DJ489-1. Plasmids were Ste2-T326-GFP (pDJ469), Ste2-G56L-T326-GFP (pDJ646), Ste2-C59R-T326-GFP (pDJ647), Ste2-H94P-T326-GFP (pDJ648), Ste2-GFP (pDJ658), Ste2-G56L-GFP (pDJ659), Ste2-C59R-GFP (pDJ660) and Ste2-H94P-GFP (pDJ661).

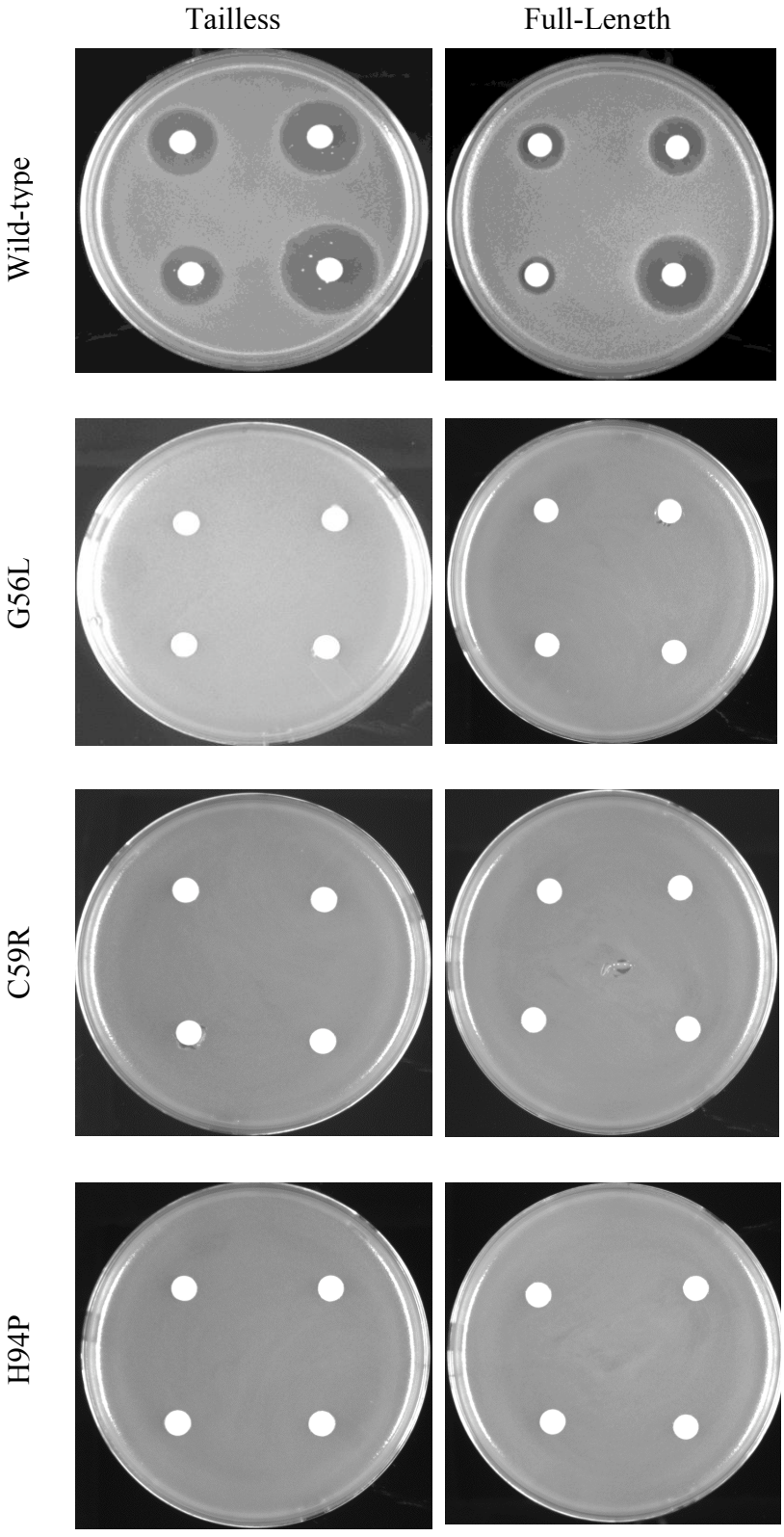
Tailless
Full-Length
Wild-type
G56L
C59R
H94P

**Figure 4-15.** Full-length Ste2-G56L-GFP, Ste2-C59R-GFP and Ste2-H94P-GFP do not promote α-factor sensitivity. Each filter disk contained α-factor (1, 0.5, 0.25 and 0.125 nmol, proceeding counter-clockwise from bottom right). Cells expressed receptors containing no amino acid substitution (wild-type) or containing the G56L, the C59R or the H94P substitution as indicated at the left of each row. In the first column, cells expressed tailless Ste2-T326-GFP, Ste2-G56L-T326-GFP, Ste2-C59R-T326-GFP or Ste2-S145P-T326-GFP. In the second column, cells expressed full-length Ste2-GFP, Ste2-G56L -GFP, Ste2-C59R -GFP or Ste2-S145P -GFP. Recipient strain was DJ1378-A-1. Plasmids were Ste2-T326-GFP (pDJ469), Ste2-G56L-T326-GFP (pDJ646), Ste2-C59R-T326-GFP (pDJ647), Ste2-H94P-T326-GFP (pDJ648), Ste2-GFP (pDJ658), Ste2-G56L-GFP (pDJ659), Ste2-C59R-GFP (pDJ660) and Ste2-H94P-GFP (pDJ661). –Ura+CAA growth medium was used. Plates were incubated for 2 days at 30° C.

**DXE motifs in C-terminus of Ste2 facilitate ER export**

The di-acidic ER exit motif, DXE, has been identified in the C-terminal region of vesicular stomatitis viral glycoprotein (VSVG) and potassium channel Kir2.1 (Nishimura and Balch, 1997; Stockklausner *et al.*, 2001). DXE was also required for efficient transport of the plant potassium ion channel, the nucleotide sugar transporter GONST1 and Golgi membrane protein CASP to the plasma membrane in plant cells (Hanton *et al.*, 2005; Mikosch *et al.*, 2006). DXE has also been found in the yeast membrane proteins, general amino acid permease (Gap1p) and Sys1p (Votsmeier and Gallwitz, 2001; Malkus *et al.*, 2002), and the DXE on both yeast proteins has been shown to facilitate efficient ER export. In yeast cells, Sys1 protein is a Golgi/endosomal membrane protein. Disruption of the DXE motif results in partial retention of Sys1 protein in the ER (Votsmeier and Gallwitz, 2001). The C-terminal cytoplasmic domain of Sys1p containing the DXE motif showed efficient binding to the Sec23p-Sec24p COPII subcomplex, and an *in vitro* assay indicated that the Sys1p tail lost its binding ability to Sec23p-Sec24p when the DLE motif was replaced by the ALA sequence (Votsmeier and Gallwitz, 2001).

As I described above, the C-terminal cytoplasmic domain of Ste2 facilitates ER export. However, specific sequences that are important in this process have not yet been identified. Interestingly, the cytoplasmic domain of Ste2 contains two DXE motifs (residue 370-371 and 417-419). To test whether these sequences serve as ER export signals, I constructed mutant forms of the various *STE2* alleles in which the aspartyl codon for both DXE motifs was replaced with an alanyl codon. These AXE substitutions

were assumed to have minimal consequences on other structural features of the C-terminal domain of Ste2. Fluorescent images of cells expressing the DXE and AXE forms of Ste2-S141P-GFP and Ste2-S141P-GFP indicated that DXE motifs are essential for exit of these mutant receptors from the ER (Fig. 4-16). Similarly, AXE forms of Ste2-C59R-GFP and Ste2-H94P-GFP also showed an ER localization (Fig. 4-17). However, the AXE forms of wild-type Ste2-GFP and the Ste2-G56L-GFP mutant retained the ability to exit the ER and accumulated in the vacuole. These results suggest that other sequence(s) in the C-terminus of Ste2, in addition DXE, also play a lesser role in ER export that is apparent when export signals in the main body of the receptor are partially functional. Interestingly, cells expressing the AXE form of the Ste2-S141P-GFP mutant showed $\alpha$-factor sensitivity that was intermediate between full-length Ste2-S141P-GFP and truncated Ste2-S141P-T326-GFP (Fig. 4-18). This result is also consistent with the presence of additional ER exit sequences in the C-terminal domain that are weaker than DXE.

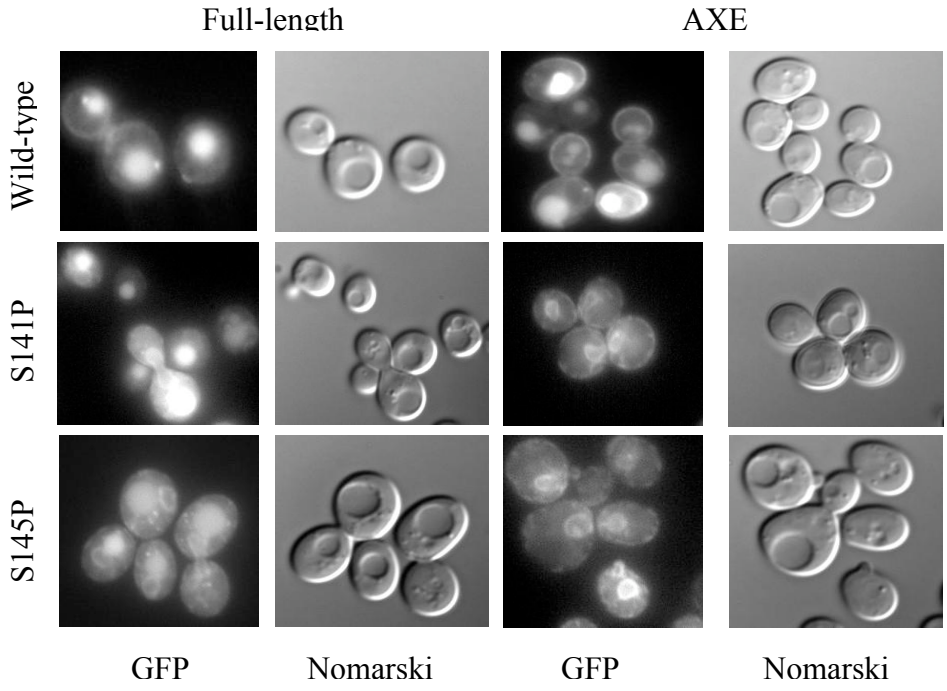


**Figure 4-16.** DXE motifs provide the ER export signal in Ste2-S141P and Ste2-S145P. GFP fluorescence images and Nomarski images are indicated below each column. Cells expressed receptors containing no amino acid substitution (wild-type) or containing the S141P or the S145P substitution as indicated at the left of each row. In the first two columns, cells expressed full-length receptors: Ste2-GFP, Ste2-S141P-GFP or Ste2-S145P-GFP. In the last two columns, cells expressed full-length receptors in which both DXE motifs had been changed to AXE: Ste2-AXE-GFP, Ste2-S141P-AXE-GFP or Ste2-S145P-AXE-GFP. Recipient strain was DJ489-1. Plasmids were Ste2-GFP (pDJ658), Ste2-S141P-GFP (pDJ662), Ste2-S145P-GFP (pDJ663), Ste2-AXE-GFP (pDJ665), Ste2-S141P-AXE-GFP (pDJ669) and Ste2-S145P-AXE-GFP (pDJ670).

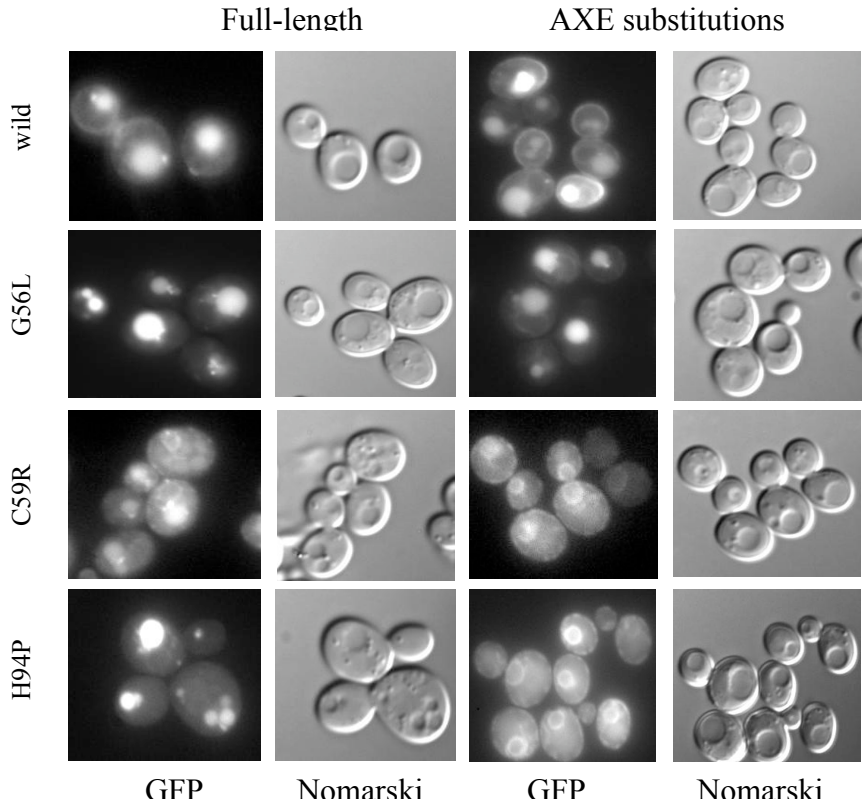


**Figure 4-17.** DXE motifs provide the ER export signal in Ste2-C59R and Ste2-SH94P but not in Ste2-G56L. GFP fluorescence images and Nomarski images are indicated below each column. Cells expressed receptors containing no amino acid substitution (wild-type) or containing the G56L, the C59R or the H94P substitution as indicated at the left of each row. In the first two columns, cells expressed full-length receptors: Ste2-GFP, Ste2-G56L-GFP, Ste2-C59R-GFP or Ste2-H94P-GFP. In the last two columns, cells expressed full-length receptors in which both DXE motifs had been changed to AXE: Ste2-AXE-GFP, Ste2-G56L-AXE-GFP, Ste2-C59R-AXE-GFP or Ste2-H94P-AXE-GFP. Recipient strain was DJ489-1. Plasmids were Ste2-GFP (pDJ658), Ste2-G56L-GFP (pDJ659), Ste2-C59R-GFP (pDJ660), Ste2H94P-GFP (pDJ661), Ste2-AXE-GFP (pDJ665), Ste2-G56L-AXE-GFP (pDJ666), Ste2-C59R-AXE-GFP (pDJ667) and Ste2-H94P-AXE-GFP (pDJ668).

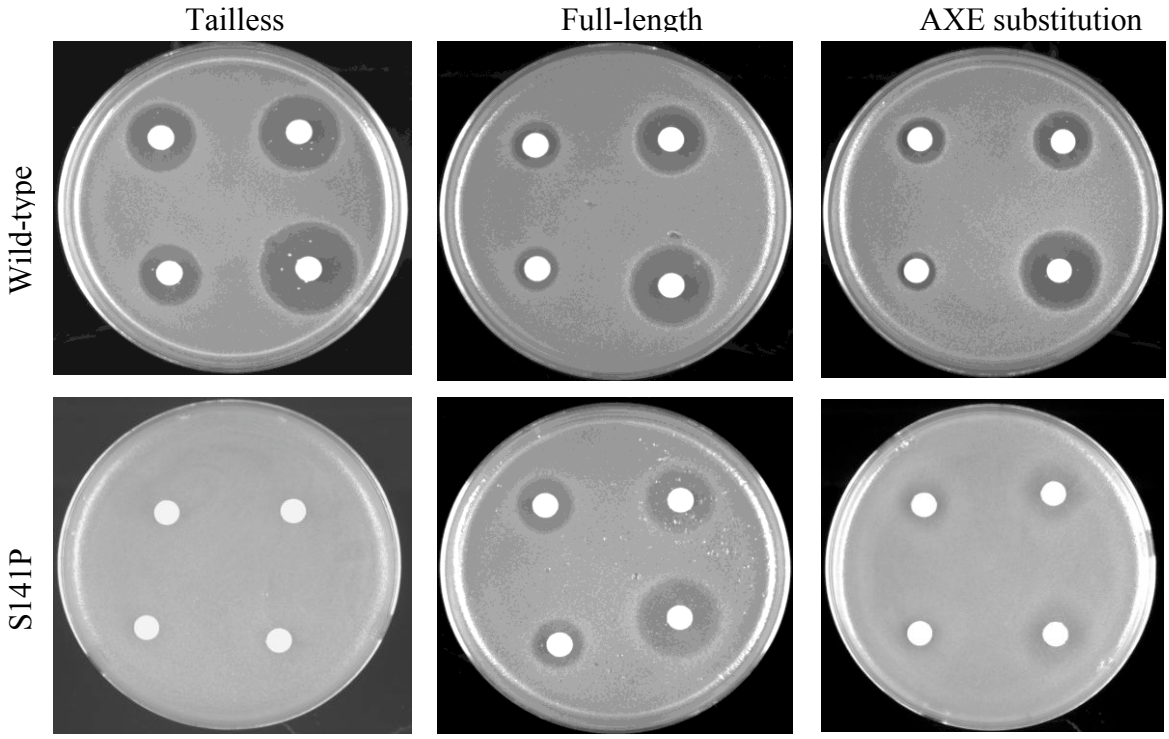


**Figure 4-18**. The DXE motifs necessary for full α-factor sensitivity of Ste2-S141P. Each filter disk contained α-factor (1, 0.5, 0.25 and 0.125 nmol, proceeding counter-clockwise from bottom right). Cells expressed receptors containing no amino acid substitution (wild-type) or containing the S141P substitution as indicated at the left of each row. In the first column, cells expressed tailless Ste2-T326-GFP or Ste2-S141P-T326-GFP. In the third column, cells expressed full-length Ste2-GFP or Ste2-S141P- GFP. In the second column, cells expressed full-length Ste2-AXE-GFP or Ste2-S141P-AXE-GFP. Recipient strain was DJ1378-A-3. Plasmids were Ste2-T326-GFP (pDJ469), Ste2-S141P-T326-GFP (pDJ649), Ste2-GFP (pDJ658), Ste2-S141P-GFP (pDJ662), Ste2-AXE GFP (pDJ665) and Ste2-S141P-AXE GFP (pDJ669). –Ura+CAA growth medium was used. Plates were incubated for two days at 30° C.

## Discussion

My data strongly suggest that at least two signals are involved in the ER export trafficking. One signal is in the C-terminal domain of Ste2 and a second signal is provided by structural features in the main body of the receptor (the hepta helical domain). The two signals are recognized independently, in that receptors containing either signal are able to exit from the ER. I further identified two DXE motifs within the C-terminal tail of Ste2 that facilitate the ER export; however, sequences on the C-terminal tail other than the two DXE motifs apparently play a weaker role in ER export since the full-length Ste2-S141P-AXE receptor provides weak α-factor sensitivity that is not seen the truncated Ste2-S141P-T326 receptor. To identify structural defects in the main body of Ste2, four ER retention mutants were obtained from two different screening strategies: the ER retention mutant screening method and complementation mutant screening method. My data suggest the proper conformational structure of Ste2 receptors serve as the second independent ER export signal.

Six motif sequences have been identified as ER export signals. Four motifs were found in GPCRs and these motifs are FxxxFxxxF in dopamine D1 receptor (Bermak *et al.*, 2001), ExxxLL in the vasopressin V2 receptor (Schulein *et al.*, 1998), $F(X)_6LL$ in AT1R and α2b-AR (Duvernay *et al.*, 2004) and FnxxLLxxxL in vasopressin V3 receptor (Robert *et al.*, 2005). These motifs described on the Chapter 1 are important for proper cell surface targeting. However, the molecular mechanism indicating how these motifs regulate receptor export from the ER remains unclear, and it is unknown whether these

motifs associate directly with the COPII complex. It has been proposed that these motifs provide the specific site for directing the receptors into vesicles that bud from the ER. It is also possible that these motifs provide a docking site for the cellular machinery that recognizes whether membrane proteins are properly folded and therefore competent for transport out of the ER. Ste2 does not contain those four motifs found in these GPCRs based on sequence analysis suggesting the α-factor may contain other signals for efficient ER export.

Two other ER export signals, the C-terminal domain dihydrophobic motif (Kappeler *et al.*, 1997; Nakamura *et al.*, 1998) and diacid (DXE) motif (Votsmeier and Gallwitz, 2001; Malkus *et al.*, 2002), have been characterized in non-GPCR membrane proteins in yeast. These two motifs interact directly with COPII components for efficient ER export. The dihydrophobic motif is not found on the Ste2. However, I identified two DXE motifs in the C-terminal domain of Ste2, and I determined that the two DXE motifs in the C-terminal domain of Ste2 facilitate ER export. Replacing the two DXE motifs with AXE sequence resulted in significant retention of the Ste2 mutant proteins in ER even though the rest of the C-terminal domain was present. However, redundant pathways apparently exist for ER export since wild-type receptors that lack the C-terminal domain are able to exit the ER with reduced efficiency.

In addition to the two DXE motifs, other sequences may be present in the C-terminal domain of Ste2 that play a lesser role in ER export. Based on the α-factor sensitivity assay, the S141P-AXE substitution mutant provided partial α-factor sensitivity suggesting cell surface targeting of mutant receptors. Although S141P-AXE resulted in

larger halo zones than Ste2-S141P-T326, the zones were significantly smaller and more turbid than zones produced with full-length Ste2-S141P. The Ste2-G56L-GFP mutant is only weakly retained in the ER. Based on images from the fluorescence microscope, the full-length Ste2-G56L-AXE-GFP receptors exited the ER more efficiently than truncated Ste2-G56L-GFP. This result is also consistent with sequences other than the two DXE motifs playing a minor role in ER export.

Interestingly, inspection of the amino acid sequence of other yeast GPCRs suggests that DXE is an ER export signal. Multiple sequence alignments of α-factor receptors from different species of budding yeast (*Kluyveromyces lactis*, *Saccharomyces bayanus* and *Saccharomyces paradoxus*) indicate the presence of DXE in the same position in the C-terminal tail. Two other G protein coupled receptors (Ste3 and Gpr1) in *S. cerevisiae* contain at least one DXE motif in the C-terminal tail suggesting that the DXE motif may serve a conserved role in ER export in yeast. An exception, the α-factor receptor of *Saccharomyces pastorianus* has a very short cytoplasmic C-terminal tail and does not contain the DXE motif. Apparently, in *S. pastorianus*, the signals in the main body of the receptor are sufficient to promote ER export.

The view that the main body of Ste2 contains an ER export signal is based on the partial ability of tailless wild-type receptors to reach the plasma membrane, whereas tailless mutant receptors are retained in the ER. In principle, the signal could reflect specific sequence motifs in the primary sequence, conformations associated with the tertiary structure or acquisition of quaternary structure. It is possible that mutants disrupting the conformational structure are recognized as misfolded protein and retained

in ER. However, in that case, it is hard to explain why a misfolded truncated mutant (for example Ste2-S141P-T326) can be corrected by simply adding back the C-terminal domain of Ste2 but not by adding back the C-terminal domain containing AXE substitutions. It seems unlikely that the main body of Ste2 contains an ER export motif in the primary sequence since I have identified ER retention mutants containing substitutions dispersed among TMI, TMII and TMIII, although the folded main body of Ste2 may present a "three dimensional" motif serving as an ER export signal. It is possible that defects in the tertiary structure of the mutant Ste2 lead to ER retention in monomers and that these defects are corrected by forming oligomeric complex with another Ste2 receptor. In this model, Ste2-S141P-T326 may resume its proper three dimensional structure when it associates with wild-type Ste2 receptors. Mutants such Ste2-C59R-T326 and Ste2-H94P-T326 are retained in the ER since they fail to form homo- or hetero-oligomers.

It is possible that Ste2 oligomerization itself serves as an ER export signal or helps receptors meet the ER quality control standards for efficient ER exit. At least three mechanisms are possible. First, each monomer may possess a weak export signal and the effective ER export signal can be reached cumulatively by forming oligomers. A second possibility is that an unidentified retention signal is masked by forming oligomers. The ER retention signal would be exposed only in the misfolded Ste2 receptors or the receptors unable to form Ste2 oligomers. Therefore, a Ste2 monomer may be sensed as a "misfolded" protein and retained in the ER. Finally, an oligomer-sensing chaperone may

recognize repeated structures in the oligomeric receptor complexes and direct them to the ER exit site.

The phenotype of the Ste-S145P-T326-GFP was more complex than Ste-S141P-T326-GFP. The original truncated Ste2-F55L, S145P-T326-GFP double substitution mutant resulted in α-factor sensitivity when the cells also expressed the full-length Ste2-S184R. However, the Ste-S145P-T326-GFP single mutant did not provide α-factor sensitivity when expressed with binding-defective mutant Ste2-S184R. Yet, the single Ste-S145P-T326-GFP mutant resulted in ER retention, and ER export was restored by coexpression with wild-type Ste2. The loss of function in Ste2-S145P is consistent with the previous report (Sommers and Dumont, 1997). The α-factor sensitivity assay suggested that full-length Ste2-S145P is also impaired in some aspect of signal transduction (i. e., ligand binding, the ligand-induced conformational change and/or G protein coupling). Therefore, the F55L substitution somehow corrects the signal defect of Ste2-S145P but does not correct the ER export defect.

Degradation of mutant Ste2-GFP fusion proteins is dependent on two proteolytic pathways located in the ER and in the vacuole. The endoplasmic reticulum-associated degradation (ERAD) pathway represents the primary means of quality control within the secretory pathway. Disruption of main ubiquitin ligase Hrd1p (Der3p) resulted in stabilization of mutant receptors. However, Hrd1p-dependent proteolysis cannot account for all of the loss of the mutant receptors because, in the *der3* mutant, the steady-state level of mutant Ste2 was never as high as the wild-type Ste2 control. Other

protein/proteins must also be involved in direct interaction with the Ste2 receptors that lead to the ER retention and degradation. Such proteins remain to be determined.

Overton et al (2003) reported that amino acid substitutions at G56 or G60 in the $^{56}$GxxxG$^{60}$ motif result in a decreased ability of the receptors to form oligomers. However, the authors probably over-estimate the severity of the oligomerization defect associated with their mutants, based on two potentially flawed observations: (1) lack of FRET between tailless G56L-CFP and G56L-YFP or G56A-CFP and G56A-YFP, and (2) the failure of Ste2-G56A-GFP to undergo ligand-induced endocytosis when co-expressed with wild-type receptors. First, the lack of FRET may have been a consequence of free CFP and YFP that were likely to have resulted from partial degradation of the fusion proteins. In my experiments, the GFP-tagged receptors are cleaved at a significant rate producing free GFP. Second, the apparent failure of G56A-GFP to undergo endocytosis may have been because most of the Ste2-G56A-GFP that appeared to be at the cell surface was actually located in the cortical ER just beneath the cell surface. Moreover, the loss of endocytosis activity of the various mutants (i. e., the reduction in fluorescent endocytic structures after $\alpha$-factor treatment) is roughly proportional to the reduction in cell-surface $\alpha$-factor binding sites before endocytosis is induced.

# CHAPTER V

# CORRELATION BETWEEN OLIGOMERIZATION AND ER EXPORT OF STE2

A large body of evidence suggests that GPCRs form oligomers before reaching the cell surface. A study of the serotonin 5-$HT_{2C}$ receptor has provided direct evidence for oligomer formation by using a microscopic technique that measures FRET efficiencies and indicates that the receptors form homodimers/oligomers in the ER (Herrick-Davis *et al.*, 2006). These types of observations raise the possibility that oligomerization plays a role in correct trafficking of GPCRs. The best example involves GABA receptors. GABAb R1 is retained in ER when expressed alone, and it is targeted to the cell surface when it forms dimers with GABAb R2 thereby masking an ER retention signal (Jones *et al.*, 1998; White *et al.*, 1998). This result indicates that heterodimerization is required for GABA receptor trafficking to the cell surface. In addition, the efficient plasma membrane trafficking of $\alpha$-$_{1D}$adrenergic requires co-expression of β-adrenergic receptors (Uberti *et al.*, 2005). In some cases, receptor interactions can have a negative impact on receptor trafficking as well. For example, a mutant form of V2 vasopressin receptor that is retained in the ER associates with wild-type receptors and prevents the complexes from reaching the cell surface (Zhu and Wess, 1998; Morello *et al.*, 2001). Similarly, mutant forms of the β-adrenergic receptor

also prevent cell surface targeting of the wild-type β-adrenergic receptor, and defects in a putative dimerization motif (GxxxGxxxL) in TM6 reduce cell surface expression (Salahpour *et al.*, 2004).

In the previous chapter, my results indicate that at least two independent signals promote ER export of the Ste2 protein. One signal is in the C-terminal tail. The other signal is in the heptahelical domain of the receptor. My results from ER retention mutant screening and complementation mutant screening suggested that dimerizaton of Ste2p is necessary for Ste2p in an ER quality checkpoint control. Previously, only the first transmembrane domain in the Ste2 receptor has been implicated in functioning as a dimerizaton interface since transmembrane I self-associates based on FRET assay (Overton *et al.*, 2003). Further investigation indicated that disruption of $^{56}$GxxxG$^{60}$ motif in the first transmembrane in the intact receptors resulted in reduced FRET activity.

## Results

This chapter describes an in vivo assay to address the issue of whether mutant receptors form homodimers with themselves or heterodimers with wild-type receptors. With this assay, I tested whether oligomerization of Ste2 accounts for the ER export signal that resides in the heptahelical domain of the receptor. The basis of my assay rests on the assumption that full-length Ste2 can promote ER export of mutant truncated Ste2 marked with GFP if and only if the two receptors form a complex. The approach was applied to the *ste2* mutants, described in Chapter 4, affecting transmembrane helices I, II and III. Cells expressing both truncated Ste2-T326-GFP and full-length wild-type Ste2 served as a positive control for the formation of homo-oligomers. As noted previously (Yesilaltay and Jenness, 2000), Ste2-T326-GFP that would otherwise accumulate in the ER (see Fig. 4-14) escapes to the cell surface in cells that express full length Ste2. For cells expressing Ste2-G56L-T326-GFP together with full length wild-type Ste2, the Ste2-G56L-T326-GFP fluorescence accululated in the vacuole instead of the ER (compare Fig. 5-1 with Fig. 4-14), indicating that Ste2-G56L-T326-GFP also form hetero-oligomers with the wild-type receptors. This results at least qualitatively, contradicts the published work (Overton *et al.*, 2003); however, as discussed below, it is possible that oligomers are disrupted only when both potential binding partners are mutant. In contrast, for cells expressing either Ste2-C59R-T326-GFP or Ste2-H94P-T326-GFP together with full-length wild-type Ste2, the fluorescent mutant receptors remained in the ER

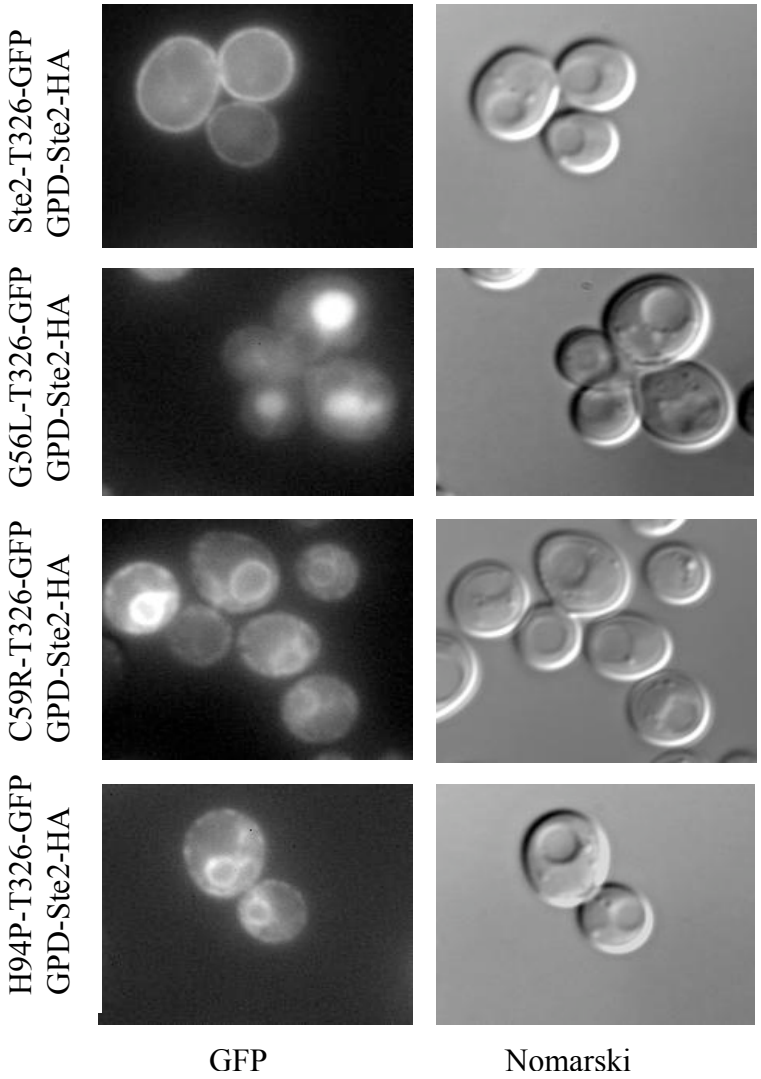


**Figure 5-1.** Effect of over-produced wild-type receptors on Ste2-G56L-T326-GFP, Ste2-C59R-T326-GFP and Ste2-H94P-T326-GFP. GFP fluorescent images and Nomarski images are indicated below each column. Indicated at the left of each row, cells expressed GFP-tagged truncated receptors containing no amino acid substitution (Ste2-T326-GFP), G56L (G56L-T326-GFP), C59R (C59R-T326-GFP) or H94P (H94P-T326-GFP). All cells expressed HA-tagged full-length wild-type receptors under the control of the GPD transcriptional promoter (GPD-Ste2-HA). Recipient strain was DJ489-1. Plasmids were pDJ469 (Ste2-T326-GFP), pDJ646 (Ste2-G56L-T326-GFP), pDJ647 (Ste2-C59R-T326-GFP), pDJ648 (Ste2-H94P-T326-GFP) and pDJ685 (GDP-Ste2-HA).

(compare Fig. 5-1 with Fig. 4-14), suggesting that both mutants fail to form hetero-oligomers. Results for the two mutants identified in the complementation screening strategy are depicted in Fig. 5-2. For cells expressing either Ste2-S141P-T326-GFP or Ste2-S145P-T326-GFP together with full-length wild-type Ste2, the fluorescent mutant receptors accumulated at the cell surface instead of the ER (compare Fig. 5-2 with Fig. 4-12), indicating the formation of hetero-oligomers. The result is consistent with my previous complementation test (Chapter 4) indicating that the Ste2-S141P-T326-GFP receptors promote α-factor sensitivity when they are permitted to interact with Ste2-S184R receptors.

I considered the possibility that the Ste2-H94P-T326-GFP receptor forms heterooligomer with the wild-type receptor and that the complexes are retained in the ER because the mutant receptor exerts a dominant negative effect on the exit of the hetero-oligomeric complex from the ER. A reciprocal experiment was designed in which the wild-type full-length Ste2 was tagged with GFP and the truncated mutant receptor was expressed under the direction of the GPD promoter. If hetero-oligomeric complexes were to form and were to be retained in the ER, then Ste2-GFP fluorescence would accumulate in the perinuclear location. Ste2-GFP progressed to the vacuole when expressed alone (Fig. 5-3 top panel). Ste2-H94-GFP progressed to the vacuole when expressed alone (Fig. 5-3 2$^{nd}$ panel). In the reciprocal experiment, for cells expressing full-length Ste2-GFP together with truncated Ste2-H94P-T326, the full-length Ste2-GFP accumulates in the vacuole indicating that Ste2-H94P-T326 does not cause dominant retention of receptor complexes. (Fig. 5-3, 3$^{rd}$ from top two panels). In the negative

control experiment, for cells expressing full-length Ste2-H94P-GFP together with truncated Ste2-H94P-T326, the full-length Ste2-H94P-GFP accumulates in the vacuole (Fig. 5-3 buttom panel). I conclude that Ste2-H94P-T326 does not exhibit a dominant retention phenotype, consistent with failure of the mutant receptor to form hetero-oligomeric complexes. The oligomerization assay was also adapted to detect homo-oligomeric complexes by taking advantage of the ability of the full-length mutants to exit the ER (Fig. 4-12 and Fig. 4-14). In the assay, the truncated mutant receptors tagged with GFP were expressed together with full-length mutant receptors. The full-length mutant receptors were expressed under the direction of the GPD transcriptional promoter. Cells expressing truncated Ste2-G56L-T326-GFP and full-length Ste2-G56L displayed fluorescence that was largely confined to the vacuole (compare Fig. 5-4 with Fig. 4-14), indicating that receptors containing the G56L substitution in the $^{56}$GxxxG$^{60}$ motif retain the ability to form homo-oligomeric complexes as well as hetero-oligomeric complexes. In contrast, for cells expressing truncated Ste2-C59R-T326-GFP together with full-length Ste2-C59R or for cells expressing truncated Ste2-H94P-T326-GFP together with full-length Ste2-H94P, the GFP signal was retained in ER indicating the C59R and H94P substitutions prevent homo-oligomer formation (Fig. 5-4). Results for the two mutants identified in the complementation screening strategy are depicted in Fig. 5-5. When Ste2-S141P-T326-GFP was expressed with Ste2-S141P and when Ste2-S145P-T326-GFP was expressed with Ste2-S145P, the GFP signal also failed to exit the ER, indicating that both the S141P and the S145P substitutions block the formation of homo-oligomers even though hetero-oligomers form

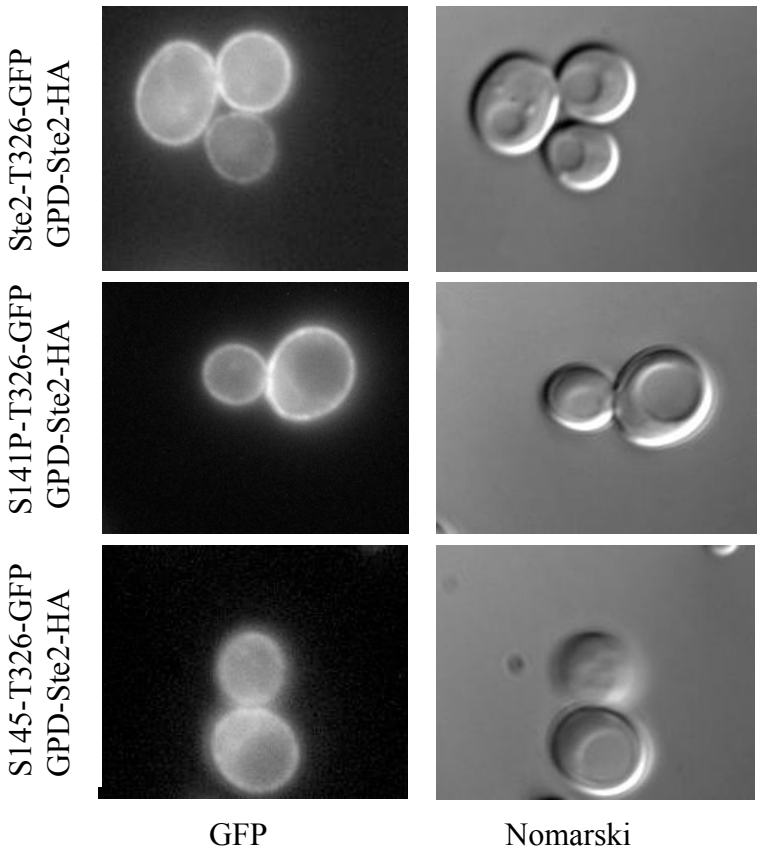


**Figure 5-2.** Effect of over-produced wild-type receptors on Ste2-S141P-T326-GFP and Ste2-S145P-T326-GFP. GFP fluorescent images and Nomarski images are indicated below each column. Indicated at the left of each row, cells expressed GFP-tagged truncated receptors containing no amino acid substitution (Ste2-T326-GFP), S141P (S141P-T326-GFP), or S145P (S145P-T326-GFP). All cells expressed HA-tagged full-length wild-type receptors under the control of the GPD transcriptional promoter (GPD-Ste2-HA). Recipient strain was DJ489-1. Plasmids were pDJ469 (Ste2-T326-GFP), pDJ649 (Ste2-S141-T326-GFP), pDJ650 (Ste2-S145P-T326-GFP) and pDJ685 (GDP-Ste2-HA).

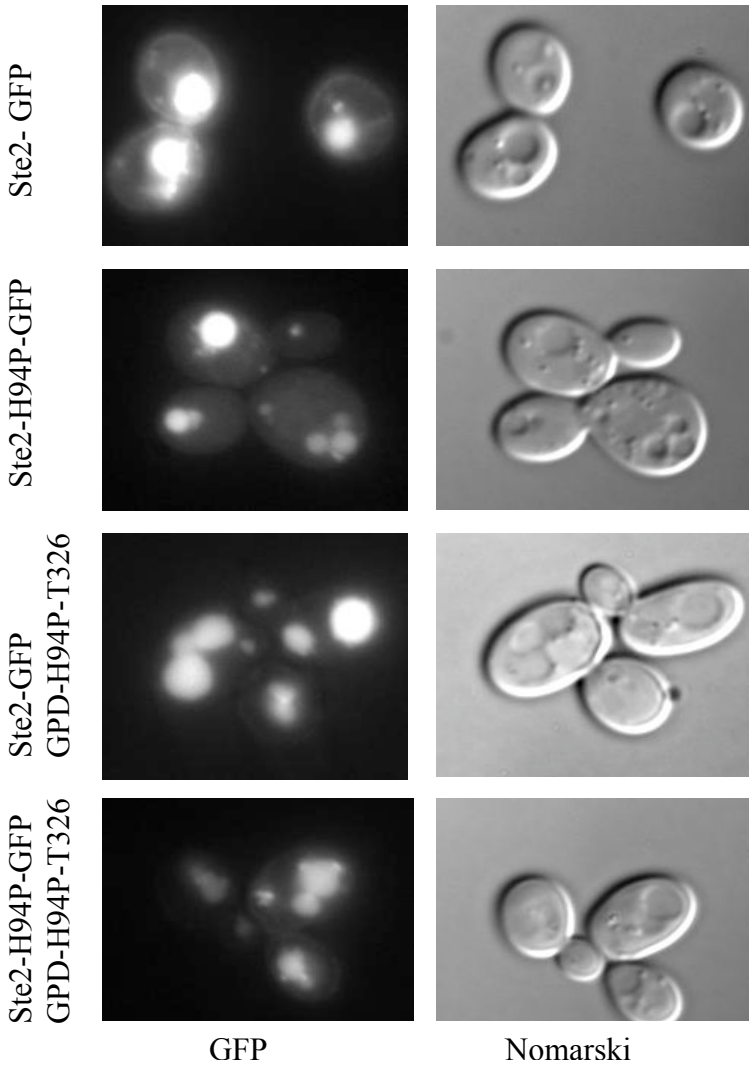


**Figure 5-3.** ER retained Ste2-H94P-T326 receptors do not impose a dominant effect on full-length receptors. GFP fluorescence images and Nomarski images are indicated below each column. Cells expressing indicated untagged full-length Ste2 and Ste2-H94PGFP proteins are shown at the left. The first row, cells expressing full-length Ste2-GFP. The second row, cells expressing Ste2-H94P-GFP. The third row, cells expressing Ste2-GFP and over-expressed Ste2-H94P-T326-HA. Bottom row, cells expressing Ste2-H94P-GFP and over-expressed Ste2-H94P-T326-HA. Ste2-H94P-T326-HA was expressed under the control of the GPD transcriptional promoter (GPD-H94P-T326). Recipient strain was DJ489-1. Plasmids were pDJ469 (Ste2-T326-GFP), pDJ646 (Ste2-G56L-T326-GFP), pDJ647 (Ste2-C59R-T326-GFP), pDJ648 (Ste2-H94P-T326-GFP) and pDJ685 (GDP-Ste2-HA).

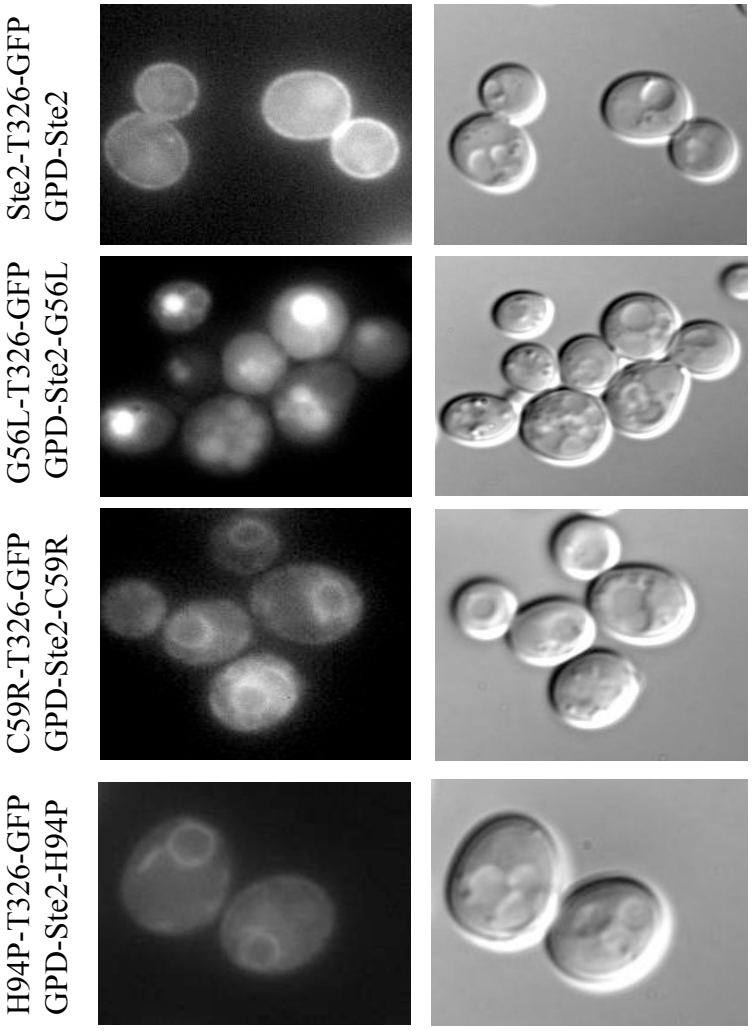
Ste2-T326-GFP
GPD-Ste2
G56L-T326-GFP
GPD-Ste2-G56L
C59R-T326-GFP
GPD-Ste2-C59R
H94P-T326-GFP
GPD-Ste2-H94P
GFP
Nomarski

**Figure 5-4.** Effect of over-produced full-length Ste2-G56L, Ste2-C59P and Ste2-H94P receptors on localization of Ste2-G56L-T326-GFP, Ste2-C59R-T326-GFP and Ste2-H94P-T326-GFP, respectively. GFP fluorescent images and Nomarski images are indicated below each column. Indicated at the left of each row, cells expressed GFP-tagged truncated receptors containing no amino acid substitution (Ste2-T326-GFP), G56L (G56L-T326-GFP), C59R (C59R-T326-GFP) or H94P (H94P-T326-GFP), as well as over-produced full-length HA-tagged receptors containing no amino acid substitution (GPD-Ste2), G56L (GPD-Ste2-G56L), C59R (GPD-Ste2C59R) or H94P (GPD-Ste2H94P). Over-produced full-length receptors were expressed under the control of the GPD transcriptional promoter. Recipient strain was DJ489-1. Plasmids were pDJ469 (Ste2-T326-GFP), pDJ646 (Ste2-G56L-T326-GFP), pDJ647 (Ste2-C59R-T326-GFP), pDJ648 (Ste2-H94P-T326-GFP), pDJ685 (GDP-Ste2), pDJ686 (GDP-Ste2-G56L), pDJ687 (GDP-Ste2-C59R) and pDJ688 (GDP-Ste2-H94P).

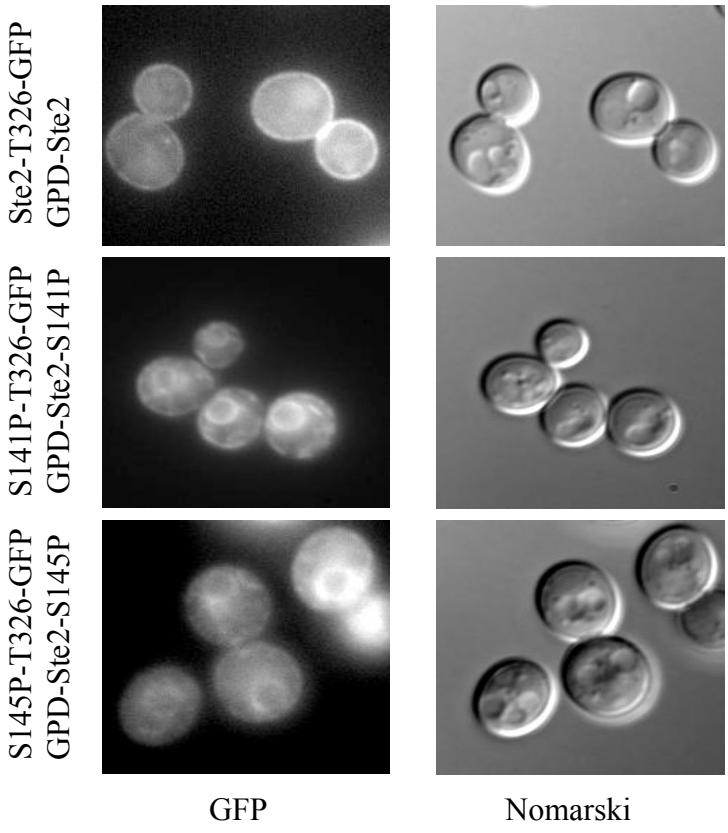


**Figure 5-5.** Effect of over-produced full-length Ste2-S141P and Ste2-S145P receptors on localization of Ste2-S141P-T326-GFP and Ste2-S145P-T326-GFP, respectively. GFP fluorescent images and Nomarski images are indicated below each column. Indicated at the left of each row, cells expressed GFP-tagged truncated receptors containing no amino acid substitution (Ste2-T326-GFP), S141P (S141P-T326-GFP) or S145P (S145P-T326-GFP), as well as over-produced full-length HA-tagged receptors containing no amino acid substitution (GPD-Ste2), S141P (GPD-Ste2-S141P) or S145P (GPD-Ste2-S145P). Over-produced full-length receptors were expressed under the control of the GPD transcriptional promoter. Recipient strain was DJ489-1. Plasmids were pDJ469 (Ste2-T326-GFP), pDJ649 (Ste2-S141-T326-GFP), pDJ650 (Ste2-S145P-T326-GFP), pDJ685 (GDP-Ste2), pDJ689 (GDP-Ste2-S141P) and pDJ690 (GDP-Ste2-S145P).

(compare Fig. 5-2 and Fig. 5-5).

In order to summarize results from Chapters 4 and 5 in a more quantified format, I counted the cells that showed specific localization patterns and tabulated the results. Independent experiments representing each of the different Ste2 mutant combinations were performed at least three times, and over 100 cells were evaluated for each experiment. Each of the cells in a microscopic field was assigned to one of five localization patterns depicted in Fig. 5-6. For the localization pattern designated ER (Fig. 5-6A), the cells show a fluorescent perinuclear ring and weaker fluorescence near the cell surface, reflecting the cortical ER. I cannot exclude the possibility that a small amount of plasma membrane localization is also present. For the vacuole pattern (Fig. 5-6B), the fluorescence accumulates in one or more round filled structures. When examined, each of these structures coincided with a structure that was visible in the Nomarski image. Some of the cells (especially the wild-type Ste2-GFP cells) that were scored as the vacuole pattern also showed very faint fluorescence at the cell surface. The localization pattern, designated Vac+ER (Fig. 5-6C), was a mixture of the vacuole and the ER pattern. For the PM pattern (Fig. 5-6D), the cell surface was visible with no perinulear fluorescence and little or no vacuolar fluorescence. In the PM+ER pattern (Fig. 5-6E), the cell surface was brighter than the perinuclear ring.

Table 5-1 shows the results from cells expressing truncated receptors alone (see Fig. 4-14). The bulk of the truncated wild-type receptors (Ste2-T326-GFP) accumulated at the cell surface, and two-thirds of the cells showed some ER staining as well, consistent with the mild ER retention phenotype reported previously (Yesilaltay and Jenness, 2000).

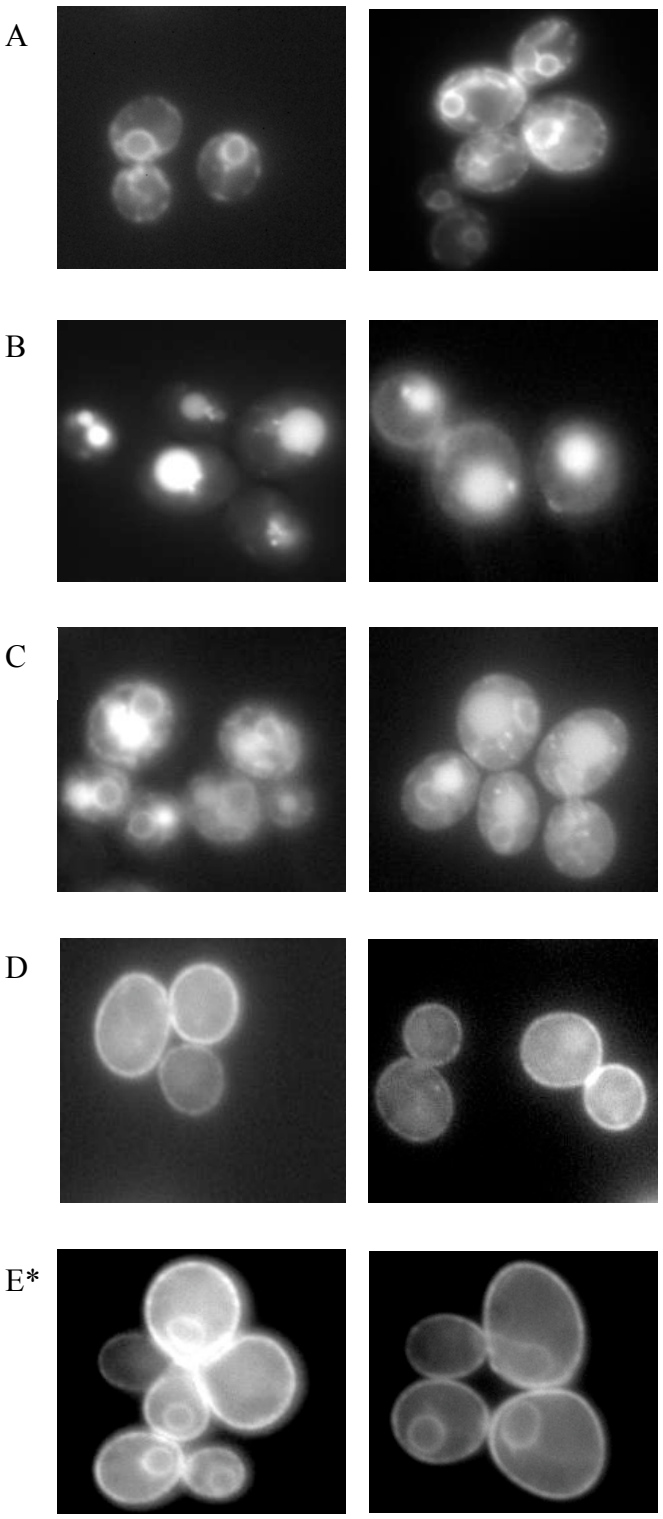
A
B
C
D
E*

Figure 5-6. Scoring method for the tabulated results in Tables 6-1,2 3 and 4. (A) endoplasmic reticulum (ER) (B) vacuole (Vac). (C) ER+ Vac (D) plasma membrane (PM) (E) PM+ER * PM+ER was only observed for the Ste2-T326-GFP receptors.

| Truncated Ste2 | ER (%) | Vacuole (%) | ER+Vac (%) | ER+PM (%) | PM (%) |
|---|---|---|---|---|---|
| Ste2-T326-GFP | - | - | - | 66±2 | 34±2 |
| Ste2-G56L-T326-GFP | 6±2 | 17±2 | 78±2 | - | - |
| Ste2-C59R-T326-GFP | 100 | - | - | - | - |
| Ste2-H94P-T326-GFP | 100 | - | - | - | - |
| Ste2-S141P-T326-GFP | 100 | - | - | - | - |
| Ste2-S145P-T326-GFP | 100 | - | - | - | - |

Table 5-1. Tabulated results for the subcellular localization of truncated mutant receptors. Cells expressing the indicated truncated receptor were scored for subcellular localization as shown in Fig. 6. Each entry is the average percentage of the total and the standard deviation for three independent experiments. More than 100 cells were scored for each experiment. The recipient strain was DJ489-1. Plasmids were pDJ469 (Ste2-T326-GFP), pDJ646 (Ste2-G56L-T326-GFP), pDJ647 (Ste2-C59R-T326-GFP), pDJ648 (Ste2-H94P-T326-GFP), pDJ649 (Ste2-S141P-T326-GFP) and pDJ650 (Ste2-S145P-T326-GFP).

For cells expressing the truncated mutant receptors, Ste2-C59R-T326-GFP, Ste2-H94P-T326-GFP, Ste2-S141P-T326-GFP and Ste2-S145P-T326-GFP, essentially the entire fluorescent signal was retained in the ER. However, in the cells expressing Ste2-G56L-T326-GFP most of the cells accumulated fluorescence in both the ER and vacuole, suggesting Ste2-G56L-T326-GFP exits from ER at a slow rate.

Table 5-2 shows the localization results for the full-length mutant receptors. For the wild-type Ste2-GFP, the bulk of the GFP fluorescence accumulated in the vacuole due to endocytosis of the full-length protein (Li *et al.*, 1999). Unlike the truncated mutant receptors (Table 5-1), the full-length mutant receptors exited the ER to varying efficiencies. Nearly 100% of the Ste2-G56L-GFP and Ste2-H94P-GFP exited the ER and accumulated in the vacuole. Ste2-C59R, Ste2-S141P and Ste2-S145P exited the ER at a reduced efficiency. These results indicate that the C-terminal domain plays a significant role in promoting the export of wild-type and mutant receptors from the ER.

Table 5-3 summarizes the results obtained with cells expressing GFP-tagged truncated receptors together with overproduced wild-type Ste2. In comparing Table 5-3 with Table 5-1, the results demonstrate that both Ste2-C59R-T326-GFP and Ste2-H94P-T326-GFP fail to form heterodimers with full-length wild-type Ste2 since all of GFP was retained in the ER. In contrast, the Ste2-S141P-T326-GFP and Ste2-S145P-T326-GFP mutant receptors form heterodimers with wild-type Ste2, based on the shift in GFP signal the from ER (Table 5-1) to the plasma membrane and the vacuole (Table 5-3). Again, the tabulated results confirmed the previous observation

| Full-length Ste2 | ER (%) | Vacuole (%) | ER+Vac (%) | PM (%) |
|---|---|---|---|---|
| Ste2 | - | 100 | - | - |
| Ste2-G56L | - | 99±1 | - | 1±1 |
| Ste2-C59R | 36±3 | 21±4 | 43±6 | - |
| Ste2-H94P | 1±1 | 97±2 | 2±2 | - |
| Ste2-S141P | 20±1 | 53±3 | 27±2 | - |
| Ste2-S145P | 28±11 | 42±14 | 30±5 | - |

Table 5-2. Tabulated results for the subcellular localization of full-length receptors. Cells expressing the indicated full-length receptor were scored for subcellular localization as shown in Fig. 6-6. Each entry is the average percentage of the total and the standard deviation for three independent experiments. More than 100 cells were scored for each experiment. The recipient strain was DJ489-1. Plasmids were pDJ658 (Ste2-GFP), pDJ659 (Ste2-G56L-GFP), pDJ660 (Ste2-C59R-GFP), pDJ661 (Ste2-H94P-GFP), pDJ662 (Ste2-S141P-GFP) and pDJ663 (Ste2-S145P-GFP).

| Ste2-HA / Truncated Mutants | ER (%) | Vacuole (%) | ER+Vac (%) | PM (%) |
|---|---|---|---|---|
| Ste2-HA / Ste2-T326-GFP | - | 19±3 | - | 81±3 |
| Ste2-HA / G56L-T326-GFP | 2±2 | 83±2 | 15±3 | - |
| Ste2-HA / C59R-T326-GFP | 100 | - | - | - |
| Ste2-HA / H94P-T326-GFP | 99±1 | - | 1±1 | - |
| Ste2-HA / S141P-T326-GFP | - | 23±5 | 1±1 | 76±4 |
| Ste2-HA / S145P-T326-GFP | 2±2 | - | 1±1 | 97±2 |

Table 5-3. Tabulated results for the subcellular localization of truncated mutant receptors in the presence of untagged wild-type receptors. Cells expressing the indicated truncated receptor and over-expressing full-length Ste2-HA were scored for subcellular localization as shown in Fig. 5-6. Over-expressed Ste2-HA receptors were expressed under the control of the GDP transcriptional promoter. Each entry is the average percentage of the total and the standard deviation for three independent experiments. More than 100 cells were scored for each experiment. The recipient strain was DJ489-1. Plasmids were pDJ685 (Ste2-HA), pDJ469 (Ste2-T326-GFP), pDJ646 (Ste2-G56L-T326-GFP), pDJ647 (Ste2-C59R-T326-GFP), pDJ648 (Ste2-H94P-T326-GFP), pDJ649 (Ste2-S141P-T326-GFP) and pDJ650 (Ste2-S145P-T326-GFP).

(Fig. 5-1) in that, for over 80% of the cells, all of the truncated Ste2-G56L-T326-GFP exited ER, suggesting that most but not all of the Ste2-G56L-T326-GFP mutant receptors form heterdimers with wild-type Ste2.

Table 5-4 summarizes the localization pattern of GFP-tagged truncated mutants, when they are co-expressed with full-length receptors containing the same amino acid substitution. As expected, the Ste2-C59R-T326-GFP and Ste2-H94P-T326-GFP receptors were retained in the ER, consistent with the results in Table 5-3. Interesting, the truncated Ste2-S141P-T326-GFP and Ste2-S145P-T326-GFP were also retained completely in the ER (Table 5-4), indicating both mutants failed to form homodimers even though they formed heterodimers efficiently (Table 5-3). Ste2-G56L-T326-GFP showed a similar localization pattern in Table 5-3 and Table 5-4, indicating that Ste2-G56L-T326-GFP forms both homo-oligomers and hetero-oligomers. These results appear to be inconsistent with the findings of Overton et al. (2003), who found that the Ste2-G56L substitution resulted in only a baseline level of oligomerization as judged by their FRET assay.

Both Ste2-C59R and Ste2-H94P were substitution that may severely disrupt receptor structure. The Ste2-C59R mutation replaces a small side chain with in a large and positively charged side chain, and the H94P substitute is expected cause in a kink in the TM2 helix. I constructed additional mutants that causes less sevre effect, Ste2-C59A and Ste2-H94A, to test whether the original phenotypes depended on the presence of disruptive residues. Cells expressing Ste2-C59A-T326-GFP showed an α-factor

| Full-length / Truncated Receptor | ER (%) | Vacuole (%) | ER+Vac (%) | PM (%) |
|---|---|---|---|---|
| Ste2-HA / Ste2-T326-GFP | - | 22±4 | - | 78±4 |
| G56L-HA / G56L-T326-GFP | 5±2 | 77±6 | 18±7 | - |
| C59R-HA / C59R-T326-GFP | 100 | - | - | - |
| H94P-HA / H94P-T326-GFP | 100 | - | - | - |
| S141P-HA / S141P-T326-GFP | 99±1 | 1±1 | - | - |
| S145P-HA / S145P-T326-GFP | 99±1 | 1±1 | - | - |

Table 5-4. Tabulated results for the subcellular localization of truncated mutant receptors in the presence of untagged full-length mutant receptors. Cells expressing the indicated GFP-tagged truncated receptor and over-expressing the HA-tagged full-length receptor indicated were scored for subcellular localization as shown in Fig. 5-6. Over-expressed receptors were expressed under the control of the GDP transcriptional promoter. Each entry is the average percentage of the total and the standard deviation for three independent experiments. More than 100 cells were scored for each experiment. The recipient strain was DJ489-1. Plasmids were pDJ685 (Ste2-HA), pDJ686 (Ste2-G56L-HA), pDJ687 (Ste2-C59R-HA), pDJ688 (Ste2-H94P-HA), pDJ689 (Ste2-S141P-HA), pDJ690 (Ste2-S145P-HA), pDJ469 (Ste2-T326-GFP), pDJ646 (Ste2-G56L-T326-GFP), pDJ647 (Ste2-C59R-T326-GFP), pDJ648 (Ste2-H94P-T326-GFP), pDJ649 (Ste2-S141P-T326-GFP) and pDJ650 (Ste2-S145P-T326-GFP).

**A.**

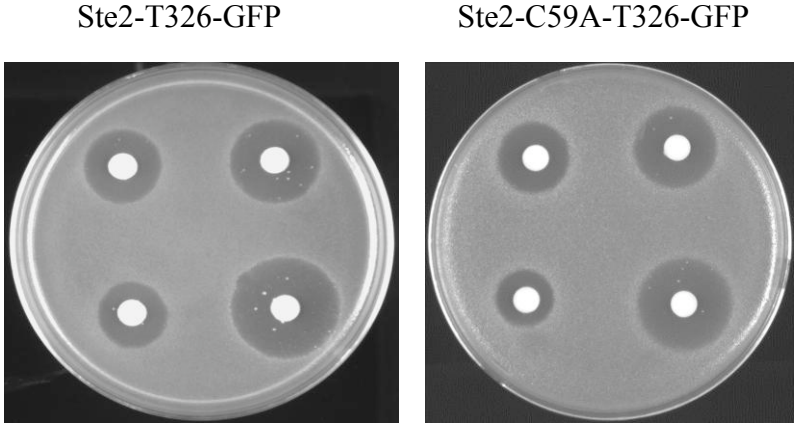
Ste2-T326-GFP
Ste2-C59A-T326-GFP

**B.**

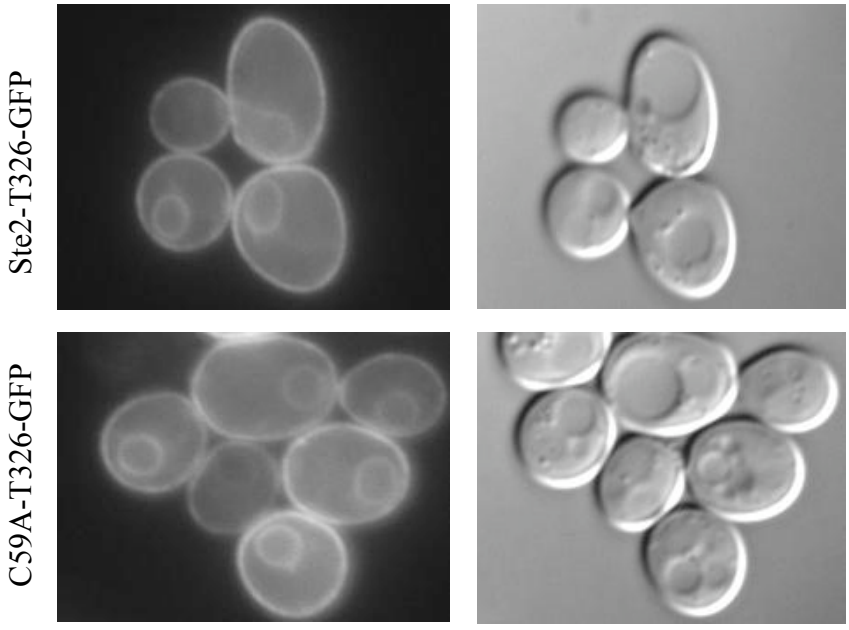
Ste2-T326-GFP
C59A-T326-GFP
GFP
Nomarski

**Figure 7.** α-factor sensitivity and subcellular localization of Ste2-C59A-GFP.
**(A)** α-factor sensitivity test. Each filter disk containing different amount of α-factor (1, 0.5, 0.25 and 0.125 nmol, proceeding counter-clockwise from bottom right) was placed on a lawn of the indicated yeast cells and then incubated for two days 30° C. Yeast cells expressing the indicated mutant are shown on the top. **(B)** Subcellular localization of truncated wild-type Ste2-T326-GFP and mutant Ste2-C59A-T326-GFP fusion proteins. GFP fluorescence images and Nomarski images are indicated below each column. Culture medium was -Ura+CAA. Recipient strain was DJ489-1. Plasmids were pDJ469 (Ste2-T326-GFP) and pDJ652 (Ste2-C59A-T326-GFP).

sensitivity (Fig. 5-7A) and intracellular localization (Fig. 5-7B) that was similar to wild-type control cells. I conclude that the phenotype associated with Ste2-C59R-T326-GFP receptors results from the presence of arginine rather than the absence of cysteie. In contrast, the truncated Ste2-H94A-T326-GFP receptor showed a strong ER retention phenotype, and the full-length Ste2-H94A-GFP receptors accumulated in the vacuole (Fig. 5-8). These phenotypes are similar to respective phenotypes associated with the original Ste2-H94P-T326-GFP and Ste2-H94P-GFP mutant receptors. Interestingly, both truncated Ste2-H94A-T326-GFP and full-length Ste2-H94A-GFP show α-factor sensitivity (Fig. 5-9). The result suggested that although most of the truncated Ste2-H94A-T326-GFP receptors were retained in the ER, some mutant protein must reach the cell surface. The different localization in the truncated Ste2-C59R-T326-GFP and Ste2-C59A-T326-GFP suggested ER retention of Ste2-C59R-T326-GFP was due to the nonspecific occlusion of this site. In addition, it was located within the $^{56}$GxxxG$^{60}$ motif. Therefore, it was possible that larger amino acid substitution (C to R) resulted in the disruption of dimer interface. In contrast, although truncated Ste2-H94A-T326-GFP can resume α-factor sensitivity, the halo zone was significantly smaller comparing with truncated wild-type Ste2-T326-GFP. The result suggested the H94 was not only important in dimerization, it also provided a positive contribution in α-factor signaling.

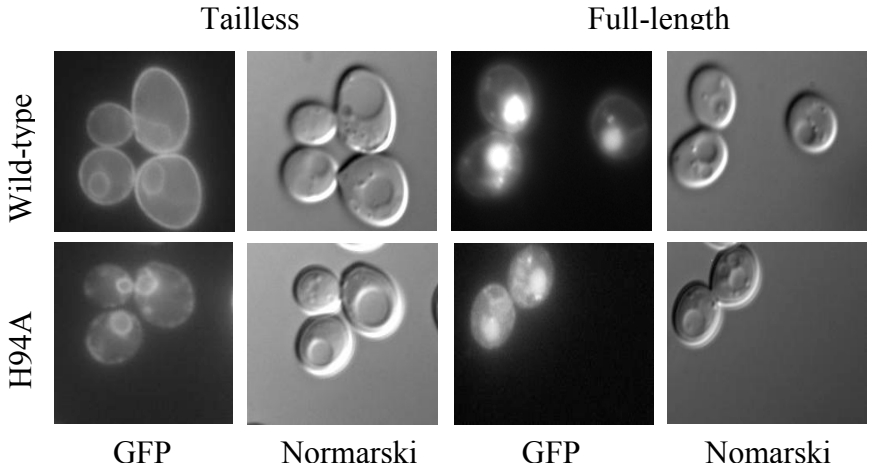


**Figure 8.** Subcellular localization of Ste2-H94A-T326-GFP and Ste2-H94A-GFP. GFP fluorescence images and Nomarski images are indicated below each column. In the first two columns, cells expressed Ste2-T326 (wild-type) or Ste2-H94A-326 (H94A). In the last two columns, cells expressed full-length Ste2 (wild-type) or Ste2-H94A-GFP (H94A). The recipient strain was DJ489-1. Plasmids were pDJ469 (Ste2-T326-GFP), pDJ658 (Ste2-GFP), pDJ653 (Ste2-H94A-T326-GFP) and pDJ664 (Ste2-H94A-GFP).

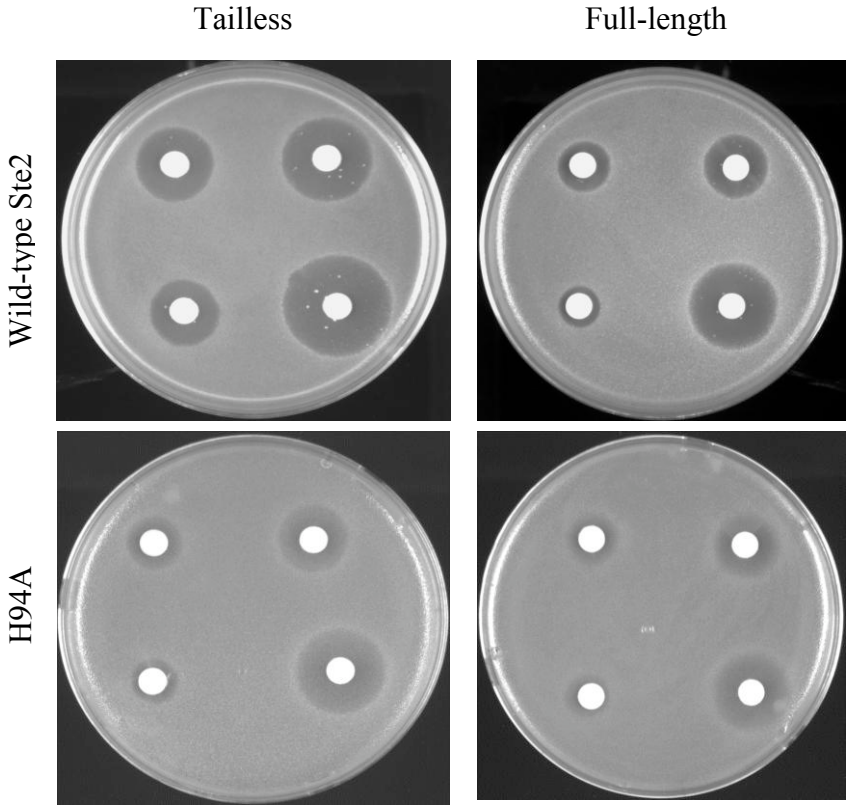


**Figure 9.** Ste2-H94A-T326-GFP and Ste2-H94A-GFP α-factor sensitivity tests. Each filter disk containing α-factor (1, 0.5, 0,25 and 0,125 nmol, proceeding counter-clockwise from bottom right) was placed on a lawn of the indicated cells and then incubated for two days at 30° C. In the first column, cells expressed tailless Ste2-T326-GFP (Wild-type) or Ste2-H94A-T326-GFP (H94A). In the second column, cells expressed full-length Ste2-GFP (Wild-type) or Ste2-H94A-GFP (H94A). Culture medium was –Ura+CAA. The recipient strain was DJ489-1. Plasmids were pDJ469 (Ste2-T326-GFP), pDJ658 (Ste2-GFP), pDJ653 (Ste2-H94A-T326-GFP) and pDJ664 (Ste2-H94A-GFP).

## Discussion

In this chapter, oligomerization of Ste2 in the ER was analyzed using an in vivo assay devised to address whether the two classes of mutants identified in Chapter 4 can form hetero-oligomers or homo-oligomers. As the basis of the assay, I tested whether GFP-tagged mutant receptors that are retained in the ER can be exported when co-expressed with untagged proteins that exit the ER. The data obtained from fluorescence microscopic images were quantified by counting single cells representing different phenotypic groups. The results suggest that Ste2-C59R and Ste2-H94P fail to form homooligomers or hetero-oligomers in the ER, that Ste2-G56L is partially defective for homooligomer and heterodimer formation, and that Ste2-S141P and Ste2-S145P fail to form homo-oligomers even though they form hetero-oligomers with wild-type receptors. I considered the possibility that the failure of GFP-tagged truncated mutants to be rescued by full-length receptors was due to a dominant-negative effect of the truncated receptors on ER exit and not due to failure to form oligomers. The inability of the overexpressed Ste2-H94P-T326 to retain the full-length wild-type Ste2-GFP or full-length mutant Ste2-H94P-GFP in the ER is inconsistent with this hypothesis. Results from Chapter 4 suggest that independent signals for ER export are located in the C-terminal tail of the receptor and in the heptahelical domain. From the Chapter 5 results, it is clear that the signal(s) in the C-terminal tail do not require oligomerization, whereas the failure of the mutants affecting the heptahelical domain are consistent with the hypothesis that oligomerization provides the second ER export signal.

Overall, my results indicate that TM domains I (containing Cys59), II (containing His94) and III (containing Ser141 and Ser145), are important for receptor oligomerization as well as for ER export. One possibility for the failure to form oligomeric complexes is that the mutant receptors are grossly unfolded. This does not appear to be the case for Ste2-S141P and Ste2-S145P since they are capable of recognizing and associating with wild-type full-length receptors. Moreover, the full-length Ste2-S141P receptors that escape the ER are functional, and Ste2-S141-T326 forms functional complexes with α-factor binding defective receptors and G protein-coupling defective receptors. I also tested less severe mutants of the affected codons C59 and H94. Two substitution mutations, C59A and H94A, were included in this study. Consistent with earlier studies with full-length Ste2-C59A (David *et al.*, 1997; Yesilaltay and Jenness, 2000), I found that truncated Ste2-C59A localizes properly on the cell surface and α-factor sensitivity is indistinguishable from truncated wild-type Ste2. Amino acid C59 is located within the $^{56}$GxxxG$^{60}$ motif. Substitution of cysteine with a bulky charged amino acid such as arginine into the proposed dimer interface may cause a steric contact problem between adjoining subunits; also the presence of arginine at position 58 may aggravate the presence of arginine in the neighboring position 59. However, I cannot rule out the possibility that the C59R substitution leads to a grossly misfolded receptor. Unlike Ste2-C59A-T326, truncated Ste2-H94A-T326 was retained in ER. Apparently, some of the Ste2-H94A and Ste2-H94A-T326 receptors were able to reach the plasma membrane in an active form since the mutants showed some (albeit reduced) α-factor sensitivity. It is possible that the Ste2-H94A receptor reflects a leaky

oligomer mutant; therefore, a small amount of mutant receptors escape the quality control machinery in the ER and reach the plasma membrane by forming weak oligomers. The partial function of Ste2-H94A and Ste2-H94A-T326 suggests that they are not grossly misfolded. Further investigation is required to test whether the Ste2-H94A can form homo or hetero dimers.

Most GPCRs appear to form dimers or higher oligomeric complexes. However, the functional significance for dimerization has been built mainly on the requirement for intracellular trafficking. The importance of dimerization on cell-surface targeting was implied for several GPCRs such as GABA receptors (Jones *et al.*, 1998; White *et al.*, 1998), β2-adrenergic receptor (Salahpour *et al.*, 2004) and D2 dopamine receptors (Lee *et al.*, 2000). However, whether oligomerizaton is required for functional coupling to heterotrimeric G-proteins remains inconclusive. Leukotriene B4 receptor (BLT1 receptor) reconstituted with G-protein with solution-phase neutron-scattering experiments suggest that one G-protein binds to a receptor dimer (Baneres and Parello, 2003). In the best-known heterodimeric complex, the GABA receptor complex, GABA b1 and GABA b2 are required for proper location and normal function; however, only one subunit couples to a G-protein and the other subunit binds the agonist. The conclusion is based on normal receptor heterodimer function when the agonist-binding GABA b1 subunit contains a defect in third intracellular loop, whereas the heterodimers are not functional when the same third-loop defect affects the agonist-binding-defective GABA b2 subunit (Duthey *et al.*, 2002). For the metabotropic glutamate receptor, upon activation, only one heptahelical domain of the homodimer is turned on (Hlavackova *et al.*, 2005). Recently,

it has been speculated that dimerization of GPCRs may play a role in facilitating the activation of heterotrimeric G proteins. In studies of rhodopsin, monomers activate G proteins, however, the activation process is faster when the rhodopsin is organized into dimers or higher order oligomers (Jastrzebska *et al.*, 2004; Ridge and Palczewski, 2007).

Two results in this chapter provide suggestive evidence indicating that dimers containing two functional receptors are not required for the α-factor response. First, the ability of the truncated receptors, Ste2-F204S-T326 and Ste2-S141P-T326, to complement is consistent with this view. Since Ste2-S141P-T326 reaches the plasma membrane only when it associates with Ste2-F204S-T326, the only receptor dimers on the cell surface that contain an α-factor binding site will be heterodimers. Furthermore, since F204S-T326 will not undergo ligand-induced conformational changes and since no detectable conformational changes are transduced between subunits (Chapter 3), the single Ste2-S141P-T326 receptor is expected to be the only subunit in the heterodimer that can reach the activated state. The second piece of evidence is the α-factor sensitivity associated with full-length Ste2-S141P. The observation that full-length Ste2-S141P cannot rescue the truncated Ste2-S141P-T326-GFP from the ER, suggests that receptors containing the S141P substitution cannot form homodimers. Therefore, full-length Ste2-S141P receptors that reach the cell surface are expected to be in a monomeric state, implying that monomers at the cell surface are active. My results support the view that dimerization of two active Ste2 receptors is not required for G-protein coupling and that a single monomer of Ste2-S141P is able to activate a G-protein.

Recent evidence has shown that rhodopsin can form two-dimensional arrays of dimers and a model derived from atomic force microscopy analysis suggested that TM4 and TM5 were involved in intradimer contact, while TM1, TM2 and TM6 may facilitate contacts between dimer rows (Fotiadis *et al.*, 2003; Liang *et al.*, 2003). So far, rhodopsin is the only GPCR that has been clearly demonstrated to form higher-order oligomers using atomic force microscopy (AFM) as the analytical method. Cross-linking studies consistent with previous results further refine the model of a rhodopsin and reveal three major interfaces contributing to oligomerization (Fotiadis *et al.*, 2006). The intradimeric contact involves two symmetric interactions, each between TM4 from one subunit with TM5 from the adjacent subunit, resulting in a two-fold axis of symmetry. This is the most extensive (and presumably the strongest) contact and is supported by *in vivo* crosslinking experiments in COS cells (Kota *et al.*, 2006). The weakest interaction is the row-row contact in which TM1 from one subunit interacts with TM1 in an adjacent subunit.

Results presented in this study indicate that TM1 (C59R), TM2 (H94P) and TM3 (S141P and S145P) are important for ER export and receptor oligomerization. My study does not exclude the possibility that other TM domains are also involved in ER trafficking and formation of oligomeric complexes. This study also raises the possibility that more than one contact site is operating in the oligomerization of Ste2. It is not possible to identify unambiguously which TMs are involved in direct contact since no high-resolution crystal structure of Ste2 is available. Overton et al (2003) showed that TM1 could self-associate, suggesting that TM1 may provide the direct contact interface

in whole receptors as well. In this model, mutant receptors affecting TM2 and TM3 may fail to form oligomers because they alter the global structure of the Ste2 such that they indirectly perturb the intersubunit contact site in the TM1. However, it seems inconsistent with this view that the strongest mutant identified by Overton et al (2003), Ste2-G56L, blocks homodimerization only partially, whereas it completely blocks receptor function. In contrast, Ste2-S141P retains receptor function when it reaches the plasma membrane, even though it completely blocks homodimer formation.

Fig. 5-10 depicts a model in which TM3 participates in a direct contact interface. In this model, a symmetric axis and two symmetric contacts exist between Ste2 oligomers. In each contact, TM3 from one subunit associates with an unidentified site on the other subunit, and is analogous to the intradimer interface in rhodopsin involving TM4 and TM5. This model explains why the mutants that disrupt TM3 (Ste2-S141p and Ste2-S145P) fail to form homodimers even though they form heterodimers with wild-type receptors. The heterodimers form one of the two contacts present in the wild-type homodimer, whereas the mutant homodimers form neither of the two contacts. The model also requires that the mutant affects only local structures in that it impairs only one of the two contact sites. Consistent with local disruption, full-length Ste2-S141p retains its responsiveness to $\alpha$-factor, and the Ste2-S141p and Ste2-S145P receptors retain sufficient tertiary structure to interact with wild-type receptors. However, if this model reflects the only subunit interface, then other dimer-defective mutants (Ste2-G56L, Ste2-C59R and Ste2-H94P) may cause more global structural defects that lead to the disruption of both interface contact sites. In this model, TM3 is

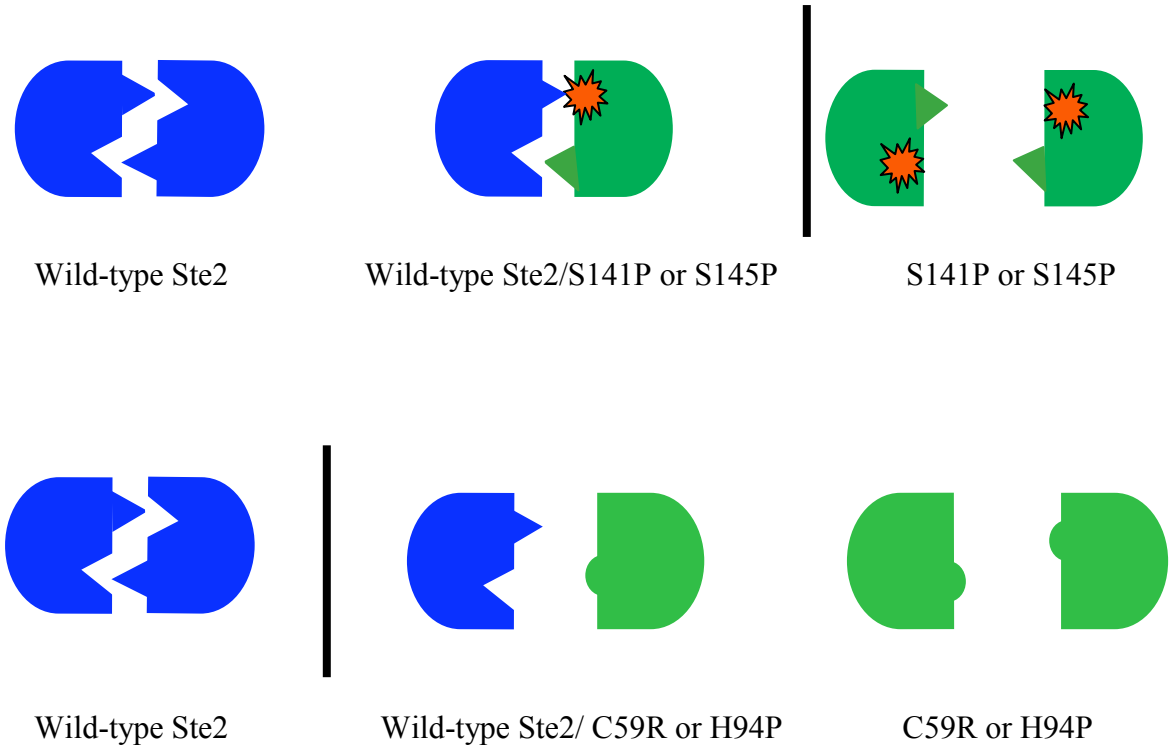


**Figure 10.** Model for heterodimers in the S141P and S145P mutants. Two different types of dimer-defective Ste2 mutants were identified in this study. One type of Ste2 mutant (Ste2-S141p and Ste2-S145P) formed heterdimers but failed to form homodimers. The other type of mutant (Ste2-C59R and Ste2-H94P) failed to form homodimers or heterodimers. If a two-fold rotational axis of symmetry exists in the Ste2 dimer, then wild-type receptors may form duplicate symmetrical contacts (similar to the proposed helix4-helix5 contacts in rhodopsin dimers). If S141P or S145P disrupt one of the two contacts, then wild-type Ste2 may still form one of the contacts with either S141P or S145P in heterodimers. S141P and S145P would be unable to form homodimers because the dimers lack both of the symmetric contacts. The symmetric axis may be disrupted in Ste2-C59R and Ste2-H94P mutants, which would result in failure to form either homodimers or heterodimers.

predicted to be the direct contact interface, whereas disruption of TM1 or TM2 leads to indirect effect. The two models described above are not mutually exclusive. It is possible that Ste2 oligomerization requires multiple contact interfaces and different interfaces function cooperatively. Therefore, mutation in any one of the interfaces can cause the global conformational structure changes of the Ste2, which results in failure of Ste2 oligomerization.

# CHAPTER VI

# GENERAL DISCUSSION

The data presented in this thesis aims to extend the understanding of protein-protein interaction between two Ste2 subunits and the functional significance of Ste2 oligomerization. A diagram of Ste2 (Fig. 6-1) shows positions of amino acid changes in the Ste2 mutants used throughout this study. The four ER retention mutants that were isolated in this study showed oligomerization defects. Here, I summarize and discuss the role that the endocytosis signal sequence plays in ligand-mediated endocytosis of α-factor receptor oligomers, the role that the two DXE motifs play in ER export trafficking, and the role that receptor oligomerization plays in ER export.

**Endocytosis signal plays a passive role in ligand-mediated endocytosis**

My data suggest that the endocytosis signal sequence plays only a passive role in the control of ligand-induced endocytosis. I present evidence indicating that the endocytosis machinery recognizes the ligand-induced conformational change and the endocytosis signal sequence *in trans* when cells express two different receptors, where one receptor is defective in ligand binding (Ste2-F204S) and the other receptor lacks the endocytosis signal sequence (Ste2-T326-GFP). I have proposed a model to explain how the endocytosis machinery recognizes these two independent signals. However, the

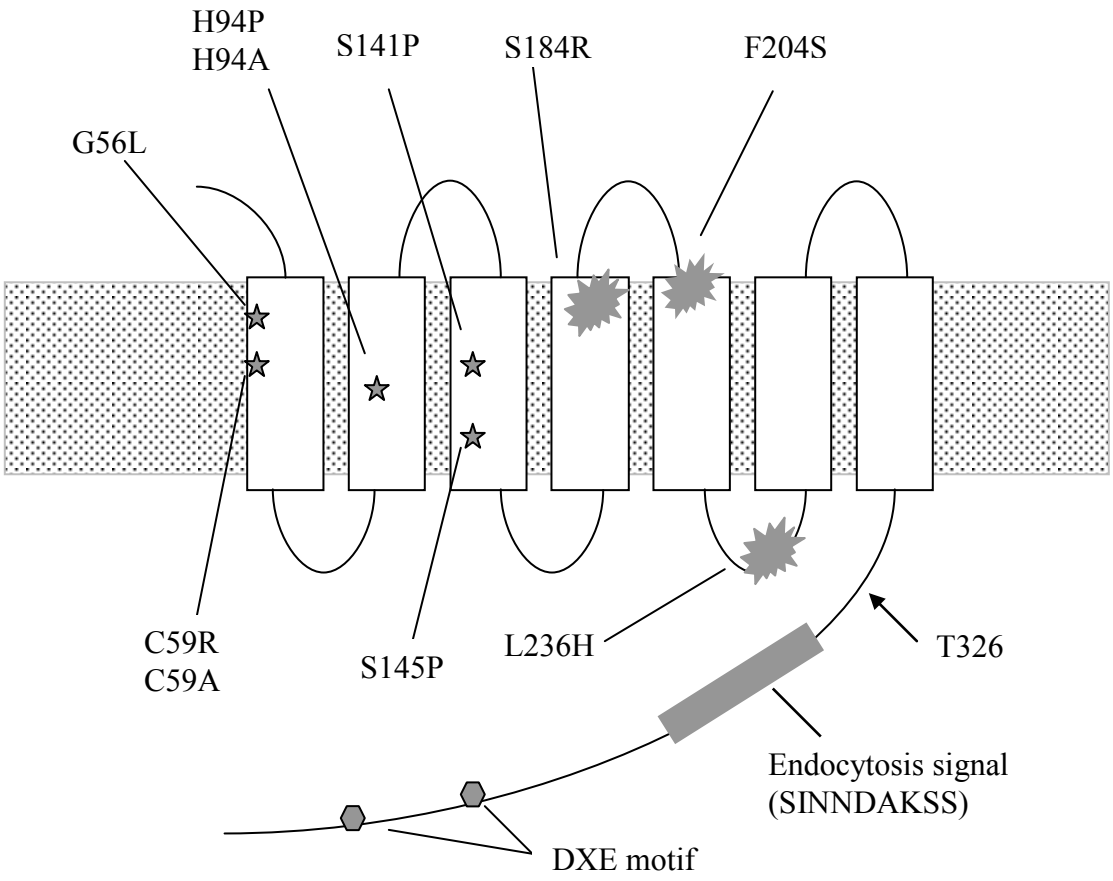


**Figure 6-1.** Summary of mutants of the α-factor receptor. The positions of the amino acid changes in receptor mutants used in this study are shown. Ste-S184R and Ste2-F204S are binding defective mutants. Ste2-L236G is a G-protein coupling mutant. The endocytosis motif SINNDAKSS sequence is denoted in gray box. The position of T326 truncation is marked with an arrow. The two ER export motifs DXE are denoted by the gray hexagons. Mutants predicted to be involved in Ste2 dimerization are denoted by the gray stars.

data presented here do not address the question of whether the two signals must come from receptors in the same complex. For example, in the presence of α-factor, the endocytosis defective receptor, Ste2-T326, may be internalized if the endocytosis signal is targeted to the cell surface without being part of a receptor complex. A positive result would strongly suggest that receptor oligomerization is not required to bring the ligand-induced conformational change and the endocytosis signal sequence together. It is also possible that oligomerization is not required at all for endocytosis. Full-length dimer-defective Ste2-S141P reaches the cell surface and the vacuole. This result suggests that oligomerization of Ste2 may not be required for endocytosis. However, at this time, it is unclear whether Ste2-S141P forms dimers after reaching the cell surface, and it is unclear whether the receptors in the vacuole have transitted the plasma membrane.

**At least two independent ER export signals are involved in the Ste2 ER export**

Two independent ER export signals were identified in this study. At least one signal is contained in the C-terminal tail, and at least one signal is located in the main body of Ste2. Mutant receptors that contain either of these signals can exit from the ER.

**The DXE motif is the major ER export signal in the C-terminal tail**

I identified two DXE motifs in the C-terminal tail of the receptor that facilitate ER export. Substitution of two DXE motifs with AXE resulted in significant ER retention of Ste2-C59R, Ste2-H94P, Ste2-S141P and Ste2-S145P. Based on sequence alignments, DXE motif is conserved among Ste2 homologs in related yeasts, suggesting a role in

facilitating ER export trafficking. DXE motifs are present in the C-terminal tails of Ste2 homologs for 12 of the 16 budding yeast species examined (Fig. 6-2). It is not present in the three species containing very short C-terminal tails (*Saccharomyces pastorianus, Pichia guilliermondii and Pichia stipitis*). DXE is also missing in the Ste2 homolog from the *Lachancea kluyveri*. These species may depend on the signals in the main body of the receptor for ER export. Two other GPCRs in *S. cerevisiae*, Ste3 and Gpr1, also contain DXE in the C-terminal domain. Therefore DXE appears to be a common ER export signal for GPCRs in budding yeasts.

Three observations indicated that a weak ER export signal may exist in the C-terminal tail in addition to the DXE motifs. First, despite its ER retention, Ste2-S141P-AXE showed α-factor sensitivity that was significantly less than Ste2-S141P but greater than truncated Ste2-S141P-T326. Second, Ste2-G56L-AXE exited the ER more efficiently than Ste2-G56L-T326. Third, Ste2-AXE did not show the trace ER localization that was observed for Ste2-T326. Together, my data suggest that another unidentified sequence in the C-terminal tail plays a role in ER export of Ste2 and remains to be identified.

My studies have not addressed the question of whether both DXE motifs are required for ER export of Ste2. The answer to this question requires the construction and analysis of mutants containing single substitution of the DXE motif.

**Correlation between Ste2 oligomerization and ER export**

My results indicate that the ER exit signal associated with the main body of the

## C-Terminal Cytoplasmic Domains of Budding Yeasts

*Ashbya gossypii* YIAVLLVSLSLPLSSVWATAANNATVPPFLNAHSLTSRYKAESWYTDSKNDAGSFSSSEN
*Candida albicans* QISLLLIILMLPLSSLWAQTANNTHNINSSPSLSFISRHHS-SDSSRSGGSNTIVSNGGS
*Candida dubliniensis* QISLLLIILMLPLSSLWAQTANNIHNINSSPSLSFISRHHSSDNNSNINTIVNGNNNHLY
*Candida glabrata* PIANLFVVLSLPLSSIWANTSNNSSRSPKYWKNSQTNKSNGSFVSSISVNSDSQNPLYKK
*Debaryomyces hansenii* AVSVLLVVLSLPFSSMWASAANNNPTPTSSTLAFLNRSDSNNSDSSTIVGNRFSLFPGKL
*Kluyveromyces lactis* SIATLLVVLSLPLTSIWAAAANDAPSASTFYRQFNPYSAQNRDDSSSYSYGKAFSDKYSF
*Lachancea kluyveri* SIATLLVTLSLPLSSMWATSANNSSH-PSSINTQF--RQRNYDDVSFKTGITSFYSESSK
*Lodderomyces elongisporus* NMALFLVVAFLPLSSLWAQTANTTKKIESSPSMSFITRRKSEDESPLAANDEDRLRKFTT
*Pichia guilliermondii* SVSMMIIVLSLPASSMWAAAAN-ASSAPSSAASSLFRYTTSDSDRTLETKSDHFIMKHES
*Pichia stipitis* -ISYLLVVLSLPVSSIWAATANNSPQLPSSATLSFMNKTTSHFSES----------
*Saccharomyces bayanus* TVATLLAVLSLPLSSMWATAANNASK-PNTITSDFTTSTNGFYPGGFSSFQADSINSDAK
*Saccharomyces cerevisiae* TVATLLAVLSLPLSSMWATAANNASK-TNTITSDFTTSTDRFYPGTLSSFQTDSINNDAK
*Saccharomyces paradoxus* TVATLLAVLSLPLSSMWATAANNSSK-TNTITSDFTTSTDRFYPGTLSSFQTDSINNDAK
*Saccharomyces pastorianus* TVATLLAVLSRPLSSKWATAANNASK-PTTINSDFTTSTNGFYPGGY----------
*Vanderwaltozyma polyspora* VIATLLVVLSLPLSSMWASAANNSPK-----PSSFTTDYSNKNPSDTPSFYSQSISSSMK
*Yarrowia lipolytica* GVAYLMVVLSLPLSSIWATAVH**DDE**MQSNYLLSALKDGHVQPSESKLKTVFLNRLRPFST

*Ashbya gossypii* CGSGYRHG----RYSNNGGSSPHQCTGGDNTVI**DIE**KCQYRVNPTPHTSGQFAFNQDSLE
*Candida albicans* NGGGGGGGNFPVSGIDAQLPP**DIE**KILHEDNNYKLLNSNNESVNDGDIIINDEGMITKQI
*Candida dubliniensis* NSNSNSNSNSNSNGNGNGKFSKLNTNGSSPFTLKGDSGSLMLQMTSNSNNGNNGNINAGN
*Candida glabrata* IVRFTSKGDTTRSIVSDSTLAEVGKYSMQDVSNSNFECRDL**DFE**KVKHTCENFGRISETY
*Debaryomyces hansenii* SKSSTTDSSIEKTMKDLSHTTSNHQEDSPTTLTDFRLQNDQSFYFSNLSAPPS--**DIE**QI
*Kluyveromyces lactis* SNSPQTSDGCSSKELELSTQLEM**DLE**SGESFMDRAKRSDFVSSPGSTDATVIKQLKASNI
*Lachancea kluyveri* PSSKYRHTNNLYDLYPVSRTSNSRCNGYPNDGSKLAPNPNCVGHNGSTMSVNDKNGAHAT
*Lodderomyces elongisporus* TLDLSGNKNNTTNNNNNSNNINNNMSNINYPSTGLGEDDKSFIFEMEPSRERAAIEEIDL
*Pichia guilliermondii* HNSSPNSSPLTLVQKRISDATLELPKELEDLIDSTSI----------
*Pichia stipitis* ----------
*Saccharomyces bayanus* SSFRSRLYDLYPRRKESISDKHSERTFVDGTAN**DIE**KNQFYQLPT----------
*Saccharomyces cerevisiae* SSLRSRLYDLYPRRKETTSDKHSERTFVSETAD**DIE**KNQFYQLPTPTSSKNTRIGPFADA
*Saccharomyces paradoxus* SSLRSRLYDLYPRRKELTSDKHSERTFVAEAAN**DIE**KNQFYQLPTPTSSKNTRIGPFADT
*Saccharomyces pastorianus* ----------
*Vanderwaltozyma polyspora* SKFPSKFIPFNFKSKDNSSDTRSENTYIGNY**DME**KNGSPNHSYSSKDQSEVYTIGVSSMH
*Yarrowia lipolytica* TTNR**DDE**SSVDSPAMPSPESDVTFLNTGFECDEKM----------

## C-Terminal Cytoplasmic Domains of Budding Yeasts (continued)


**Figure 6-2.** DXE motifs in the C-terinal tails of Ste2 homologs.

receptor correlates with the ability of the mutant receptors to form oligomers. Wild-type truncated Ste2-T326-GFP reached cell surface based on the fluorescence microscopy, whereas the four mutant forms of the truncated receptor that failed to form oligomers (Ste2-C59R-T326. Ste2-H94P-T326, Ste2-S141P-T326 and Ste2-S145P-T326) also fail to exit the ER. Furthermore, the ER-retained truncated Ste2-S141P-T326 and Ste2-S145P-T326 mutants were delivered to the cell surface when allowed to form hetero-oligomers with wild-type Ste2. The data suggest that oligomerization of Ste2 can serve as an ER export signal. Oligomerization of GPCRs is important for cell surface expression in other receptor systems such as the β-adrenergic receptor and the GABA receptor (Jone *et al*., 1998; White *et al*., 1998; Salhpour *et al*., 2004). In principle, oligomerization could facilitate ER export either by concentrating multiple weak ER export signals or by shielding an ER retention signal.

**Mutations affecting Ste2 oligomerization**

Knowledge of interaction among Ste2 transmembrane helices has been hampered due to a lack of a high-resolution crystal structure. However, common features in the structure of Ste2 can be achieved by comparing it with rhodopsin. One possible arrangement of the helical domains in Ste2, depicted in Fig. 6-3B, is based on a model proposed by Eiler *et al* (2005). The translational positions of the helices are based on rhodopsin. The relative rotations of the helices are inferred from helix packing moments and from conserved sequences at the proposed helix interfaces. The structure has been refined by using molecular dynamics computer programs. Other models using different

(A) Rhodopsin

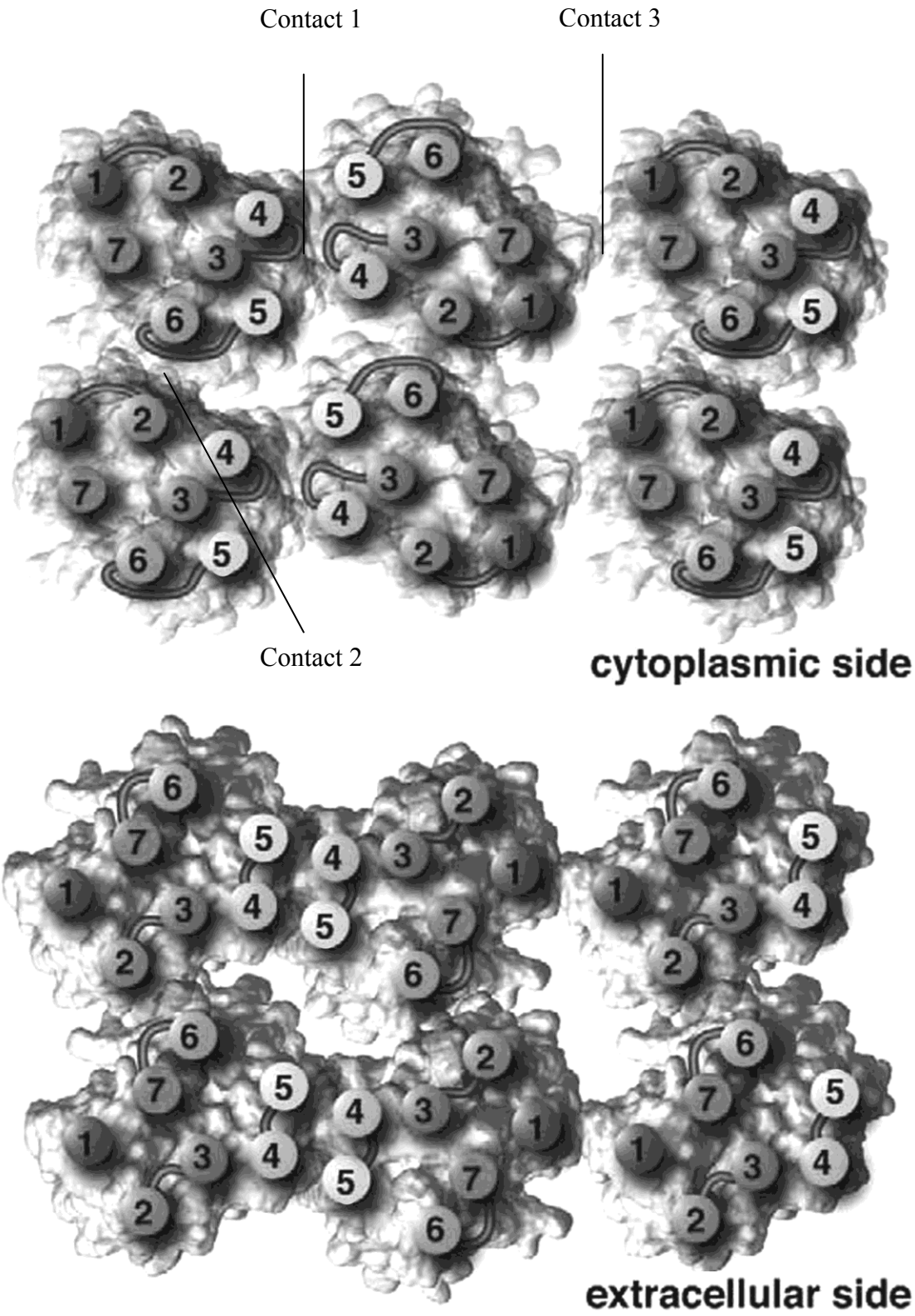
Contact 1
Contact 3
Contact 2
cytoplasmic side
extracellular side

(B) Ste2

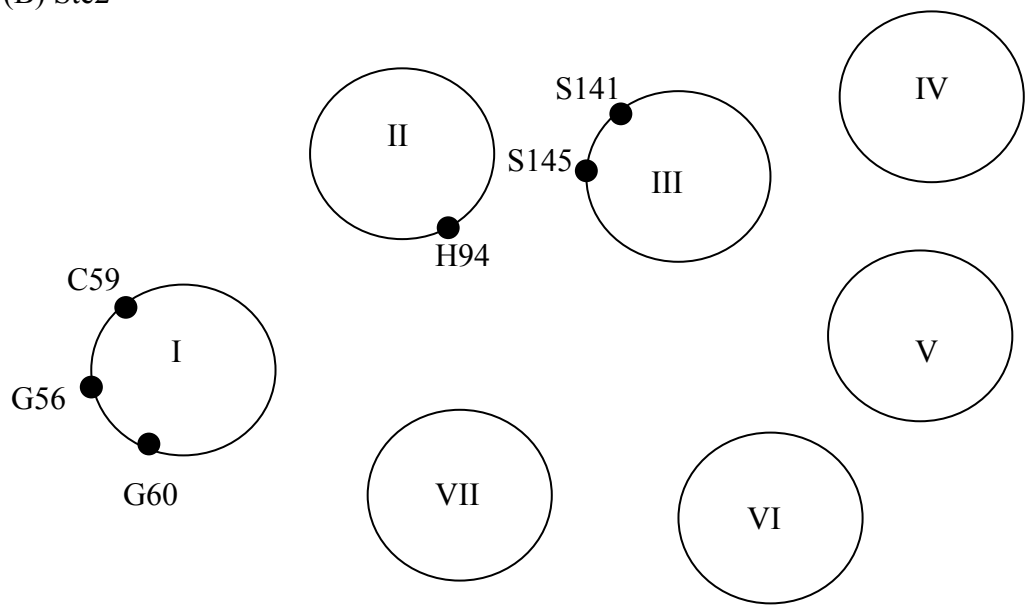


**Figure 6-3**. Models for transmembrane domain arrangement in rhodopsin and Ste2. (A) Transmembrane domain arrangement in rhodopsin adapted from Fotiadis et al (2004). Three different contacts intradimeric (contact 1), interdimeric (contact 2) and row–row (contact 3) are shown. (B) Transmembrane domain arrangement in Ste2. The locations of each residue (G56, C59, G60, H94, S141, and S145) are indicated based on the analysis shown on Eilers *et al* (2005).

assumptions give somewhat different helix rotations (Parrish *et al*., 2002; Lin *et al*., 2005). The potential oligomeric structure of GPCRs (Fig. 6-3A) is based on the x-ray crystal structure of rhodopsin and on atomic force microscopy of rhodopsin in retinal disk membranes (Fotiadis *et al.*, 2004; Fotiadis *et al.*, 2006). This model of rhodopsin proposes three different types of contacts among rhodopsin monomers: intradimeric (contact 1), interdimeric (contact 2) and row–row (contact 3). In disk membranes, the oligomeric structure is extended in two dimensions to produce a sheet of interacting receptors. The model suggestes that TMIV and TMV are the main contact interfaces (contact 1) between two monomers (Fotiadis *et al.*, 2004). Cooperative interactions among the three contact interfaces may be required to maintain the stability of the oligomeric structure. Therefore, a mutation affecting any these contacts may have a profound consequence for the oligomerization. This possibility is confirmed by the $\alpha_{1b}$-adrenoceptor oligomerization. The $\alpha_{1b}$-adrenoceptor is believed to form a higher-order oligomer, based on three-color fluorescence resonance energy transfer (3-FRET) analysis to detect the higher-order oligomeric complexes in single living cells. Oligomerization is important for receptor maturation, surface delivery and function (Lopez-Gimenez *et al.*, 2007). Transmembrane domain I and transmembrane domain IV were proposed to contribute two symmetrical protein-protein interaction interfaces (contact 1 and contact 3 in Fig. 6-3A), and a "daisy-chain" structure was proposed to link the monomers into higher-order oligomers (Carrillo *et al.*, 2004; Lopez-Gimenez *et al.*, 2007). Mutations that lead to amino acid substitutions in transmembrane domain IV

disrupt oligomerization and have profound consequences for cell surface delivery and function (Lopez-Gimenez *et al.*, 2007).

Ste2 may also form higher order oligomeric complexes rather than only simple dimeric complexes, suggesting the existence of more than one interaction interface. These interface contacts may work cooperatively such that mutations affecting any single interface may disrupt the oligomeric structure. However, further investigation is required to address this question.

The GxxxG motif in TMI of Ste2 is conserved and is the only predicted dimerization motif (Overton *et al.*, 2003; Eilers *et al.*, 2005). The sequence is conserved in the Ste2 family and a similar sequence is present in rhodopsin ($^{38}$SxxxA$^{42}$) but absent in the Ste3 family (Eilers *et al.*, 2005). These two glycines are predicted to be oriented outward, away from the interior of the helical bundles based on the model of Eilers *et al* (2005). However, although G56L was the most severe glycine substitution in GxxxG as judged by the FRET assay (Overton *et al*., 2003), G56L was found to form both hetero-oligomers and homo-oligomers in this study, albeit at a reduced efficiency. In terms of the proposed GPCR oligomeric structure (Fig. 6-3A), Ste-G56L is likely to cause a partial disruption of contact 3.

In this study, the C59R substitution caused a severe disruption of oligomerization. C59 is a non-conserved residue located within $^{56}$GxxxG$^{60}$ motif. In the model of Eilers *et al* (2005), it faces outward and is part of the same helix packing moment as G56. Therefore, substitution of cysteine with a bulky charged amino acid such as arginine may cause a steric contact problem between adjoining subunits. This possibility is consistent

with the observation that the truncated Ste2-C59A localizes properly on the cell surface, and its α-factor sensitivity is indistinguishable from that of the truncated wild-type Ste2. In the rhodopsin model (Fig. 6-3A), the C59R may cause a severe disruption of contact 3; however, I cannot rule out the possibility that C59R causes a more global disruption of receptor structure.

Residue H94 is moderately conserved among the Ste2 homologs (normally either arginine or histidine). H94 forms hydrogen-bonds with R58 (TMI) and interacts with Q135 (TMIII) in the model of Eilers *et al*., (2005). The H94P substitution is expected to cause a kink in the TM2 helix and disrupt the hydrogen-bond with TMI. My results are consistent with the prediction that H94 would serve to stabilize the TMI and TMII interaction of the Ste2 (Eilers *et al.*, 2005) Since truncated H94P and H94A both lead to ER retention. In this view, H94P and H94A may be similar to C59R in disrupting contact 3 (Fig. 6-3A). Again, I cannot rule out the possibility that substitutions at H94 cause global disruptions in receptor structure.

The Ste2-S141P and Ste2-S145P mutants represent a class of mutant receptors that are qualitatively different from Ste2-C59R and Ste2-H94P. The phenotype does not appear to reflect a global disruption of receptor structure since Ste2-S141P and Ste2-S145P form heterooligomers with wild-type receptors and since the Ste2-S141P and Ste2-F55L,S145P receptors that reach the plasma membrane are active. Both S141 and S145 are near the cytoplasmic end of TMIII, the most interior of the seven helices in rhodopsin and in the Ste2 model (Eilers *et al*., 2005). Therefore, possibility for direct contact between TMIII and helices in adjacent receptors is limited. S141 faces outward

in the model of Eilers *et al* (2005) and is weakly conserved. S145 is highly conserved among Ste2 homologs and is believed to form hydrogen bonds with TMII (Eilers *et al*., 2005). In term of rhodopsin oligomeric structure (Fig. 6-3A), the S141P and S145P substitutions could influence TMII or TMVI, indirectly affecting contact 2. It is also possible that the kink in TMIII caused by S141P and S145P could affect cytoplasmic loop 2. Residues in this loop have been implicated in contact 2 (Liang *et al*., 2003). As discussed previously (Fig. 5-10), the ability of mutant receptors to form hetero- but not homooligomers may be a consequence of redundant symmetric contacts between receptors. Contact 1 (Fig. 6-3A) contains symmetric redundant interactions between TMIV and TMV. Also, two receptor dimers (joined by contact 1 or contact 3) are bound by two symmetric and redundant contact 2 sites.

S141 and S145 have been implicated in receptor structural changes. Previous results showed that S141P is an intragenic suppressor for Ste2-F204S and Ste2-Y266C (Lin *et al.*, 2005). My data also showed the S141P complement Ste2-F204S and Ste2-L236H mutants by forming hetero-oligomers. The loss of function in Ste2-S145P can be rescued by second mutation F55L (in the original double mutant). F55L also suppresses the G-protein defect in Ste2-Y266C (Lin *et al.*, 2005). Therefore, F55L may serve as a global suppressor in Ste2 by stabilizing the Ste2 structure. Interestingly, S141P, S145L and S145T cause mild agonist-independent activation of the receptor (Lin *et al*., 2005). Therefore, the oligomeric structures that require S141 and S145 may help to constrain the unliganded receptor in the inactive conformation.

Based on the model of rhodopsin (Fig. 6-3A), different TM domains in Ste2 may be involved in different contacts, such as the intradimeric, interdimeric or row–row contacts in the higher-order structure. Together, these interactions may constitute a cooperative network that can be broken by single mutations in the *STE2* gene. On the one hand, single mutations in *STE2* causing global disruption of multiple contacts may lead to inability to form higher oligomeric complex. On the other hand, mutations in *STE2* causing the local disruption of single receptor contact may disrupt the higher order structure by breaking the cooperative network of interactions.

Several unaddressed questions are discussed below. First, I did not address whether the hetero-oligomer formation between Ste2-T326 and Ste2-S141P-T326 is sufficient to promote exit of Ste2-S141P-T-326 from the ER even though coexpression of Ste2-S141P-T326 and Ste2-F204S-T326 showed full $\alpha$-factor sensitivity, implying that Ste2-S141P-T-326 exits from the ER and reaches cell surface. Second, although Ste2-G56L still can form homo-oligomers or hetero-oligomers; however, unlike the truncated Ste2-T326-GFP, most of Ste2-G56L-T326-GFP accumulated in the vacuole instead of remaining on the cell surface (Fig. 5-4 and Fig. 5-5) in the coexpression experiments. This result suggests that the Ste2-G56L that escapes the ER is diverted to the vacuole by a post-ER quality control process. It will be of interest to determine whether these defective receptors are diverted to the vacuole before reaching the plasma membrane, as has been shown for the Ste2-3 temperature-sesitive receptor (Jenness *et al*., 1997). It would be also be interesting to determine whether trafficking to the plasma membrane can be restored by disrupting elements of the post-ER quality control process (Li *et al*.,

1997). Third, my data suggest TMI, II and III are involved directly or indirectly in Ste2 oligomerization. It remains unclear whether other domains influence contact interfaces as well. No repeated mutants were recovered in both of my mutant screens, suggesting that mutants from both screening methods have not been saturated. More screening and mutants are required to map out the direct dimer contacts between Ste2 subunits.

# BIBLOGRAPHY

AbdAlla, S., Lother, H., and Quitterer, U. (2000). AT1-receptor heterodimers show enhanced G-protein activation and altered receptor sequestration. Nature *407*, 94-98.

Angers, S., Salahpour, A., and Bouvier, M. (2001). Biochemical and biophysical demonstration of GPCR oligomerization in mammalian cells. Life Sci *68*, 2243-2250.

Angers, S., Salahpour, A., Joly, E., Hilairet, S., Chelsky, D., Dennis, M., and Bouvier, M. (2000). Detection of beta 2-adrenergic receptor dimerization in living cells using bioluminescence resonance energy transfer (BRET). Proc Natl Acad Sci U S A *97*, 3684-3689.

Arnason, T., and Ellison, M.J. (1994). Stress resistance in Saccharomyces cerevisiae is strongly correlated with assembly of a novel type of multiubiquitin chain. Mol Cell Biol *14*, 7876-7883.

Bai, M., Trivedi, S., and Brown, E.M. (1998). Dimerization of the extracellular calcium-sensing receptor (CaR) on the cell surface of CaR-transfected HEK293 cells. J Biol Chem *273*, 23605-23610.

Baker, E.K., Colley, N.J., and Zuker, C.S. (1994). The cyclophilin homolog NinaA functions as a chaperone, forming a stable complex in vivo with its protein target rhodopsin. Embo J *13*, 4886-4895.

Baneres, J.L., Martin, A., Hullot, P., Girard, J.P., Rossi, J.C., and Parello, J. (2003). Structure-based analysis of GPCR function: conformational adaptation of both agonist and receptor upon leukotriene B4 binding to recombinant BLT1. J Mol Biol *329*, 801-814.

Baneres, J.L., and Parello, J. (2003). Structure-based analysis of GPCR function: evidence for a novel pentameric assembly between the dimeric leukotriene B4 receptor BLT1 and the G-protein. J Mol Biol *329*, 815-829.

Bayburt, T.H., Leitz, A.J., Xie, G., Oprian, D.D., and Sligar, S.G. (2007). Transducin activation by nanoscale lipid bilayers containing one and two rhodopsins. J Biol Chem *282*, 14875-14881.

Bays, N.W., Gardner, R.G., Seelig, L.P., Joazeiro, C.A., and Hampton, R.Y. (2001). Hrd1p/Der3p is a membrane-anchored ubiquitin ligase required for ER-associated degradation. Nat Cell Biol *3*, 24-29.

Belden, W.J., and Barlowe, C. (2001). Role of Erv29p in collecting soluble secretory proteins into ER-derived transport vesicles. Science *294*, 1528-1531.

Benkirane, M., Jin, D.Y., Chun, R.F., Koup, R.A., and Jeang, K.T. (1997). Mechanism of transdominant inhibition of CCR5-mediated HIV-1 infection by ccr5delta32. J Biol Chem *272*, 30603-30606.

Bermak, J.C., Li, M., Bullock, C., and Zhou, Q.Y. (2001). Regulation of transport of the dopamine D1 receptor by a new membrane-associated ER protein. Nat Cell Biol *3*, 492-498.

Bockaert, J., and Pin, J.P. (1999). Molecular tinkering of G protein-coupled receptors: an evolutionary success. Embo J *18*, 1723-1729.

Bordallo, J., Plemper, R.K., Finger, A., and Wolf, D.H. (1998). Der3p/Hrd1p is required for endoplasmic reticulum-associated degradation of misfolded lumenal and integral membrane proteins. Mol Biol Cell *9*, 209-222.

Bouley, R., Sun, T.X., Chenard, M., McLaughlin, M., McKee, M., Lin, H.Y., Brown, D., and Ausiello, D.A. (2003). Functional role of the NPxxY motif in internalization of the type 2 vasopressin receptor in LLC-PK1 cells. Am J Physiol Cell Physiol *285*, C750-762.

Bourne, H.R. (1997). How receptors talk to trimeric G proteins. Curr Opin Cell Biol *9*, 134-142.

Brodsky, J.L., and McCracken, A.A. (1999). ER protein quality control and proteasome-mediated protein degradation. Semin Cell Dev Biol *10*, 507-513.

Bukusoglu, G., and Jenness, D.D. (1996). Agonist-specific conformational changes in the yeast alpha-factor pheromone receptor. Mol Cell Biol *16*, 4818-4823.

Carrillo, J.J., Lopez-Gimenez, J.F., and Milligan, G. (2004). Multiple interactions between transmembrane helices generate the oligomeric alpha1b-adrenoceptor. Mol Pharmacol *66*, 1123-1137.

Carvalho, P., Goder, V., and Rapoport, T.A. (2006). Distinct ubiquitin-ligase complexes define convergent pathways for the degradation of ER proteins. Cell *126*, 361-373.

Chabre, M., and le Maire, M. (2005). Monomeric G-protein-coupled receptor as a functional unit. Biochemistry *44*, 9395-9403.

Chan, W.Y., Soloviev, M.M., Ciruela, F., and McIlhinney, R.A. (2001). Molecular determinants of metabotropic glutamate receptor 1B trafficking. Mol Cell Neurosci *17*, 577-588.

Chapple, J.P., and Cheetham, M.E. (2003). The chaperone environment at the cytoplasmic face of the endoplasmic reticulum can modulate rhodopsin processing and inclusion formation. J Biol Chem *278*, 19087-19094.

Chen, Q., and Konopka, J.B. (1996). Regulation of the G-protein-coupled alpha-factor pheromone receptor by phosphorylation. Mol Cell Biol *16*, 247-257.

Chinault, S.L., Overton, M.C., and Blumer, K.J. (2004). Subunits of a yeast oligomeric G protein-coupled receptor are activated independently by agonist but function in concert to activate G protein heterotrimers. J Biol Chem *279*, 16091-16100.

Chini, B., and Parenti, M. (2009). G-protein coupled receptors, cholesterol and palmitoylation: facts about fats. J Mol Endocrinol.

Chu, D.S., Pishvaee, B., and Payne, G.S. (1996). The light chain subunit is required for clathrin function in Saccharomyces cerevisiae. J Biol Chem *271*, 33123-33130.

Claing, A., Chen, W., Miller, W.E., Vitale, N., Moss, J., Premont, R.T., and Lefkowitz, R.J. (2001). beta-Arrestin-mediated ADP-ribosylation factor 6 activation and beta 2-adrenergic receptor endocytosis. J Biol Chem *276*, 42509-42513.

Cook, L.B., Zhu, C.C., and Hinkle, P.M. (2003). Thyrotropin-releasing hormone receptor processing: role of ubiquitination and proteasomal degradation. Mol Endocrinol *17*, 1777-1791.

Couve, A., Kittler, J.T., Uren, J.M., Calver, A.R., Pangalos, M.N., Walsh, F.S., and Moss, S.J. (2001). Association of GABA(B) receptors and members of the 14-3-3 family of signaling proteins. Mol Cell Neurosci *17*, 317-328.

Cvejic, S., and Devi, L.A. (1997). Dimerization of the delta opioid receptor: implication for a role in receptor internalization. J Biol Chem *272*, 26959-26964.

D'Hondt, K., Heese-Peck, A., and Riezman, H. (2000). Protein and lipid requirements for endocytosis. Annu Rev Genet *34*, 255-295.

Damian, M., Martin, A., Mesnier, D., Pin, J.P., and Baneres, J.L. (2006). Asymmetric conformational changes in a GPCR dimer controlled by G-proteins. Embo J *25*, 5693-5702.

Damian, M., Mary, S., Martin, A., Pin, J.P., and Baneres, J.L. (2008). G protein activation by the leukotriene B4 receptor dimer. Evidence for an absence of trans-activation. J Biol Chem *283*, 21084-21092.

David, N.E., Gee, M., Andersen, B., Naider, F., Thorner, J., and Stevens, R.C. (1997). Expression and purification of the Saccharomyces cerevisiae alpha-factor receptor (Ste2p), a 7-transmembrane-segment G protein-coupled receptor. J Biol Chem *272*, 15553-15561.

Davis, R.E., Ye, V.Z., Macdonald, G.J., and Duggan, K.A. (1995). Vasoactive intestinal peptide regulates angiotensin II catabolism in the rabbit. Acta Physiol Scand *153*, 255-261.

Deslauriers, B., Ponce, C., Lombard, C., Larguier, R., Bonnafous, J.C., and Marie, J. (1999). N-glycosylation requirements for the AT1a angiotensin II receptor delivery to the plasma membrane. Biochem J *339 ( Pt 2)*, 397-405.

Dong, C., Filipeanu, C.M., Duvernay, M.T., and Wu, G. (2007). Regulation of G protein-coupled receptor export trafficking. Biochim Biophys Acta *1768*, 853-870.

Dong, C., and Wu, G. (2006). Regulation of anterograde transport of alpha2-adrenergic receptors by the N termini at multiple intracellular compartments. J Biol Chem *281*, 38543-38554.

Dosil, M., Giot, L., Davis, C., and Konopka, J.B. (1998). Dominant-negative mutations in the G-protein-coupled alpha-factor receptor map to the extracellular ends of the transmembrane segments. Mol Cell Biol *18*, 5981-5991.

Dosil, M., Schandel, K.A., Gupta, E., Jenness, D.D., and Konopka, J.B. (2000). The C terminus of the Saccharomyces cerevisiae alpha-factor receptor contributes to the formation of preactivation complexes with its cognate G protein. Mol Cell Biol *20*, 5321-5329.

Dulic, V., Egerton, M., Elguindi, I., Raths, S., Singer, B., and Riezman, H. (1991). Yeast endocytosis assays. Methods Enzymol *194*, 697-710.

Duncan, M.C., Cope, M.J., Goode, B.L., Wendland, B., and Drubin, D.G. (2001). Yeast Eps15-like endocytic protein, Pan1p, activates the Arp2/3 complex. Nat Cell Biol *3*, 687-690.

Dunn, R., and Hicke, L. (2001). Multiple roles for Rsp5p-dependent ubiquitination at the internalization step of endocytosis. J Biol Chem *276*, 25974-25981.

Dupre, S., Urban-Grimal, D., and Haguenauer-Tsapis, R. (2004). Ubiquitin and endocytic internalization in yeast and animal cells. Biochim Biophys Acta *1695*, 89-111.

Duthey, B., Caudron, S., Perroy, J., Bettler, B., Fagni, L., Pin, J.P., and Prezeau, L. (2002). A single subunit (GB2) is required for G-protein activation by the heterodimeric GABA(B) receptor. J Biol Chem *277*, 3236-3241.

Duvernay, M.T., Zhou, F., and Wu, G. (2004). A conserved motif for the transport of G protein-coupled receptors from the endoplasmic reticulum to the cell surface. J Biol Chem *279*, 30741-30750.

Dwyer, N.D., Troemel, E.R., Sengupta, P., and Bargmann, C.I. (1998). Odorant receptor localization to olfactory cilia is mediated by ODR-4, a novel membrane-associated protein. Cell *93*, 455-466.

Egner, R., and Kuchler, K. (1996). The yeast multidrug transporter Pdr5 of the plasma membrane is ubiquitinated prior to endocytosis and degradation in the vacuole. FEBS Lett *378*, 177-181.

Eilers, M., Hornak, V., Smith, S.O., and Konopka, J.B. (2005). Comparison of class A and D G protein-coupled receptors: common features in structure and activation. Biochemistry *44*, 8959-8975.

Ellgaard, L., and Helenius, A. (2003). Quality control in the endoplasmic reticulum. Nat Rev Mol Cell Biol *4*, 181-191.

Engqvist-Goldstein, A.E., and Drubin, D.G. (2003). Actin assembly and endocytosis: from yeast to mammals. Annu Rev Cell Dev Biol *19*, 287-332.

Ernst, O.P., Gramse, V., Kolbe, M., Hofmann, K.P., and Heck, M. (2007). Monomeric G protein-coupled receptor rhodopsin in solution activates its G protein transducin at the diffusion limit. Proc Natl Acad Sci U S A *104*, 10859-10864.

Feng, Y., and Davis, N.G. (2000). Akr1p and the type I casein kinases act prior to the ubiquitination step of yeast endocytosis: Akr1p is required for kinase localization to the plasma membrane. Mol Cell Biol *20*, 5350-5359.

Foley, D.A., Sharpe, H.J., and Otte, S. (2007). Membrane topology of the endoplasmic reticulum to Golgi transport factor Erv29p. Mol Membr Biol *24*, 259-268.

Fotiadis, D., Jastrzebska, B., Philippsen, A., Muller, D.J., Palczewski, K., and Engel, A. (2006). Structure of the rhodopsin dimer: a working model for G-protein-coupled receptors. Curr Opin Struct Biol *16*, 252-259.

Fotiadis, D., Liang, Y., Filipek, S., Saperstein, D.A., Engel, A., and Palczewski, K. (2003). Atomic-force microscopy: Rhodopsin dimers in native disc membranes. Nature *421*, 127-128.

Fotiadis, D., Liang, Y., Filipek, S., Saperstein, D.A., Engel, A., and Palczewski, K. (2004). The G protein-coupled receptor rhodopsin in the native membrane. FEBS Lett *564*, 281-288.

Fromant, M., Blanquet, S., and Plateau, P. (1995). Direct random mutagenesis of gene-sized DNA fragments using polymerase chain reaction. Anal Biochem *224*, 347-353.

Fukushima, Y., Oka, Y., Saitoh, T., Katagiri, H., Asano, T., Matsuhashi, N., Takata, K., van Breda, E., Yazaki, Y., and Sugano, K. (1995). Structural and functional analysis of the canine histamine H2 receptor by site-directed mutagenesis: N-glycosylation is not vital for its action. Biochem J *310 ( Pt 2)*, 553-558.

Gaborik, Z., Mihalik, B., Jayadev, S., Jagadeesh, G., Catt, K.J., and Hunyady, L. (1998). Requirement of membrane-proximal amino acids in the carboxyl-terminal tail for expression of the rat AT1a angiotensin receptor. FEBS Lett *428*, 147-151.

Galan, J.M., Moreau, V., Andre, B., Volland, C., and Haguenauer-Tsapis, R. (1996). Ubiquitination mediated by the Npi1p/Rsp5p ubiquitin-protein ligase is required for endocytosis of the yeast uracil permease. J Biol Chem *271*, 10946-10952.

Galvez, T., Duthey, B., Kniazeff, J., Blahos, J., Rovelli, G., Bettler, B., Prezeau, L., and Pin, J.P. (2001). Allosteric interactions between GB1 and GB2 subunits are required for optimal GABA(B) receptor function. Embo J *20*, 2152-2159.

Gao, Z., Ni, Y., Szabo, G., and Linden, J. (1999). Palmitoylation of the recombinant human A1 adenosine receptor: enhanced proteolysis of palmitoylation-deficient mutant receptors. Biochem J *342 ( Pt 2)*, 387-395.

Gehret, A.U., Bajaj, A., Naider, F., and Dumont, M.E. (2006). Oligomerization of the yeast alpha-factor receptor: implications for dominant negative effects of mutant receptors. J Biol Chem *281*, 20698-20714.

George, S.R., Fan, T., Xie, Z., Tse, R., Tam, V., Varghese, G., and O'Dowd, B.F. (2000). Oligomerization of mu- and delta-opioid receptors. Generation of novel functional properties. J Biol Chem *275*, 26128-26135.

Gimelbrant, A.A., Haley, S.L., and McClintock, T.S. (2001). Olfactory receptor trafficking involves conserved regulatory steps. J Biol Chem *276*, 7285-7290.

Gitan, R.S., and Eide, D.J. (2000). Zinc-regulated ubiquitin conjugation signals endocytosis of the yeast ZRT1 zinc transporter. Biochem J *346 Pt 2*, 329-336.

Glickman, M.H., and Ciechanover, A. (2002). The ubiquitin-proteasome proteolytic pathway: destruction for the sake of construction. Physiol Rev *82*, 373-428.

Gomes, I., Gupta, A., Filipovska, J., Szeto, H.H., Pintar, J.E., and Devi, L.A. (2004). A role for heterodimerization of mu and delta opiate receptors in enhancing morphine analgesia. Proc Natl Acad Sci U S A *101*, 5135-5139.

Goudet, C., Kniazeff, J., Hlavackova, V., Malhaire, F., Maurel, D., Acher, F., Blahos, J., Prezeau, L., and Pin, J.P. (2005). Asymmetric functioning of dimeric metabotropic glutamate receptors disclosed by positive allosteric modulators. J Biol Chem *280*, 24380-24385.

Govers, R., van Kerkhof, P., Schwartz, A.L., and Strous, G.J. (1997). Linkage of the ubiquitin-conjugating system and the endocytic pathway in ligand-induced internalization of the growth hormone receptor. Embo J *16*, 4851-4858.

Gripentrog, J.M., Jesaitis, A.J., and Miettinen, H.M. (2000). A single amino acid substitution (N297A) in the conserved NPXXY sequence of the human N-formyl peptide receptor results in inhibition of desensitization and endocytosis, and a dose-dependent shift in p42/44 mitogen-activated protein kinase activation and chemotaxis. Biochem J *352 Pt 2*, 399-407.

Guo, W., Shi, L., and Javitch, J.A. (2003). The fourth transmembrane segment forms the interface of the dopamine D2 receptor homodimer. J Biol Chem *278*, 4385-4388.

Guo, W., Urizar, E., Kralikova, M., Mobarec, J.C., Shi, L., Filizola, M., and Javitch, J.A. (2008). Dopamine D2 receptors form higher order oligomers at physiological expression levels. Embo J *27*, 2293-2304.

Hague, C., Uberti, M.A., Chen, Z., Bush, C.F., Jones, S.V., Ressler, K.J., Hall, R.A., and Minneman, K.P. (2004a). Olfactory receptor surface expression is driven by association with the beta2-adrenergic receptor. Proc Natl Acad Sci U S A *101*, 13672-13676.

Hague, C., Uberti, M.A., Chen, Z., Hall, R.A., and Minneman, K.P. (2004b). Cell surface expression of alpha1D-adrenergic receptors is controlled by heterodimerization with alpha1B-adrenergic receptors. J Biol Chem *279*, 15541-15549.

Hamm, H.E. (1998). The many faces of G protein signaling. J Biol Chem *273*, 669-672.

Hanton, S.L., Renna, L., Bortolotti, L.E., Chatre, L., Stefano, G., and Brandizzi, F. (2005). Diacidic motifs influence the export of transmembrane proteins from the endoplasmic reticulum in plant cells. Plant Cell *17*, 3081-3093.

Hanyaloglu, A.C., and von Zastrow, M. (2008). Regulation of GPCRs by endocytic membrane trafficking and its potential implications. Annu Rev Pharmacol Toxicol *48*, 537-568.

Hartwell, L.H. (1980). Mutants of Saccharomyces cerevisiae unresponsive to cell division control by polypeptide mating hormone. J Cell Biol *85*, 811-822.

Hasson, M.S., Blinder, D., Thorner, J., and Jenness, D.D. (1994). Mutational activation of the STE5 gene product bypasses the requirement for G protein beta and gamma subunits in the yeast pheromone response pathway. Mol Cell Biol *14*, 1054-1065.

Hauser, M., Kauffman, S., Lee, B.K., Naider, F., and Becker, J.M. (2007). The first extracellular loop of the Saccharomyces cerevisiae G protein-coupled receptor Ste2p undergoes a conformational change upon ligand binding. J Biol Chem *282*, 10387-10397.

Hebert, T.E., and Bouvier, M. (1998). Structural and functional aspects of G protein-coupled receptor oligomerization. Biochem Cell Biol *76*, 1-11.

Hebert, T.E., Moffett, S., Morello, J.P., Loisel, T.P., Bichet, D.G., Barret, C., and Bouvier, M. (1996). A peptide derived from a beta2-adrenergic receptor transmembrane domain inhibits both receptor dimerization and activation. J Biol Chem *271*, 16384-16392.

Heese-Peck, A., Pichler, H., Zanolari, B., Watanabe, R., Daum, G., and Riezman, H. (2002). Multiple functions of sterols in yeast endocytosis. Mol Biol Cell *13*, 2664-2680.

Hermosilla, R., Oueslati, M., Donalies, U., Schonenberger, E., Krause, E., Oksche, A., Rosenthal, W., and Schulein, R. (2004). Disease-causing V(2) vasopressin receptors are retained in different compartments of the early secretory pathway. Traffic *5*, 993-1005.

Hermosilla, R., and Schulein, R. (2001). Sorting functions of the individual cytoplasmic domains of the G protein-coupled vasopressin V(2) receptor in Madin Darby canine kidney epithelial cells. Mol Pharmacol *60*, 1031-1039.

Hernanz-Falcon, P., Rodriguez-Frade, J.M., Serrano, A., Juan, D., del Sol, A., Soriano, S.F., Roncal, F., Gomez, L., Valencia, A., Martinez, A.C., and Mellado, M. (2004). Identification of amino acid residues crucial for chemokine receptor dimerization. Nat Immunol *5*, 216-223.

Herrick-Davis, K., Weaver, B.A., Grinde, E., and Mazurkiewicz, J.E. (2006). Serotonin 5-HT2C receptor homodimer biogenesis in the endoplasmic reticulum: real-time visualization with confocal fluorescence resonance energy transfer. J Biol Chem *281*, 27109-27116.

Hicke, L. (1997). Ubiquitin-dependent internalization and down-regulation of plasma membrane proteins. Faseb J *11*, 1215-1226.

Hicke, L. (2001). Protein regulation by monoubiquitin. Nat Rev Mol Cell Biol *2*, 195-201.

Hicke, L., and Dunn, R. (2003). Regulation of membrane protein transport by ubiquitin and ubiquitin-binding proteins. Annu Rev Cell Dev Biol *19*, 141-172.

Hicke, L., and Riezman, H. (1996). Ubiquitination of a yeast plasma membrane receptor signals its ligand-stimulated endocytosis. Cell *84*, 277-287.

Hicke, L., Zanolari, B., and Riezman, H. (1998). Cytoplasmic tail phosphorylation of the alpha-factor receptor is required for its ubiquitination and internalization. J Cell Biol *141*, 349-358.

Hlavackova, V., Goudet, C., Kniazeff, J., Zikova, A., Maurel, D., Vol, C., Trojanova, J., Prezeau, L., Pin, J.P., and Blahos, J. (2005). Evidence for a single heptahelical domain being turned on upon activation of a dimeric GPCR. Embo J *24*, 499-509.

Hochstrasser, M. (1996). Ubiquitin-dependent protein degradation. Annu Rev Genet *30*, 405-439.

Holtzman, D.A., Yang, S., and Drubin, D.G. (1993). Synthetic-lethal interactions identify two novel genes, SLA1 and SLA2, that control membrane cytoskeleton assembly in Saccharomyces cerevisiae. J Cell Biol *122*, 635-644.

Horak, J. (2003). The role of ubiquitin in down-regulation and intracellular sorting of membrane proteins: insights from yeast. Biochim Biophys Acta *1614*, 139-155.

Horak, J., and Wolf, D.H. (2001). Glucose-induced monoubiquitination of the Saccharomyces cerevisiae galactose transporter is sufficient to signal its internalization. J Bacteriol *183*, 3083-3088.

Howard, J.P., Hutton, J.L., Olson, J.M., and Payne, G.S. (2002). Sla1p serves as the targeting signal recognition factor for NPFX(1,2)D-mediated endocytosis. J Cell Biol *157*, 315-326.

Hwang, C.S., and Varshavsky, A. (2008). Regulation of peptide import through phosphorylation of Ubr1, the ubiquitin ligase of the N-end rule pathway. Proc Natl Acad Sci U S A *105*, 19188-19193.

Illing, M.E., Rajan, R.S., Bence, N.F., and Kopito, R.R. (2002). A rhodopsin mutant linked to autosomal dominant retinitis pigmentosa is prone to aggregate and interacts with the ubiquitin proteasome system. J Biol Chem *277*, 34150-34160.

Jacob, C., Cottrell, G.S., Gehringer, D., Schmidlin, F., Grady, E.F., and Bunnett, N.W. (2005). c-Cbl mediates ubiquitination, degradation, and down-regulation of human protease-activated receptor 2. J Biol Chem *280*, 16076-16087.

Jastrzebska, B., Maeda, T., Zhu, L., Fotiadis, D., Filipek, S., Engel, A., Stenkamp, R.E., and Palczewski, K. (2004). Functional characterization of rhodopsin monomers and dimers in detergents. J Biol Chem *279*, 54663-54675.

Jayadev, S., Smith, R.D., Jagadeesh, G., Baukal, A.J., Hunyady, L., and Catt, K.J. (1999). N-linked glycosylation is required for optimal AT1a angiotensin receptor expression in COS-7 cells. Endocrinology *140*, 2010-2017.

Jenness, D.D., Li, Y., Tipper, C., and Spatrick, P. (1997). Elimination of defective alpha-factor pheromone receptors. Mol Cell Biol *17*, 6236-6245.

Jenness, D.D., and Spatrick, P. (1986). Down regulation of the alpha-factor pheromone receptor in S. cerevisiae. Cell *46*, 345-353.

Jones, K.A., Borowsky, B., Tamm, J.A., Craig, D.A., Durkin, M.M., Dai, M., Yao, W.J., Johnson, M., Gunwaldsen, C., Huang, L.Y., Tang, C., Shen, Q., Salon, J.A., Morse, K., Laz, T., Smith, K.E., Nagarathnam, D., Noble, S.A., Branchek, T.A., and Gerald, C. (1998). GABA(B) receptors function as a heteromeric assembly of the subunits GABA(B)R1 and GABA(B)R2. Nature *396*, 674-679.

Jordan, B.A., and Devi, L.A. (1999). G-protein-coupled receptor heterodimerization modulates receptor function. Nature *399*, 697-700.

Kaksonen, M., Sun, Y., and Drubin, D.G. (2003). A pathway for association of receptors, adaptors, and actin during endocytic internalization. Cell *115*, 475-487.

Kaksonen, M., Toret, C.P., and Drubin, D.G. (2005). A modular design for the clathrin- and actin-mediated endocytosis machinery. Cell *123*, 305-320.

Kaksonen, M., Toret, C.P., and Drubin, D.G. (2006). Harnessing actin dynamics for clathrin-mediated endocytosis. Nat Rev Mol Cell Biol *7*, 404-414.

Kalatskaya, I., Schussler, S., Blaukat, A., Muller-Esterl, W., Jochum, M., Proud, D., and Faussner, A. (2004). Mutation of tyrosine in the conserved NPXXY sequence leads to constitutive phosphorylation and internalization, but not signaling, of the human B2 bradykinin receptor. J Biol Chem *279*, 31268-31276.

Kappeler, F., Klopfenstein, D.R., Foguet, M., Paccaud, J.P., and Hauri, H.P. (1997). The recycling of ERGIC-53 in the early secretory pathway. ERGIC-53 carries a cytosolic

endoplasmic reticulum-exit determinant interacting with COPII. J Biol Chem *272*, 31801-31808.

Kaykas, A., Yang-Snyder, J., Heroux, M., Shah, K.V., Bouvier, M., and Moon, R.T. (2004). Mutant Frizzled 4 associated with vitreoretinopathy traps wild-type Frizzled in the endoplasmic reticulum by oligomerization. Nat Cell Biol *6*, 52-58.

Klco, J.M., Lassere, T.B., and Baranski, T.J. (2003). C5a receptor oligomerization. I. Disulfide trapping reveals oligomers and potential contact surfaces in a G protein-coupled receptor. J Biol Chem *278*, 35345-35353.

Kolling, R., and Hollenberg, C.P. (1994). The ABC-transporter Ste6 accumulates in the plasma membrane in a ubiquitinated form in endocytosis mutants. Embo J *13*, 3261-3271.

Konopka, J.B., Jenness, D.D., and Hartwell, L.H. (1988). The C-terminus of the S. cerevisiae alpha-pheromone receptor mediates an adaptive response to pheromone. Cell *54*, 609-620.

Kota, P., Reeves, P.J., Rajbhandary, U.L., and Khorana, H.G. (2006). Opsin is present as dimers in COS1 cells: identification of amino acids at the dimeric interface. Proc Natl Acad Sci U S A *103*, 3054-3059.

Kraft, K., Olbrich, H., Majoul, I., Mack, M., Proudfoot, A., and Oppermann, M. (2001). Characterization of sequence determinants within the carboxyl-terminal domain of chemokine receptor CCR5 that regulate signaling and receptor internalization. J Biol Chem *276*, 34408-34418.

Krupnick, J.G., and Benovic, J.L. (1998). The role of receptor kinases and arrestins in G protein-coupled receptor regulation. Annu Rev Pharmacol Toxicol *38*, 289-319.

Laporte, S.A., Oakley, R.H., Zhang, J., Holt, J.A., Ferguson, S.S., Caron, M.G., and Barak, L.S. (1999). The beta2-adrenergic receptor/betaarrestin complex recruits the clathrin adaptor AP-2 during endocytosis. Proc Natl Acad Sci U S A *96*, 3712-3717.

Leavitt, L.M., Macaluso, C.R., Kim, K.S., Martin, N.P., and Dumont, M.E. (1999). Dominant negative mutations in the alpha-factor receptor, a G protein-coupled receptor encoded by the STE2 gene of the yeast Saccharomyces cerevisiae. Mol Gen Genet *261*, 917-932.

Lee, S.P., O'Dowd, B.F., Ng, G.Y., Varghese, G., Akil, H., Mansour, A., Nguyen, T., and George, S.R. (2000). Inhibition of cell surface expression by mutant receptors demonstrates that D2 dopamine receptors exist as oligomers in the cell. Mol Pharmacol *58*, 120-128.

Levoye, A., Dam, J., Ayoub, M.A., Guillaume, J.L., Couturier, C., Delagrange, P., and Jockers, R. (2006). The orphan GPR50 receptor specifically inhibits MT1 melatonin receptor function through heterodimerization. Embo J *25*, 3012-3023.

Li, Y., Kane, T., Tipper, C., Spatrick, P., and Jenness, D.D. (1999). Yeast mutants affecting possible quality control of plasma membrane proteins. Mol Cell Biol *19*, 3588-3599.

Liang, Y., Fotiadis, D., Filipek, S., Saperstein, D.A., Palczewski, K., and Engel, A. (2003). Organization of the G protein-coupled receptors rhodopsin and opsin in native membranes. J Biol Chem *278*, 21655-21662.

Lin, C.H., MacGurn, J.A., Chu, T., Stefan, C.J., and Emr, S.D. (2008). Arrestin-related ubiquitin-ligase adaptors regulate endocytosis and protein turnover at the cell surface. Cell *135*, 714-725.

Lin, J.C., Duell, K., Saracino, M., and Konopka, J.B. (2005). Identification of residues that contribute to receptor activation through the analysis of compensatory mutations in the G protein-coupled alpha-factor receptor. Biochemistry *44*, 1278-1287.

Liu, J., Maurel, D., Etzol, S., Brabet, I., Ansanay, H., Pin, J.P., and Rondard, P. (2004). Molecular determinants involved in the allosteric control of agonist affinity in the GABAB receptor by the GABAB2 subunit. J Biol Chem *279*, 15824-15830.

Lopez-Gimenez, J.F., Canals, M., Pediani, J.D., and Milligan, G. (2007). The alpha1b-adrenoceptor exists as a higher-order oligomer: effective oligomerization is required for receptor maturation, surface delivery, and function. Mol Pharmacol *71*, 1015-1029.

Malkus, P., Jiang, F., and Schekman, R. (2002). Concentrative sorting of secretory cargo proteins into COPII-coated vesicles. J Cell Biol *159*, 915-921.

Marchese, A., Paing, M.M., Temple, B.R., and Trejo, J. (2008). G protein-coupled receptor sorting to endosomes and lysosomes. Annu Rev Pharmacol Toxicol *48*, 601-629.

Marchese, A., Raiborg, C., Santini, F., Keen, J.H., Stenmark, H., and Benovic, J.L. (2003). The E3 ubiquitin ligase AIP4 mediates ubiquitination and sorting of the G protein-coupled receptor CXCR4. Dev Cell *5*, 709-722.

Margeta-Mitrovic, M., Jan, Y.N., and Jan, L.Y. (2000). A trafficking checkpoint controls GABA(B) receptor heterodimerization. Neuron *27*, 97-106.

Martin, N.P., Lefkowitz, R.J., and Shenoy, S.K. (2003). Regulation of V2 vasopressin receptor degradation by agonist-promoted ubiquitination. J Biol Chem *278*, 45954-45959.

McLatchie, L.M., Fraser, N.J., Main, M.J., Wise, A., Brown, J., Thompson, N., Solari, R., Lee, M.G., and Foord, S.M. (1998). RAMPs regulate the transport and ligand specificity of the calcitonin-receptor-like receptor. Nature *393*, 333-339.

McNiven, M.A. (1998). Dynamin: a molecular motor with pinchase action. Cell *94*, 151-154.

Medintz, I., Wang, X., Hradek, T., and Michels, C.A. (2000). A PEST-like sequence in the N-terminal cytoplasmic domain of Saccharomyces maltose permease is required for glucose-induced proteolysis and rapid inactivation of transport activity. Biochemistry *39*, 4518-4526.

Mentesana, P.E., and Konopka, J.B. (2001). Mutational analysis of the role of N-glycosylation in alpha-factor receptor function. Biochemistry *40*, 9685-9694.

Meusser, B., Hirsch, C., Jarosch, E., and Sommer, T. (2005). ERAD: the long road to destruction. Nat Cell Biol *7*, 766-772.

Mikosch, M., Hurst, A.C., Hertel, B., and Homann, U. (2006). Diacidic motif is required for efficient transport of the K+ channel KAT1 to the plasma membrane. Plant Physiol *142*, 923-930.

Milasta, S., Pediani, J., Appelbe, S., Trim, S., Wyatt, M., Cox, P., Fidock, M., and Milligan, G. (2006). Interactions between the Mas-related receptors MrgD and MrgE alter signalling and trafficking of MrgD. Mol Pharmacol *69*, 479-491.

Milligan, G., Parenty, G., Stoddart, L.A., and Lane, J.R. (2007). Novel pharmacological applications of G-protein-coupled receptor-G protein fusions. Curr Opin Pharmacol *7*, 521-526.

Morello, J.P., Salahpour, A., Petaja-Repo, U.E., Laperriere, A., Lonergan, M., Arthus, M.F., Nabi, I.R., Bichet, D.G., and Bouvier, M. (2001). Association of calnexin with wild type and mutant AVPR2 that causes nephrogenic diabetes insipidus. Biochemistry *40*, 6766-6775.

Munn, A.L. (2001). Molecular requirements for the internalisation step of endocytosis: insights from yeast. Biochim Biophys Acta *1535*, 236-257.

Munn, A.L., Stevenson, B.J., Geli, M.I., and Riezman, H. (1995). end5, end6, and end7: mutations that cause actin delocalization and block the internalization step of endocytosis in Saccharomyces cerevisiae. Mol Biol Cell *6*, 1721-1742.

Nakamura, N., Yamazaki, S., Sato, K., Nakano, A., Sakaguchi, M., and Mihara, K. (1998). Identification of potential regulatory elements for the transport of Emp24p. Mol Biol Cell *9*, 3493-3503.

Navratil, A.M., Farmerie, T.A., Bogerd, J., Nett, T.M., and Clay, C.M. (2006). Differential impact of intracellular carboxyl terminal domains on lipid raft localization of the murine gonadotropin-releasing hormone receptor. Biol Reprod *74*, 788-797.

Nelson, G., Chandrashekar, J., Hoon, M.A., Feng, L., Zhao, G., Ryba, N.J., and Zuker, C.S. (2002). An amino-acid taste receptor. Nature *416*, 199-202.

Nelson, G., Hoon, M.A., Chandrashekar, J., Zhang, Y., Ryba, N.J., and Zuker, C.S. (2001). Mammalian sweet taste receptors. Cell *106*, 381-390.

Newpher, T.M., Smith, R.P., Lemmon, V., and Lemmon, S.K. (2005). In vivo dynamics of clathrin and its adaptor-dependent recruitment to the actin-based endocytic machinery in yeast. Dev Cell *9*, 87-98.

Ng, G.Y., Mouillac, B., George, S.R., Caron, M., Dennis, M., Bouvier, M., and O'Dowd, B.F. (1994). Desensitization, phosphorylation and palmitoylation of the human dopamine D1 receptor. Eur J Pharmacol *267*, 7-19.

Ng, G.Y., O'Dowd, B.F., Lee, S.P., Chung, H.T., Brann, M.R., Seeman, P., and George, S.R. (1996). Dopamine D2 receptor dimers and receptor-blocking peptides. Biochem Biophys Res Commun *227*, 200-204.

Nishimura, N., and Balch, W.E. (1997). A di-acidic signal required for selective export from the endoplasmic reticulum. Science *277*, 556-558.

Nishimura, N., Bannykh, S., Slabough, S., Matteson, J., Altschuler, Y., Hahn, K., and Balch, W.E. (1999). A di-acidic (DXE) code directs concentration of cargo during export from the endoplasmic reticulum. J Biol Chem *274*, 15937-15946.

Nomura, R., Suzuki, Y., Kakizuka, A., and Jingami, H. (2008). Direct detection of the interaction between recombinant soluble extracellular regions in the heterodimeric metabotropic gamma-aminobutyric acid receptor. J Biol Chem *283*, 4665-4673.

Oksche, A., Dehe, M., Schulein, R., Wiesner, B., and Rosenthal, W. (1998). Folding and cell surface expression of the vasopressin V2 receptor: requirement of the intracellular C-terminus. FEBS Lett *424*, 57-62.

Otte, S., and Barlowe, C. (2002). The Erv41p-Erv46p complex: multiple export signals are required in trans for COPII-dependent transport from the ER. Embo J *21*, 6095-6104.

Overton, M.C., and Blumer, K.J. (2000). G-protein-coupled receptors function as oligomers in vivo. Curr Biol *10*, 341-344.

Overton, M.C., and Blumer, K.J. (2002). The extracellular N-terminal domain and transmembrane domains 1 and 2 mediate oligomerization of a yeast G protein-coupled receptor. J Biol Chem *277*, 41463-41472.

Overton, M.C., Chinault, S.L., and Blumer, K.J. (2003). Oligomerization, biogenesis, and signaling is promoted by a glycophorin A-like dimerization motif in transmembrane domain 1 of a yeast G protein-coupled receptor. J Biol Chem *278*, 49369-49377.

Pagano, A., Rovelli, G., Mosbacher, J., Lohmann, T., Duthey, B., Stauffer, D., Ristig, D., Schuler, V., Meigel, I., Lampert, C., Stein, T., Prezeau, L., Blahos, J., Pin, J., Froestl, W., Kuhn, R., Heid, J., Kaupmann, K., and Bettler, B. (2001). C-terminal interaction is essential for surface trafficking but not for heteromeric assembly of GABA(b) receptors. J Neurosci *21*, 1189-1202.

Pankevych, H., Korkhov, V., Freissmuth, M., and Nanoff, C. (2003). Truncation of the A1 adenosine receptor reveals distinct roles of the membrane-proximal carboxyl terminus in receptor folding and G protein coupling. J Biol Chem *278*, 30283-30293.

Paquin, N., Menade, M., Poirier, G., Donato, D., Drouet, E., and Chartrand, P. (2007). Local activation of yeast ASH1 mRNA translation through phosphorylation of Khd1p by the casein kinase Yck1p. Mol Cell *26*, 795-809.

Parrish, W., Eilers, M., Ying, W., and Konopka, J.B. (2002). The cytoplasmic end of transmembrane domain 3 regulates the activity of the Saccharomyces cerevisiae G-protein-coupled alpha-factor receptor. Genetics *160*, 429-443.

Payne, G.S., Baker, D., van Tuinen, E., and Schekman, R. (1988). Protein transport to the vacuole and receptor-mediated endocytosis by clathrin heavy chain-deficient yeast. J Cell Biol *106*, 1453-1461.

Percherancier, Y., Planchenault, T., Valenzuela-Fernandez, A., Virelizier, J.L., Arenzana-Seisdedos, F., and Bachelerie, F. (2001). Palmitoylation-dependent control of degradation, life span, and membrane expression of the CCR5 receptor. J Biol Chem *276*, 31936-31944.

Perez-Otano, I., Schulteis, C.T., Contractor, A., Lipton, S.A., Trimmer, J.S., Sucher, N.J., and Heinemann, S.F. (2001). Assembly with the NR1 subunit is required for surface expression of NR3A-containing NMDA receptors. J Neurosci *21*, 1228-1237.

Petaja-Repo, U.E., Hogue, M., Laperriere, A., Bhalla, S., Walker, P., and Bouvier, M. (2001). Newly synthesized human delta opioid receptors retained in the endoplasmic

reticulum are retrotranslocated to the cytosol, deglycosylated, ubiquitinated, and degraded by the proteasome. J Biol Chem *276*, 4416-4423.

Petaja-Repo, U.E., Hogue, M., Leskela, T.T., Markkanen, P.M., Tuusa, J.T., and Bouvier, M. (2006). Distinct subcellular localization for constitutive and agonist-modulated palmitoylation of the human delta opioid receptor. J Biol Chem *281*, 15780-15789.

Pidasheva, S., Grant, M., Canaff, L., Ercan, O., Kumar, U., and Hendy, G.N. (2006). Calcium-sensing receptor dimerizes in the endoplasmic reticulum: biochemical and biophysical characterization of CASR mutants retained intracellularly. Hum Mol Genet *15*, 2200-2209.

Prezeau, L., Richman, J.G., Edwards, S.W., and Limbird, L.E. (1999). The zeta isoform of 14-3-3 proteins interacts with the third intracellular loop of different alpha2-adrenergic receptor subtypes. J Biol Chem *274*, 13462-13469.

Prinster, S.C., Holmqvist, T.G., and Hall, R.A. (2006). Alpha2C-adrenergic receptors exhibit enhanced surface expression and signaling upon association with beta2-adrenergic receptors. J Pharmacol Exp Ther *318*, 974-981.

Rands, E., Candelore, M.R., Cheung, A.H., Hill, W.S., Strader, C.D., and Dixon, R.A. (1990). Mutational analysis of beta-adrenergic receptor glycosylation. J Biol Chem *265*, 10759-10764.

Raths, S., Rohrer, J., Crausaz, F., and Riezman, H. (1993). end3 and end4: two mutants defective in receptor-mediated and fluid-phase endocytosis in Saccharomyces cerevisiae. J Cell Biol *120*, 55-65.

Ray, K., Hauschild, B.C., Steinbach, P.J., Goldsmith, P.K., Hauache, O., and Spiegel, A.M. (1999). Identification of the cysteine residues in the amino-terminal extracellular domain of the human Ca(2+) receptor critical for dimerization. Implications for function of monomeric Ca(2+) receptor. J Biol Chem *274*, 27642-27650.

Reddy, P.S., and Corley, R.B. (1998). Assembly, sorting, and exit of oligomeric proteins from the endoplasmic reticulum. Bioessays *20*, 546-554.

Reid, H.M., and Kinsella, B.T. (2007). Palmitoylation of the TPbeta isoform of the human thromboxane A2 receptor. Modulation of G protein: effector coupling and modes of receptor internalization. Cell Signal *19*, 1056-1070.

Remelli, R., Robbins, M.J., and McIlhinney, R.A. (2008). The C-terminus of the metabotropic glutamate receptor 1b regulates dimerization of the receptor. J Neurochem *104*, 1020-1031.

Reneke, J.E., Blumer, K.J., Courchesne, W.E., and Thorner, J. (1988). The carboxy-terminal segment of the yeast alpha-factor receptor is a regulatory domain. Cell *55*, 221-234.

Ridge, K.D., and Palczewski, K. (2007). Visual rhodopsin sees the light: structure and mechanism of G protein signaling. J Biol Chem *282*, 9297-9301.

Riezman, H. (1985). Endocytosis in yeast: several of the yeast secretory mutants are defective in endocytosis. Cell *40*, 1001-1009.

Robert, J., Clauser, E., Petit, P.X., and Ventura, M.A. (2005). A novel C-terminal motif is necessary for the export of the vasopressin V1b/V3 receptor to the plasma membrane. J Biol Chem *280*, 2300-2308.

Rocheville, M., Lange, D.C., Kumar, U., Sasi, R., Patel, R.C., and Patel, Y.C. (2000). Subtypes of the somatostatin receptor assemble as functional homo- and heterodimers. J Biol Chem *275*, 7862-7869.

Rodriguez-Frade, J.M., Vila-Coro, A.J., de Ana, A.M., Albar, J.P., Martinez, A.C., and Mellado, M. (1999). The chemokine monocyte chemoattractant protein-1 induces functional responses through dimerization of its receptor CCR2. Proc Natl Acad Sci U S A *96*, 3628-3633.

Rohrer, J., Benedetti, H., Zanolari, B., and Riezman, H. (1993). Identification of a novel sequence mediating regulated endocytosis of the G protein-coupled alpha-pheromone receptor in yeast. Mol Biol Cell *4*, 511-521.

Rondard, P., Huang, S., Monnier, C., Tu, H., Blanchard, B., Oueslati, N., Malhaire, F., Li, Y., Trinquet, E., Labesse, G., Pin, J.P., and Liu, J. (2008). Functioning of the dimeric GABA(B) receptor extracellular domain revealed by glycan wedge scanning. Embo J *27*, 1321-1332.

Roth, A.F., and Davis, N.G. (1996). Ubiquitination of the yeast a-factor receptor. J Cell Biol *134*, 661-674.

Roth, A.F., Feng, Y., Chen, L., and Davis, N.G. (2002). The yeast DHHC cysteine-rich domain protein Akr1p is a palmitoyl transferase. J Cell Biol *159*, 23-28.

Rothman, J.H., Hunter, C.P., Valls, L.A., and Stevens, T.H. (1986). Overproduction-induced mislocalization of a yeast vacuolar protein allows isolation of its structural gene. Proc Natl Acad Sci U S A *83*, 3248-3252.

Sadeghi, H.M., Innamorati, G., Dagarag, M., and Birnbaumer, M. (1997). Palmitoylation of the V2 vasopressin receptor. Mol Pharmacol *52*, 21-29.

Salahpour, A., Angers, S., Mercier, J.F., Lagace, M., Marullo, S., and Bouvier, M. (2004). Homodimerization of the beta2-adrenergic receptor as a prerequisite for cell surface targeting. J Biol Chem *279*, 33390-33397.

Saliba, R.S., Munro, P.M., Luthert, P.J., and Cheetham, M.E. (2002). The cellular fate of mutant rhodopsin: quality control, degradation and aggresome formation. J Cell Sci *115*, 2907-2918.

Sanchez-Laorden, B.L., Sanchez-Mas, J., Martinez-Alonso, E., Martinez-Menarguez, J.A., Garcia-Borron, J.C., and Jimenez-Cervantes, C. (2006). Dimerization of the human melanocortin 1 receptor: functional consequences and dominant-negative effects. J Invest Dermatol *126*, 172-181.

Sato, K., and Nakano, A. (2004). Reconstitution of coat protein complex II (COPII) vesicle formation from cargo-reconstituted proteoliposomes reveals the potential role of GTP hydrolysis by Sar1p in protein sorting. J Biol Chem *279*, 1330-1335.

Sawutz, D.G., Lanier, S.M., Warren, C.D., and Graham, R.M. (1987). Glycosylation of the mammalian alpha 1-adrenergic receptor by complex type N-linked oligosaccharides. Mol Pharmacol *32*, 565-571.

Schandel, K.A., and Jenness, D.D. (1994). Direct evidence for ligand-induced internalization of the yeast alpha-factor pheromone receptor. Mol Cell Biol *14*, 7245-7255.

Schulein, R., Hermosilla, R., Oksche, A., Dehe, M., Wiesner, B., Krause, G., and Rosenthal, W. (1998). A dileucine sequence and an upstream glutamate residue in the intracellular carboxyl terminus of the vasopressin V2 receptor are essential for cell surface transport in COS.M6 cells. Mol Pharmacol *54*, 525-535.

Sevier, C.S., Weisz, O.A., Davis, M., and Machamer, C.E. (2000). Efficient export of the vesicular stomatitis virus G protein from the endoplasmic reticulum requires a signal in the cytoplasmic tail that includes both tyrosine-based and di-acidic motifs. Mol Biol Cell *11*, 13-22.

Shea, L., and Linderman, J.J. (1997). Mechanistic model of G-protein signal transduction. Determinants of efficacy and effect of precoupled receptors. Biochem Pharmacol *53*, 519-530.

Shenoy, S.K., and Lefkowitz, R.J. (2003a). Multifaceted roles of beta-arrestins in the regulation of seven-membrane-spanning receptor trafficking and signalling. Biochem J *375*, 503-515.

Shenoy, S.K., and Lefkowitz, R.J. (2003b). Trafficking patterns of beta-arrestin and G protein-coupled receptors determined by the kinetics of beta-arrestin deubiquitination. J Biol Chem *278*, 14498-14506.

Shenoy, S.K., McDonald, P.H., Kohout, T.A., and Lefkowitz, R.J. (2001). Regulation of receptor fate by ubiquitination of activated beta 2-adrenergic receptor and beta-arrestin. Science *294*, 1307-1313.

Shih, S.C., Prag, G., Francis, S.A., Sutanto, M.A., Hurley, J.H., and Hicke, L. (2003). A ubiquitin-binding motif required for intramolecular monoubiquitylation, the CUE domain. Embo J *22*, 1273-1281.

Shih, S.C., Sloper-Mould, K.E., and Hicke, L. (2000). Monoubiquitin carries a novel internalization signal that is appended to activated receptors. Embo J *19*, 187-198.

Sommers, C.M., and Dumont, M.E. (1997). Genetic interactions among the transmembrane segments of the G protein coupled receptor encoded by the yeast STE2 gene. J Mol Biol *266*, 559-575.

Sprague, G.F., Jr., and Herskowitz, I. (1981). Control of yeast cell type by the mating type locus. I. Identification and control of expression of the a-specific gene BAR1. J Mol Biol *153*, 305-321.

Springael, J.Y., and Andre, B. (1998). Nitrogen-regulated ubiquitination of the Gap1 permease of Saccharomyces cerevisiae. Mol Biol Cell *9*, 1253-1263.

Stockklausner, C., Ludwig, J., Ruppersberg, J.P., and Klocker, N. (2001). A sequence motif responsible for ER export and surface expression of Kir2.0 inward rectifier K(+) channels. FEBS Lett *493*, 129-133.

Strous, G.J., van Kerkhof, P., Govers, R., Ciechanover, A., and Schwartz, A.L. (1996). The ubiquitin conjugation system is required for ligand-induced endocytosis and degradation of the growth hormone receptor. Embo J *15*, 3806-3812.

Sun, Y., Martin, A.C., and Drubin, D.G. (2006). Endocytic internalization in budding yeast requires coordinated actin nucleation and myosin motor activity. Dev Cell *11*, 33-46.

Tan, P.K., Howard, J.P., and Payne, G.S. (1996). The sequence NPFXD defines a new class of endocytosis signal in Saccharomyces cerevisiae. J Cell Biol *135*, 1789-1800.

Tanaka, K., Nagayama, Y., Nishihara, E., Namba, H., Yamashita, S., and Niwa, M. (1998). Palmitoylation of human thyrotropin receptor: slower intracellular trafficking of the palmitoylation-defective mutant. Endocrinology *139*, 803-806.

Tao, Y.X., Johnson, N.B., and Segaloff, D.L. (2004). Constitutive and agonist-dependent self-association of the cell surface human lutropin receptor. J Biol Chem *279*, 5904-5914.

Tazawa, H., Takahashi, S., and Zilliacus, J. (2003). Interaction of the parathyroid hormone receptor with the 14-3-3 protein. Biochim Biophys Acta *1620*, 32-38.

Terrell, J., Shih, S., Dunn, R., and Hicke, L. (1998). A function for monoubiquitination in the internalization of a G protein-coupled receptor. Mol Cell *1*, 193-202.

Terrillon, S., Barberis, C., and Bouvier, M. (2004). Heterodimerization of V1a and V2 vasopressin receptors determines the interaction with beta-arrestin and their trafficking patterns. Proc Natl Acad Sci U S A *101*, 1548-1553.

Tetsuka, M., Saito, Y., Imai, K., Doi, H., and Maruyama, K. (2004). The basic residues in the membrane-proximal C-terminal tail of the rat melanin-concentrating hormone receptor 1 are required for receptor function. Endocrinology *145*, 3712-3723.

Thevenin, D., Lazarova, T., Roberts, M.F., and Robinson, C.R. (2005a). Oligomerization of the fifth transmembrane domain from the adenosine A2A receptor. Protein Sci *14*, 2177-2186.

Thevenin, D., Roberts, M.F., Lazarova, T., and Robinson, C.R. (2005b). Identifying interactions between transmembrane helices from the adenosine A2A receptor. Biochemistry *44*, 16239-16245.

Toret, C.P., and Drubin, D.G. (2006). The budding yeast endocytic pathway. J Cell Sci *119*, 4585-4587.

Toret, C.P., Lee, L., Sekiya-Kawasaki, M., and Drubin, D.G. (2008). Multiple pathways regulate endocytic coat disassembly in Saccharomyces cerevisiae for optimal downstream trafficking. Traffic *9*, 848-859.

Tsai, B., and Rapoport, T.A. (2002). Unfolded cholera toxin is transferred to the ER membrane and released from protein disulfide isomerase upon oxidation by Ero1. J Cell Biol *159*, 207-216.

Tulipano, G., Stumm, R., Pfeiffer, M., Kreienkamp, H.J., Hollt, V., and Schulz, S. (2004). Differential beta-arrestin trafficking and endosomal sorting of somatostatin receptor subtypes. J Biol Chem *279*, 21374-21382.

Uberti, M.A., Hague, C., Oller, H., Minneman, K.P., and Hall, R.A. (2005). Heterodimerization with beta2-adrenergic receptors promotes surface expression and functional activity of alpha1D-adrenergic receptors. J Pharmacol Exp Ther *313*, 16-23.

van Koppen, C.J., and Nathanson, N.M. (1990). Site-directed mutagenesis of the m2 muscarinic acetylcholine receptor. Analysis of the role of N-glycosylation in receptor expression and function. J Biol Chem *265*, 20887-20892.

Votsmeier, C., and Gallwitz, D. (2001). An acidic sequence of a putative yeast Golgi membrane protein binds COPII and facilitates ER export. Embo J *20*, 6742-6750.

Wang, X., Matteson, J., An, Y., Moyer, B., Yoo, J.S., Bannykh, S., Wilson, I.A., Riordan, J.R., and Balch, W.E. (2004). COPII-dependent export of cystic fibrosis transmembrane conductance regulator from the ER uses a di-acidic exit code. J Cell Biol *167*, 65-74.

Watanabe, R., and Riezman, H. (2004). Differential ER exit in yeast and mammalian cells. Curr Opin Cell Biol *16*, 350-355.

Weiner, J.L., Guttierez-Steil, C., and Blumer, K.J. (1993). Disruption of receptor-G protein coupling in yeast promotes the function of an SST2-dependent adaptation pathway. J Biol Chem *268*, 8070-8077.

White, J.F., Grodnitzky, J., Louis, J.M., Trinh, L.B., Shiloach, J., Gutierrez, J., Northup, J.K., and Grisshammer, R. (2007). Dimerization of the class A G protein-coupled neurotensin receptor NTS1 alters G protein interaction. Proc Natl Acad Sci U S A *104*, 12199-12204.

White, J.H., Wise, A., Main, M.J., Green, A., Fraser, N.J., Disney, G.H., Barnes, A.A., Emson, P., Foord, S.M., and Marshall, F.H. (1998). Heterodimerization is required for the formation of a functional GABA(B) receptor. Nature *396*, 679-682.

Whorton, M.R., Bokoch, M.P., Rasmussen, S.G., Huang, B., Zare, R.N., Kobilka, B., and Sunahara, R.K. (2007). A monomeric G protein-coupled receptor isolated in a high-density lipoprotein particle efficiently activates its G protein. Proc Natl Acad Sci U S A *104*, 7682-7687.

Whorton, M.R., Jastrzebska, B., Park, P.S., Fotiadis, D., Engel, A., Palczewski, K., and Sunahara, R.K. (2008). Efficient coupling of transducin to monomeric rhodopsin in a phospholipid bilayer. J Biol Chem *283*, 4387-4394.

Wolfe, B.L., Marchese, A., and Trejo, J. (2007). Ubiquitination differentially regulates clathrin-dependent internalization of protease-activated receptor-1. J Cell Biol *177*, 905-916.

Yesilaltay, A. (2001). Oligomerizaton and endocytosis of the α-factor receptor, University of Massachusetts, Worcester.

Yesilaltay, A., and Jenness, D.D. (2000). Homo-oligomeric complexes of the yeast alpha-factor pheromone receptor are functional units of endocytosis. Mol Biol Cell *11*, 2873-2884.

Yuan, H., Michelsen, K., and Schwappach, B. (2003). 14-3-3 dimers probe the assembly status of multimeric membrane proteins. Curr Biol *13*, 638-646.

Zagouras, P., Ruusala, A., and Rose, J.K. (1991). Dissociation and reassociation of oligomeric viral glycoprotein subunits in the endoplasmic reticulum. J Virol *65*, 1976-1984.

Zanolari, B., Raths, S., Singer-Kruger, B., and Riezman, H. (1992). Yeast pheromone receptor endocytosis and hyperphosphorylation are independent of G protein-mediated signal transduction. Cell *71*, 755-763.

Zeng, F.Y., and Wess, J. (1999). Identification and molecular characterization of m3 muscarinic receptor dimers. J Biol Chem *274*, 19487-19497.

Zerangue, N., Schwappach, B., Jan, Y.N., and Jan, L.Y. (1999). A new ER trafficking signal regulates the subunit stoichiometry of plasma membrane K(ATP) channels. Neuron *22*, 537-548.

Zhang, Z., Sun, S., Quinn, S.J., Brown, E.M., and Bai, M. (2001). The extracellular calcium-sensing receptor dimerizes through multiple types of intermolecular interactions. J Biol Chem *276*, 5316-5322.

Zhou, F., Filipeanu, C.M., Duvernay, M.T., and Wu, G. (2006). Cell-surface targeting of alpha2-adrenergic receptors -- inhibition by a transport deficient mutant through dimerization. Cell Signal *18*, 318-327.

Zhu, L., Imanishi, Y., Filipek, S., Alekseev, A., Jastrzebska, B., Sun, W., Saperstein, D.A., and Palczewski, K. (2006). Autosomal recessive retinitis pigmentosa and E150K mutation in the opsin gene. J Biol Chem *281*, 22289-22298.

Zhu, X., and Wess, J. (1998). Truncated V2 vasopressin receptors as negative regulators of wild-type V2 receptor function. Biochemistry *37*, 15773-15784.